



Universidade de Aveiro
Ano 2022

**Sara Cristiana Lopes
Peixoto**

**Efeitos dos nanomateriais no microbioma do solo:
aplicação de nano-agroquímicos e biosólidos**

**Effects of nanomaterials on soil microbiome: nano-
agrochemicals and biosolids applications**



Universidade de Aveiro
Ano 2022

**Sara Cristiana Lopes
Peixoto**

**Efeitos dos nanomateriais no microbioma do solo:
aplicação de nano-agroquímicos e biosólidos**

**Effects of nanomaterials on soil microbiome: nano-
agrochemicals and biosolids applications**

Tese apresentada à Universidade de Aveiro para cumprimento dos requisitos necessários à obtenção do grau de Doutor em Biologia e Ecologia das Alterações Globais, realizada sob a orientação científica da Doutora Isabel da Silva Henriques, Professora auxiliar do Departamento de Ciências da Vida, Faculdade de Ciências e Tecnologia, Universidade de Coimbra e da Doutora Susana Patrícia Mendes Loureiro, Professora auxiliar com agregação do Departamento de Biologia da Universidade de Aveiro.

Apoio financeiro da FCT e do FSE no âmbito do III Quadro Comunitário de Apoio. Bolsa de doutoramento atribuída a Sara Peixoto: SFRH/BD/117738/2016

Dedico este trabalho à minha prima Anabela (*in memorium*).

o júri

presidente

Doutor Carlos Fernandes da Silva
Professor Catedrático, Universidade de Aveiro

vogais

Doutora Paula Maria Lima e Castro
Professora Catedrática, Universidade Católica Portuguesa

Doutora Paula Maria de Melim Vasconcelos de Vitorino Morais
Professor Associado com agregação, Universidade de Coimbra

Doutor Newton Carlos Marcial Gomes
Investigador Principal, Universidade de Aveiro

Doutora Isabel da Silva Henriques (Orientadora)
Professora Auxiliar, Universidade de Coimbra

Doutor Tiago Manuel Ferreira Natal da Luz
Investigador Doutorado, Universidade de Coimbra

agradecimentos

Em primeiro lugar gostaria de agradecer às minhas orientadoras que me receberam amavelmente nos seus respetivos laboratórios e sempre se disponibilizaram para me ajudar a atingir todas as metas propostas. Sem dúvida que a concretização deste trabalho não seria possível sem o vosso enorme contributo científico. Agradeço particularmente à Dr. Isabel Henriques, pela imensa ajuda em todo o trabalho, pela confiança, pelos conselhos e também pelas inúmeras chamadas de atenção que me foi dando durante estes anos. À Dr. Susana Loureiro, que desde o primeiro momento se prontificou a ajudar-me na elaboração do plano de trabalho, pela confiança, ajuda e a todas as oportunidades que me facultou para o desenvolvimento do trabalho. Agradeço ainda, a ambas, por me ensinarem como fazer boa ciência com profissionalismo e muita dedicação ao trabalho.

Também agradeço à Fundação de Ciência e Tecnologia (FCT) pela bolsa atribuída e ao programa doutoral em Biologia e Ecologia das Alterações Globais pela possibilidade de participação em congressos/seminários. Ao departamento de Biologia da Universidade de Aveiro e ao CESAM por terem fornecido todas as condições para a realização da tese.

Gostaria também de agradecer a todos os colegas de laboratório, pertencentes ao microlab e ao applEE, que me foram acompanhando neste processo. Gostaria de agradecer especialmente ao pessoal do microlab, Patrícia Matos, Rita Almeida, Rafael Tavares, Isabel Silva, Frederico Leitão, Cristina Torcato e Marta Alves, pela paciência, ajuda no laboratório, pela amizade e por todos os momentos de convívio. Também deixo um agradecimento ao pessoal do applEE: Rui Morgado, Marija Prodana, Joana Neves, Violeta Ferreira, Catarina Malheiro e Évila Damasceno, pela ajuda, pela disponibilidade e por demonstrarem o quão bom é trabalhar em equipa.

Às amigas de sempre pelo apoio incondicional e que mesmo à distância estiveram sempre presentes, Carla, Inês e Joana. E claro não posso deixar de agradecer novamente às colegas e amigas Rita e Patrícia pela paciência e pelas imensas palavras de apoio e conforto que me foram dando nos momentos mais complicados, tanto ao nível profissional como pessoal.

Por fim gostaria de agradecer à minha família por todo o apoio, carinho e paciência. E um agradecimento especial à minha afilhada Inês pela playlist de música infantil que me obrigou a ouvir durante a fase de escrita desta tese, sem dúvida nunca pensei que o “Fungagá da bicharada” fosse um ótimo estímulo para a concentração!

palavras-chave

Nanopesticidas, nanopartículas de prata sulfatada, comunidade microbiana do solo, *Porcellionides pruinosus*, mesocosmos, avaliação de risco.

resumo

A aplicação frequente de agroquímicos e/ou de biosólidos na agricultura poderá levar a um aumento acentuado da concentração, bem como a possível persistência de nanomateriais (NMs) em solos agrícolas. Alguns destes NMs são caracterizados pelas suas propriedades antimicrobianas, podendo afetar as comunidades microbianas do solo, essenciais na manutenção da função e equilíbrio do ecossistema. Um impacto negativo na qualidade, na fertilidade e nos processos biogeoquímicos do solo, poderá resultar em perdas económicas no sector agrícola. Assim, o objetivo principal desta tese consistiu em avaliar o efeito de NMs no microbioma do solo, e demonstrar a potencialidade dos parâmetros microbiológicos na avaliação do risco ambiental destes NMs. Para isso, foram testados, sob diferentes cenários de exposição, vários NMs com formulações à base de cobre: o nanopesticida comercial Kocide®3000, nanopartículas de óxido de cobre (nCuO) e nanopartículas de hidróxido de cobre [nCu(OH)₂], e à base de prata, com nanopartículas de prata sulfatada (Ag₂S NPs). Nestes cenários, a presença e/ou ausência de elementos edáficos (invertebrados e plantas) essenciais à manutenção do funcionamento do solo, foram consideradas. Transversalmente, o microbioma do solo foi avaliado ao nível estrutural e composicional (Eletroforese em Gel de Gradiente Desnaturante e sequenciação massiva paralela) e funcional (atividade enzimática do solo, perfil fisiológico da comunidade e abundância de grupos bacterianos por métodos cultiváveis e/ou qPCR). Particularmente para os NMs à base de cobre, uma exposição longa do nanopesticida comercial (90 dias), em microcosmos e com concentrações recomendadas para áreas vitícolas, influenciou a estrutura/riqueza da comunidade bacteriana e fúngica do solo e a regulação do ciclo de carbono. Com a inclusão de organismos decompositores (*Porcellionides pruinosus*) neste ensaio, estas diferenças não foram observadas, sugerindo uma atenuação do efeito deste nanopesticida no microbioma do solo. Aquando da simulação de condições mais realistas, a aplicação de diferentes NMs à base de cobre em mesocosmos (na presença de invertebrados e plantas), resultou na redução da abundância de classes bacterianas envolvidas na regulação da matéria orgânica do solo (dependendo da formulação testada), e atividades enzimáticas associadas aos ciclos de enxofre, carbono e azoto, após 28 dias de exposição. Foi também detetado um efeito mais rápido destes NMs no microbioma da rizosfera (14 dias) quando comparado com o efeito no microbioma do solo não rizosférico, sugerindo uma dissolução mais rápida destes NMs devido à ação dos exsudados radiculares. Relativamente aos NMs de prata, os resultados sugerem que a exposição da prata sulfatada afeta o microbioma do solo principalmente ao nível da regulação do ciclo do carbono (redução da atividade da β-glucosidase, e o aumento da abundância de classes bacterianas envolvidas na degradação da celulose). Após análise de previsão de função, a exposição a prata alterou o funcionamento do processo de nitrificação. Verificou-se também o aparecimento de variantes dos genes *amoA* e *nxB* nos solos contaminados, sugerindo assim a substituição de grupos bacterianos que apresentam estes genes. Por fim, este trabalho evidencia a relevância da inclusão do microbioma do solo como um parâmetro essencial na avaliação de risco dos NMs, sob cenários de exposição mais realistas, para uma compreensão mais profunda do impacto destes compostos no ambiente terrestre. Evidencia também a necessidade da implementação de legislação específica para a avaliação de risco ambiental destes compostos.

keywords

Nanopesticides, silver sulfide nanoparticles, soil microbial community, *Porcellionides pruinosus*, indoor mesocosms, risk assessment.

abstract

The frequent application of agrochemicals and/or biosolids in agriculture may lead to an increased concentration and persistence of nanomaterials (NMs) in agricultural soils. Some of these NMs are characterized by their antimicrobial properties, affecting the microbial communities in soil, which are essential in maintaining ecosystem's function and balance. A negative impact of these NMs on soil quality, fertility and biogeochemical processes could result in economic losses to the agricultural sector. Thus, the main aim of this thesis was to evaluate the effect of NMs on the soil microbiome and demonstrate the potential of several microbiological endpoints for the risk assessment of these NMs. For this, several NMs were tested, under different exposure scenarios, with copper-based formulations: the commercial nanopesticide Kocide®3000, copper oxide nanoparticles (nCuO) and copper hydroxide nanoparticles [nCu(OH)₂]; and a silver sulfide nanoparticle (Ag₂S NPs), simulating aging of AgNPs. In these experiments, the presence and/or absence of edaphic elements (invertebrates and plants), essential to the maintenance of soil functioning, was considered. Crosswise, the soil microbiome was evaluated at the structural, compositional (Denaturing Gradient Gel Electrophoresis and massive parallel sequencing), and functional levels (soil enzymatic activity, community-level physiological profiling and abundance of bacterial groups using culture-dependent methods and/or qPCR technique). Particularly for copper-based NMs, a long exposure to the commercial nanopesticide (90 days) in microcosms, using recommended concentrations for vineyard areas, influenced the structure/richness of the soil bacterial and fungal communities and the regulation of the carbon cycle. With the inclusion of decomposer organisms (*Porcellionides pruinosus*), these differences were not observed, suggesting an attenuated effect of this nanopesticide on the soil microbiome. Simulating more realistic conditions, the application of different copper-based NMs in mesocosms (in the presence of plants and invertebrates), resulted in a reduced abundance of bacterial classes involved in the regulation of soil organic matter and in the nitrogen cycle (depending on the tested formulation), and enzymatic activities associated with the sulfur, carbon and nitrogen cycles, after 28 days of exposure. Also, an earlier effect of these NMs in the rhizosphere microbiome (14 days) was detected compared to the effect on the non-rhizosphere soil microbiome, suggesting a faster dissolution of these NMs resulting from the root exudates activity. Regarding silver NMs, the results suggest that the exposure to Ag₂S NPs affect the soil microbiome involved in the regulation of the carbon cycle (reduced β-glucosidase activity, and increased abundance of bacterial classes involved in the degradation of cellulose). The function prediction analysis revealed that silver exposure changes the functioning of the nitrification process. It was also verified the emergence of variants of genes *amoA* and *nxrB* in silver-treated soils, suggesting the replacement of bacterial groups that comprise these genes. Finally, this work highlights the relevance of including the soil microbiome as an essential endpoint in the risk assessment of NMs, using a more realistic exposure scenario, for a deeper understanding of the impact of these compounds on the terrestrial environment. This work also highlights the need for specific regulation in the risk assessment of these compounds in the environment.

Table of Contents

Table of Contents

<i>List of Figures</i>	vi
<i>List of Tables</i>	xiv
<i>List of Abbreviations</i>	xviii
CHAPTER 1: GENERAL INTRODUCTION	
<i>1.Nanomaterials</i>	3
1.1. Life cycle of nano-enabled products and release into the environment	5
1.2. Metal-based nanomaterials released intentionally in soils	6
1.3. Metal-based nanomaterials released unintentionally in soils	8
<i>2.Metal-based nanomaterials in agroecosystem</i>	9
2.1. Concentrations of metallic nanomaterials in the terrestrial compartment....	9
2.2. Transformations of metal-based nanomaterials in soils	11
2.3. Fate of metal-based nanomaterials in soils.....	13
<i>3.Bioavailability and toxicity of metal-based nanomaterials in soils</i>	14
3.1. Toxicity mechanisms of metal-based nanomaterials to Bacteria and Fungi	15
<i>4.Impact of metal nanomaterials in soil biota</i>	17
4.1. Soil microbiome	17
4.2. Soil microbiome in the presence of plants and invertebrates	26
4.2.1. Model or potential model organisms in soil ecotoxicology and their relation with soil microbiome.....	26
<i>5.Soil microbiome as an endpoint in the Environment Risk Assessment (ERA): current knowledge gaps</i>	29
<i>6.References</i>	31
CHAPTER 2: HYPOTHESES, GOALS AND OUTLINE OF THIS THESIS	
<i>1.Hypotheses</i>	45
<i>2.Goals</i>	46
<i>3.Outline of this thesis</i>	47
CHAPTER 3: LONG-TERM EFFECTS OF $\text{Cu}(\text{OH})_2$ NANOPESTICIDE EXPOSURE ON SOIL MICROBIAL COMMUNITIES	
<i>1.Introduction</i>	54
<i>2.Material and methods</i>	56
2.1. Experimental set up	56
2.2. Copper dissolution analysis	57
2.3. Assessment of bacterial growth and heterotrophic plate counts (HPC)	58
2.4. Molecular analysis	58
2.4.1. Total DNA extraction.....	58
2.4.2. PCR reaction	58
2.4.3. Denaturing Gradient Gel Electrophoresis	59
2.5. Assessment of microbial activity.....	60
2.5.1. Community level physiological profiling (CLPP)	60
2.5.2. Enzymatic activity.....	61
2.6. Statistical analysis	61
<i>3.Results</i>	62
3.1. Copper in soil porewater.....	62
3.2. Structural effects of $\text{Cu}(\text{OH})_2$ nanopesticide on soil microbial community	64
3.2.1. Assessment of heterotrophic bacterial counts	64
3.2.2. Soil bacterial communities	65

3.2.3. Soil fungal communities.....	69
3.3. Effects of Cu(OH) ₂ nanopesticide on microbial activity.....	71
3.3.1. Community level physiological profiling (CLPP).....	71
3.3.2. Enzymatic activity.....	73
4. Discussion.....	76
5. Conclusions.....	80
6. Acknowledgements.....	81
7. References.....	81
8. Supplementary data.....	87
8.1. List of Figures.....	87
8.2. List of Tables.....	90

CHAPTER 4: RESPONSES OF SOIL MICROBIOME TO COPPER-BASED NANOMATERIALS FOR AGRICULTURAL APPLICATIONS

<i>Abstract</i>	97
<i>1. Introduction</i>	98
<i>2. Material and Methods</i>	100
2.1. Copper-based nanoparticles characterization.....	100
2.2. Copper exposure.....	101
2.3. Chemical extraction test to assess soil-bound ionic Cu.....	102
2.4. Culture-dependent analysis of soil microbiome.....	102
2.5. Enzymatic activity.....	103
2.6. Community level physiological profiling.....	103
2.7. Microbiome analysis.....	103
2.8. Statistical analysis.....	104
<i>3. Results</i>	104
3.1. General trends in extractable Cu for amended soil.....	104
3.2. Effects on culturable bacteria.....	106
3.3. Treatment effects on enzymatic activity.....	106
3.4. Effects on carbon substrates utilization.....	108
3.5. Metagenomic analysis.....	111
3.6. Functional prediction.....	117
<i>4. Discussion</i>	120
4.1. Pattern of bound ionic Cu in soil.....	120
4.2. Copper exposure affects the soil microbiome activity and function.....	120
4.3. Copper exposure affects the soil microbiome structure and composition.....	122
<i>5. Conclusions</i>	125
<i>6. Acknowledgements</i>	126
<i>7. References</i>	126
<i>8. Supplementary material</i>	133
8.1. List of Figures.....	133
8.2. List of Tables.....	135

CHAPTER 5: COPPER-BASED NANOMATERIALS ALTER THE RHIZOSPHERE BACTERIAL COMMUNITY

<i>Abstract</i>	147
<i>1. Introduction</i>	148
<i>2. Material and Methods</i>	150
2.1. Copper-based nanoparticles exposure.....	150
2.2. PCR-DGGE analysis.....	151
2.3. Enzymatic activity.....	151

2.4. Statistical analysis	152
3. <i>Results</i>	152
3.1. Effects of copper on soil bacterial community structure and diversity	152
3.2. Effects of copper on enzymatic activity	156
4. <i>Discussion</i>	159
4.1. Effects of copper-based nanomaterials on soil bacterial rhizosphere.....	159
4.2. Distinct effects of copper-based nanomaterials on soil bacterial rhizosphere and bulk	161
4.3. The environmental and agronomic relevance.....	162
5. <i>Conclusion</i>	163
6. <i>Acknowledgements</i>	164
7. <i>References</i>	164
8. <i>Supplementary material</i>	169
8.1. List of Figures.....	169
8.2. List of Tables	170

CHAPTER 6: IMPACT OF Ag₂S NPS ON SOIL BACTERIAL COMMUNITY – A TERRESTRIAL MESOCOSM APPROACH

<i>Abstract</i>	175
1. <i>Introduction</i>	176
2. <i>Material and methods</i>	178
2.1. Silver exposure	178
2.2. Mesocosm setup	179
2.3. Soil chemical analysis	180
2.4. Culture-dependent analysis of SBC.....	181
2.5. Enzymatic activity	182
2.6. Community level physiological profiling (CLPP)	182
2.7. PCR-DGGE	183
2.8. Statistical analysis	184
3. <i>Results</i>	185
3.1. Effects on culturable bacteria	186
3.2. Treatment effects on enzymatic activity.....	187
3.3. Effects on carbon source consumption.....	188
3.4. Effects on SBC structure and diversity.....	190
3.5. Relationship between structure and functions of SBC	192
4. <i>Discussion</i>	193
4.1. Effects of silver on SBC function.....	193
4.2. Effects of silver on SBC structure and diversity	197
4.3. Environmental relevance and integrative analysis between structure and functional levels of SBC.....	198
5. <i>Conclusions</i>	198
6. <i>Acknowledgements</i>	199
7. <i>References</i>	199
8. <i>Supplementary material</i>	205
8.1. Nanoparticle's characterization	205
8.2. List of Figures.....	205
8.3. List of Tables	207

CHAPTER 7: THE IMPACT OF SILVER SULFIDE NANOPARTICLES AND SILVER IONS IN SOIL MICROBIOME

<i>Abstract</i>	213
-----------------------	-----

<i>1.Introduction</i>	214
<i>2.Materials and Methods</i>	216
2.1. Experimental design	216
2.2. Molecular analysis of soil microbiome	217
2.2.1. DNA extraction and Illumina high-throughput sequencing	217
2.2.1.1. In silico metagenome analysis	217
2.2.2. Real-time polymerase chain reaction (qPCR).....	218
2.2.3. Diversity of <i>amoA</i> and <i>nxrB</i> gene variants.....	218
2.3. Statistical analysis	219
<i>3.Results</i>	220
3.1. Effects of Ag ₂ S NPs and AgNO ₃ on soil microbiome.....	220
3.1.1. Effect on soil microbiome after 14 days of exposure	220
3.1.2. Effect on soil microbiome after 28 days of exposure	229
3.2. Abundance and diversity of ammonia-oxidizing bacteria (AOB) and nitrite-oxidizing bacteria (NOB)	231
<i>4.Discussion</i>	234
4.1. Silver exposure affects the soil microbiome structure and composition..	235
4.2. Silver exposure affects the soil microbiome function	237
4.2.1. Silver exposure affects the nitrification process	238
<i>5.Conclusions</i>	240
<i>6.Acknowledgements</i>	240
<i>7.References</i>	241
<i>8.Supplementary material</i>	248
8.1. List of Figures.....	248
8.2. List of Tables	254
CHAPTER 8: GENERAL DISCUSSION AND CONCLUDING REMARKS	
<i>1.General Discussion</i>	265
H _I : Metal-based ENMs induce changes in soil microbiome	265
H _{II} : Distinct formulations of ENMs distinctly affect the soil microbiome function, structure and composition.....	271
H _{III} : The presence of invertebrates influences the effects of metal-based ENMs on soil microbiome	272
H _{IV} : Metal-based ENMs affect the soil rhizosphere bacterial community.....	273
H _V : The metal-based ENMs change the nitrogen cycle	274
<i>2.Final remarks and future directions</i>	276
<i>3.References</i>	279
ANNEXES:	
A1. Copyright Licence Terms and Conditions for Figures in Chapter 1.	A1

List of Figures

CHAPTER 1: GENERAL INTRODUCTION

Figure 1. Metal-based engineered nanomaterials production volume (Mg) (Values were obtained from the average of global production volume and then transformed in Log-scale). Adapted from: Janković and Plata, 2019.....5

Figure 2. Scheme of ENMs sources and release routes in the terrestrial environment. Green arrows indicate release to the soil (unintentionally release) and red arrows indicate ENMs release pathways ending up in waste management or end-of-life treatments, from where release in soil can also occur. Adapted from: Loureiro et al., 2018.6

Figure 3. Predicted environmental concentrations in Europe regarding the presence of AgNPs (tonnes Ag released per km²) (Kuenen *et al.*, 2020) or copper (mg Cu kg⁻¹ vineyards soil) (Ballabio *et al.*, 2018).....11

Figure 4. Conceptual diagram of the major transformations that engineered nanomaterials (ENMs) might undergo in the environment. In figure was described the physical, chemical and biological transformations. Based on: Lowry *et al.*, 2012.13

Figure 5. Schematic overview of the main fate-determining parameters of ENMs in soil-water systems. 1. ENMs leaching from biosolids, 2. Colloid generation, 3. Homoaggregation, 4. Fragmentation, 5. Sedimentation, 6. Heteroaggregation, 7. Size exclusion, 8. Straining, 9. Deposition, 10. Convective transport, and 11. Bioturbation. 12. Biodegradation and/or bioaccumulation. Adapted from: Cornelis *et al.* 2014.14

Figure 6. Nanoparticles and ions mode of action in (A) bacteria and (B) fungi cells. 1. Disruption of cell wall and pore formation, 2. Passage through outer membrane porin, 3. DNA damage, 4. Increase of intracellular reactive oxygen species (ROS) concentration, 5. Inhibition of protein synthesis, 6. Uncoupling of respiratory chain, and 7. Mitochondria damage. Adapted from: McNeilly *et al.*, 2021 and Lakshmeesha *et al.*, 2020.16

Figure 7. Schematic of three biogeochemical cycles of carbon, nitrogen and phosphorous in terrestrial ecosystems. Arrows show the transfer of phosphorous - P (blue), carbon - C (orange), and nitrogen - N (green) between ecosystem compartment. Ecological processes in bold indicate the mediation by Bacteria. In scheme: ECM: ectomycorrhizas (fungi). Adapted from: Lladó et al., 2017.19

Figure 8. Model or potential model organisms used in ecotoxicological assays. In figure: A: wheat (*Triticum* spp.); B: earthworm (*Eisenia* spp.); C: terrestrial isopods (*Porcellionides pruinosus*); and D: mealworms (*Tenebrio molitor*).27

CHAPTER 2: HYPOTHESES, GOALS AND OUTLINE OF THIS THESIS

Figure 1. The scheme of the experimental approaches used in Chapters 3 to 7 to investigate effects of different metallic nanomaterials on soil microbiome. In figure, H (I to V) and G (I to VI) refers the hypothesis and goals of this thesis, respectively.49

CHAPTER 3: LONG-TERM EFFECTS OF $\text{Cu}(\text{OH})_2$ NANOPESTICIDE EXPOSURE ON SOIL MICROBIAL COMMUNITIES

Figure 1. The dissolution of $\text{Cu}(\text{OH})_2$ -nanopesticide and $\text{Cu}(\text{OH})_2$ -ionic in soil porewater after 2 and 90 days of exposure, in the absence (A)) or in the presence of *Porcellionides pruinosus* (B)). The data was expressed as $\mu\text{g} (\text{Cu}) \text{L}^{-1}$ of porewater (\pm standard deviation). The soil treatments included the non-exposed soil (CT), soil exposed to $\text{Cu}(\text{OH})_2$ -nanopesticide and soil exposed to $\text{Cu}(\text{OH})_2$ -ionic, at two different concentrations (single and season). Different letters (^{a,b}) indicate statistical significance ($p \leq 0.05$) between treatments and the respective control, using the three-way ANOVA (Tukey HSD).64

Figure 2. Long-term effect, 90 days of exposure of $\text{Cu}(\text{OH})_2$ on soil heterotrophic bacteria count, as measured by CFU g^{-1} soil (\pm standard deviation), in the absence (A) or in the presence of *Porcellionides pruinosus* (B). The soil treatments included the non-exposed soil (CT), soil exposed to $\text{Cu}(\text{OH})_2$ -nanopesticide and to $\text{Cu}(\text{OH})_2$ -ionic, at the season application rate. Different letters (^{a,b}) indicates a statistic significant ($p \leq 0.05$) among the soil treatments and *Porcellionides pruinosus* presence, using the two-way ANOVA (Tukey HSD).65

Figure 3. Principal Coordinates analysis (PCoA) of DGGE profiles representing the structural effects of the nanopesticide and of ionic $\text{Cu}(\text{OH})_2$ on soil bacterial communities in the absence (A)) or in the presence of *Porcellionides pruinosus* (B)). The PCoA was constructed based on Jaccard similarity from DGGE profiling at 90 days of exposure. Soil treatments included the non-exposed soil (CT), soil exposed to $\text{Cu}(\text{OH})_2$ -nanopesticide and to $\text{Cu}(\text{OH})_2$ -ionic, at two different application rates (single or season).66

Figure 4. Principal Coordinates analysis (PCoA) of DGGE profiles representing the structural effects of the nanopesticide and of ionic $\text{Cu}(\text{OH})_2$ on soil fungal communities in the absence (A)) or in the presence of *Porcellionides pruinosus* (B)). The PCoA was constructed based on Jaccard similarity from DGGE profiling at 90 days of exposure. Soil treatments included the non-exposed soil (CT), soil exposed to $\text{Cu}(\text{OH})_2$ -nanopesticide and to $\text{Cu}(\text{OH})_2$ -ionic, at two different application rates (single or season).....70

Figure 5. Average Well Color Development - AWCD representing the carbon consumption ($n=5 \pm$ standard deviation) of the soil community exposed to the nanopesticide and of ionic $\text{Cu}(\text{OH})_2$, in the absence (A)) or in the presence of *Porcellionides pruinosus* (B)). The soil treatments included the non-exposed soil (CT), soil exposed to $\text{Cu}(\text{OH})_2$ -nanopesticide and to $\text{Cu}(\text{OH})_2$ -ionic, at two different application rates (single or season).72

Figure 6. Substrate Average Well Color Development (SAWCD) index representing the functional effects of the nanopesticide and of ionic $\text{Cu}(\text{OH})_2$ on soil microbiome in the absence (A) or in the presence of *Porcellionides pruinosus* (B). The SAWCD was calculated based on 144 h from Ecoplate incubate at 90 days of exposure. Values are presented per mean of 5 replicates per treatment. The soil treatments included the non-exposed soil (CT), soil exposed to $\text{Cu}(\text{OH})_2$ -nanopesticide and to $\text{Cu}(\text{OH})_2$ -ionic, two different application rates (single or season).73

Figure 7. Principal Coordinates analysis (PCoA) of soil enzymatic activities representing the functional effects of the nanopesticide and of ionic $\text{Cu}(\text{OH})_2$ on soil microbiome in the absence (A)) or in the presence of *Porcellionides pruinosus* (B)). The PCoA was constructed based on Euclidean distance from soil enzymatic activities at 90 days of exposure. Soil treatments included the non-exposed soil (CT), soil exposed to $\text{Cu}(\text{OH})_2$ -nanopesticide and to $\text{Cu}(\text{OH})_2$ -ionic, at two different application rates (single or season). The

vectors represent each enzymatic activity tested and were constructed based on Pearson correlation ($R > 0.2$).75

Figure S1. The electrophoresis of DGGE gel, of the non-exposed soil bacterial community (A) and fungal community (B) in the absence or in the presence of *Porcellionides pruinosus*, after 90 days of exposure or initial fungal community – day 2 (B). Lane Mk refers to DGGE marker for bacterial communities (A): I - RAI 70; II - RAN 60; III - RAI 3; IV - RAI 43; V - RAN 18; VI - RAN 12; VII - RAN 140; VIII - RAI 76 (Henriques et al., 2004). Also, Lane Sr refers to sample r5 from non-exposed soils in the presence of *Porcellionides pruinosus*, used as a reference position on the DGGE gel (B).87

Figure S2. Soil enzymatic activities representing the functional effects of the $\text{Cu}(\text{OH})_2$ -nanopesticide and $\text{Cu}(\text{OH})_2$ -ionic, at two different application (single or season) [dehydrogenase - DHA (A and B), β -glucosidase - β G (C and D), arylsulfatase - AS (E and F), acid phosphatase -AP (G and H) and urease - UA activities (I and J)]. These effects were evaluated for soils in the absence (A C, E, G and I) or in the presence of *Porcellionides pruinosus* (B, D, F, H and J). The data is represented by the mean \pm standard deviation. The soil treatments included the non-exposed soil (CT), soil exposed to $\text{Cu}(\text{OH})_2$ - nanopesticide and to $\text{Cu}(\text{OH})_2$ - ionic, at two different concentrations (single or season application). Asterisks (*) indicate a statistically significant difference ($p < 0.05$) between nanopesticide or ionic $\text{Cu}(\text{OH})_2$ treatments towards the respective control.88

Figure S3. Principal Coordinates Analysis (PCoA) of soil enzymatic activities representing the functional effects of the nanopesticide and of ionic $\text{Cu}(\text{OH})_2$ on soil microbiome. The PCoA was constructed based on Euclidean distance from soil enzymatic activities, at 90 days of exposure. Soil treatments included the non-exposed soil (CT), soil exposed to $\text{Cu}(\text{OH})_2$ -nanopesticide and to $\text{Cu}(\text{OH})_2$ -ionic, at two different concentrations (single or season application). These treatments also included the absence or in the presence of *P. pruinosus*.89

CHAPTER 4: RESPONSES OF SOIL MICROBIOME TO COPPER-BASED NANOMATERIALS FOR AGRICULTURAL APPLICATIONS

Figure 1. Diethylenetriaminepentaacetic acid (DTPA) extractable Cu in Lufa 2.2 treated with $\text{Cu}(\text{OH})_2$ -i, Kocide[®]3000, $\text{nCu}(\text{OH})_2$, or nCuO , after day -2 (soil-spiking), day 0 (input soil organisms), day 14 and day 28. The data was expressed as $\text{mg}(\text{Cu}) \text{kg}^{-1}$ of soil [average ($n = 3$) \pm standard deviation]. The DTPA extractable Cu in non-treated soil (CT) was measured in all soil treatments and presented values below the detection level ($< \text{LOD}$). Asterisks (*) indicate significant differences between Cu-treated soil towards the $\text{Cu}(\text{OH})_2$ -i treated soil (one-way ANOVA, Tukey HSD method; $p < 0.05$), for each sampling time.105

Figure 2. Average colony forming units (CFUs) in non-treated Lufa 2.2 soil (CT) and in soil spiked with $\text{Cu}(\text{OH})_2$ -i, Kocide[®]3000, $\text{nCu}(\text{OH})_2$, or nCuO , sampled at day 0 and 28. Heterotrophic bacteria (HB) were counted in nutrient agar medium and P-solubilizing bacteria in National Botanical Research Institute Phosphate (NBRIP) medium (B). Different letters (^{a,b,c}) indicate significant differences regarding the time of exposure and treatments for each culture media, using the three-way ANOVA (Tukey HSD method; $p < 0.05$).106

Figure 3. Enzymatic activity measured in Lufa 2.2 non-treated soil (CT) and soil spiked with $\text{Cu}(\text{OH})_2$ -i, Kocide[®]3000, $\text{nCu}(\text{OH})_2$ or nCuO , and sampled at day -2, 0, 14 and 28. The data represent the average enzymatic activity ($n=3 \pm$ standard deviation) of dehydrogenase (A), arylsulfatase (B), β -glucosidase (C), acid phosphatase (D), and urease (E).

Asterisks (*) indicate significant differences between Cu-treated samples towards the CT soil (two-way ANOVA, Tukey HSD method; $p < 0.05$), for each sampling time. 108

Figure 4. Community-level physiological profiles (CLPP) measured in non-treated Lufa 2.2 soil (CT) or spiked with $\text{Cu}(\text{OH})_2\text{-i}$, Kocide[®]3000, $\text{nCu}(\text{OH})_2$ or nCuO , sampled at day 0, 14 and 28. The data represent the mean ($n=3 \pm$ standard deviation) of area under curve (AUC). The AUC was calculated based on the trapezoidal integration function. Asterisks (*) indicate significant differences ($p < 0.05$) between Cu-treated soils and CT soil (two-way ANOVA, Tukey HSD test), for each sampling time. 109

Figure 5. Substrate average well colour development (SAWCD) measured in Lufa 2.2 soil spiked with $\text{Cu}(\text{OH})_2\text{-i}$, Kocide[®]3000, $\text{nCu}(\text{OH})_2$ or nCuO , sampled at days 0, 14 and 28. Non-treated soil (CT) was included. The data represent the mean ($n=3$) of SAWCD index. Asterisks (*) indicate significant differences ($p < 0.05$) between treated soils and respective CT soil (two-way ANOVA, Tukey HSD method), for each sampling time. 110

Figure 6. Soil microbiome structure from non-treated soil (CT) and soil treated to $\text{Cu}(\text{OH})_2\text{-i}$, Kocide[®]3000, $\text{nCu}(\text{OH})_2$, or nCuO , after 0 and 28 days of exposure. Cluster analysis (A) and principal coordinate analysis (B - day 0 and C - day 28) were constructed based on Bray-Curtis similarity after square root transformation on OTU abundance. 112

Figure 7. Relative abundance (%) of classes and unidentified classes affiliated with phylum or kingdom in non-treated Lufa 2.2. soil (CT) or in spiked soil with $50 \text{ mg (Cu) kg}^{-1}$ soil of $\text{Cu}(\text{OH})_2\text{-i}$, Kocide[®]3000, $\text{nCu}(\text{OH})_2$, or nCuO , after 0 (A) and 28 (B) days of exposure. Data represent the average of three replicates per treatment. Asterisks (*) indicate significant differences between copper-treated samples and the respective control (CT) ($p < 0.05$; Tukey HSD). 113

Figure 8. Genera and unidentified genera affiliated with family, class or kingdom significantly affected by $50 \text{ mg (Cu) kg}^{-1}$ soil of copper formulations [$\text{Cu}(\text{OH})_2\text{-i}$, Kocide[®]3000, $\text{nCu}(\text{OH})_2$, or nCuO] (one-way ANOVA; $p < 0.05$), after day 0 and 28 of exposure. The direction (positive or negative variation) and the magnitude of the responses are indicated on the x-axis, which shows the percentage of variation to the control (CT). Data represent the average of three replicates per treatment. Bold letters indicate the most abundant genera (relative abundance $> 1\%$). 114

Figure S1. Diversity of carbon substrates used by the microbial community. Soil treatments included the non-treated soils (CT) and spiked soils with $\text{Cu}(\text{OH})_2\text{-i}$, Kocide[®]3000, $\text{nCu}(\text{OH})_2$, or nCuO , based on optical density (570 nm, read=168h) of Biolog[®]Ecoplate data after 28 days of exposure. Different letters (^{a,b,c}) indicate significant differences ($p < 0.05$) regarding the soil treatments, using the one-way ANOVA (Tukey HSD). 133

Figure S2. Rarefaction curves of observed OTUs as function of the number of reads (sequences per sample). Results of three replicates are presented for control soil (CT) and copper-treated soil [$50 \text{ mg (Cu) kg}^{-1}$ soil of Kocide[®]3000, nCuO , $\text{nCu}(\text{OH})_2$ and $\text{Cu}(\text{OH})_2\text{-i}$]. The soil sampling was done at day 0 (A) and day 28 (B). 134

CHAPTER 5: COPPER-BASED NANOMATERIALS ALTER THE RHIZOSPHERE BACTERIAL COMMUNITY

Figure 1. Denaturing gradient gel electrophoresis (DGGE) analysis, targeting the bacterial community (16S rRNA gene) from rhizosphere (A, B, and C) or bulk (D, E, and F) soil. Soil treatments included: non-treated soil (CT), and soil treated with 50 mg (Cu)

kg⁻¹ soil as Cu(OH)₂-i, Kocide[®]3000, nCu(OH)₂, or nCuO, after 14 (■ blue symbols) and 28 (■ green symbols) days of exposure. Clustering analysis (A and D) and Principal coordinate analysis (PCoA) (B, C, E, and F), were constructed based on Jaccard similarity of DGGE relative abundance data (n=3).....154

Figure 2. Richness (number of bands; S), Shannon-Wiener (diversity index; H') and Pielou's (evenness index; J') indexes calculated for bacterial communities from rhizosphere (A, C and E) or bulk soil (B, D, and F). Soil treatments included the non-exposed or exposed to Cu(OH)₂-i, or Kocide[®]3000, or nCuO or nCu(OH)₂, after day 14 (■ blue symbols) or 28 (■ green symbols). Values are presented per mean ± standard deviation. Asterisk (*) indicates a significant difference between soil treatments and respective control (one-way ANOVA, p<0.05; Tukey HSD).....156

Figure 3. Enzymatic activity measured in Lufa 2.2 non-exposed soil (CT) and in soil spiked with Cu(OH)₂-i, Kocide[®]3000, nCu(OH)₂, or nCuO, and sampled from rhizosphere at day 14 and 28. The data represent the average enzymatic activity (n=3 ± standard deviation) of dehydrogenase (A), β-glucosidase (B), arylsulfatase (C), acid phosphatase (D) and urease (E). Asterisks (*) indicate significant differences between exposed samples towards the respective control (one-way ANOVA, Tukey HSD method; p<0.05), for each sampling point158

Figure S1. Soil enzymatic activity measured in rhizosphere and bulk soil, sampled at day -2, 0, 14 and 28. Soil treatments included the non-exposed soil (CT) and soil spiked with Cu(OH)₂-i, or Kocide[®]3000, or nCu(OH)₂, or nCuO. The data represent the average of enzymatic activity (n=3 ± standard deviation) of dehydrogenase (DHA), arylsulfatase (AS), β-glucosidase (βG) acid phosphatase (AP) and urease (UA) activities. The vectors represent each enzymatic activity tested.169

CHAPTER 6: IMPACT OF Ag₂S NPS ON SOIL BACTERIAL COMMUNITY – A TERRESTRIAL MESOCOSM APPROACH

Figure 1. Scheme of the temporal procedures during the 28 days of the mesocosm experiment.....180

Figure 2. Silver content in soils (A) and silver dissolution into soil porewater (B), after 0 (2 days after soil spiking) and 28 days of exposure. The data was expressed as mg (Ag) kg⁻¹ of soil (A) and as μg (Ag) L⁻¹ of porewater [average (n=3) ± standard deviation]. The treatments included: the non-exposed soil (CT), soil exposed to Ag₂S NPs and soil exposed to AgNO₃. Different letters (a,b) indicate statistical significance (p<0.05) between soil treatments and the time of exposure, using the two-way ANOVA (Tukey post-hoc test, p<0.05).....186

Figure 3. Soil colony forming units (CFUs) measured in Lufa 2.2 soil, sampled at day 0 and 28 from the mesocosm experiment, previously spiked with AgNO₃ and Ag₂S NPs. CFUs are presented as % of variation on CFUs (Log₁₀ g⁻¹ soil) (± standard deviation) from the respective control (non-exposed soil), n=3. Heterotrophic bacteria in nutrient agar (NA) medium (A); and P-solubilizing bacteria in National Botanical Research Institute Phosphate (NBRIP) medium (B). The grey bars represent the soil samples collected at the beginning of the mesocosm soil experiment (day 0), and the white bars represent samples after 28 days. Asterisks (*) indicate significant differences using two-way ANOVA (Dunnnett's post-hoc test), p<0.05) relative to the respective control.186

Figure 4. Soil enzymatic activity measured in Lufa 2.2 soil, sampled at days 0, 14 and 28 from the mesocosm experiment, previously spiked with AgNO₃ and Ag₂S NPs. Also, the non-exposed soil was included in this experiment (CT). The data represent the mean (n=3) of enzymatic activity (± standard deviation) of dehydrogenase (A), β-glucosidase (B),

acid phosphatase (C) and arylsulfatase (D) activities. Different letters (a, b) indicate a significant difference using two-way ANOVA (Tukey post-hoc test, $p < 0.05$), among treatments.188

Figure 5. Community-level and physiological profile (CLPP) measured in Lufa 2.2 soil, sampled at days 0, 14 and 28 from the mesocosm experiment, previously spiked with AgNO_3 and Ag_2S NPs. For further comparison the non-exposed soil (CT) was included. The area under the curve (AUC) was calculated based on a trapezoidal integration function (A) over time; (B) after day 28, the Pyruvic acid methyl ester, β -methyl-D-glucoside, and L-arginine consumption; and (C) substrate average well colour development (SAWCD) after 14 and 28 days of exposure. The data represent the mean ($n=3$) of AUC (\pm standard deviation). Letters (^{a, b}) represent significant differences using two-way ANOVA (Tukey HSD, $p < 0.05$.) between treatments.189

Figure 6. Denaturing gradient gel electrophoresis (DGGE) analysis of the V3 region of the 16S rRNA gene amplified from SBC from non-exposed soil (CT), soil exposed to Ag_2S NPs and AgNO_3 , after 0, 14 and 28 days of exposure. Cluster analysis (A); and Principal component analysis (PCoA) (B), were constructed based on Bray-Curtis similarity after square root transformation of DGGE relative abundance data ($n=3$).....190

Figure 7. Principal coordinates analysis (PCoA) ordinations based on Bray-Curtis similarity showing the spatial distribution of SBC structures among the different soil treatments: non-exposed soil (CT) and exposed soil to Ag_2S NPs or AgNO_3 ($n=3$), after 28 days of exposure. The vectors represent a functional variable (Black: enzymatic activity and CLPP) or a chemical variable (Red: silver ion presence (Figure 2) in soil pore-water) that presented a correlation ≥ 0.6 with SBC structure: AP - Acid Phosphatase; β G - β -Glucosidase; HB - Heterotrophic bacteria; P-SB - Phosphatase-Solubilizing Bacteria.192

Figure S1. Characterization of Ag_2S NPs colloids, A) TEM image with scale bar 200 nm); B) size distribution by analysis of the TEM images (20.4 ± 11.9 nm; 613 nanoparticles analyzed); C) normalized UV-vis spectra in colloidal dispersion (mili-Q water).....205

Figure S2. Clustering analysis (A and C) and Principal Coordinate Analysis (PCoA) (B and D) of SBC from upper layers [S1 (0-4 cm) and S2 (4-6 cm)] and bottom layers [S3 (10-12 cm) and S4 (12-16 cm)] of mesocosm columns with control soil (CT), soil spiked with Ag_2S NPs and soil spiked with AgNO_3206

CHAPTER 7: THE IMPACT OF SILVER SULFIDE NANOPARTICLES AND SILVER IONS IN SOIL MICROBIOME

Figure 1. Structural changes in soil microbiome exposed to Ag_2S NPs or AgNO_3 , represented in cluster analysis [A and B] and Principal Coordinate analysis (PCoA) [C and D]. Results of three replicates ($n=3$) are presented for non-exposed soil (CT) and for each treatment [$10 \text{ mg (Ag) kg}^{-1}$ soil of AgNO_3 and Ag_2S NPs]. The soil sampling was done at day 14 [A and C] and day 28 [B and D].221

Figure 2. Relative abundance of 15 most abundant classes of soil microbiome, after day 14 (A) and 28 (B). Results of three replicates (R1, R2 and R3) are presented for non-exposed soil (CT) and for each silver treatment [$10 \text{ mg (Ag) kg}^{-1}$ soil of AgNO_3 and Ag_2S NPs]. Asterisks (*) and bold names (classes) indicate significant differences towards the respective CT, for each sampling time (one-way ANOVA, $p < 0.05$; Tukey HSD).223

Figure 3. Relative abundance of the genera and unidentified genera affiliated with family or class significantly ($p < 0.05$) affected by Ag_2S NPs or AgNO_3 treatments, after 14 (A) or 28 (B) days of exposure. Average of three replicates ($n=3$) is presented for control (CT) and for each silver treatment [$10 \text{ mg (Ag) kg}^{-1}$ soil of AgNO_3 and Ag_2S NPs]. Asterisk (*) indicates a significant difference between soil treatments and control samples, for each sampling time. Bold affiliation (genera or unidentified genera affiliated with family or class) name indicates a significant difference among silver forms (AgNO_3 vs. Ag_2S NPs), for each sampling time (one-way ANOVA, $p < 0.05$; Tukey HSD).224

Figure 4. Relative abundance of the most represented OTUs (30 most abundant per treatment) in exposed soil at both 14 and 28 days of exposure. The color code represents the relative OTU abundance (%) in each sample. Asterisks (*) indicate significant differences towards the respective control (CT), for each sampling time (two-way ANOVA, $p < 0.05$; Tukey HSD). Bold genera names indicate significant differences between silver treatments (AgNO_3 vs. Ag_2S NPs), for each sampling time (two-way ANOVA, $p < 0.05$; Tukey HSD).226

Figure 5. Copy numbers per gram of soil of 16S rRNA gene (A), and the ratio of *amoA*/16S rRNA gene (B), and *nxB*/16S rRNA gene (C) as determined by qPCR. Values represent a mean \pm standard deviation of three replicates. Results are presented for non-treated soil (CT) and for soil treated with $10 \text{ mg (Ag) kg}^{-1}$ soil of AgNO_3 or Ag_2S NPs. The soil sampling was done at days 14 and 28. Different letters (a, b) indicate a significant difference among soil treatments for each sampling time (two-way ANOVA, $p < 0.05$; Tukey HSD).232

Figure 6. Clustering analysis of DGGE profiles of the *nxB* (A) and *amoA* (B) genes amplified from Lufa 2.2 soil (CT) and soil exposed to $10 \text{ mg (Ag) kg}^{-1}$ soil of Ag_2S NPs or AgNO_3 . Soil sampling was done at days 14 and 28. The cluster was constructed based on Dice similarity.234

Figure S1. Rarefaction curves of OTUs as function of the number of reads. Results of three replicates are presented for control (CT) and for each treatment [$10 \text{ mg (Ag) kg}^{-1}$ soil of AgNO_3 and Ag_2S NPs]. The soil sampling was done at day 14 (A) and day 28 (B). The sequencing effort reaches an average of 53117.248

Figure S2. Nitrogen metabolism of soil microbiome exposed to $10 \text{ mg (Ag) kg}^{-1}$ of Ag_2S NPs or AgNO_3 . The data was based on predicted relative abundance of nitrogen-related genes. Different colors (■ no differences; ■ differences at day 14; and ■ differences at day 28) represent significant differences in the silver forms towards the respective control (two-way ANOVA; Tukey HSD; $p < 0.05$). The arrows indicate the significant increased (\uparrow) or decreased (\downarrow) in the relative abundance of genes between silver treatments (blue: Ag_2S NPs; red: AgNO_3) toward the respective control (two-way ANOVA; Tukey HSD; $p < 0.05$).249

Figure S3. Melting curves for *nxB* gene amplified from Lufa 2.2 soil (CT), and soils exposed to 10 mg kg^{-1} of Ag_2S NPs or AgNO_3 , after 14 and 28 days of exposure.250

Figure S4. Melting curves for *amoA* gene amplified from Lufa 2.2 soil (CT), soils exposed to 10 mg kg^{-1} of Ag_2S NPs or AgNO_3 , after 14 and 28 days of exposure.251

Figure S5. Multiple Sequence Alignments of *nxB* sequences, using Clustal Omega software. Treatments represented the soil microbiome exposed to $10 \text{ mg (Ag) kg}^{-1}$ soil

of Ag₂S NPs or AgNO₃ or non-exposed (CT), at 14 and 28 days of exposure. Grey color indicates differences in nucleotides compared between treatments.....252

Figure S6. Multiple sequence alignment of *amoA* variants, using Clustal Omega software. A representative of each variant per treatment was included. Treatments include soil exposed for 14 and 28 days to 10 mg (Ag) kg⁻¹ soil Ag₂S NPs or AgNO₃ or non-exposed (CT). Grey color indicates differences in nucleotides compared between treatments.253

CHAPTER 8: GENERAL DISCUSSION AND CONCLUDING REMARKS

Figure 1. Nitrogen metabolism of soil microbiome exposed to silver- [Ag₂S NPs or AgNO₃ at 10 mg (Ag) kg⁻¹] or copper- based NMs [Kocide[®]3000, nCu(OH)₂, nCuO, or Cu(OH)₂-i at 50 mg (Cu) kg⁻¹]. The data was only based on predicted relative abundance of nitrogen-related genes, previously described in Chapter 4 and Chapter 7, using the Piphillin software. Green and blue arrows indicate the steps in the nitrogen cycle significantly affected by silver- or copper- based NMs exposure, respectively. Gray arrows indicate the steps in the nitrogen cycle not affected by NMs exposure.....275

List of Tables

CHAPTER 1: GENERAL INTRODUCTION

Table 1. Properties and applications of different nanoparticles. Adapted from: EPA, 2017.	4
Table 2. Some ENMs-based agrochemicals commercially available.	7
Table 3. Effects of silver (Ag) and/or copper (Cu) based ENMs/ENPs in soil microorganisms, under distinct exposure scenarios.	22

CHAPTER 3: LONG-TERM EFFECTS OF $\text{Cu}(\text{OH})_2$ NANOPESTICIDE EXPOSURE ON SOIL MICROBIAL COMMUNITIES

Table 1. The richness (number of bands; S), Shannon-Wiener (diversity index; H') and Pielou's (evenness index; J) indexes of the soil bacterial and fungal communities exposed to $\text{Cu}(\text{OH})_2$ in nanopesticide or ionic form, after 90 days of soil exposure. These effects were assessed in the absence or presence of <i>Porcellionides pruinosus</i> . Values are presented per mean \pm standard deviation. The soil treatments included the non-exposed soil (CT), soil exposed to $\text{Cu}(\text{OH})_2$ -nanopesticide and to $\text{Cu}(\text{OH})_2$ -ionic, at two different concentrations (single and season application).	68
Table S1. Number of invertebrates, <i>Porcellionides pruinosus</i> , per replicate in each soil treatment, at the beginning of the experiment (day 2) and after 90 days of soil exposure. Soil treatments included the non-exposed soil (CT), soil exposed to $\text{Cu}(\text{OH})_2$ -nanopesticide and to $\text{Cu}(\text{OH})_2$ -ionic, at two different concentrations, at two different application rates (single or season).	90
Table S2. Soil pH for each treatment, at the beginning of the experiment and after 90 days of soil exposure. Soil treatments included the non-exposed soil (CT), soil exposed to $\text{Cu}(\text{OH})_2$ -nanopesticide and to $\text{Cu}(\text{OH})_2$ -ionic, at two different concentrations, at two different application rates (single or season). Data was expressed as average and standard deviation (SD).	91
Table S3. Heatmap for carbon sources utilization by the soil microbiome, non-exposed (CT), or exposed to $\text{Cu}(\text{OH})_2$ nanopesticide or ionic form at two different application rates (single or season). These carbon utilizations were analyzed after 90 days of soil exposure. These effects were assessed in the absence or presence of <i>Porcellionides pruinosus</i>	92
Table S4. Carbon consumption of the soil communities measured during the 144 h of the Biolog [®] Ecoplate incubation. Data were expressed in terms of Confidence intervals, with a 95% of significance. Bold numbers indicates a significant difference between time of incubation for each soil treatment [non-exposed soil, $\text{Cu}(\text{OH})_2$ -ionic or $\text{Cu}(\text{OH})_2$ -nanopesticide]. Repeated measure ANOVA, Tukey HSD, $p \leq 0.05$	93

CHAPTER 4: RESPONSES OF SOIL MICROBIOME TO COPPER-BASED NANOMATERIALS FOR AGRICULTURAL APPLICATIONS

Table 1. Relative abundance of the 15 most abundant OTUs per treatment in control soil and soil spiked with different copper formulations. Asterisks (*) indicate significant differences in relative abundances towards the respective control ($p < 0.05$; Tukey HSD).....	116
Table 2. Inference of pathways affected by exposure to 50 mg (Cu) kg^{-1} soil, as different formulation of copper [$\text{Cu}(\text{OH})_2\text{-i}$, Kocide [®] 3000, $\text{nCu}(\text{OH})_2$, nCuO]. The soil sampling was done at day 28. The significative decrease (■) and increase (■) of the relative abundance of function-related sequences towards the non-treated soil (CT) are highlighted (Tukey HSD; $p < 0.05$). White colour represents no statistically significant effects towards the CT	118
Table S1. Statistical significance ($p < 0.05$), using the two-way ANOVA (Tukey HSD test), for the copper dissolution in spiked soil with copper-based (nano)materials [$\text{Cu}(\text{OH})_2\text{-i}$, Kocide [®] 3000, $\text{nCu}(\text{OH})_2$, or nCuO]. The table represents the copper formulations for each sampling time (day -2, 0, 14 and 28).....	135
Table S2. Statistical significance ($p < 0.05$), using the two-way ANOVA (Tukey HSD test), for the enzymatic activity from non-treated soil (CT) and spiked soil with copper (nano)materials [$\text{Cu}(\text{OH})_2\text{-i}$, Kocide [®] 3000, $\text{nCu}(\text{OH})_2$, or nCuO]. In the table are represented two factors: (1) copper formulations and (2) sampling time (day 0, 14 and 28).	136
Table S3. Statistical significance, using the two-way ANOVA (Tukey HSD test), for the substrate well colour development (SAWCD). In the table are represented the two factors considered to the analysis: (1) copper formulation [Kocide [®] 3000, $\text{nCu}(\text{OH})_2$, nCuO and $\text{Cu}(\text{OH})_2\text{-i}$] and (2) sampling time (day 0, 14 and 28).....	137
Table S4. Statistical significance, using the two-way ANOVA (Tukey HSD test, $p < 0.05$), for each carbon substrate utilized (from Biolog [®] Ecoplate) by the microbial community from non-treated (CT) and spiked soil with copper [$\text{Cu}(\text{OH})_2\text{-i}$, Kocide [®] 3000, $\text{nCu}(\text{OH})_2$, or nCuO]. Data was based on the optical density (590 nm). In this analysis was considered two factors: (1) soil treatments and (2) sampling time (days 0, 14 and 28).	138
Table S5. Number of reads and OTUs per sample after each sequence data processing step.	139
Table S6. Diversity indexes calculated based on metagenomic analysis from non-treated soil (CT) and spiked soil with $\text{Cu}(\text{OH})_2\text{-i}$, Kocide [®] 3000, $\text{nCu}(\text{OH})_2$, or nCuO , after day 0 and 28. Average values ($n=3 \pm$ standard deviation) for each soil treatment.....	140
Table S7. Statistical significance ($p < 0.05$) for each class in the soil treatments from non-treated soil or spiked soil with copper [$\text{Cu}(\text{OH})_2\text{-i}$, Kocide [®] 3000, $\text{nCu}(\text{OH})_2$, or nCuO]. Two factors were considered (two-way ANOVA; Tukey HSD method, $p < 0.05$): (1) soil treatments and (2) sampling time (day 0 and 28) for each class.	141
Table S8. Statistical significance ($p < 0.05$) for each genus affiliated across the soil treatments [CT, soil spiked with $\text{Cu}(\text{OH})_2\text{-i}$, Kocide [®] 3000, $\text{nCu}(\text{OH})_2$, or nCuO]	

after 0, and 28 days of exposure, using the one-way ANOVA for each sampling time (Tukey HSD method; $p < 0.05$). 142

Table S9. Statistical significance ($p < 0.05$) for the 15 most abundant OTU from non-treated soil or spiked soil with copper [$\text{Cu}(\text{OH})_2\text{-i}$, Kocide[®]3000, $\text{nCu}(\text{OH})_2$, or nCuO]. Two factors were considered (two-way ANOVA; Tukey HSD method, $p < 0.05$): (1) soil treatments and (2) sampling time (day 0 and 28) for each OTU. 143

CHAPTER 5: COPPER-BASED NANOMATERIALS ALTER THE RHIZOSPHERE BACTERIAL COMMUNITY

Table S1. Permanova analysis regarding the bacterial community structure, by DGGE analysis, from rhizosphere and bulk soil. Treatments included: the non-exposed soil or exposed soil to 50 mg (Cu) kg^{-1} soil of $\text{Cu}(\text{OH})_2\text{-i}$, or Kocide[®]3000, or nCuO or $\text{nCu}(\text{OH})_2$, after 14 and 28 days of exposure. Data was paired-wised test based on 999 permutations. 170

Table S2. Statistical significance ($p < 0.05$) for diversity indexes in non-exposed soil or exposed soil to 50 mg (Cu) kg^{-1} soil of $\text{Cu}(\text{OH})_2\text{-i}$, Kocide[®]3000, nCuO or $\text{nCu}(\text{OH})_2$, using the one-way ANOVA (Tukey HSD test). 171

Table S3. Statistical significance ($p < 0.05$) for enzymatic activity in non-exposed rhizosphere soil or exposed rhizosphere soil to 50 mg (Cu) kg^{-1} soil of $\text{Cu}(\text{OH})_2\text{-i}$, Kocide[®]3000, nCuO or $\text{nCu}(\text{OH})_2$, using the one-way ANOVA (Tukey HSD test). 172

CHAPTER 6: IMPACT OF Ag_2S NPS ON SOIL BACTERIAL COMMUNITY – A TERRESTRIAL MESOCOSM APPROACH

Table 1. Diversity indexes from SBC structure analysis were analysed over time and considering the following soil treatments: CT (non-exposed soil), and spiked soil with AgNO_3 and Ag_2S NPs. The diversity indexes included: the richness (S), Pielou (J') and Shannon-Wiener index (H'). The data represent the mean of each diversity index ($n=3 \pm$ standard deviation). Different letters (^{a, b}) indicate statistical difference using two-way ANOVA (Tukey post-hoc test, $p < 0.05$) among treatments and within exposure time.. 191

Table S1. Percentage of dissolution measured by ICP-MS of Ag_2S -NPs measured in ultrapure water (UPW) stock solution at a nominal concentration of 1 mg (Ag) L^{-1} . Data was expressed by mean and standard deviation (mean \pm SD). 207

Table S2. Soil $\text{pH}(\text{CaCl}_2)$ measured of mesocosm columns. Top-soil (0-4 cm), with control soil (CT), soil spiked with Ag_2S NPs and soil spiked with AgNO_3 . Data was expressed by mean and standard deviation (mean \pm SD). 208

Table S3. Diversity indexes calculated based on DGGE analysis among soil treatments and soil depth in mesocosm core. The soil treatments consist in: CT (non-exposed soil), spiked soil with AgNO_3 and Ag_2S NPs were analysed for each soil layers (S1, S2, S3, and S4) after 28 days. Different letters (a, b) correspond to significant differences ($p < 0.05$) between soil treatments (CT vs. Ag_2S NP vs. AgNO_3) for each layers, after 28 days of exposure..... 209

Table S4. Statistical significance (using the Two-way ANOVA) for the area under curve (AUC) values for each substrate tested in Biolog [®] Ecoplate. In the table are represented the two factors considered to the analysis: (1) silver treatment (Ag ₂ S NP or AgNO ₃) and (2) sampling time (Day 14 and 28). (*) Asterisks indicate significant changes in AUC using Tukey HSD (p<0.05), for each substrate, comparing the silver treatment towards the CT (non-exposed soil).....	210
--	-----

CHAPTER 7: THE IMPACT OF SILVER SULFIDE NANOPARTICLES AND SILVER IONS IN SOIL MICROBIOME

Table 1. Species richness (number of OTU; S), diversity (Shannon-Wiener index; H') and evenness (Pielou's evenness index; J') index of the soil bacterial communities exposed to Ag ₂ S NPs and AgNO ₃ or non-exposed soil (CT) (OTU based profile). Values presented are mean ± standard deviation. Asterisks (*) indicate significant differences between silver treatments toward the respective CT (two-way ANOVA; Tukey HSD; p<0.05).	222
---	-----

Table 2. Functional inference for the soil microbiome exposed to 10 mg (Ag) kg ⁻¹ soil for AgNO ₃ and Ag ₂ S NPs, at day 14 and 28. The average values (n=3) for each silver treatment and control (CT) were computed using the Piphillin software. The arrows indicate a decrease (↓) and increase (↑) in relative abundance of genes encoding the listed functions/products toward the respective CT. Statistical differences across the treatments were highlighted in dark-blue (■ significantly decrease) and light-blue (■significantly increase) using two-way ANOVA (Tukey HSD, p<0.05).	227
--	-----

Table S1. Primer sequences and thermocycling conditions for ammonia-oxidizing bacteria (amoA gene) and nitrite-oxidizing bacteria (nxrB gene), and total bacteria (16S rRNA gene).....	254
---	-----

Table S2. Number of reads and OTUs per sample after each sequence data processing step.	255
---	-----

Table S3. Statistical analysis of the relative abundance of soil genera, at day 14, using the one-way ANOVA. Treatments represented the soil microbiome non-exposed (CT), and soils exposed to Ag ₂ S NPs or AgNO ₃ . In table, multi-comparisons, using the Tukey HSD test, were done considering differences between sampling treatment. The confidence value p<0.05.	256
---	-----

Table S4. Statistical analysis of the abundance of the most represented OTUs (30 most abundant per treatment) in exposed soil at days 14 and 28. Two-way ANOVA was applied considering a p<0.05 (Tukey HSD method).	258
---	-----

Table S5. Statistical analysis of the relative abundance of soil genera, at day 28, using the one-way ANOVA. Treatments represented the soil microbiome non-exposed (CT), and soils exposed to Ag ₂ S NPs or AgNO ₃ . In table, multi-comparisons, using the Tukey HSD test, were done considering differences between sampling treatment. The confidence value p<0.05.	260
---	-----

List of Abbreviations

Ag ₂ S NPs	Silver sulfide nanoparticles
AgNPs	Silver nanoparticles
AI	Active ingredient
ANOVA	Analysis of variance
AOA	Ammonia-oxidising archaea
AOB	Ammonia-oxidising bacteria
AP	Acid phosphatase activity
AS	Arylsulfatase activity
C	Carbon
CAGR	Compound annual growth rate
CLPP	Community-Level Physiological Profile
Cu	Copper
DGGE	Denaturing Gradient Gel Electrophoresis
DHA	Dehydrogenase activity
ENMs	Engineered nanomaterials
ERA	Environmental risk assessment
EU	European Union
HPC	Heterotrophic plate counts
ISO	International Organization for Standardization
N	Nitrogen
nCu(OH) ₂	Copper hydroxide nanoparticles
nCuO	Copper oxide nanoparticles
NGS	Next generation sequencing
NMs	Nanomaterials
P	Phosphorous
<i>P. pruinus</i>	<i>Porcellionides pruinus</i>
PEC	Predicted concentration in the environment
P-SB	Phosphorous-solubilizing bacteria
qPCR	quantitative PCR
ROS	Reactive Oxygen Species
REACH	European Chemicals Agency

SBC	Soil Bacterial Community
UA	Urease activity
WHC	Water holding capacity
ZVI	nanoscale Zero-Valent Iron
β G	β -glucosidase activity

Chapter 1

General introduction

1. Nanomaterials

Currently, nanotechnology provides new nanomaterials (NMs) to supply industrial and human needs. NMs were defined by the European Commission (2011/696/EU), in 2011, as “(...) *a natural, incidental or manufactured material containing particles, in an unbound stage or as an aggregate or as an agglomerate and where for 50% or more external dimensions is in the size range 1 nm-100nm*”. Also, the NMs can be defined as nano-objects with one, two, or three external dimensions in the nanoscale (1-100 nm), accordingly to the International Organization for Standardization (ISO/TS 80004-1:2015).

Although materials in the nano-size range can be naturally present in the environment, engineered NMs (ENMs) attracted more attention in the industrial sector. As a result of the large area-to-volume ratio (higher than $60 \text{ m}^2 \text{ cm}^{-3}$; as indicated in 2011/696/EU) and size-dependent properties (particularly particles smaller than 20 nm), ENMs have novel/unique properties and behaviours, that make them suitable for nanotechnology applications (Auffan *et al.*, 2009). These ENMs represent an enormous class of compounds that can be grouped based on dimension, morphology, state, and chemical composition (Saleh, 2020). Regarding chemical nature of ENMs, they can be classified in five categories: carbon, metal (including metal oxides), quantum dots, dendrimers, and composite NMs (EPA, 2017), as described in Table 1. Among all of them, metal-based ENPs (*e.g.*, AgNPs and CuONPs) are the most widely used in different applications/products such as paints, cosmetics, agrochemicals, among others (EPA, 2017), as briefly described in Table 1.

Table 1. Properties and applications of different nanoparticles. Adapted from: EPA, 2017.

Type of ENMs	Some examples	Physical and chemical properties	Applications
Carbon-based	Fullerenes and carbon nanotubes (CNTs).	Stable, limited reactivity, high thermal and electrical conductivity.	Biomedical applications, sensors and components in electronics, automotive industries.
Metal-based	Gold, Silver, Copper metal oxides: titanium dioxide (TiO ₂), zinc oxide (ZnO), Zerovalent iron (nZVI).	High reactivity, photolytic properties and antimicrobial properties.	Paints, cosmetics, agrochemicals.
Quantum Dots	Quantum dots made from cadmium selenide (CdSe), cadmium telluride (CdTe), indium phosphide (InP) and zinc selenide (ZnSe).	Reactive core composed of metals or semiconductors controls the material's optical properties.	Medical bioimaging, targeted therapeutics, solar cells, photonics and telecommunication.
Dendrimers	Hyperbranched polymers, dendrigraft polymers and dendrons.	Three-dimensional nanostructures engineered to carry encapsulated molecules in their inner void spaces or attached to the surface.	Drug delivery systems, polymer materials, chemical sensors and modified electrodes.
Composite NMs	Produced using two different NMs or NMs combined with larger, bulk-type materials.	Electrical, catalytic, magnetic, mechanical, thermal or imaging features.	Potential applications in drug delivery and cancer detection.

Recently, Mordor Intelligence estimates that the global economic impact of ENMs will reach 57.6 billion USD in 2026, at a compound annual growth rate (CAGR) of over 19.86% during the forecast period 2020-2026 (Mordor Intelligence, 2020). The global production of metal-based ENMs was projected over-time, as observed in Figure 1. Metal oxides, like SiO₂, ZnO and Al₂O₃ presented an estimated highest production volume (metric tons - Mg) per year, in which in 2025 will range from 532185-4534963 Mg (SiO₂), 49500-497000 Mg (ZnO) and 12250-79954 Mg (Al₂O₃). In fact, these ENMs can be used in diverse applications, and for this reason present a very high production volume in comparison to the other ENMs (Janković and Plata, 2019). Interestingly, ENMs that have been essentially used as bactericides and/or fungicides (*e.g.*, in textile, paints and agrochemicals), such as Ag and CuO, represent relatively small current markets (410-798 Mg and 16000-830 Mg, respectively in 2025) (Janković and Plata, 2019).

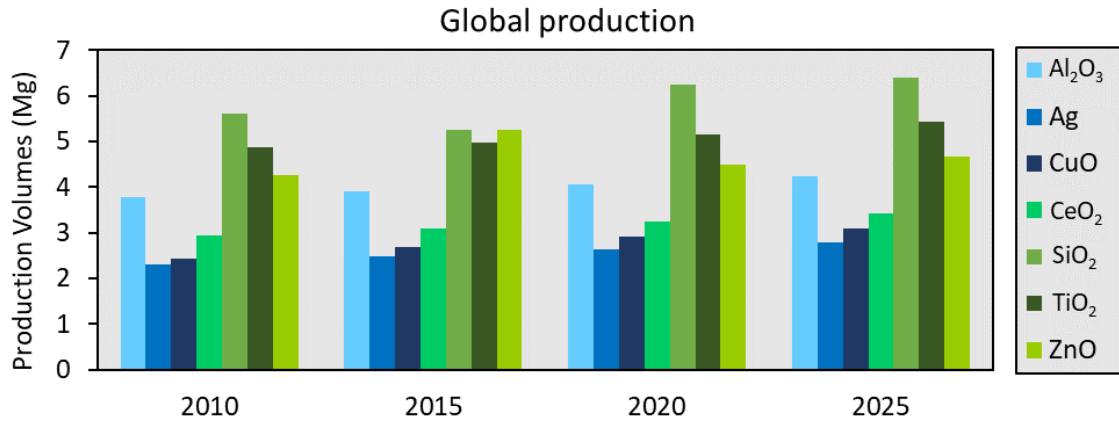


Figure 1. Metal-based engineered nanomaterials production volume (Mg) (Values were obtained from the average of global production volume and then transformed in Log-scale). Adapted from: Janković and Plata, 2019.

1.1. Life cycle of nano-enabled products and release into the environment

Despite the advantages of nano-enabled products, the environmental risks linked with metallic ENMs are not completely known. During the life cycle of a nano-enabled product (*i.e.*, production, manufacturing, use, recycling and end-of-life), ENMs can be released and possibly reach diverse environmental compartments, *e.g.*, air, soil and water systems. Three different releasing pathways of ENMs are well recognized: (1) accidental release; (2) intentionally, via use or application of nano-enabled products (*e.g.*, nano-agrochemicals) and (3) unintentionally, via wastewater, sewage sludge, or landfills (Gottschalk *et al.*, 2009; Sun *et al.*, 2014). From this point of view, Figure 2 represents the probable sources and exposure routes of ENMs, that can potentially lead to their release during their life-cycle, focusing on that ending-up in the terrestrial system. In fact, the agricultural soil is identified as the major environmental compartment that may be a final sink for different ENMs (Cornelis *et al.*, 2014).

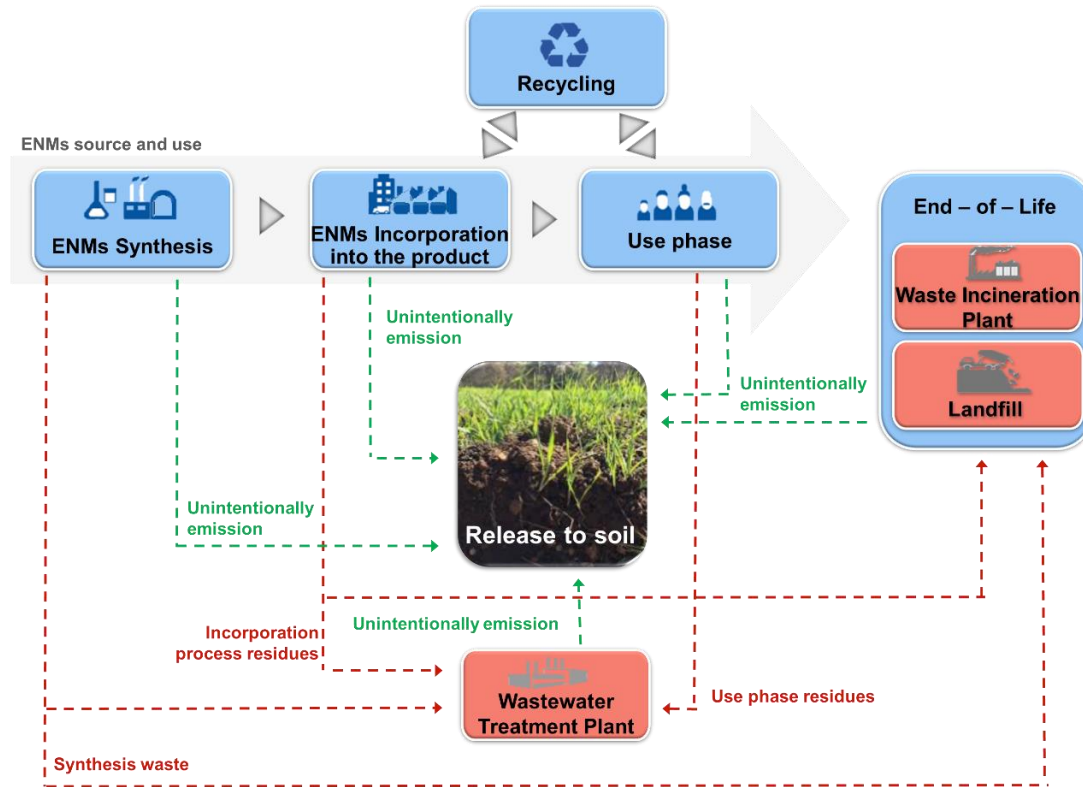


Figure 2. Scheme of ENMs sources and release routes in the terrestrial environment. Green arrows indicate release to the soil (unintentionally release) and red arrows indicate ENMs release pathways ending up in waste management or end-of-life treatments, from where release in soil can also occur. Adapted from: Loureiro *et al.*, 2018.

As demonstrated in Figure 2, the ENPs can be released to soil in distinct stages of the nano-product life-cycle. Generally, the synthesis and manufacturing phases are controlled processes, representing a low risk of ENMs release into the soil (Loureiro *et al.*, 2018). On the other hand, the use phase and end-of-life stages may present the main contamination route to the soil compartment (Loureiro *et al.*, 2018).

1.2. Metal-based nanomaterials released intentionally in soils

A wide-range of metallic ENMs can deliberately enter the terrestrial compartment, as a consequence of nano-agrochemicals applications (He *et al.*, 2019). These products strive to improve the agri-food sector by increasing the efficiency of chemical inputs and offering solutions to agricultural and environmental problems, by improving food productivity and security, or diminishing the environmental contamination risks. Table 2 summarizes some commercially available nano-products, such as fertilizers, pesticides and remediation products.

Table 2. Some ENMs-based agrochemicals commercially available.

	Commercial product	ENPs	Content	Company
Remediation products	Nano-Goethite	Pristine iron oxides stabilized with HA	Catalytic effect on bioremediation and adsorption of heavy metals	University of Duisburg-Essen, Germany
	NANOFER 25S	Zero valent iron (ZVI)	Remediation of groundwater	NANO IRON, s.r.o., Czech Republic
	FerMEG12	ZVI	Remediation of soil and groundwater	UVR-FIA GmbH, Germany
Nano-fertilizers	Nano-Gro™	Zeolite	Plant growth regulator and immunity enhancer	Agro Nanotechnology Corp., FL, United States
	Nano-Ag Answer®	Silver	Plant growth, reduction in water needs, and reduction in predatory pests	Urth Agriculture, CA, United States
	Biozar Nano-Fertilizer	Iron, zinc and manganese	Improve the fertility of soils and various agricultural plants	Fanavar Nano-Pazhooohesh Markazi Company, Iran
	Nano Max NPK Fertilizer	Chitosan	Promote the growth of green leaves and photosynthesis; increases carbohydrates, oil fats and proteins in crop.	JU Agri Sciences Pvt. Ltd, Janakpuri, New Delhi, India
	Master Nano Chitosan Organic Fertilizer	Chitosan	Promote plant growth, enhanced resistance against Fungi and Bacteria.	Pannaraj Intertrade, Thailand
Nano-pesticides	Kocide®3000	Copper hydroxide	Plant protection; fungicide and bactericide.	Dupont Ltd, United States
	NANOCU	Copper	Promote plant growth; fungicide and bactericide.	Bio Nano Technology, Egypt
	Banner MAXX	Propiconazole	Fungicide.	Syngenta Crop Protection AG, Switzerland
	Nanosulf®Spray	Sulfur	Promote plant growth; fungicide.	Alert Biotech, India
	Nanosulf®Drenching	Sulfur	Promote plant growth; fungicide.	Alert Biotech, India
	Zerebra®agro Zeroxxe® Zeromix®	Silver	Promote plant growth; fungicide and bactericide.	AgroKhimProm Group, Russia and Commonwealth of Independent States, Grand Harvest Research Innovation Company

Particularly for nanoremediation products, ENMs are released in a controlled manner into the soil to reduce pollutants in contaminated areas (by degradation and

immobilization processes) (Thangadurai *et al.*, 2020). Due to low costs, environmental compatibility and high reactivity, nanoscale zero-valent iron (ZVI) is the most broadly used ENPs for this application (Ezzatahmadi *et al.*, 2017). Concerning nano-fertilizers, they can improve the yield and quality of food crops with increased nutrient usage efficiency, through encapsulation of nutrients (macro- and/or micro- nutrients) within the ENMs, as for example Biozar Nano-Fertilizer (which uses the iron, zinc and manganese NPs) (Mardalipour *et al.*, 2014). On the other hand, nano-pesticides involve either ENPs of an active ingredient (AI) or other engineered small structures with useful antimicrobial properties, to protect the food-crop production. Currently, at least four types of ENMs have resulted in nano-enabled commercial pesticides, available on the market: (1) copper NPs [Cu_2O NPs, CuO NPs and $\text{Cu}(\text{OH})_2$] as fungicides and bactericides to control diseases on fruit trees, and vegetables (for example: bacterial spot caused by *Xanthomonas*), (2) colloidal silver to combat fungal pathogens on seeds, tubers, and vegetative plants; (3) sulfur as miticides and fungicides, used to improve root growth and seed production; and (4) propiconazole NPs, to prevent fungal cell growth by inhibiting sterol biosynthesis in root system or surface stem (He *et al.*, 2019). The application of copper-based nanopesticides in agroecosystems is still being debated in the scientific community. Nevertheless, Kocide[®]3000 [a pesticide with nano $\text{Cu}(\text{OH})_2$ as an active ingredient] is already available in the United States of America (USA) market and can be applied in both organic and conventional farms (Keller *et al.*, 2017). In general, these products have shown slow degradation and controlled release of the active ingredient for long-time, which is a great advantage in comparison to conventional pesticides (Lowry *et al.*, 2019). The nano-form in this pesticide is expected to make them more stable and improve their efficacy against microorganisms (bactericide and fungicide properties), which can increase food production by reducing costs to the farmer (Lowry *et al.*, 2019). However, the possible risks associated with these products do not only come from the accumulation of copper in the soil, but also from its antimicrobial broad-spectrum activity against non-target microorganisms. A possible effect on the soil microbiome may lead to negative consequences to soil fertility/quality and to human health (via food chain) (Kah *et al.*, 2021).

1.3. Metal-based nanomaterials released unintentionally in soils

The unintentionally release of ENMs in terrestrial compartment can happen in different steps of the life cycle of a nano-enabled product. First of all, these products can be

damaged during the use phase for several reasons, such as mechanical action or chemical corrosion (Loureiro *et al.*, 2018). On the other hand, at the end-of-life stage of nano-enabled products, ENMs reach the terrestrial compartment through the application of landfill disposal and wastewater treatment plants (WWTP) in this system (Loureiro *et al.*, 2018). The landfill disposal is the most commonly used method to discard the ENMs-products; however, it depends on the country's regulations. Particularly for WWTP, ENMs can reach this compartment from different steps in the life-cycle stages of nano-products (*e.g.*, synthesis, manufacturing and use phase; as described in Figure 2). During the primary and secondary treatments in WWTP, most ENMs (around 91%) can be removed from effluents (Gottschalk *et al.*, 2009), remaining attached to the sludge. This sludge is then used in some countries as a farm-land fertilizer (biosolids), resulting in agroecosystems contamination (Gottschalk *et al.*, 2009). In Europe, around 10 million tons of dry sewage sludge are produced per year, of which about 40% is applied to agricultural lands as fertilizer (Roig *et al.*, 2012). AgNPs are the metallic ENPs most widely used in commercial products (*e.g.*, electronics, textiles, and medical devices) mainly due to their antimicrobial properties (Giese *et al.*, 2018). Many studies reported these nanoparticles in sewage sludge (Kaegi *et al.*, 2011; Colman *et al.*, 2013).

2. Metal-based nanomaterials in agroecosystem

2.1. Concentrations of metallic nanomaterials in the terrestrial compartment

Due to the rapidly growing market of products containing nano-sized particles (like, silver and copper), an increased concentration of these substances in the terrestrial compartment is expected. This increased concentration may lead to a negative impact in soil functioning. For this reason, in the last years, efforts to estimate both Ag and Cu predicted concentration in the environment (PEC) have been made. Particularly for AgNPs, in general, a range concentration of ng kg^{-1} soil have been estimated, assuming different exposure scenarios (Mueller and Nowack, 2008; Gottschalk *et al.*, 2009; Sun *et al.*, 2014; Gottschalk *et al.*, 2015; Giese *et al.*, 2018). In 2018, Giese and their collaborators estimated the PEC for 2050 in the range of 0.24 – 792.23 ng kg^{-1} in sludge soil; with a maximum of 10 $\mu\text{g kg}^{-1}$ for agricultural soils (Giese *et al.*, 2018). Based on Denmark data, Ag NMs concentration was predicted in a range from 6 to 21 ng kg^{-1} in agricultural soils and 50–530 ng kg^{-1} in sludge-treated soils (Gottschalk *et al.*, 2015). A

study by Sun *et al.* (2014) estimated the PEC of Ag NMs in the European Union to range from 30 to 80 ng kg⁻¹ in natural soils and from 1290 to 1390 ng kg⁻¹ in sludge-treated soils by 2020, using a dynamic probabilistic model. Muller and Nowack (2008) suggested that the PEC for AgNPs in soil could reach 0.02 or 0.1 µg kg⁻¹ in a realistic or in a high-emission scenario, respectively. Recently, Kuenen and collaborators (2020) estimated the tonnes of AgNPs released per km² soil for European countries (Figure 3). In this study, the sludge-treated, natural and urban soils were considered. Portugal, Czech Republic, France, United Kingdom and Belgium presented the highest released tonnes of silver per km² soil, for instance 1.14 x10⁻⁰⁷, 1.16 x10⁻⁰⁷, 1.35 x10⁻⁰⁷ and 1.52 x10⁻⁰⁷, 1.99 x10⁻⁰⁷, respectively.

Copper, in its different forms, has been extensively used in agriculture for long time. For this reason, Cu concentration is critical for environmental risk assessment (ERA) (Keller *et al.*, 2017). Copper can be released into soils via biosolids application or deliberately applied as part of (nano)agrochemicals. Concerning the nanoparticulate form, copper-based NPs concentrations in biosolids are expected to be below µg kg⁻¹ soil (Keller *et al.*, 2017). However, higher concentrations were projected due to (nano)pesticides application, in which rates of 0.05 to 0.8 g m⁻² (or 0.5–8 kg ha⁻¹) per event were used (*e.g.*, Kocide[®]3000). This corresponds to around 10–50 mg per plant, depending on application amount (*i.e.*, repeated application at 2–4 weeks intervals - Kocide[®]3000) and planting density (Keller *et al.*, 2017). Recurrent application of copper pesticides (in both nano and conventional form) may result in increased concentration of copper in agricultural soils. In this line, Ballabio and co-workers (2018) estimated the Cu concentration in European Union lands (top-soil) of 49.26 mg kg⁻¹ for vineyards soils, by using a model based on the LUCAS Topsoil database, as represented in Figure 3.

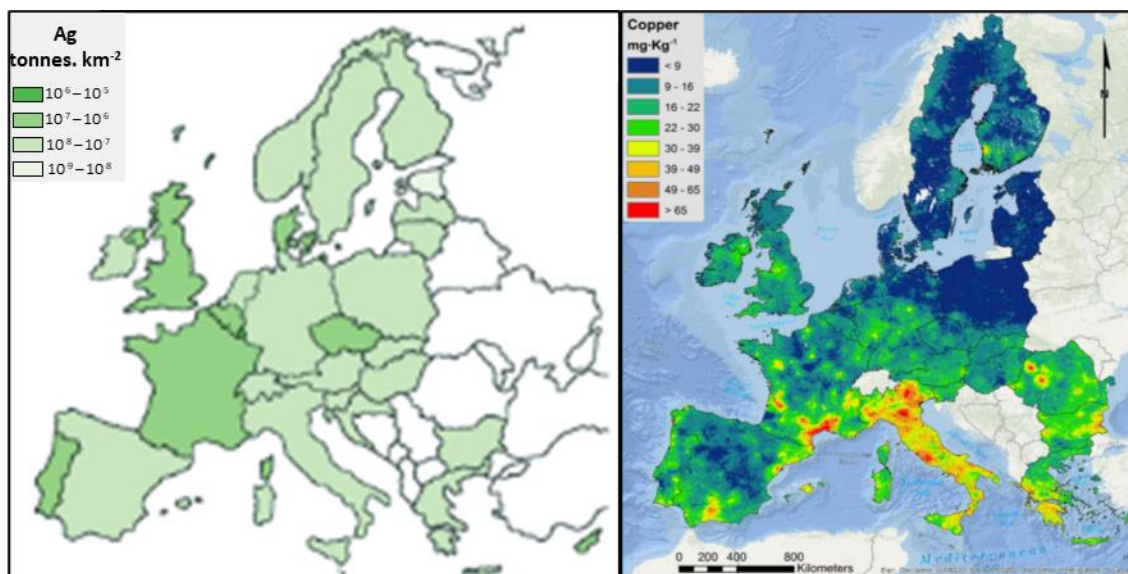


Figure 3. Predicted environmental concentrations in Europe regarding the presence of AgNPs (tonnes Ag released per km²) (Kuenen *et al.*, 2020) or copper (mg Cu kg⁻¹ vineyards soil) (Ballabio *et al.*, 2018).

Due to their persistence and recurrent detection in the terrestrial compartment, their toxicity and potential human exposure, both Ag and Cu were suggested as emerging contaminants. Thus, from an environmental risk assessment perspective, the study of ENMs transformation and mobility is fundamental to understand their toxicity in the agroecosystem.

2.2. Transformations of metal-based nanomaterials in soils

Generally, metal-ENMs are very dynamic and reactive in the environment and several chemical, physical, or biological transformations may occur in the terrestrial environment (Figure 4). Physical processes mainly include aggregation and/or agglomeration (Cornelis *et al.*, 2014). The aggregation process results from the compression of the electrical double layers on the particle surfaces in high ionic strength conditions (Cornelis *et al.*, 2014). In the environment, ENMs tend to aggregate with particles of the same nature (homo-aggregation) and/or with other ENMs or with soil particles/constituents (*e.g.*, soil organic matter) or different ENMs (hetero-aggregation) (Cornelis *et al.*, 2014). Depending on the duration of the aggregation (in both homo or hetero) process, particles with larger sizes can be formed, leading to a decreased toxicity (Zhang *et al.*, 2020). The soil organic matter can also influence this process, in which high content of organic matter in soils can inhibit (homo or hetero) aggregation with other NPs (Klitzke *et al.*, 2015).

Chemical processes include dissolution and subsequent speciation changes, like redox reactions (*e.g.*, oxidation and sulfidation), photochemical reactions, and corona formation (Cornelis *et al.*, 2014). In fact, dissolution is a very common chemical transformation of metal-based ENMs, which occurs when an ion detaches from the particle and migrates through the electrical double layer into the solution. Generally, ionic species dissolution contributes to the toxicity for organisms and microorganisms (Zhang *et al.*, 2020). This step is usually accompanied by sulfidation of ENPs, frequently described for most metal ENMs (*e.g.*, Ag, Cu and Zn) in WWTP (Kaegi *et al.*, 2011; Banerjee and Jain, 2018; Gogos *et al.*, 2017). This sulfidation state may result in changes in particle size, surface charge, and solubility and are often thought to be caused by core-shell (*e.g.*, Ag to Ag₂S) formation, where the Ag₂S layer gradually increases. Eventually these changes will influence the fate, bioavailability and toxicity (Lead *et al.*, 2018). Generally, the sulfidation makes the ENMs exert less toxicity to organisms and microorganisms, due to higher stability and consequent lower ionic dissolution, but also depending on their sulfidation state or extent. Dissolution also depends on this sulfidation state but also on aggregation, organic matter coating, and other ions present (Adeleye *et al.*, 2014, Conway *et al.*, 2015). For instance, highly aggregated ENPs have a reduced surface area, which decreases the dissolution rate.

Biologically mediated processes include biodegradation and biomodification (Cornelis *et al.*, 2014). ENMs can aggregate in the rhizosphere, on root surfaces or in biological fluids (*e.g.*, xylem and phloem). Dissolution, degradation, redox reactions, or chelation may take place in the cell wall/membrane, cytoplasm, or extracellularly via enzyme-assisted reactions or through interaction with reactive oxygen species (Lowry *et al.*, 2012).

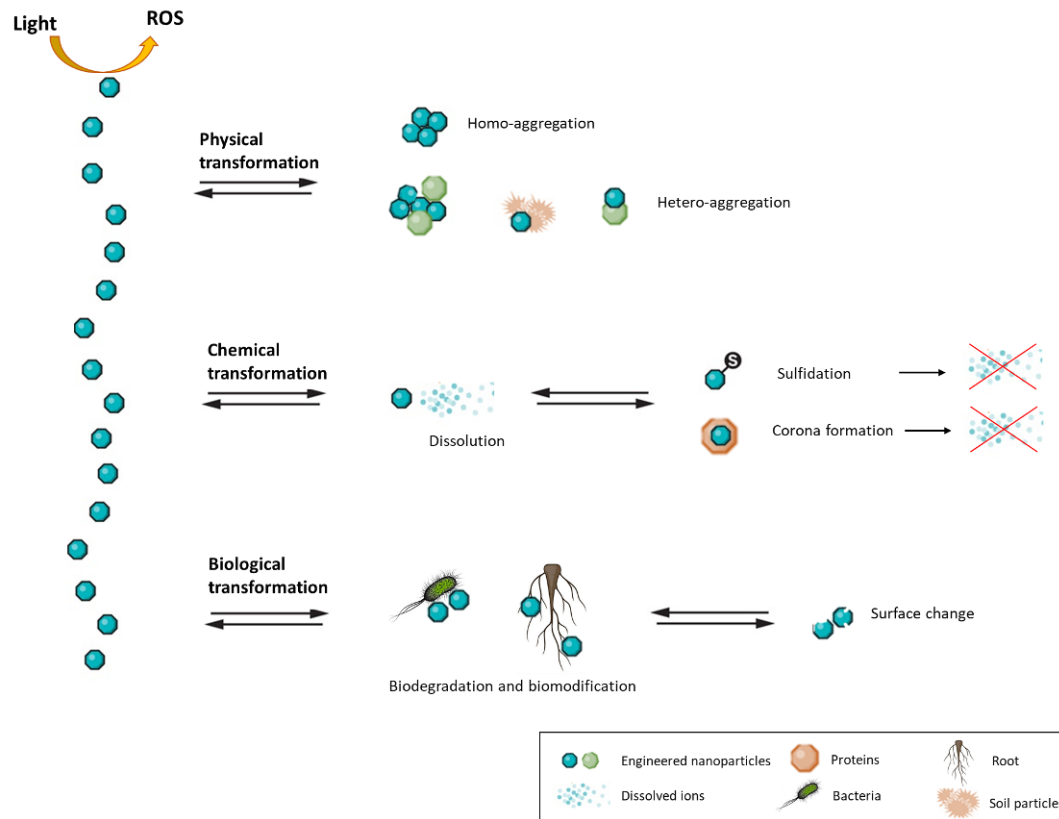


Figure 4. Conceptual diagram of the major transformations that engineered nanomaterials (ENMs) might undergo in the environment. In figure was described the physical, chemical and biological transformations. Based on: Lowry *et al.*, 2012.

2.3. Fate of metal-based nanomaterials in soils

To date, the fate of these materials was consensually characterized in the soil porewater system (Cornelis *et al.*, 2014), as schematized in Figure 5. In fact, soils are porous systems formed by mineral and organic particles combined with liquid and gaseous phases. Generally, the organic matter-rich soils presented an ENPs dispersion increased, and consequently, their mobility in porous media also increase. On the other hand, the clay particles can decrease the ENMs mobility by destabilize charged ENPs (positively or negatively) (Zhou *et al.*, 2012). Moreover, these processes are greatly influenced by the pH and ionic strength in soil solution (Cornelis *et al.*, 2014). Also, the mobility of ENPs decreases dramatically with finer texture, an effect that has indeed been found experimentally in several column tests on ENPs (Cornelis *et al.*, 2014). The presence of organisms has also been demonstrated to be a driver in the mobility of ENMs in soil, in a process called bioturbation (Baccaro *et al.*, 2019). One example is the activity of earthworms, which can bury and move the AgNPs in vertical and/or horizontal direction (Baccaro *et al.*, 2019). Also, the bioaccumulation of ENMs can occur in organisms

(externally or internally), regardless of the exposure regime (by ingesting or taking up ENMs via soil, sediment, air, water or food) (Petersen *et al.* 2019).

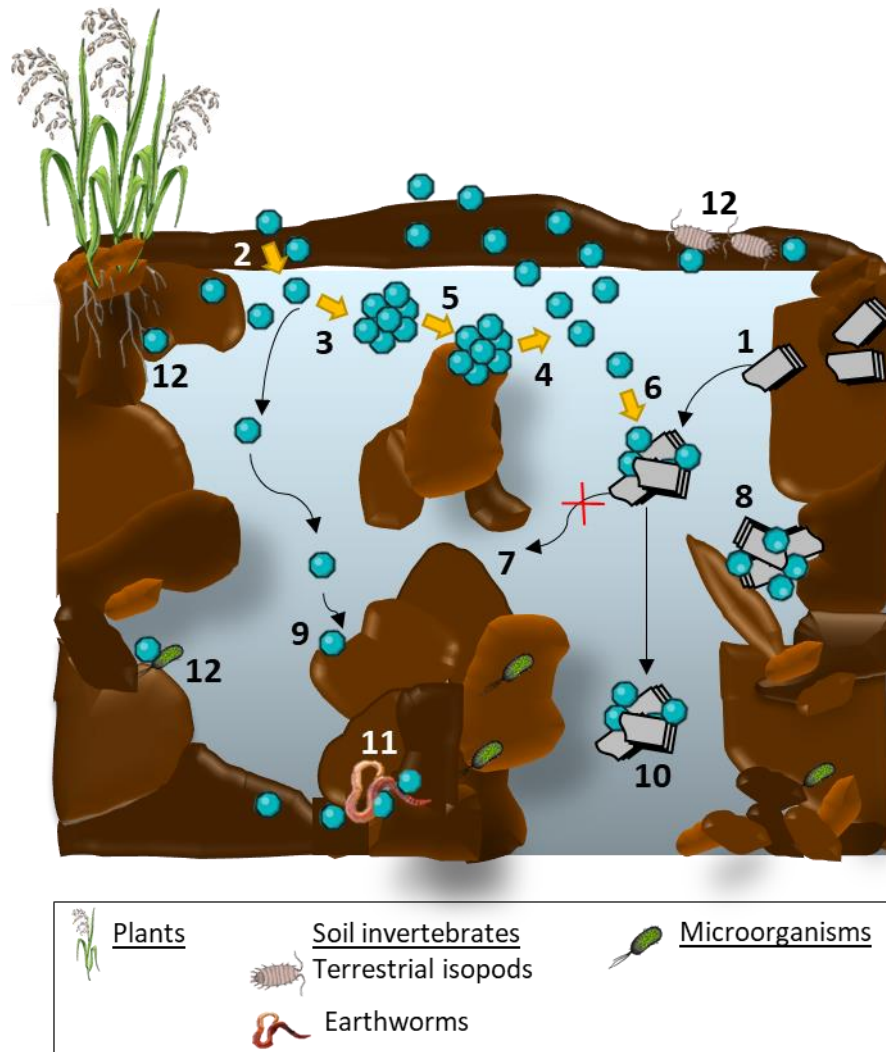


Figure 5. Schematic overview of the main fate-determining parameters of ENMs in soil-water systems. 1. ENMs leaching from biosolids, 2. Colloid generation, 3. Homoaggregation, 4. Fragmentation, 5. Sedimentation, 6. Heteroaggregation, 7. Size exclusion, 8. Straining, 9. Deposition, 10. Convective transport, and 11. Bioturbation. 12. Biodegradation and/or bioaccumulation. Adapted from: Cornelis *et al.* 2014.

3. Bioavailability and toxicity of metal-based nanomaterials in soils

Once in soils, bioavailability of ENMs is key in toxicity for different organisms (vertebrates, invertebrates, plants) and/or microorganisms. In general, this process can be defined as the fraction of chemical that is available or can be made available for uptake with potential to cause toxic effects in biota (Allen, 2002). Soil characteristics,

route of exposure, and the ENMs' characteristics determine the bioavailability of these substances (Zhang *et al.*, 2020).

3.1. Toxicity mechanisms of metal-based nanomaterials to Bacteria and Fungi

Several *in vitro* studies reported that metallic ENMs exert toxicity, and some toxic mechanisms for Bacteria and Fungi are illustrated in Figure 6 (Nel *et al.*, 2009; Schultz *et al.*, 2018). The ENPs accumulate and dissolve in the bacterial membrane, leading to alterations in membrane permeability (McQuillan, 2014). The aggregation state of ENPs and the membrane composition influence the toxicity of ENPs. For instance, homo-aggregation decreases the cell smoothness and thickness, while hetero-aggregation may not exert toxic effects (Stoimenov *et al.*, 2002). Regarding bacterial membrane (Figure 6 A), Gram-negative showed to be less susceptible to ENPs due to, essentially, the presence of the outer membrane (Schultz *et al.*, 2018). Metal ions and/or ENPs can penetrate the cell membrane (internalization and translocation), which may result in degradation of intracellular ATP and interruption in DNA duplication (Lok *et al.*, 2007). Also, both ionic and nanosized particles may generate reactive oxygen species (ROS) causing damage to the cellular structures (McNeilly *et al.*, 2021). Particularly for fungal communities (Figure 6 B), five distinct mode of action was already reported regarding different ENMs exposure, which include disruption of cell wall, DNA damage, inhibition of protein synthesis, mitochondria damage and the ROS generation (Lakshmeesha *et al.*, 2020).

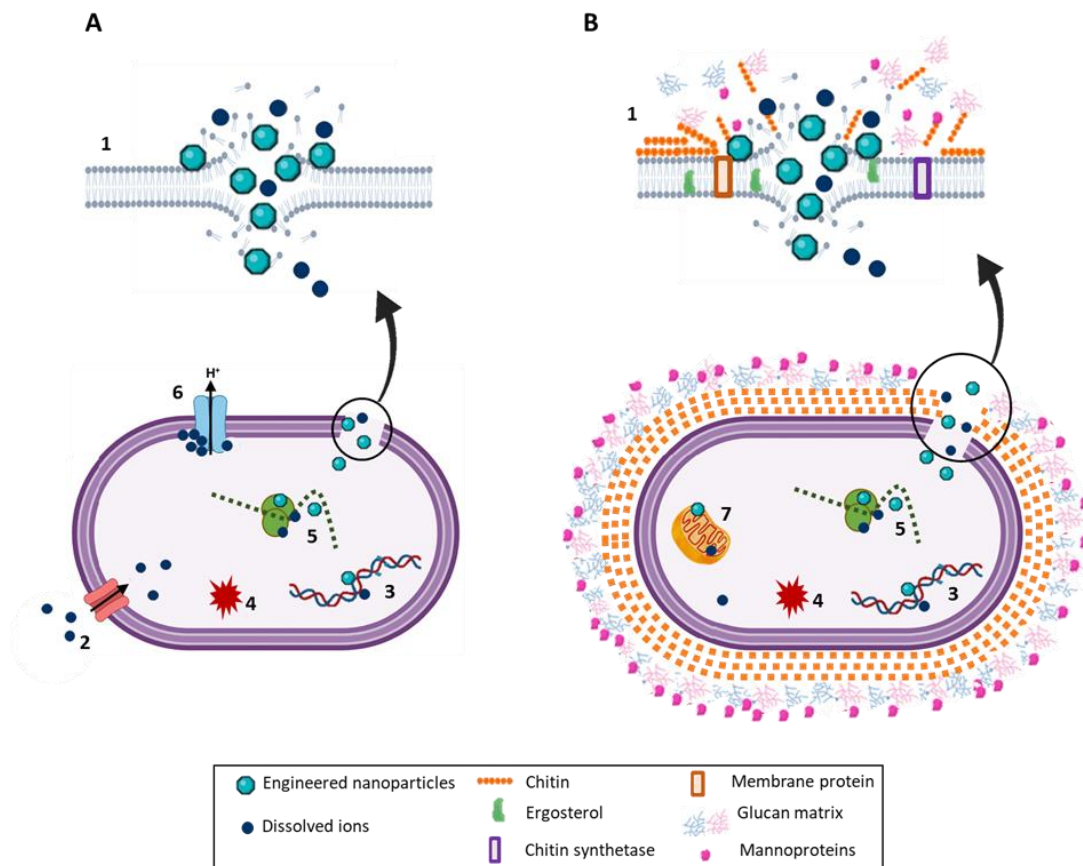


Figure 6. Nanoparticles and ions mode of action in (A) bacteria and (B) fungi cells. 1. Disruption of cell wall and pore formation, 2. Passage through outer membrane porin, 3. DNA damage, 4. Increase of intracellular reactive oxygen species (ROS) concentration, 5. Inhibition of protein synthesis, 6. Uncoupling of respiratory chain, and 7. Mitochondria damage. Adapted from: McNeilly *et al.*, 2021 and Lakshmeesha *et al.*, 2020.

Nevertheless, some bacteria can activate resistance mechanisms to survive in NMs-contaminated soils, such as (1) the efflux pumps and (2) the communication cell-to-cell by *Quorum Sensing* (QS). Concerning the efflux pumps activity, the activation of this mechanism promotes the exportation of metallic ions/particles from inside the bacterial cell, regulating their cell homeostasis (McNeilly *et al.*, 2021). The upregulation of Cu efflux proteins (*e.g.*, involved in the Sil/Cus systems) has been documented in silver-tolerant bacteria from contaminated soils with AgNPs (McNeilly *et al.*, 2021). The QS as suggested as a mechanism that enable bacteria to adapt to environmental/chemical changes, through the production and release of small-molecules signals (*e.g.*, N-acyl-l-homoserine lactones) into extracellular environment (Gómez-Gómez *et al.*, 2019). The increase of these signals can promote the transcription of target genes which activate a

cascade of cellular processes, promoting the tolerance of bacteria (Gómez-Gómez *et al.*, 2019).

4. Impact of metal nanomaterials in soil biota

4.1. Soil microbiome

Due to their bioavailability, persistence in the environment and their antimicrobial properties, Ag- and Cu- based ENMs may affect target and non-target soil microbiome. Soil microbiome can be defined as the microorganisms that live together in soil ecosystems, in both bulk and rhizosphere area (Santaella and Plancot, 2020). Naturally, healthy soils presented a high diversity and abundance of microorganisms (Santaella and Plancot, 2020). For instance, Bacteria and Fungi are the most abundant microorganisms found in the terrestrial compartment, typically presenting a 10^2 – 10^4 times more biomass than the Protists, Archaea and Viruses (Fierer *et al.*, 2017). Although there is no “standard” soil core microbiome, the first Atlas of soil bacterial taxa identified the most abundant and ubiquitous classes from 237 soil samples (derived from six continents and 18 countries), namely Alphaproteobacteria, Betaproteobacteria, Actinobacteria and Acidobacteria (Delgado-Baquerizo *et al.*, 2018). Regarding fungal communities, a study conducted by Tedersoo *et al.*, (2014) reported that the phyla Ascomycota, Basidiomycota, and Chytridiomycota were the most abundant soil fungi across the 365 sites globally distributed. Nevertheless, this composition can be influenced by soil properties (*e.g.*, soil type, salinity, nutrients and oxygen availability); climatic conditions, geographic location and soil horizon, and presence of other organisms (Santaella and Plancot, 2020; Delgado-Baquerizo *et al.*, 2018). In the presence of plants, rhizosphere soil (soil surrounding the roots) displays a distinct microbiome composition compared to the bulk soil, which the abundance of Proteobacteria, Actinobacteria, Alphaproteobacteria and Bacteroidetes increase in the rhizosphere soil, as already reported for grassland (Shi *et al.*, 2015), cropland (Donn *et al.*, 2015) and forest (Gschwendtner *et al.*, 2016) soils. This distinct composition may result from the presence of root exudates, which alter the soil properties and the carbon content in the soil (Philippot *et al.*, 2013). For example, a decrease in soil pH has been observed in rhizosphere soils, resulting from the release of protons (H^+) by root exudates (Knauff *et al.*, 2003). Also, the roots secrete exudates containing carbon in the form of soluble (called primary metabolites), such as vitamins, purines, inorganic ions,

organic acid and amino acids, which can be an additional source of carbon and energy for soil microorganisms (Berendsen *et al.*, 2012, Philippot *et al.*, 2013). Some secondary metabolites, such as siderophores and nucleosides, can also be produced by the root to defend the plants against pathogens, also altering the microbiome composition and structure (Berendsen *et al.*, 2012; Ebadollahi *et al.*, 2019). On the other side, the root exudates can also stimulate the abundance of microorganisms beneficial to plant growth and defence against phytopathogens, such as plant-growth promoting rhizobacteria (PGPR) (Yuan *et al.*, 2018).

Generally, soil microbiome plays a role in terrestrial ecosystem services associated with soil fertility and crop production (Santaella and Plancot, 2020; FAO, 2016). In fact, 80-90% of soil functioning is mediated by soil microorganisms (Nannipieri and Badalucco, 2003). For instance, the soil formation and structure, water retention, gaseous exchanges and carbon sink, biogeochemical cycling (*e.g.*, phosphorus, carbon, and nitrogen), plant development, degradation of pollutants and pathogens control can be regulated by the soil microbiome; and vice-versa (Jansson and Hofmockel, 2020).

Regarding biogeochemical cycling (Figure 7), the ability of the microorganisms to use atmospheric gases (*e.g.*, hydrogen, carbon dioxide, nitric oxide, nitrous oxide), and/or transform dead material into an available form reusable to other organisms, can influence and regulate the entire nutrient cycling in terrestrial system (Jansson and Hofmockel, 2020).

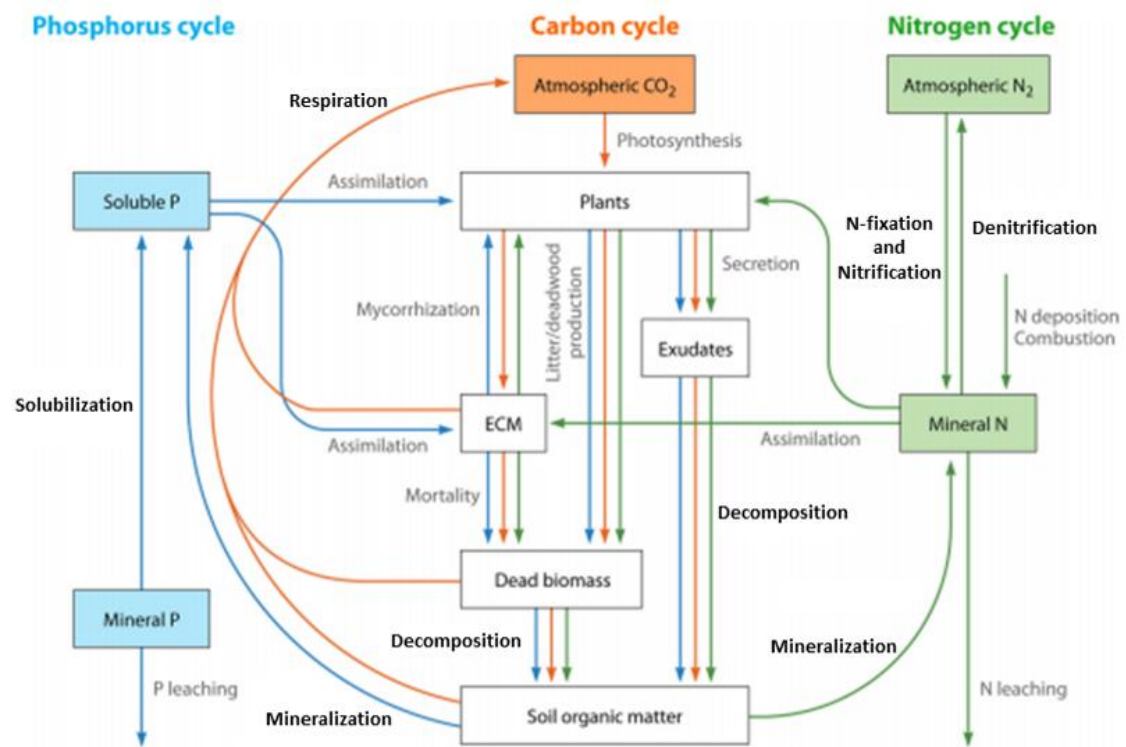


Figure 7. Schematic of three biogeochemical cycles of carbon, nitrogen and phosphorous in terrestrial ecosystems. Arrows show the transfer of phosphorous - P (blue), carbon - C (orange), and nitrogen - N (green) between ecosystem compartment. Ecological processes in bold indicate the mediation by Bacteria. In scheme: ECM: ectomycorrhizas (fungi). Adapted from: Lladó *et al.*, 2017.

For instance, members of Bacteria (*e.g.*, species of *Azotobacter*, *Bacillus*, *Burkholderia*) and Fungi (*e.g.*, species of *Actinomyces*, *Rhizoctonia*, *Aspergillus*) can mineralize phosphorous, making it available for plants growth (Nautiyal, 1999). The activity of phosphatases can also mediate this process, in which the phosphate can be released from organic phosphate ester during organic matter decay (Nannipieri *et al.*, 2018). This process contributes not only to increase crop productivity but it also increases soil fertility, highlighting its crucial role in agriculture systems. Soil microbiome can also be involved in the flux of C in terrestrial ecosystem, essential due to its mediation in the decomposition of plant debris and mineralization processes. For instance, the decomposition of plant debris is mediated by several microorganisms, such as some members of Actinobacteria and Acidobacteria, which can return some carbon to the atmosphere (Lladó *et al.*, 2017). Several soil enzymes (*e.g.*, endocellulases, exocellulases, and β -glucosidases) can also play a major role in C cycle, namely in the degradation of cellulose, which is the most accessible polymer present in the plant biomass.

On the other side, the most limiting nutrient for plant growth is nitrogen (N) (Lladó *et al.*, 2017). In fact, the nitrogen mineralization is a crucial process to soil fertility, in which organic nitrogen is converted to inorganic forms available to the plants (Lladó *et al.*, 2017). Also, this process can be directly associated to decomposition, nitrogen fixation, nitrification and denitrification (Lladó *et al.*, 2017). Concerning nitrogen fixation, this process is mediated by members of Bacteria, converting the inorganic to organic nitrogen ($N_2 \rightarrow NH_3$), which makes nitrogen available for plants growth and for activities of other organisms (Nelson *et al.*, 2016). This process can be catalysed by nitrogenases encoded by *nifD* and *nifK* genes, and a di-nitrogenase reductase subunit encoded by *nifH* gene; and is mainly mediated by ubiquitous N-fixing bacteria like Alphaproteobacteria (*Bradyrhizobium*, *Azospirillum*, *Hyphomicrobium*, and *Gluconacetobacter*) and Deltaproteobacteria (*Geobacter* spp.) (Lladó *et al.*, 2017). The nitrification is a limiting step in N cycling involving the oxidation of ammonium (NH_4^+) to nitrite (NO_2^-), which can be mediated by ammonia-oxidising bacteria (AOB) and/or archaea (AOA) (Nelson *et al.*, 2016). In fact, AOB were indicated as most abundant in soils than AOA (Nelson *et al.*, 2016). The final step of the N cycle involves the returning of nitrogen gas to the atmosphere via the denitrification process (Nelson *et al.*, 2016). In this process, nitrate is reduced to nitrogen gas through some intermediary compounds namely: nitrite, nitric oxide and nitrous oxide ($NO_3 \rightarrow NO_2 \rightarrow NO \rightarrow N_2O \rightarrow N_2$). This process is mediated by chemolithoautotrophic bacteria, like species of *Pseudomonas* and *Bacillus*, and archaeal species (Clark *et al.* 2012). Additionally, several genes have been identified which are involved in the different steps of the microbial denitrification process (Nelson *et al.*, 2016). For instance, *nap* and *nar* genes which encode for nitrate reductase ($NO_3 \rightarrow NO_2$); *nir* genes that encode for nitrite reductase ($NO_2 \rightarrow NO$); *nor* genes nitric oxide reductase ($NO \rightarrow N_2O$) and *nos* genes which encode for nitrous oxide reductase ($N_2O \rightarrow N_2$).

So, in response to emerging contaminants, the function, abundance, structure and composition of soil microorganisms may change (Holden *et al.*, 2014). Since they play an important role in ecosystem health and function, any changes in these microbial communities will affect the whole ecosystem (Holden *et al.*, 2014). Several microbial responses to the contaminants were already suggested, such as (1) tolerance, (2) functional redundancy, (3) resilience and (4) affected/susceptible (Allison and Martiny, 2008). For instance, the microbial communities can support/tolerate the effect of contaminants and remaining similar to the initial composition (Allison and Martiny,

2008). Concerning the resilience response, the initial composition of microbial community can return to its original composition after being disturbed (Allison and Martiny, 2008). The shifts in community structure/composition could also be neutral on ecosystems functioning, in which some tolerant microorganisms can perform a similar function of the eliminated/sensitive microorganisms - functional redundancy (Allison and Martiny, 2008). On the other hand, microbial communities can have their composition/structure permanently affected by the contaminant (susceptible).

In the last years, many studies were conducted to assess the effects of Ag- and Cu-based ENMs on soil microbiome, as described in Table 3. In these studies, Ag-based ENPs were described to alter soil bacterial community structure, diversity, composition and enzymatic activity, as well as nitrifying communities' abundance (inferred from *amoA* gene abundance) (Peyrot *et al.*, 2014; Samarajeewa *et al.*, 2017; Forstner *et al.*, 2019; Bao *et al.*, 2016; Doolette *et al.*, 2016). Recently, most studies focused on aged AgNPs (Ag₂S NPs) and compared their impact with other silver forms, being observed the following toxic pattern: AgNO₃ > AgNPs > Ag₂S NPs (Bao *et al.*, 2016; Doolette *et al.*, 2016; Schultz *et al.*, 2018). However, comparisons among studies are difficult due to of the use of distinct concentrations, distinct soil characteristics, lab-scale designs (exposure scenarios), microbial endpoints analysed and time of exposure. Similarly, several studies have established that Cu-based NMs can also affect composition, abundance, diversity and structure of soil microbiome, as well as soil enzymatic activity (Carley *et al.*, 2020; Samarajeewa *et al.*, 2020; Zhang *et al.*, 2019; Zhang *et al.*, 2020; Simonin *et al.*, 2018 a, b). Microorganisms related with denitrification, nitrogen-fixation and nitrification processes have been reported to change in CuO NPs treated soils, under distinct experimental designs and/or duration (Guan *et al.*, 2020; Zhao *et al.*, 2020; Simonin *et al.*, 2018b). Nevertheless, the impact of nano-Cu(OH)₂ in the microbial-mediators in the nitrogen cycle was poorly explored. In the last years, the increased concern in the application of Cu-based NMs in agriculture resulted in an increased study of these NMs in soil, under more realistic exposure scenarios (*e.g.*, using outdoor mesocosm experiments) at longer exposure periods and environmental relevant concentrations (Simonin *et al.*, 2018b; Carley *et al.*, 2020). However, a knowledge gap concerning the impact of Ag- and Cu- based ENMs in soil microbiome (*e.g.*, composition, structure and function) in the presence of different organisms (including plants and invertebrates) was noted in the studies described in Table 3.

Table 3. Effects of silver (Ag) and/or copper (Cu) based ENMs/ENPs in soil microorganisms, under distinct exposure scenarios.

ENMs	Soil type	Duration (days)	Concentrations (mg kg ⁻¹)	Biota	Test complexity	Microbial endpoint	Main conclusions	Reference
AgNO ₃ ; AgNPs (PVP, 44 nm); Ag ₂ SNPs (152 nm)	Natural soil (pH=5.1)	28	0.1 to 72 (AgNO ₃); 0.1 to 456 (AgNPs); 0.1 to 2285 (Ag ₂ S NPs).	-	Microcosm	Gene quantification (<i>amoA</i> gene); Metagenomic analysis; Soil nitrification (OECD 216).	Toxic effect increasing in the order: AgNO ₃ >AgNP>Ag ₂ S NPs	Doolette <i>et al.</i> , 2016
AgNO ₃ ; AgNPs (35-nm and 75 nm), and AgNPs (PVP; 30-50 nm)	Freshwater sediments	45	0.001	-	Microcosm	Enumeration of heterotrophic bacteria; Soil enzyme activities; Metagenomic analysis.	AgNPs affect sediment microbial biomass and enzyme activity.	Bao <i>et al.</i> , 2016
AgNPs and sodium acetate	Sandy soil (pH=5.70), with or without compost amendment	42	0.00125 to 30	-	Microcosms	Soil enzymatic activities.	Enzyme activities were inhibited as a function of the Ag concentration in the soil.	Peyrot <i>et al.</i> , 2014
AgNPs (15–20 nm) amended sludge	Natural soil (pH=5.4)	90	1 and 10	-	Mesocosms	Bacterial and fungal community diversity and structure.	AgNPs was mainly converted in Ag ₂ S. AgNPs alter microbial diversity.	Forstner <i>et al.</i> , 2019
Ag ₂ S-containing sludge	Two natural soils (pH=5.5) with salinity gradient	150	30	Rice (<i>Oryza sativa L.</i>)	Microcosms	Plant growth; Gene quantification (<i>amoA</i> , <i>nxrB</i> gene and <i>narG</i> , <i>napA</i> , <i>nirS</i> , and <i>nosZ</i>)	The availability of Ag ₂ S increased with salinity. Ag ₂ S posed a low risk for plants and soil microorganisms.	Wu <i>et al.</i> , 2020

AgNPs (PVP; 20 nm)	Sandy loam soil (pH=5.8)	49 and 63	49, 124, 287, 723 and 1815	-	Microcosms	Heterotrophic bacteria count; Enzyme activities; DGGE; Metagenomic analysis.	Negative effects on microbial growth, diversity, and enzymatic activities.	Samarajeewa <i>et al.</i> , 2017
Kocide®3000 [DuPont; Cu(OH) ₂ nanoparticles]	Natural soil (sandy-clay- loam soil; pH=5.8), with or without fertilization (commercial Osmocote fertilizer)	365 (terrestrial)	6.68 mg/L per event (x 3 events)	<i>Trifolium pratense</i> , <i>Chamaecrista fasciculata</i> , <i>Medicago sativa</i> , <i>Brassica napus</i> , <i>Cichorium intybus</i> , <i>Sorghastrum nutans</i> , and <i>Urochloa ramosa</i> .	Mesocosms (outdoor)	Metagenomic analysis (bacterial, fungal, and total eukaryotic community)	No toxic effects. Shifts in the sediment communities of the wetland mesocosms were found (protists, fungi, and algae).	Carley <i>et al.</i> , 2020
Kocide®3000 [DuPont; Cu(OH) ₂ nanoparticles]	Natural soil (sandy-clay- loam soil; pH=5.8), with or without fertilization (commercial Osmocote fertilizer)	365	6.68 mg/L per event (x 3 events, under three different nutrient addition)	<i>Trifolium pratense</i> , <i>Chamaecrista fasciculata</i> , <i>Brassica napus</i> , <i>Cichorium intybus</i> , <i>Sorghastrum nutans</i> , and <i>Urochloa ramosa</i> .	Mesocosms (outdoor)	Plant growth; Nitrogen fixation rate; Enzymatic activities.	Soil enzyme activities were significantly reduced (after the first and the third exposure). Fertilization levels mitigate the effect of Kocide®3000.	Simonin <i>et al.</i> , 2018a

CuO NPs (28 nm) and CuSO ₄	Lufa 2.1 soil (pH adjusted to 7.6)	28	0.5 (CuSO ₄) and 50 (CuO NPs and CuSO ₄).	<i>Triticum aestivum</i>	Microcosms	Plant growth; Gene quantification (<i>nifH</i> , <i>amoA</i> , <i>nxrA</i> , <i>narG</i> , <i>nirS</i> , <i>norB</i> and <i>nosZ</i>).	Cu treatments reduced nitrate accumulation in the bulk soil, increase in the rhizosphere	Guan <i>et al.</i> , 2020
Cu(OH) ₂ -nanopesticide; Cu(OH) ₂ -nanorods; Cu(OH) ₂ -ionic and CuSO ₄ .	Natural soil (loamy soil; pH=7.7)	21	0.5, 5, and 50.	-	Microcosms	Enzymatic activities; Metagenomic analysis (bacterial communities).	Different formulation of Cu(OH) ₂ differently affected soil bacterial abundance, diversity, soil enzymatic activity and community compared to CuSO ₄ .	Zhang <i>et al.</i> , 2020
CuO NPs	Natural soil (red soil; pH=6.2)	2.5	10, 100, 500.	-	Microcosms	Enzymatic activities; Gene quantification (<i>narG</i> , <i>nirK</i> , <i>nirS</i> and <i>nosZ</i>); and Metagenomic analysis (bacterial communities).	CuO NPs exposure decreased the enzymatic activities in soil. Denitrifying functional genes and bacterial communities' composition were changed after CuO NPs exposure.	Zhao <i>et al.</i> , 2020
CuO NPs (50 nm)	Natural soils (Sandy-Loam: pH=7; Loam: pH=6.4; Silty-Clay: pH=6.9; Silty-Clay: pH=8.2; Silty-Clay-Loam: pH=7.8)	90	0.1, 1, and 100.	<i>Triticum aestivum</i>	Microcosms	Soil enzymatic activities; Gene quantification (<i>amoA</i> gene).	CuO NPs reduced the microbial activities (denitrification, nitrification, and soil respiration) at 100 mg/kg dry soil.	Simonin <i>et al.</i> , 2018b

Cu(OH) ₂ -nanopesticide; synthesized Cu(OH) ₂ ; Cu(OH) ₂ -ionic and CuSO ₄ .	Agricultural soil (pH=8.2)	14	0.5, 5 and 50	-	Microcosms	Gene quantification (<i>nth</i> gene); and Metagenomic analysis (bacterial communities).	Cu(OH) ₂ nanopesticides changed the soil microbial communities composition, and reduced nitrile hydratase activity.	Zhang <i>et al.</i> , 2019
CuO NPs (<50 nm)-amended biosolids CuSO ₄ .	Sandy loam soil (pH=5.2)	49 and 77	27, 54, 123, 265 and 627	-	Microcosms	Heterotrophic bacteria count; Community-level physiological profiling; Metagenomic analysis; Soil nitrification rate, Organic matter decomposition; Soil respiration; and Enzymatic activities.	Negative impact on soil microbial communities, compared to CuSO ₄ .	Samarajeewa <i>et al.</i> , 2020

4.2. Soil microbiome in the presence of plants and invertebrates

At agroecosystem level, the presence of different organisms is expected to change the abundance and structure of the soil microbiome. In general, the plants and the soil invertebrates are indicated as the main biotic factors to influence the composition and structure of these soil microbial communities (Bray and Wickings, 2019). Concerning the plants, the litter input, rhizodeposition and root exudates can influence the soil microbiome composition and abundance, as previously described in section 4.1 (Chapter 1). On the other hand, the soil invertebrates influence the soil microbiome by distinct pathways: (1) the dispersal of microorganisms throughout soils, (2) grazing on microbial biomass, and (3) nutrient inputs into soils (Bray and Wickings, 2019). The bacterial input and distribution in soil compartment via invertebrate faeces may also have an impact on decomposition and biogeochemical cycling of soil nutrients (Zimmer and Topp 1998; Swart *et al.*, 2020; Oliveira *et al.*, 2021). For instance, the anoxic conditions in the gut of worms may promote the spread and distribution of anaerobic bacteria in soil, which may stimulate the denitrification process (Sun *et al.*, 2020). The N-rich faeces can also stimulate the growth of nitrifiers bacteria, which can stimulate the nitrification process in soil (Zimmer and Topp, 1998). Additionally, soil organisms' activity promotes changes in the abiotic factors, such as the oxygen levels (*e.g.*, burrowing), pH (*e.g.*, root exudates), and nutrient content (*e.g.*, organic matter) in soils (Abd El-Wakeil, 2015), which may alter the soil microbiome composition and structure. Therefore, soil microbiome responses to contaminants can be altered.

4.2.1. Model or potential model organisms in soil ecotoxicology and their relation with soil microbiome

As a crucial part of the agroecosystem, a range of soil organisms are inevitably exposed to ENMs and may be negatively affected, including plants and soil invertebrates, Figure 8.



Figure 8. Model or potential model organisms used in ecotoxicological assays. In figure: A: wheat (*Triticum* spp.); B: earthworm (*Eisenia* spp.); C: terrestrial isopods (*Porcellionides pruinosus*); and D: mealworms (*Tenebrio molitor*).

The wheat is the most used plant in ecotoxicology assays (Figure 8 A). For instance, *Triticum* spp. is a monocotyledonous plant with an annual life-cycle. This cultivar is globally widespread and can serve as a food source for 30% of the human population (FAO, 2016). Copper-based NMs can inhibit wheat seed germination (Lee *et al.*, 2008), plant/root growth (Gao *et al.*, 2018), reducing the genes involved in denitrification processes (Guan *et al.*, 2020), and stimulate the abundance of genes associated with nitrification processes (Guan *et al.*, 2020). Likewise, some studies reported that silver-based NPs influence the wheat growth and the regulation of nitrogen cycle (Wang *et al.*, 2015). Also, wheat plants can accumulate both Cu and Ag based NMs in their root and shoot tissues (Gao *et al.*, 2018; Wang *et al.*, 2015). On the other hand, soil microorganisms have a clear relationship with plants, being the first line of defence against soil-borne pathogens, determining the plant microbiome composition, establishing an intrinsic relation with root surface, and stimulating the crop productivity (Raaijmakers and Weller, 1998, Zhang *et al.*, 2020, Singh and Jha, 2017). Specifically for wheat, *Pseudomonas* spp. in soils can control the soil root diseases of wheat caused by fungus *Gaeumannomyces graminis* var. *tritici* (Raaijmakers and Weller, 1998). Nevertheless, previous studies demonstrated that *Pseudomonas chlororaphis* O6 is susceptible to Ag, CuO, and ZnO NPs (Dimkpa *et al.*, 2011 a, b), which might impair the protective effect for the plant health.

Similarly, soil invertebrates can be suitable model organisms to study the impact of ENMs exposure in terrestrial systems. For instance, earthworms (Figure 8 B) have an important role in soil processes, such as organic matter decomposition, redistribution, and soil structure formation. *Eisenia Andrei* and/or *fetida* are shown to be sensitive in responses to ENMs in soil, in the various approaches such as avoidance behaviour (Li *et*

al., 2011), bioaccumulation/bioturbation (Baccaro *et al.*, 2019), biomarkers (Li *et al.*, 2011) and gut microbiome composition (Swart *et al.*, 2020; Wu *et al.*, 2020). From the microbiome point of view, earthworms may have a positive impact on nitrogen cycling in soil. In fact, the reduced oxygen levels make the earthworm gut a favourable environment for denitrifying bacteria. Consequently, these denitrifying bacteria can be distributed in soil via faeces, which may lead to an increased rate of denitrification in the soil (Wu *et al.*, 2020). However, in Ag₂S NPs contaminated soil, the accumulated Ag content in earthworm gut resulted in a decreased abundance of denitrifying (*e.g.*, genus *Bacillus*) in both soil and organisms' gut (Wu *et al.*, 2020). Additionally, Ag₂S NPs also decreased the copy number of nitrification gene (*nxrB*) and denitrification genes (*napA*, *nirS*, and *nosZ*) in the earthworm' gut (Wu *et al.*, 2020). This impact can negatively affect gut homeostasis and terrestrial functioning regulation.

Also, terrestrial arthropod from the order Isopoda are important detritivores, playing an important role in decomposition processes (van Gestel *et al.*, 2018). Through litter decomposing, these organisms contribute to microbial activity, abundance and nutrient cycling in soil (Orgiazzi *et al.*, 2016). The species *Porcellionides pruinosus* (Figure 8 C) is a cosmopolitan species widely distributed into the terrestrial compartment, which has been suggested as a model organism in ecotoxicology, due to their sensitivity to organic pollutants (Loureiro *et al.*, 2006b; van Gestel *et al.*, 2018). They are mostly exposed to environmental contaminants through the uropods or soil ingestion. *P. pruinosus* was used to assess the effects of ENMs (Tourinho *et al.*, 2012; Tourinho *et al.*, 2015; Morgado *et al.*, 2021), combination of chemicals (Morgado *et al.*, 2016), or to assess soil quality and contamination by the avoidance food consumption, biomass change bioassays and bioaccumulation of metals (Loureiro *et al.*, 2006a, b, Morgado *et al.*, 2021). The soil microbiome is already described as a crucial factor in the gut homeostasis and nutrition for these terrestrial isopods. For instance, the isopod-associated bacterial communities are considered a well-established resident (in hepatopancreas) or transients (in hindgut - faeces) in isopods' gut. The soil microbiome can also contribute to the processing of the ingested detritus or become a source of nutrients for isopods (Zimmer and Topp, 1998). The Proteobacteria and Bacteroidetes showed to be the most abundant phyla in the gut of *P. pruinosus* (Delhoumi *et al.*, 2020; Oliveira *et al.*, 2021), which some bacterial members can be involved in the lignocellulose degradation. These bacterial groups are affected by the metal-based NMs (Fajardo *et al.*, 2019), which may disturb the functional role of terrestrial isopods as

litter decomposers and regulators of nutrient cycling in soil ecosystems. On the other hand, the distinct avoidance to AgNPs, Ag₂S and CeO NPs contaminated food have been described in isopods behaviour, which may have resulted from the changes in the palpability of food derived from the alteration of food microbiome composition (Zidar *et al.*, 2019).

Concerning mealworms (*e.g.*, *Tenebrio molitor*; Figure 8 D), this organism was suggested as a potential model-organism to assess the impact of ENMs in soils (Khodaparast *et al.*, 2021), due to their long-term larval stage (3 or 4 months) and relevance in the feed sector (Morales-Ramos *et al.*, 2010). In the environment, *T. molitor* can act as a decomposer organism for decay plant material and dead insects (Jung *et al.*, 2014). Recently it was demonstrated that this organism can ingest (via food or soil), accumulate (in their body tissues) and eliminate (by faeces) silver [*e.g.*, pristine AgNPs, Ag₂S NPs and AgNO₃ (Khodaparast *et al.*, 2021)] and copper-based NMs [Kocide[®]3000, ionic Cu(OH)₂ and Champion (Morgado *et al.*, 2021)]. As the other invertebrates, microorganisms present in gut of *T. molitor* play an important role in their ability to adapt to different foods and/or to protect them from pathogen infections. Also, few genera from mealworm gut microbiome (*e.g.*, genera *Citrobacter* and *Kosakonia*.) were suggested to enable plastics' degradation (polystyrene and polyethylene), highlighting their relevance in the terrestrial ecosystem remediation (Brandon *et al.*, 2018).

5. Soil microbiome as an endpoint in the Environment Risk Assessment (ERA): current knowledge gaps

In terms of soil microbiome as an endpoint, only a few standardized methods are included in current guidelines for environmental risk assessment. These methodologies include the bacterial nitrogen transformation, respiration, biomass, and enzymatic activities (ECHA, 2017). However, most of these bacterial endpoints are focused on a specific bacterial group, which does not reflect the response of the broad soil microbiome as a complex community. Therefore, the development of strategies to screen and evaluate the community-level effects of contaminants, using methodologies based on structural, compositional and functional levels, is an essential step for the relevant prognostic and diagnostic ERA of these new products (*i.e.*, nanopesticides) and aged compounds (*i.e.*, sulfidized silver nanoparticles). Thus, the use of methodologies

targeting the single and community-level (*e.g.*, next-generation sequencing analysis) are widely recommended and should be comprised as an endpoint in the ERA regulation of metallic ENMs.

Concerning the nanomaterials regulation, no specific methodologies currently are standardized to study the toxic impact of nanopesticides or their properties like active ingredient in non-target soil microorganisms and organisms (Grillo *et al.*, 2020). Also, no ENMs-based pesticide is listed in the European Union Pesticides Database of active substances approved for use in European countries (Grillo *et al.*, 2020). In fact, in Europe, nano-enable products have been regulated under the European chemicals agency (REACH), which included the collection of environmental performance data prior to the commercialization. At the moment, only four different legal acts containing specific provisions for NMs, including several product-specific regulations, were created for cosmetics (EC/1223/ 2009), food (EU/1169/ 2011), biocides (EU/528/ 2012) and medical devices (Directive 2001/83/EC) (Miernicki *et al.*, 2019). In contrast, the United States of America (USA) and China, which are the countries that mostly use nanotechnology in different fields, have not yet regulated the use and/or production of nano-enable products, like nanopesticides (Miernicki *et al.*, 2019). Thus, the following knowledge gaps in this field were identified: (1) the need of studies on the impact of these NMs in the terrestrial compartment, considering the source (*i.e.*, intentionally or deliberated) and transformations of ENMs in soil (*i.e.*, aged forms of NMs, like in the sulfidation state), (2) the need for specific regulation for these NMs (*e.g.*, nanopesticides must be regulated differently from conventional pesticides) and (3) the need for standardization of methodologies for ecotoxicology/microbial assays.

Regarding the current ecotoxicology studies, the impact of metal-based ENMs has been assessed targeting endpoints related to the organisms' reproduction, mortality, accumulation, among others. However, the study of the impact of ENMs on the soil microbiome when edaphic elements are present, which act as drivers of the microbial composition, structure and activity, is still in its early stages. Furthermore, the use of complex exposure designs, such as mesocosms, has rarely been considered in these ecotoxicology studies.

6. References

- Abd El-Wakeil, K. F. (2015). Effects of terrestrial isopods (Crustacea: Oniscidea) on leaf litter decomposition processes. *The Journal of Basic & Applied Zoology*, 69, 10-16.
- Adeleye, A. S., Conway, J. R., Perez, T., Rutten, P., Keller, A. A. (2014). Influence of extracellular polymeric substances on the long-term fate, dissolution, and speciation of copper-based nanoparticles. *Environmental Science & Technology*, 48(21), 12561-12568.
- Petersen, E. J., Mortimer, M., Burgess, R. M., Handy, R., Hanna, S., Ho, K. T., Holden, P. (2019). Strategies for robust and accurate experimental approaches to quantify nanomaterial bioaccumulation across a broad range of organisms. *Environmental Science: Nano*, 6(6), 1619-1656.
- Allen, H.E. (2002). Terrestrial ecosystems: an overview. *In Bioavailability of Metals in terrestrial Ecosystems: Importance of partitioning for Bioavailability to Invertebrates, Microbes and Plants.* (pp. 1-16). Society of Environmental Toxicology and Chemistry.
- Allison, S. D., Martiny, J. B. (2008). Resistance, resilience, and redundancy in microbial communities. *Proceedings of the National Academy of Sciences*, 105 (1), 11512-11519.
- Auffan, M., Rose, J., Wiesner, M.R., Bottero, J.-Y. (2009). Chemical stability of metallic nanoparticles: a parameter controlling their potential cellular toxicity *invitro*. *Environmental Pollution*, 157, 1127-1133.
- Baccaro, M., Harrison, S., van den Berg, H., Sloot, L., Hermans, D., Cornelis, G., van den Brink, N. W. (2019). Bioturbation of Ag₂S-NPs in soil columns by earthworms. *Environmental Pollution*, 252, 155-162.
- Ballabio, C., Panagos, P., Lugato, E., Huang, J. H., Orgiazzi, A., Jones, A., Montanarella, L. (2018). Copper distribution in European topsoils: An assessment based on LUCAS soil survey. *Science of The Total Environment*, 636, 282-298.
- Banerjee, P., Jain, P. K. (2018). Mechanism of sulfidation of small zinc oxide nanoparticles. *RSC advances*, 8(60), 34476-34482.

- Bao, S., Wang, H., Zhang, W., Xie, Z., Fang, T. (2016). An investigation into the effects of silver nanoparticles on natural microbial communities in two freshwater sediments. *Environmental Pollution*, 219, 696-704.
- Berendsen, R. L., Pieterse, C. M., Bakker, P. A. (2012). The rhizosphere microbiome and plant health. *Trends in Plant Science*, 17(8), 478-486.
- Brandon, A. M., Gao, S. H., Tian, R., Ning, D., Yang, S. S., Zhou, J., Criddle, C. S. (2018). Biodegradation of polyethylene and plastic mixtures in mealworms (larvae of *Tenebrio molitor*) and effects on the gut microbiome. *Environmental Science & Technology*, 52(11), 6526-6533.
- Bray, N., Wickings, K. (2019). The roles of invertebrates in the urban soil microbiome. *Frontiers in Ecology and Evolution*, 7, 359.
- Carley, L. N., Panchagavi, R., Song, X., Davenport, S., Bergemann, C. M., McCumber, A. W., Simonin, M. (2020). Long-term effects of copper nanopesticides on soil and sediment community diversity in two outdoor mesocosm experiments. *Environmental Science & Technology*, 54(14), 8878-8889.
- Clark, I. M., Buchkina, N., Jhurrea, D., Goulding, K. W., Hirsch, P. R. (2012). Impacts of nitrogen application rates on the activity and diversity of denitrifying bacteria in the Broadbalk Wheat Experiment. *Philosophical Transactions of the Royal Society B: Biological Sciences*, 367(1593), 1235-1244.
- Colman, B. P., Arnaout, C. L., Anciaux, S., Gunsch, C. K., Hochella Jr, M. F., Kim, B., Bernhardt, E. S. (2013). Low concentrations of silver nanoparticles in biosolids cause adverse ecosystem responses under realistic field scenario. *PloS one*, 8(2), e57189.
- Conway, J. R., Beaulieu, A. L., Beaulieu, N. L., Mazer, S. J., Keller, A. A. (2015). Environmental stresses increase photosynthetic disruption by metal oxide nanomaterials in a soil-grown plant. *Acs Nano*, 9(12), 11737-11749.
- Cornelis, G., Hund-Rinke, K., Kuhlbusch, T., Van den Brink, N., Nickel, C. (2014). Fate and bioavailability of engineered nanoparticles in soils: a review. *Critical Reviews in Environmental Science & Technology*, 44(24), 2720-2764.
- Delgado-Baquerizo, M., Oliverio, A. M., Brewer, T. E., Benavent-González, A., Eldridge, D. J., Bardgett, R. D., Fierer, N. (2018). A global atlas of the dominant bacteria found in soil. *Science*, 359(6373), 320-325.

- Delhoumi, M., Catania, V., Zaabar, W., Tolone, M., Quatrini, P., Achouri, M. S. (2020). The gut microbiota structure of the terrestrial isopod *Porcellionides pruinosus* (Isopoda: Oniscidea). *The European Zoological Journal*, 87(1), 357-368.
- Dimkpa, C. O., Calder, A., Britt, D. W., McLean, J. E., Anderson, A. J. (2011 a). Responses of a soil bacterium, *Pseudomonas chlororaphis* O6 to commercial metal oxide nanoparticles compared with responses to metal ions. *Environmental Pollution*, 159(7), 1749-1756.
- Dimkpa, C. O., Calder, A., Gajjar, P., Merugu, S., Huang, W., Britt, D. W., Anderson, A. J. (2011 b). Interaction of silver nanoparticles with an environmentally beneficial bacterium, *Pseudomonas chlororaphis*. *Journal of Hazardous Materials*, 188(1-3), 428-435.
- Donn, S., Kirkegaard, J. A., Perera, G., Richardson, A. E., Watt, M. (2015). Evolution of bacterial communities in the wheat crop rhizosphere. *Environmental Microbiology*, 17(3), 610-621.
- Doolette, C. L., Gupta, V. V., Lu, Y., Payne, J. L., Batstone, D. J., Kirby, J. K., McLaughlin, M. J. (2016). Quantifying the sensitivity of soil microbial communities to silver sulfide nanoparticles using metagenome sequencing. *PLoS one*, 11(8), e0161979.
- Ebadollahi, R., Jafarirad, S., Kosari-Nasab, M., Mahjouri, S. (2019). Effect of explant source, perlite nanoparticles and TiO₂/perlite nanocomposites on phytochemical composition of metabolites in callus cultures of *Hypericum perforatum*. *Scientific Reports*, 9(1), 1-15.
- ECHA (2017) Guidance on information requirements and chemical safety assessment chapter R.7c: endpoint specific guidance. ECHA-14-G-06-EN. European Chemicals Agency. https://echa.europa.eu/documents/10162/13632/information_requirements_r7c_en.pdf/e2e23a98-adb2-4573-b450-cc0dfa7988e5. Accessed 25 May 2021.
- EPA (2017). Technical Fact Sheet – Nanomaterials. https://www.epa.gov/sites/default/files/2014-03/documents/ffrrofactsheet_emergingcontaminant_nanomaterials_jan2014_final.pdf. Accessed 25 May 2021.
- Ezzatahmadi, N., Ayoko, G. A., Millar, G. J., Speight, R., Yan, C., Li, J., Xi, Y. (2017). Clay-supported nanoscale zero-valent iron composite materials for the

- remediation of contaminated aqueous solutions: a review. *Chemical Engineering Journal*, 312, 336-350.
- Fajardo, C., Costa, G., Nande, M., Botías, P., García-Cantalejo, J., Martín, M. (2019). Pb, Cd, and Zn soil contamination: monitoring functional and structural impacts on the microbiome. *Applied Soil Ecology*, 135, 56-64.
- FAO, (2016). Wheat production and regional food security in CIS: The case of Belarus, Turkmenistan, and Uzbekistan. <https://www.fao.org/policy-support/tools-and-publications/resources-details/en/c/681891/>. Accessed 25 May 2021.
- Fierer, N. (2017). Embracing the unknown: disentangling the complexities of the soil microbiome. *Nature Reviews Microbiology*, 15(10), 579-590.
- Forstner, C., Orton, T. G., Wang, P., Kopittke, P. M., Dennis, P. G. (2019). Soil chloride content influences the response of bacterial but not fungal diversity to silver nanoparticles entering soil via wastewater treatment processing. *Environmental Pollution*, 255, 113274.
- Gao, X., Avellan, A., Laughton, S., Vaidya, R., Rodrigues, S. M., Casman, E. A., Lowry, G. V. (2018). CuO nanoparticle dissolution and toxicity to wheat (*Triticum aestivum*) in rhizosphere soil. *Environmental Science & Technology*, 52(5), 2888-2897.
- Giese, B., Klaessig, F., Park, B., Kaegi, R., Steinfeldt, M., Wigger, H., Gottschalk, F. (2018). Risks, release and concentrations of engineered nanomaterial in the environment. *Scientific Reports*, 8(1), 1-18.
- Gogos, A., Thalmann, B., Voegelin, A., Kaegi, R. (2017). Sulfidation kinetics of copper oxide nanoparticles. *Environmental Science: Nano*, 4(8), 1733-1741.
- Gómez-Gómez, B., Arregui, L., Serrano, S., Santos, A., Pérez-Corona, T., Madrid, Y. (2019). Unravelling mechanisms of bacterial quorum sensing disruption by metal-based nanoparticles. *Science of The Total Environment*, 696, 133869.
- Gottschalk, F., Lassen, C., Kjoelholt, J., Christensen, F., Nowack, B. (2015). Modeling flows and concentrations of nine engineered nanomaterials in the Danish environment. *International Journal of Environmental Research and Public Health*, 12(5), 5581-5602.
- Gottschalk, F., Sonderer, T., Scholz, R.W., Nowack, B., 2009. Modeled environmental concentrations of engineered nanomaterials (TiO₂, ZnO, Ag, CNT, fullerenes) for different regions. *Environmental Science & Technology* 43, 9216-9222.

- Grillo, R., Fraceto, L. F., Amorim, M. J., Scott-Fordsmand, J. J., Schoonjans, R., Chaudhry, Q. (2020). Ecotoxicological and regulatory aspects of environmental sustainability of nanopesticides. *Journal of Hazardous Materials*, 124148.
- Gschwendtner, S., Engel, M., Lueders, T., Buegger, F., Schloter, M. (2016). Nitrogen fertilization affects bacteria utilizing plant-derived carbon in the rhizosphere of beech seedlings. *Plant and soil*, 407(1), 203-215.
- Guan, X., Gao, X., Avellan, A., Spielman-Sun, E., Xu, J., Laughton, S., Lowry, G. V. (2020). CuO nanoparticles alter the rhizospheric bacterial community and local nitrogen cycling for wheat grown in a Calcareous soil. *Environmental Science & Technology*, 54(14), 8699-8709.
- He, X., Deng, H., Hwang, H. M. (2019). The current application of nanotechnology in food and agriculture. *Journal of Food and Drug Analysis*, 27(1), 1-21.
- Holden, P. A., Klaessig, F., Turco, R. F., Priester, J. H., Rico, C. M., Avila-Arias, H., Gardea-Torresdey, J. L. (2014). Evaluation of exposure concentrations used in assessing manufactured nanomaterial environmental hazards: are they relevant?. *Environmental Science & Technology*, 48(18), 10541-10551.
- Janković, N. Z., Plata, D. L. (2019). Engineered nanomaterials in the context of global element cycles. *Environmental Science: Nano*, 6(9), 2697-2711.
- Jansson, J. K., Hofmockel, K. S. (2020). Soil microbiomes and climate change. *Nature Reviews Microbiology*, 18(1), 35-46.
- Jung, J., Heo, A., Park, Y. W., Kim, Y. J., Koh, H., Park, W. (2014). Gut microbiota of *Tenebrio molitor* and their response to environmental change. *Journal of Microbiology and Biotechnology*, 24(7), 888-897.
- Kaegi, R., Voegelin, A., Sinnet, B., Zuleeg, S., Hagendorfer, H., Burkhardt, M., Siegrist, H. (2011). Behavior of metallic silver nanoparticles in a pilot wastewater treatment plant. *Environmental Science & Technology*, 45(9), 3902-3908.
- Kah, M., Johnston, L. J., Kookana, R. S., Bruce, W., Haase, A., Ritz, V., Gubala, V. (2021). Comprehensive framework for human health risk assessment of nanopesticides. *Nature Nanotechnology*, 16(9), 955-964.
- Keller, A. A., Adeleye, A. S., Conway, J. R., Garner, K. L., Zhao, L., Cherr, G. N., Zuverza-Mena, N. (2017). Comparative environmental fate and toxicity of copper nanomaterials. *NanoImpact*, 7, 28-40.

- Khodaparast, Z., van Gestel, C. A., Papadiamantis, A. G., Gonçalves, S. F., Lynch, I., Loureiro, S. (2021). Toxicokinetics of Silver Nanoparticles in the Mealworm *Tenebrio molitor* Exposed via Soil or Food. *Science of The Total Environment*, 146071.
- Klitzke, S., Metreveli, G., Peters, A., Schaumann, G. E., Lang, F. (2015). The fate of silver nanoparticles in soil solution—Sorption of solutes and aggregation. *Science of the Total Environment*, 535, 54-60.
- Knauff, U., Schulz, M., Scherer, H. W. (2003). Arylsufatase activity in the rhizosphere and roots of different crop species. *European Journal of Agronomy*, 19(2), 215-223.
- Kuenen, J., Pomar-Portillo, V., Vilchez, A., Visschedijk, A., van der Gon, H. D., Vázquez-Campos, S., Adam, V. (2020). Inventory of country-specific emissions of engineered nanomaterials throughout the life cycle. *Environmental Science: Nano*, 7(12), 3824-3839.
- Lakshmeesha, T. R., Murali, M., Ansari, M. A., Udayashankar, A. C., Alzohairy, M. A., Almatroudi, A., Niranjana, S. R. (2020). Biofabrication of zinc oxide nanoparticles from *Melia azedarach* and its potential in controlling soybean seed-borne phytopathogenic fungi. *Saudi Journal of Biological Sciences*, 27(8), 1923-1930.
- Lead, J. R., Batley, G. E., Alvarez, P. J., Croteau, M. N., Handy, R. D., McLaughlin, M. J., Schirmer, K. (2018). Nanomaterials in the environment: behavior, fate, bioavailability, and effects—an updated review. *Environmental toxicology and chemistry*, 37(8), 2029-2063.
- Lee, W. M., An, Y. J., Yoon, H., Kweon, H. S. (2008). Toxicity and bioavailability of copper nanoparticles to the terrestrial plants mung bean (*Phaseolus radiatus*) and wheat (*Triticum aestivum*): plant agar test for water-insoluble nanoparticles. *Environmental Toxicology and Chemistry: An International Journal*, 27(9), 1915-1921.
- Li, D., Hockaday, W. C., Masiello, C. A., Alvarez, P. J. J. (2011). Earthworm avoidance of biochar can be mitigated by wetting. *Soil Biology and Biochemistry*. 43(8), 1732–1737.
- Lladó, S., López-Mondéjar, R., Baldrian, P. (2017). Forest soil bacteria: diversity, involvement in ecosystem processes, and response to global change. *Microbiology and Molecular Biology Reviews*, 81(2), e00063-16.

- Lok, C. N., Ho, C. M., Chen, R., He, Q. Y., Yu, W. Y., Sun, H., Che, C. M. (2007). Silver nanoparticles: partial oxidation and antibacterial activities. *JBIC Journal of Biological Inorganic Chemistry*, 12(4), 527-534.
- Loureiro S., Santos S., Pinto G., Costa A., Monteiro M., Nogueira A.J.A., Soares A.M.V.M. (2006a). Toxicity Assessment of Two Soils from Jales Mine (Portugal) Using Plants: Growth and Biochemical Parameters. *Archives of Environmental Contamination and Toxicology*, 50, 182–190.
- Loureiro, S., Sampaio, A., Brandao, A., Nogueira, A. J. Soares, A. M. (2006b). Feeding behaviour of the terrestrial isopod *Porcellionides pruinosus* Brandt, 1833 (Crustacea, Isopoda) in response to changes in food quality and contamination. *Science of the Total Environment*, 369, 119-128.
- Loureiro, S., Tourinho, P. S., Cornelis, G., Van Den Brink, N. W., Díez-Ortiz, M., Vázquez-Campos, S., Van Gestel, C. A. (2018). Nanomaterials as soil pollutants. *In Soil Pollution* (pp. 161-190). Academic Press.
- Lowry G.V., Gregory K.B., Apte S.C., Lead J.R. (2012). Transformations of Nanomaterials in the Environment. *Environmental Science & Technology*, 46, 6893–6899.
- Lowry, G. V., Avellan, A., Gilbertson, L. M. (2019). Opportunities and challenges for nanotechnology in the agri-tech revolution. *Nature Nanotechnology*, 14(6), 517-522.
- Mardalipour, M., Zahedi, H., Sharghi, Y. (2014). Evaluation of nano biofertilizer efficiency on agronomic traits of spring wheat at different sowing date. *In Biological forum* (pp. 349). Research Trend.
- McNeilly, O., Mann, R., Hamidian, M., Gunawan, C. (2021). Emerging concern for silver nanoparticle resistance in *Acinetobacter baumannii* and other bacteria. *Frontiers in Microbiology*, 12.
- McQuillan JS, Shaw AM. (2014). Differential gene regulation in the Ag nanoparticle and Ag⁺-induced silver stress response in *Escherichia coli*: a full transcriptomic profile. *Nanotoxicology.*, 8, 177–184.
- Miernicki, M., Hofmann, T., Eisenberger, I., von der Kammer, F., Praetorius, A. (2019). Legal and practical challenges in classifying nanomaterials according to regulatory definitions. *Nature Nanotechnology*, 14(3), 208-216.
- Morales-Ramos, J. A., Rojas, M. G., Shapiro-Ilan, D. I., Tedders, W. L. (2010). Developmental plasticity in *Tenebrio molitor* (Coleoptera: Tenebrionidae):

- Analysis of instar variation in number and development time under different diets. *Journal of Entomological Science*, 45(2), 75-90.
- Mordor Intelligence (2020). Nanomaterials Market – Growth trends, covid-19 impact, and forecast (2021 – 2026). <https://www.researchandmarkets.com/reports/4514871/nanomaterials-market-growth-trends-covid-19>. Accessed 1 September 2021.
- Morgado, R. G., Pavlaki, M. D., Soares, A. M., Loureiro, S. (2021). Terrestrial organisms react differently to nano and non-nano Cu(OH)₂ forms. *Science of The Total Environment*, 150679.
- Morgado, R.G., Gomes, P.A.D., Ferreira, N.G.C., Cardoso, D.N., Santos, M.J.G., Soares, A.M.V.M., Loureiro, S., (2016). Toxicity interaction between chlorpyrifos, mancozeb and soil moisture to the terrestrial isopod *Porcellionides pruinosus*. *Chemosphere*, 144, 1845–1853.
- Mueller, N. C., Nowack, B. (2008). Exposure modeling of engineered nanoparticles in the environment. *Environmental Science & Technology*, 42(12), 4447-4453.
- Nannipieri P, Badalucco L. (2003). Biological processes. *In: Handbook of Processes in the Soil–Plant System: Modelling Concepts and Applications*. (pp. 57-76). The Haworth Press.
- Nannipieri, P., Trasar-Cepeda, C., Dick, R. P. (2018). Soil enzyme activity: a brief history and biochemistry as a basis for appropriate interpretations and meta-analysis. *Biology and Fertility of Soils*, 54(1), 11-19.
- Nautiyal, C. S. (1999). An efficient microbiological growth medium for screening phosphate solubilizing microorganisms. *FEMS Microbiology Letters*, 170(1), 265-270.
- Nel, A. E., Mädler, L., Velegol, D., Xia, T., Hoek, E. M. V., Somasundaran, P., Klaessig, F., Castranova, V., Thompson, M. (2009). Understanding biophysicochemical interactions at the nano-bio interface. *Nature Materials*, 8(7), 543–557.
- Nelson, M. B., Martiny, A. C., Martiny, J. B. (2016). Global biogeography of microbial nitrogen-cycling traits in soil. *Proceedings of the National Academy of Sciences*, 113(29), 8033-8040.
- Oliveira, J. M., Henriques, I., Read, D. S., Gweon, H. S., Morgado, R. G., Peixoto, S., Loureiro, S. (2021). Gut and faecal bacterial community of the terrestrial isopod

- Porcellionides pruinosus*: potential use for monitoring exposure scenarios. *Ecotoxicology*, 1-13.
- Orgiazzi, A., Bardgett, R.D., Barrios, E., Behan-Pelletier, V., Briones, M.J.I., Chotte, J-L., De Deyn, G.B., Eggleton, P., Fierer, N., Fraser, T., H., K., Jeffery, S., Johnson, N.C., Jones, A., Kandeler, E., Kaneko, N., L., P., Lemanceau, P., Miko, L., Montanarella, L., Moreira, F.M.S., R., K.S., Scheu, S., Singh, B.K., Six, J., van der Putten, W.H., Wall, D.H. (2016). Global Soil Biodiversity Atlas. (pp. 1-176). Publications Office of the European Union, Luxemburg.
- Peyrot, C., Wilkinson, K. J., Desrosiers, M., Sauvé, S. (2014). Effects of silver nanoparticles on soil enzyme activities with and without added organic matter. *Environmental Toxicology and Chemistry*, 33(1), 115-125.
- Philippot, L., Raaijmakers, J. M., Lemanceau, P., Van Der Putten, W. H. (2013). Going back to the roots: the microbial ecology of the rhizosphere. *Nature Reviews Microbiology*, 11(11), 789-799.
- Raaijmakers, J. M., and Weller, D. M. (1998). Natural plant protection by 2,4-diacetylphloroglucinol-producing *Pseudomonas* spp. in take-all decline soils. *Molecular Plant-Microbe Interactions*. 11:144-152.
- Roig, N., Sierra, J., Martí, E., Nadal, M., Schuhmacher, M., Domingo, J.L., (2012). Long-term amendment of Spanish soils with sewage sludge: Effects on soil functioning. *Agriculture, Ecosystems & Environment*. 158, 41–48.
- Saleh, T. A. (2020). Nanomaterials: classification, properties, and environmental toxicities. *Environmental Technology & Innovation*, 101067.
- Samarajeewa, A. D., Velicogna, J. R., Princz, J. I., Subasinghe, R. M., Scroggins, R. P., Beaudette, L. A. (2017). Effect of silver nano-particles on soil microbial growth, activity and community diversity in a sandy loam soil. *Environmental Pollution*, 220, 504-513.
- Samarajeewa, A. D., Velicogna, J. R., Schwertfeger, D. M., Princz, J. I., Subasinghe, R. M., Scroggins, R. P., Beaudette, L. A. (2021). Ecotoxicological effects of copper oxide nanoparticles (nCuO) on the soil microbial community in a biosolids-amended soil. *Science of The Total Environment*, 763, 143037.
- Santaella, C., Plancot, B. (2020). Interactions of nanoenabled agrochemicals with soil microbiome. *In Nanopesticides* (pp. 137-163). Springer, Cham.
- Schultz, C. L., Gray, J., Verweij, R. A., Busquets-Fité, M., Puentes, V., Svendsen, C., Matzke, M. (2018). Aging reduces the toxicity of pristine but not sulphidised

- silver nanoparticles to soil bacteria. *Environmental Science: Nano*, 5(11), 2618-2630.
- Shi, S., Nuccio, E., Herman, D. J., Rijkers, R., Estera, K., Li, J., Firestone, M. (2015). Successional trajectories of rhizosphere bacterial communities over consecutive seasons. *MBio*, 6(4), e00746-15.
- Simonin, M., Cantarel, A. A., Crouzet, A., Gervais, J., Martins, J. M., Richaume, A. (2018 b). Negative effects of copper oxide nanoparticles on carbon and nitrogen cycle microbial activities in contrasting agricultural soils and in presence of plants. *Frontiers in Microbiology*, 9, 3102.
- Simonin, M., Colman, B. P., Tang, W., Judy, J. D., Anderson, S. M., Bergemann, C. M., Bernhardt, E. S. (2018 a). Plant and microbial responses to repeated Cu(OH)₂ nanopesticide exposures under different fertilization levels in an agro-ecosystem. *Frontiers in Microbiology*, 9, 1769.
- Singh, R. P., Jha, P. N. (2017). The PGPR *Stenotrophomonas maltophilia* SBP-9 augments resistance against biotic and abiotic stress in wheat plants. *Frontiers in Microbiology*, 8, 1945.
- Stoimenov, P. K., Klinger, R. L., Marchin, G. L., Klabunde, K. J. (2002). Metal oxide nanoparticles as bactericidal agents. *Langmuir*, 18(17), 6679-6686.
- Sun, M., Chao, H., Zheng, X., Deng, S., Ye, M., Hu, F. (2020). Ecological role of earthworm intestinal bacteria in terrestrial environments: A review. *Science of the Total Environment*, 740, 140008.
- Sun, T.Y., Gottschalk, F., Hungerbühler, K., Nowack, B. (2014). Comprehensive probabilistic modelling of environmental emissions of engineered nanomaterials. *Environmental Pollution*, 185, 69–76.
- Swart, E., Goodall, T., Kille, P., Spurgeon, D. J., Svendsen, C. (2020). The earthworm microbiome is resilient to exposure to biocidal metal nanoparticles. *Environmental Pollution*, 267, 115633.
- Tedersoo, L., Bahram, M., Põlme, S., Kõljalg, U., Yorou, N. S., Wijesundera, R., Abarenkov, K. (2014). Global diversity and geography of soil fungi. *Science*, 346(6213).
- Thangadurai, D., Chakrabarty, M., Sangeetha, J. (2020). Nanoremediation of Polluted Environment: Current Scenario and Case Studies. *In Handbook of Nanomaterials and Nanocomposites for Energy and Environmental Applications*, (pp. 1-16). Springer, Cham.

- Tourinho, P. S., van Gestel, C. A., Jurkschat, K., Soares, A. M., Loureiro, S. (2015). Effects of soil and dietary exposures to Ag nanoparticles and AgNO₃ in the terrestrial isopod *Porcellionides pruinosus*. *Environmental Pollution*, 205, 170-177.
- Tourinho, P. S., Van Gestel, C. A., Lofts, S., Svendsen, C., Soares, A. M., Loureiro, S. (2012). Metal-based nanoparticles in soil: Fate, behavior, and effects on soil invertebrates. *Environmental Toxicology and Chemistry*, 31(8), 1679-1692.
- van Gestel, C. A., Loureiro, S., Primožidar (2018). Terrestrial isopods as model organisms in soil ecotoxicology: a review. *ZooKeys*, (801), 127.
- Wang, P., Menzies, N. W., Lombi, E., Sekine, R., Blamey, F. P. C., Hernandez-Soriano, M. C., Kopittke, P. M. (2015). Silver sulfide nanoparticles (Ag₂S NPs) are taken up by plants and are phytotoxic. *Nanotoxicology*, 9(8), 1041-1049.
- Wu, J., Bai, Y., Lu, B., Zhao, W., Forstner, C., Menzies, N. W., Kopittke, P. M. (2020). Silver sulfide nanoparticles reduce nitrous oxide emissions by inhibiting denitrification in the earthworm gut. *Environmental Science & Technology*, 54(18), 11146-11154.
- Yuan, J., Raza, W., Shen, Q. (2018). Root exudates dominate the colonization of pathogen and plant growth-promoting rhizobacteria. *In Root Biology* (pp. 167-180). Springer, Cham.
- Zhang, P., Guo, Z., Zhang, Z., Fu, H., White, J. C., Lynch, I. (2020). Nanomaterial transformation in the soil–plant system: implications for food safety and application in agriculture. *Small*, 16(21), 2000705.
- Zhang, P., Ma, Y., Xie, C., Guo, Z., He, X., Valsami-Jones, E., Zhang, Z. (2019). Plant species-dependent transformation and translocation of ceria nanoparticles. *Environmental Science: Nano*, 6(1), 60-67.
- Zhao, S., Su, X., Wang, Y., Yang, X., Bi, M., He, Q., Chen, Y. (2020). Copper oxide nanoparticles inhibited denitrifying enzymes and electron transport system activities to influence soil denitrification and N₂O emission. *Chemosphere*, 245, 125394.
- Zhou, D., Abdel-Fattah, A.I., and Keller, A.A. (2012). Clay particles destabilize engineered nanoparticles in aqueous environments. *Environmental Science & Technology*, 46, 7520–7526.

- Zidar, P., Kos, M., Ilič, E., Marolt, G., Drobne, D., Kokalj, A. J. (2019). Avoidance behaviour of isopods (*Porcellio scaber*) exposed to food or soil contaminated with Ag- and CeO₂-nanoparticles. *Applied Soil Ecology*, 141, 69-78.
- Zimmer, M., Topp, W. (1997). Does leaf litter quality influence population parameters of the common woodlouse, *Porcellio scaber* (Crustacea: Isopoda)? *Biology and Fertility of Soils*, 24(4), 435-441.

Chapter 2

Hypotheses, goals and outline of this thesis

1. Hypotheses

The potential of metallic ENMs to improve the quality of life and to contribute to economic growth and competitiveness of industry is widely recognized. However, the potential effects of these ENMs in terrestrial systems have received increased attention, due to their consequential release, potential persistence/accumulation into the environment and antimicrobial broad-spectrum. The deliberated application of metal-based ENMs in agricultural soils, as nano-agrochemicals or potential nano-agrochemicals [*e.g.*, Kocide[®]3000, nCu(OH)₂, nCuO] or unintentionally as part of biosolids (*e.g.*, containing Ag₂S NPs, as an aged form of silver nanoparticles), may induce changes in the soil microbiome activity, structure and composition. Therefore, this impact may result in negative consequences for the soil fertility and quality, posing a risk for the terrestrial ecosystem functions and overall services. In addition, this predicted disruption in the ecosystem may also result in economic losses in the agronomic sector, due to the interaction between soil microbiome and plants (in which soil microbiome may indirectly influence the quality/nutritional value in fruits/vegetables).

In the last three years, some studies have already shown the potential effect of these metallic ENMs on soil microbiome. However, there are few information regarding the impact of these emerging contaminants on soil microbiome in the presence of non-target soil biota, as an integrating element of an agroecosystem and as a crucial driver in soil microbiome. In fact, the activity, structure, composition and diversity of soil microbiome is widely influenced by the presence of soil invertebrates and plants, mainly due to the nutrient inputs, spread microbial communities through the soil, and changing the soil properties (*e.g.*, pH, oxygen, among others) (Bray and Wickings, 2019). As a direct consequence, the microbial responses to metal-based ENMs exposure are expected to be changed. Besides, the impact of these metallic ENMs was mainly assessed using simple experimental designs, such as microcosms as observed in Table 3 (Chapter 1). Although a simple approach can reduce environmental variables, it does not allow extrapolating the impact of these contaminants at the level of the agroecosystem.

Up to now, methodologies targeting the microbial community-level (*e.g.*, PCR-DGGE, NGS and Biolog[®]Ecoplates) are not included in the risk assessment regulations for these emerging contaminants. Thus, using different and complementary microbial

endpoints and methodologies can highlight the relevance of their inclusion in this regulation frameworks.

In order to tackle the challenge of understanding and assess metallic ENMs impact in soil microbiome using different exposure scenarios, including the non-target soil organisms and targeting distinct microbial endpoints, some hypotheses (H) will be tested in this work:

- H_I:** Metal-based ENMs induce changes in soil microbiome function, structure and composition.
- H_{II}:** Distinct formulations of ENMs distinctly affect the soil microbiome function, structure and composition.
- H_{III}:** The presence of invertebrates influences the effects of metal-based ENMs on the soil microbiome.
- H_{IV}:** Metal-based ENMs affect the soil rhizosphere bacterial community.
- H_V:** The ENMs influence the nitrogen cycle.

2. Goals

The main goal (G) of this study was to evaluate the effects of copper-based nanopesticides [Kocide[®]3000, nCuO and nCu(OH)₂] and simulated aged form of silver-based NPs (Ag₂S NPs) on the soil microbiome, at both structural/composition and functional levels, and using different exposure scenarios. To test the proposed hypothesis and to achieve the main goal, the following specific goals were established:

- G_I.** Evaluate the effect of copper-based ENMs long-term exposure on soil bacterial and fungal structure and diversity.
- G_{II}.** Evaluate the effect of copper-based ENMs long-term exposure on soil microbial function, using enzymatic assays and Community-Level Physiological Profile (CLPP).
- G_{III}.** Evaluate the effect of copper-based ENMs exposure on soil microbiome function and composition, under a more realistic exposure scenario (*i.e.*, indoor mesocosm experiments, which included soil invertebrates and plants).
- G_{IV}.** Evaluate the impact of copper-based ENMs on rhizosphere soil bacterial community, assessing soil enzymatic activity and bacterial community structure and diversity.

- Gv.** Evaluate the effect of Ag₂S NPs exposure on soil microbiome, simulating a real edaphic scenario at the agroecosystem level.
- Gvi.** Evaluate the role of Ag₂S NPs exposure in the relative abundance of nitrification related genes (*e.g.*, *amoA*, and *nxrB*) in soil microbiome, through quantitative PCR (qPCR).

3. Outline of this thesis

The current thesis is organized into eight chapters, as followed described:

Chapter 1: Introduction

In this chapter an overview and contextualization about the metal-based ENMs use and its impact in the terrestrial environment is given. Topics like metal-based ENMs source, environmental concentration and transformation, as well as its impacts on (non)target microorganisms (*e.g.*, soil microbiome) are addressed.

Chapter 2: Hypotheses, Goals and Thesis Structure

The hypothesis to test and goals to achieve in this thesis are pointed in this chapter. The chapter ends with an outline of the thesis and with a flowchart of the thesis methodology (Figure 1).

Chapter 3: Long-term effects of Cu(OH)₂-nanopesticide exposure on soil microbial communities

This study has been published in the international journal Environmental Pollution (<https://doi.org/10.1016/j.envpol.2020.116113>). In this study, the long-term impact of Cu(OH)₂-nanopesticide in soil microbiome was assessed in the absence and in the presence of *P. pruinosus* (H_I, H_{III}, G_I and G_{II}). After 90 days of exposure, analyses of several microbial endpoints, like soil enzymatic activity, carbon substrate utilization and structure of bacterial and fungal communities, were performed.

Chapter 4: Responses of soil microbiome to copper-based nanomaterials for agricultural applications

In this Chapter, structural and compositional effects of distinct formulations of copper-based NMs (50 mg kg^{-1} soil) were evaluated using indoor mesocosms (*e.g.*, multi-species design) (H_I, H_{II}, H_V, and G_{III}).

Chapter 5: Copper-based nanomaterials alter the rhizosphere bacterial community

Based on our previous work (Chapter 4), the impact of 50 mg kg^{-1} of copper-based NMs was assessed using soil enzymatic activity and bacterial community structure from rhizosphere soil. For this, the soil sampling was done considering the soil surrounding the roots of wheat (rhizosphere) (H_I, H_{II}, H_{III}, H_{IV}, and G_{IV}). These results were compared with bulk soil bacterial community (soil sampled from the top of the column mesocosm).

Chapter 6: Impact of Ag₂S NPs on soil bacterial community – a terrestrial mesocosm approach

In this work, indoor mesocosms (multi-species) were installed to investigate the effects of Ag₂S NPs (10 mg kg^{-1} soil) on the structure and function of soil microbiome (H_I, H_{III}, and G_{IV}). The study has been published in the international journal *Ecotoxicology and Environmental Safety* (<https://doi.org/10.1016/j.ecoenv.2020.111405>).

Chapter 7: The impact of Ag₂S NPs and AgNO₃ exposure in soil microbiome

Based on our previous work (Chapter 6) this chapter intended to achieve a deeper analysis of soil bacterial communities at composition and functional level (H_I, H_{III}, and G_V). Thus, we used a 16S rRNA gene metagenomics approach through Illumina technology. Also, a quantitative-PCR analysis was performed to assess the impact of Ag₂S NPs on the relative abundance of ammonia-oxidizing bacteria (AOB) and nitrite-oxidizing bacteria (NOB) (H_{IV} and G_{VI}). The current study has been published in the international journal: *Journal of Hazardous Materials* (<https://doi.org/10.1016/j.jhazmat.2021.126793>).

Chapter 8: General discussion and final conclusions

An overall discussion of the main study results and observations is provided, along with study limitations, major conclusions and future directions.

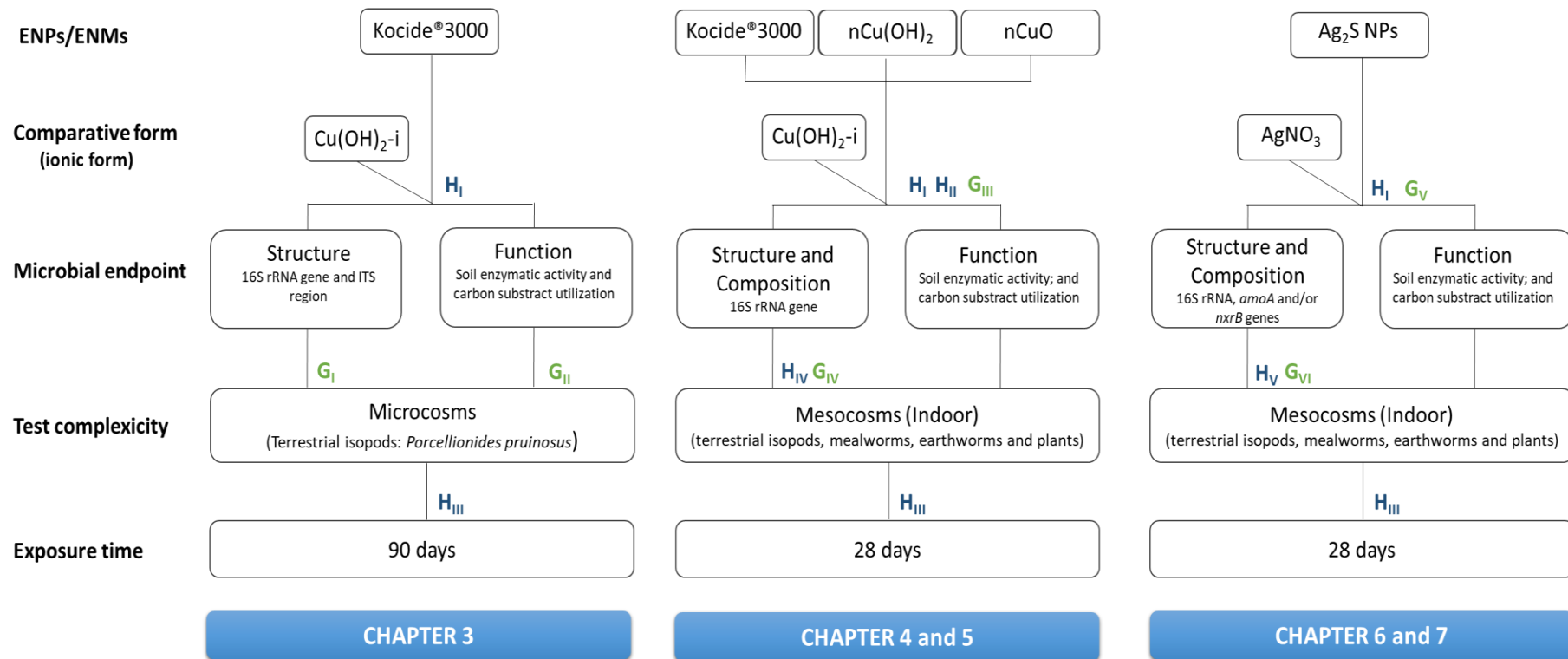


Figure 1. The scheme of the experimental approaches used in Chapters 3 to 7 to investigate effects of different metallic nanomaterials on soil microbiome. In figure, H (I to V) and G (I to VI) refers the hypotheses and goals of this thesis, respectively.

Chapter 3

Long-term effects of $\text{Cu}(\text{OH})_2$ nanopesticide exposure on soil microbial communities

Long-term effects of Cu(OH)₂ nanopesticide exposure on soil microbial communities

Peixoto, S., Henriques, I., Loureiro, S.

Environmental Pollution, 269, 116113, doi.org/10.1016/j.envpol.2020.116113

Abstract

Copper-based (nano)pesticides in agroecosystems may result in unintended consequences on non-target soil microbial communities, due to their antimicrobial broad spectrum. We studied the impact of a commercial Cu(OH)₂-nanopesticide, over 90 days, at single and season agricultural application doses, in the presence and absence of an edaphic organism (the isopod *Porcellionides pruinosus*), on microbial communities' function, structure and abundance. Results were compared to the effects of Cu(OH)₂-ionic. The nanopesticide application resulted in significant changes on both bacterial and fungal communities' structure, particularly at the season application. The exposed bacterial community presented a significantly lower richness, and higher diversity and evenness while the exposed fungal community presented lower diversity and richness. At the functional level, a significant increase on microbial ability of carbon utilization and a significant decrease on the β -glucosidase activity was observed for communities exposed to the nanopesticide. Regarding Cu forms, less pronounced effects were observed in soils spiked with Cu(OH)₂-ionic, which might result from lower Cu concentration in porewater. The presence of *P. pruinosus* did not induce significant changes in diversity indexes (fungal community) and community level physiological profiling, suggesting an attenuation of the nanopesticide effect. This study revealed that Cu(OH)₂-nanopesticide, at doses applied in agriculture, impact the soil microbial community, possibly affecting its ecological role. On the other hand, invertebrates may attenuate this effect, highlighting the importance of jointly including different interacting communities in the risk assessment of nanopesticides in soils.

Keywords: Copper hydroxide nanopesticide; Bacterial community; Fungal community; Structure; β -glucosidase activity; Community-Level Physiological Profiling.

1. Introduction

Agriculture is among the most important fields for nanotechnology application, with a recent emphasis in developing novel nano-agrochemicals (Kah, 2015). The development of these products involves the use of nano-sized particles (1-100 nm in one of their dimensions) with innovative and unique properties to improve crop productivity (Sekhon, 2014). Nanopesticides are new optimized strategies for prolonged and sustained release of ingredients and, consequently, with lower application rates than conventional pesticides and with fewer environmental consequences (Lowry *et al.*, 2019). Considering this, large amounts of nanomaterials (NM) from nanopesticides are expected in agroecosystems, due to their direct, intentional and repeated applications (Kah, 2015; Simonin *et al.*, 2018b). Nevertheless, the limited knowledge on the environmental fate and potential impacts of nanopesticides hampers the ability to estimate the specific benefits and risks of these new formulations, compared to conventional pesticides (Lowry *et al.*, 2019; Li *et al.*, 2019b; Kah *et al.*, 2018). Since there is a long worldwide tradition of using Cu-based pesticides, particularly in vineyards (Ballabio *et al.*, 2018), the contamination of agricultural soils with copper nanopesticides represents a primary environmental and toxicological concern. Recently, Ballabio and coworkers (2018) estimated the copper (Cu) concentration in EU lands of 49.26 mg kg⁻¹ for vineyards soils, by using a model based on the LUCAS Topsoil database. Due to extensive wine production, the Mediterranean area was estimated to have one the highest Cu levels in soils. Hence, for France and Italy, average Cu concentrations of 91.29 mg kg⁻¹ and 71.90 mg kg⁻¹ were estimated according to this model, respectively (Ballabio *et al.*, 2018). This may represent a potential risk to human health, because 14.6% of vineyard soil samples displayed values higher than 100 mg kg⁻¹ (Ballabio *et al.*, 2018), considered as a human health threshold. So, in order to minimize the Cu accumulation on soils, the European Commission stipulated a maximum average of 4 kg (Cu) ha⁻¹ year⁻¹ application of copper in soil, with a maximum of 28 kg (Cu) ha⁻¹ year⁻¹ in a seven-year period (European Commission, 2018).

Currently, copper-based nanopesticides are available in the market and used in agriculture. The commercial pesticide Kocide®3000 has been used in several studies and contains NM as the active ingredient [Cu(OH)₂] (Li *et al.*, 2019a; Zhang *et al.*, 2020). The copper particles in this product were characterized as nanosheets composed

by nano-needles (10-15 nm in diameter and 300-600 nm in length), and presented a great solubility in water (Li *et al.*, 2019a). Besides, the formulation of Kocide®3000 contains 26.5% of copper, while the remained noncopper ingredients are present in a percentage of 73.5% (Simonin *et al.*, 2018b). The regulation of this type of pesticides is based on the active ingredient, disregarding the novel properties acquired. Therefore, and although its application on agroecosystem protects the crops from fungal and bacterial diseases, its antimicrobial broad-spectrum may result in unintended consequences on soil microbial communities (Keiblinger *et al.*, 2018), including on non-target microorganisms involved in plant nutrition, such as mycorrhizal communities and nitrogen-fixing bacteria (Simonin *et al.*, 2018a).

Besides, in agroecosystems the presence of invertebrates might influence the bioavailability of contaminants in soils through their activity, increasing the oxygenation and the input of organic matter (Abd El-Wakeil, 2015). The microbial responses to pollutants are expected to change in the presence of invertebrates, since their activity may, for instance, increase the abundance of microbial community (*e.g.*, through the introduction of organism's faeces in soil) or promote soil aeration. For instance, isopods have an intrinsic relation with the soil microbial community because they can influence the proliferation of different bacteria/fungi, ultimately resulting in a structural and composition change of the soil microbial communities. Their faeces have a high nutritional value, and microbial colonization is prone to occur (Zimmer and Topp, 2002). One example of these organisms are terrestrial isopods, which are considered as good bio-indicators for soil quality (regarding the use of organic chemicals), and are widely distributed, being some species synanthropic (van Gestel and Loureiro, 2018). Therefore, understand how the microbial community behaves in the presence of a beneficial soil invertebrate, when exposed to chemical stressors, is crucial to derive accurate soil functional responses.

To date, the literature related to Cu nanopesticides has essentially focused on material characterization (Adeleye *et al.*, 2014; Li *et al.*, 2019a), environmental fate (Keller *et al.*, 2017), and toxicity to target-organisms, such as plants (Zhang *et al.*, 2017; Zhao *et al.*, 2017; Simonin *et al.*, 2018b) and collembola (Neves *et al.*, 2019).

Regarding microbial communities, a negative impact of Cu(OH)₂-nanopesticide has recently been reported on function-related parameters, like nitrogen cycling genes (Guan *et al.*, 2020) and soil enzymatic activities (Zhang *et al.*, 2019), and also at the structural level (Keiblinger *et al.*, 2018; Zhang *et al.*, 2020). But none has reported how

communities of different taxa (like microbes and invertebrates) are affected by this nanopesticides regarding their joint function in decomposition processes.

The objective of the present work is to investigate the long-term impact of commercial pesticide - Kocide[®]3000, described in the literature as having nanopesticide characteristics, on the soil microbial communities' structure and their functions related with different nutrient cycles (*e.g.*, soil enzymatic activity). Thus, we performed a 90-day soil microcosm experiment to assess the effects of this nanopesticide at recommended application rates for vineyard areas. Considering the need of more realism in exposure scenarios, we simulated the synergistic relationship between terrestrial isopods and microbial communities. Therefore, the synanthropic isopod *Porcellionides pruinosus* was chosen as a driver in the microbial community shift, being a copper tolerant species but there is still no information available about the influence of this organism on microbial communities previous exposed to the Cu(OH)₂-nanopesticide. Additionally, the bioavailable Cu fraction in soil porewater was also monitored to infer possible explanations for the differences in the microbial responses to Cu(OH)₂ formulations.

2. Material and methods

2.1. Experimental set up

The LUFA 2.2 soil (LUFA-Speyer, SP 2.2 1118, Speyer, Germany) was the selected soil, with the following properties: pH of 5.5 ± 0.2 (0.01 M CaCl₂); $1.61 \pm 0.2\%$ organic C; $0.17 \pm 0.02\%$ nitrogen; $7.3 \pm 1.2\%$ clay; $13.8 \pm 2.7\%$ silt; $78.9 \pm 3.5\%$ sand; $40 \pm 3.0\%$ water holding capacity (WHC); $10.0 \pm 0.70\%$ cation exchange capacity (100 cmol⁺/kg).

Microcosm experiments were performed including three conditions: uncontaminated soil – negative control (CT), soil spiked with Cu(OH)₂-nanopesticide, and soil spiked with ionic Cu(OH)₂. The commercial formulation Kocide[®]3000 was chosen as the Cu(OH)₂-nanopesticide (DuPont Co. TM, Wilmington, DE, United States). This commercial formulation has already been characterized within work done in the ERANET SIINN NanoFARM project (Li *et al.*, 2019a), showing 10–15 nm in diameter nano-needles, 300–600 nm long, with a zeta potential averaging -38 ± 3.5 mV (mean \pm s.d.). The Cu(OH)₂-ionic form used as control was purchased from Sigma-Aldrich (99 % purity, CAS 7761-88-8, Germany).

Two copper concentrations were tested, corresponding to the amount recommended by manufacturer for vineyard areas for a single application [0.45 mg (Cu) kg⁻¹ soil] and per season [19.86 mg (Cu). kg⁻¹ soil]. Soil-spiking was performed by adding the copper compounds directly into the soils, and afterwards adjusting to 50 % soil water holding capacity (WHC), by adding de-ionized water. After spiked and watered, soils were mixed manually in order to obtain a homogeneous exposure throughout replicates. For the control batch, the soil was prepared following the same protocol but using distilled water only. Soil was distributed into plastic boxes (each box containing 40 g of soil), considering 10 replicates per treatment. During the experiment, soil moisture was checked every three days and adjusted by adding distilled water. Sampling was conducted two days after soil-spiking and after 90 days. In some methodological procedures/endpoints' measurements (see below) both sampling times were used, while in others, only the 90 days sampling was used.

A similar experimental set up was also carried out with *P. pruinosus* (Crustacea, Isopoda), with three isopods per replicated microcosm, which were added at day 2 after soil spiking (or in control microcosms). Sterilized and dried food was supplied (3 discs of *Alnus glutinosa* leaves) weekly, including in the set up without isopods. Isopods were acquired from laboratory cultures maintained at the Department of Biology of the University of Aveiro (21 ± 2°C and 16:8 h light/dark photoperiod). Only adults were used yet pregnant females, isopods with abnormalities, without antenna or under molting were excluded (Tourinho *et al.*, 2015). During the experiment, no statistical differences between treatments were detected in isopods mortality (Table S1) and soil pH (Table S2).

2.2. Copper dissolution analysis

Porewater was collected by saturating 25g of soil with ultrapure water for 48 h. Samples were centrifuged at 2862 g for 90 min (Eppendorf 5810R centrifuge). The supernatant was collected and filtered using a cellulose nitrate filter (0.45 µm pore size). The HNO₃ (nitric acid trace metal basics, CAS Number 7697-37-2, purchased from Sigma-Aldrich Biotechnology LP, Germany) was added on porewater filtered samples, to reach a pH=2. Samples were stored at 4°C until posterior analysis. Then, samples were digested, for total Cu quantification by Inductively Coupled Plasma - Atomic Emission Spectroscopy (ICP-AEP) (Horiba Jobin-Yvon, France, Ultima, equipped with autosampler AS500). Calibration procedures used known copper concentrations

solutions, and only the correlation coefficient greater than 0.999 was considered. The ICP-AEP instrument detection limit was 0.7 µg l⁻¹.

2.3. Assessment of bacterial growth and heterotrophic plate counts (HPC)

Heterotrophic plate counts (HPC) were obtained using the nutrient agar (NA) (Merck, Darmstadt, Germany). Three grams of test soil were suspended into 25 mL of phosphate saline buffer (P-BS), in four sub-replicates. Suspensions were shaken at 200 rpm with twenty sterile glass beads (4 mm) for 10 min at 20°C followed by (1:100) dilutions in phosphate buffered saline. Then this dilution was placed into the medium plates and incubated at 21°C ±2, for three days.

To prevent growth of fungi, culture medium was supplemented with 0.2 mg L⁻¹ of cycloheximide (95% purity, Acros organics, New Jersey). The counts were reported as colony forming units (CFUs) per gram of soil. Only the season application from both Cu(OH)₂ forms (nanopesticide, and ionic), plus the negative control, were analysed. Also, the presence of *P. pruinosis* on contaminated soils was included in this analysis. Samples were used from the beginning of experience (after two days of soil spiking) and after 90 days of exposure.

2.4. Molecular analysis

2.4.1. Total DNA extraction

Soil (0.25 g) was collected at each sampling time and from each microcosm condition and replicate and transferred into UltraClean[®] bead tubes (MoBio Laboratories, Inc., Carlsbad, CA). DNA was extracted following the instructions of the manufacturer.

2.4.2. PCR reaction

The V3 region of the 16S rRNA gene was amplified using a nested PCR strategy. First, the 16S rRNA gene was amplified using the universal primers 27F (5'-AGAGTTTGATCCTGGCTCAG-3') and 1492R (5'-GGTTACCTTGTTACGACTT-3'). The PCR mixture (25 µL) contained: nuclease-free water (16.25 µL), NZYTaQ 2x Green Master Mix (6.25 µL; 2.5 mM MgCl₂; 200 mM dNTPs; 0.2 U/µL DNA polymerase) (NZYTech, Portugal), each primer (0.75 µL of a 10 mM solution), and DNA sample (1 µL corresponding to 50-100 ng of DNA). The amplification conditions consisted of an initial denaturation step (94°C for 3 min), followed by 30 cycles comprising the following steps: denaturation (94°C for 1 min), annealing (52°C for 1

min) and extension (72°C for 2 min), and a final extension step (72°C for 10 min). The second PCR was conducted as described above, using 1.6 µL of the first PCR product as template, and the universal primers [338f-GC (5'-GACTCCTACGGGAGGCAGCAG-3') and 518r (5'-ATTACCGCGGCTGCTGG-3')], with a GC clamp attached to the forward primer (Muyzer *et al.*, 1993). Amplification conditions were: denaturation (94 °C for 5 min), annealing (52 °C for 30 sec) and extension (72 °C for 30 sec), and a final extension step (72 °C for 30 min).

For analysis of the fungal community, PCR products were generated using primers for the ITS region: ITS1F (5'-CTTGGTCATTTAGAGGAAGTAA-3') and ITS2 (5'-GCTGCGTTCTTCATCGATGC-3'). A 40- base GC clamp (CGCCCGGGGCGCGCCCCGGGCGGGGCGGGGGCACGGGGGG) was attached to the primer ITS1F at the 5' end. The thermocycling program was: 95 °C for 5 min; and the 30 cycles with 95°C for 30 sec, 52°C for 60 sec and 72°C for 60 sec, and the final extension 72°C for 30 min. A nested-PCR was conducted with the same PCR mixture and temperature profile as the first PCR, in Bio-Rad Thermal Cycler (Bio-Rad Laboratories, CA, USA).

Positive and negative controls were included, using as template purified bacterial (*Escherichia coli* ATCC 25922) DNA and nuclease-free water, respectively. PCR products were verified by electrophoresis (1.5% agarose gel) and stained with ethidium bromide (15 min).

2.4.3. Denaturing Gradient Gel Electrophoresis

PCR products were loaded into 8% (w/v) polyacrylamide (37.5:1, acrylamide:bisacrylamide) gels with denaturing gradient ranging from 35% to 62.5% for bacterial communities, and 10% to 50% for fungal communities [100% denaturant corresponded to 7 M urea and 40% (v/v) formamide]. The electrophoresis was performed on a D-Code Universal Mutation Detection System (Bio-Rad) with in 1X TAE buffer (Sigma-Aldrich, Germany) at 60°C in two steps, (1) for 15 min at 20 V and (2) for 16h at 70 V. Gels were stained in a solution of ethidium bromide (0.5 µg/mL) for 5 minutes and rinsed in distilled water (20 min). Images (Figure S1) were captured by the Molecular Imager[®]Gel Doc[™] XR+ System (Bio Rad Laboratories, Hercules, California, USA).

DGGE patterns were analyzed using Bionumerics Software (Applied Maths, Belgium) and cluster analysis obtained by UPGMA method (group average method) applying Jaccard coefficient.

2.5. Assessment of microbial activity

2.5.1. Community level physiological profiling (CLPP)

Community-Level Physiological Profiling (CLPP) was performed using 96-well Biolog Ecoplates™ that contained 31 different carbon sources; each plate has three replicates and control well. The rate of utilization of these carbon sources was verified by the reduction of tetrazolium violet redox dye, which changed from colorless to purple, upon microbial respiration and dehydrogenation of the respective carbon source (Zhai *et al.*, 2017). The procedure was adapted from Samarajeewa (*et al.*, 2017). Three grams of soil sampled only at day 90 were added to 27 mL of sterile water with 20 glass beads and shaken at 200 rpm for 10 min at 20°C. The suspension was diluted 100-fold to contain a bacterial density of approximately 10⁷ cell mL⁻¹, and was shaken vigorously for 30s, and then left for 45 min. Following, one hundred microliters of this solution were inoculated into each well, followed by incubation of the plates at 21°C±2.

The color development was measured by reading the Biolog®Ecoplate using a spectrophotometer (Biolog, MicroStation TM, CA, USA) at 24 h-intervals during 6 days of plates incubation.

The color development was recorded as Average Well Color Development (AWCD), defined as:

$$AWCD = \sum_{31} \frac{OD_i}{31}$$

Where, OD_{*i*} is the optical density (OD) for each well, corrected by subtracting the OD of the blank well (without a carbon source). The number (31) represents the number of wells with different carbon substrates.

Additionally, the 31 carbon substrates from Biolog®Ecoplate were divided into five groups: (1) carbohydrates, (2) carboxylic acids, (3) amines and amides, (4) amino acids, and (5) polymers. Thus, the Substrate Average Well Color Development (SAWCD) index was calculated based on optical density values obtained after 144 h of Biolog®Ecoplate incubation for each soil treatment:

$$SAWCD = \sum_n \frac{OD_i}{n}$$

Where, OD_i is the optical density (OD) for each well, corrected by subtracting the OD of the blank well. The number (n) represents the number of wells with different carbon substrates for each class.

2.5.2. Enzymatic activity

Dehydrogenase (DHA), β -glucosidase (β G), acid phosphatase (AP), and arylsulfatase (AS) and urease (UA) activities were determined according to the methods described by (Dick *et al.*, 1997), with some modifications. The DHA activity was evaluated by suspending soil (2.5 g) in a 3% of triphenyl tetrazolium chloride (TTC) solution, followed by 24 h of incubation at 37°C, in darkness (Dick *et al.*, 1997). The triphenyl formazan (TPF) produced was extracted with methanol. Then, soil samples were centrifuged (3000 rpm for 15 min) and the supernatant was measured photometrically at 485 nm. The results were expressed as μg of TPF.g⁻¹.24 h. The β G, AS and AP activities were measured using specific substrate solutions: 4-nitrophenyl β -D-glucopyranoside substrate (0.05 M) (Acros organics, 99% of purity); 4-nitrophenyl sulfate (0.05 M) (Acros organics, 99% of purity); and *p*-nitrophenyl phosphate (0.05 M) (Sigma-Aldrich, 99% of purity), respectively (Dick *et al.*, 1997; Loureiro *et al.*, 2007; Tabatabai 1994). The soil samples (0.5 g) were incubated with 0.5 mL of substrate solution and 2 mL of the modified universal buffer (MUB) with pH 6.5 (β G) or pH 6.0 (AP); or acetate buffer (0.5 M; pH=5.8) for AS activity (Tabatabai, 1994; Loureiro *et al.*, 2007). After 1 h of samples incubation at 37°C, the reaction was stopped with CaCl₂ (0.5 M) and NaOH (0.5 M). Afterward, the soil samples were centrifuged at 3000 rpm for 15 minutes, and the supernatant was measured spectrophotometrically at wavelengths of 410 nm (β G, AP, AS). The urease activity (UA) was performed based on Kandeler & Gerber (1988).

All enzymatic activities were readed in 96 wells microplates, in five replicates and fourth technical replicates (Loureiro *et al.*, 2007) using a microplate reader spectrophotometer (Thermo Scientific Multiskan Spectrum, USA).

2.6. Statistical analysis

Assumptions of homogeneity of variance and test for normality of distributions were verified applying Levene's test and Shapiro-Wilk's test, using SPSS version 12.5. A level of $p=0.05$ was considered to assume statistical significance. A three-way ANOVA was conducted to assess the effect among the soil treatments [control, Cu(OH)₂-

nanopesticide and Cu(OH)₂-ionic], concentration tested (single or season application), and the absence/presence of the *P. pruinosa* (diversity indexes) or exposure time (in porewater measurements). Additionally, the Tukey's HSD (honestly significant difference) test was applied for the post-hoc analysis, to obtain multiple comparisons between treatments.

Differences in bacterial counts were performed using a two-way ANOVA, considering the absence or presence of the *P. pruinosa* among the soil treatments.

A repeated measured ANOVA was performed to assess the effect of the carbon consumption (AWCD) during 144 h of reads of the Biolog[®]Ecoplate, considering the following factors: incubation period of the Biolog[®]Ecoplate (0 to 144 h), soil treatments [CT, Cu(OH)₂-nanopesticide and Cu(OH)₂-ionic], concentration tested (single or season application), and the absence or presence of the *P. pruinosa*. A multiple comparison between factors were performed using the Tukey's HSD, as a post-hoc analysis.

The spatial distribution of soil enzymatic activities was performed using PRIMER v6 software (Primer-E Ltd., Plymouth, UK). Principal Coordinate Analysis (PCoA) was constructed based on Euclidean distance, after the data normalized. The vectors were constructed based on Pearson correlation ($R > 0.2$) and indicates the different soil enzymatic activities. Additionally, a PERMANOVA analysis was performed (999 permutations), to obtain the statistical significances between soil treatments, exposure test concentration, *P. pruinosa* presence/absent, and time of exposure.

Also, DGGE band matrix was analyzed in PRIMER v6 software. Band position and intensity was used to calculate the richness, the Shannon-Wiener diversity (H') and Pielou's index (J'). A three-way ANOVA followed by the Tukey's HSD was used to discriminate differences in these indices. Further, two-dimensional Principal Coordinate Analysis (PCoA) was performed based on the Jaccard similarity. Also, differences in soil microbial community structure among treatments were evaluated through PERMANOVA analysis based on 999 permutations.

3. Results

3.1. Copper in soil porewater

Total copper was quantified in soil porewater (Figure 1), after 2 and 90 days of exposure (*i.e.*, soil spiking) and in the presence/absence of *P. pruinosa*.

In the absence of *P. pruinosus* (Figure 1 A)), only porewater from soils with the highest concentration (season application) of the Cu(OH)₂-nanopesticide revealed a significantly higher copper level (F=26.73; p<0.001). For these samples copper levels were detected in a range between $73.11 \pm 8.56 \mu\text{g (Cu) L}^{-1}$ and $54.15 \pm 4.39 \mu\text{g (Cu) L}^{-1}$ for 2 and 90 days of exposure, respectively. Samples from the Cu(OH)₂-ionic exposure showed similar copper levels to the control, in a range from 8.4 ± 0.56 to $17 \pm 0.45 \mu\text{g (Cu) L}^{-1}$. Over-time a slight decrease was detected in copper concentration in both contaminated soils but not significantly (F=1.55; p=0.222).

In the presence of *P. pruinosus* (Figure 1 B)), also only soils with the highest concentration of Cu(OH)₂-nanopesticide revealed a significantly higher level of copper in soil porewater (F=30.83; p<0.001). Additionally, the copper dissolution significantly decreased during the time of exposure (F= 7.26; p=0.014). For these samples, copper levels were detected in a range of $61.35 \pm 10.92 \mu\text{g (Cu) L}^{-1}$ and $35.80 \pm 2.88 \mu\text{g (Cu) L}^{-1}$, for 2 and 90 days of exposure, respectively.

Regardless the time of exposure, the presence of *P. pruinosus* did not change the levels of dissolved copper in porewater (Day 2: F= 2.86; p=0.106; Day 90: F= 1.86; p=0.188).

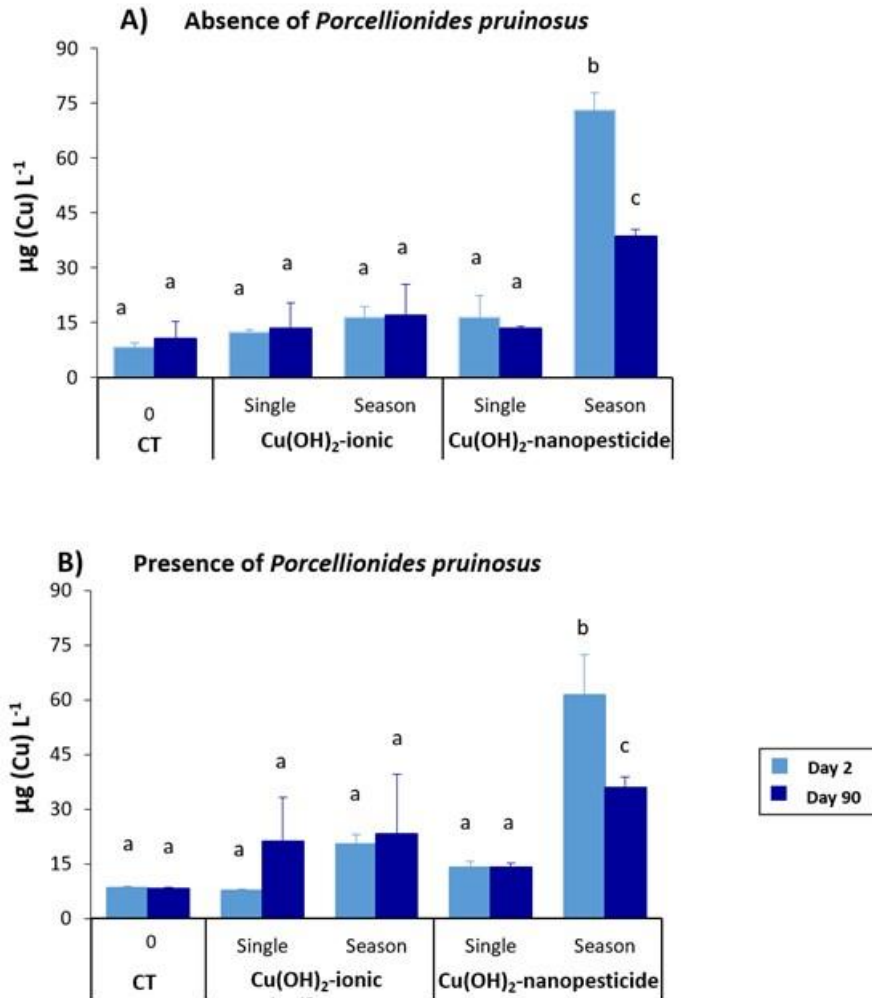


Figure 1. The dissolution of Cu(OH)₂-nanopesticide and Cu(OH)₂-ionic in soil porewater after 2 and 90 days of exposure, in the absence (A)) or in the presence of *Porcellionides pruinosus* (B)). The data was expressed as µg (Cu) L⁻¹ of porewater (± standard deviation). The soil treatments included the non-exposed soil (CT), soil exposed to Cu(OH)₂-nanopesticide and soil exposed to Cu(OH)₂-ionic, at two different concentrations (single and season). Different letters (^{a,b}) indicate statistical significance ($p \leq 0.05$) between treatments and the respective control, using the three-way ANOVA (Tukey HSD).

3.2. Structural effects of Cu(OH)₂ nanopesticide on soil microbial community

3.2.1. Assessment of heterotrophic bacterial counts

Colony forming units were determined for non-contaminated soil and the season application contaminated soil for both contaminants (Figure 2). After 90 days of exposure, the soil contaminated with Cu(OH)₂-nanopesticide presented a significant reduction ($F=57.24$; $p < 0.001$) on bacterial counts, with a reduction of 42% towards the

control soil. On the other hand, an increase of 12% was observed for samples spiked with Cu(OH)₂-ionic (F=57.24; p=0.024).

The presence of *P. pruinus* significantly increased, around 26%, the abundance of heterotrophic bacteria in control soils (F=209.65, p<0.001). Additionally, in the presence of *P. pruinus* in contaminated soils it was observed a slight increase of 0.19% CFU g⁻¹ soil for Cu(OH)₂-ionic (F=209; p=0.113) and a decrease of 48% for Cu(OH)₂-nanopesticide (F=209; p<0.001).

Besides, the Cu(OH)₂ forms exhibited a distinct and significant impact on heterotrophic bacteria counts, regardless of the *P. pruinus* presence in contaminated soils (F=200.65; p<0.001). In fact, soils contaminated with Cu(OH)₂-nanopesticide presented lower abundance of heterotrophic bacteria than soils contaminated with Cu(OH)₂-ionic.

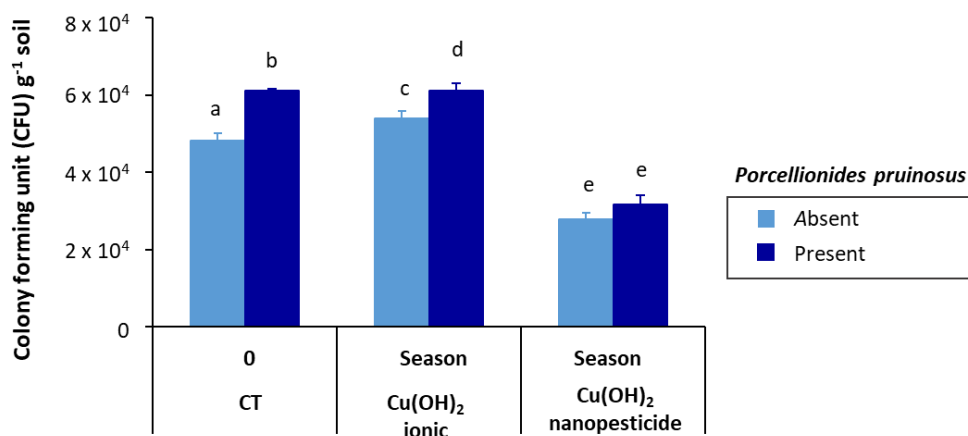


Figure 2. Long-term effect, 90 days of exposure of Cu(OH)₂ on soil heterotrophic bacteria count, as measured by CFU g⁻¹ soil (± standard deviation), in the absence (A) or in the presence of *Porcellionides pruinus* (B). The soil treatments included the non-exposed soil (CT), soil exposed to Cu(OH)₂-nanopesticide and to Cu(OH)₂-ionic, at the season application rate. Different letters (^{a,b}) indicates a statistic significant (p≤0.05) among the soil treatments and *Porcellionides pruinus* presence, using the two-way ANOVA (Tukey HSD).

3.2.2. Soil bacterial communities

Principal component analysis (PCoA) of the DGGE data of bacterial communities (Figure 3 A)) showed a significant spatial separation between contaminated soil samples and the control soil (PERMANOVA analysis: F=15.32; P < 0.001). Also, the structure of bacterial communities exposed to different copper forms was significantly different (PERMANOVA analysis: t=3.56; P=0.001) and dependent on the concentration (PERMANOVA analysis: t=2.98; P=0.001). Similar results were obtained when *P.*

pruinus was present (PCoA – Figure 3 B)): a significant spatial separation between contaminated and non-contaminated soils (PERMANOVA analysis: $F=16.55$; $P=0.001$), significant differences between communities exposed to different copper forms (PERMANOVA analysis: $t=22.17$; $P=0.001$), and differences among the concentrations tested (PERMANOVA analysis: $t=12.39$, $P=0.001$).

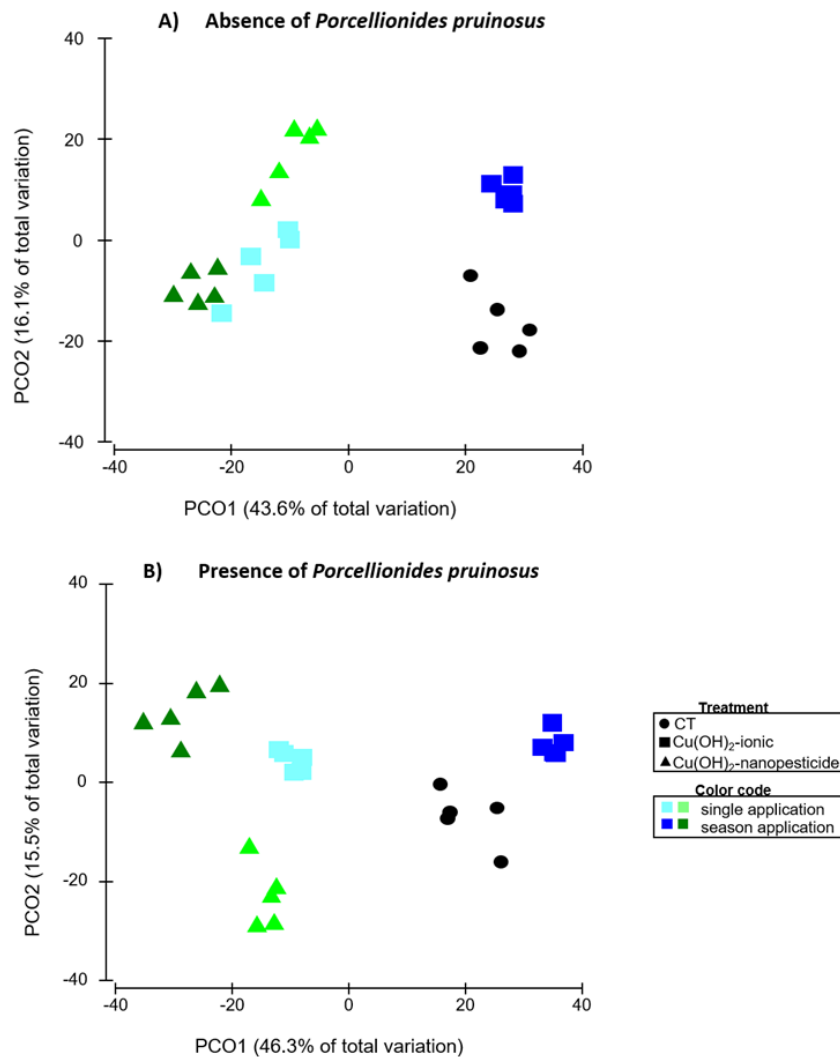


Figure 3. Principal Coordinates analysis (PCoA) of DGGE profiles representing the structural effects of the nanopesticide and of ionic $\text{Cu}(\text{OH})_2$ on soil bacterial communities in the absence (A) or in the presence of *Porcellionides pruinosus* (B). The PCoA was constructed based on Jaccard similarity from DGGE profiling at 90 days of exposure. Soil treatments included the non-exposed soil (CT), soil exposed to $\text{Cu}(\text{OH})_2$ -nanopesticide and to $\text{Cu}(\text{OH})_2$ -ionic, at two different application rates (single or season).

Richness (Table 1) was significantly lower in soils contaminated with both copper forms, towards the respective control ($F = 25.27$; $p < 0.001$). A significant lower number of bands was observed in soils with Cu(OH)₂-nanopesticide compared to soils contaminated with the ionic form ($F=39.89$, $p < 0.001$). Also, soils exposed to the season application exhibited a significantly lower richness in comparison to the single application, regardless of the copper form. On the other hand, diversity (H') and evenness (J') of the bacterial community were significantly higher in contaminated soils (H' : $F=3.30$, $p < 0.001$; J' : $F=13.95$, $p=0.001$) than in control soils, regardless of copper form ($F=3.30$, $p=0.177$). Also, at the season application rate, an increased diversity ($F=11.63$, $p=0.002$) and homogeneity ($F=7.93$, $p=0.008$) were depicted, when compared to the single application rate.

The presence of *P. pruinosis* in soils did not influence the effects of both forms of the contaminant regarding richness ($F=1.22$, $p=0.277$), evenness ($F=3.40$, $p=0.073$) nor diversity ($F=0.03$, $p=0.872$).

Table 1. The richness (number of bands; *S*), Shannon-Wiener (diversity index; *H'*) and Pielou's (evenness index; *J*) indexes of the soil bacterial and fungal communities exposed to Cu(OH)₂ in nanopesticide or ionic form, after 90 days of soil exposure. These effects were assessed in the absence or presence of *Porcellionides pruinosus*. Values are presented per mean ± standard deviation. The soil treatments included the non-exposed soil (CT), soil exposed to Cu(OH)₂-nanopesticide and to Cu(OH)₂-ionic, at two different concentrations (single and season application).

Community	Treatment	Application	S			J'			H'		
Bacterial community	Non-exposed soil	0	41 ^a	±	1	0.75 ^a	±	0.02	2.78 ^a	±	0.09
	Cu(OH) ₂ -ionic	Single	32^b	±	2	0.92^b	±	0.02	3.21^b	±	0.09
	Cu(OH) ₂ -nanopesticide	Single	31^b	±	2	0.89^c	±	0.10	3.05 ^a	±	0.35
	Cu(OH) ₂ -ionic	Season	39^c	±	2	0.92^b	±	0.03	3.37^b	±	0.08
	Cu(OH) ₂ -nanopesticide	Season	33^b	±	1	0.94^c	±	0.01	3.30^b	±	0.04
Bacterial community in the presence of <i>P. pruinosus</i>	Non-exposed soil	0	46 ^a	±	4	0.65 ^a	±	0.23	2.46 ^a	±	0.87
	Cu(OH) ₂ -ionic	Single	34^{bd}	±	2	0.84^b	±	0.07	2.97 ^a	±	0.24
	Cu(OH) ₂ -nanopesticide	Single	33^b	±	1	0.88^c	±	0.03	3.08 ^a	±	0.09
	Cu(OH) ₂ -ionic	Season	38^d	±	1	0.94^c	±	0.01	3.40^b	±	0.04
	Cu(OH) ₂ -nanopesticide	Season	29^e	±	2	0.94^c	±	0.02	3.16^c	±	0.07
Fungal community	Non-exposed soil	0	29 ^a	±	2	0.73 ^a	±	0.02	2.46 ^a	±	0.09
	Cu(OH) ₂ -ionic	Single	26 ^{ad}	±	1	0.76 ^a	±	0.03	2.48 ^{ab}	±	0.10
	Cu(OH) ₂ -nanopesticide	Single	25 ^{ade}	±	1	0.74 ^a	±	0.01	2.38 ^{ab}	±	0.05
	Cu(OH) ₂ -ionic	Season	25 ^{ade}	±	1	0.78 ^a	±	0.02	2.49 ^{ab}	±	0.07
	Cu(OH) ₂ -nanopesticide	Season	21^{bee}	±	0	0.73 ^a	±	0.04	2.24 ^{ab}	±	0.11
Fungal community in presence of <i>P. pruinosus</i>	Non-exposed soil	0	27 ^{ad}	±	1	0.66 ^b	±	0.03	2.17 ^{ab}	±	0.09
	Cu(OH) ₂ -ionic	Single	25 ^{ade}	±	1	0.67 ^b	±	0.03	2.18 ^{ab}	±	0.10
	Cu(OH) ₂ -nanopesticide	Single	22 ^{abcde}	±	7	0.70 ^b	±	0.07	2.13 ^{ab}	±	0.44
	Cu(OH) ₂ -ionic	Season	26 ^{ad}	±	2	0.66 ^b	±	0.06	2.14 ^{ab}	±	0.23
	Cu(OH) ₂ -nanopesticide	Season	18^{bc}	±	0	0.70 ^b	±	0.13	2.02^b	±	0.36

Different letters (^{a,b}) indicate differences among soil treatments for each bacterial or fungal communities, regardless of the presence of *Porcellionides pruinosus* (p<0.05; Three-way ANOVA – Tukey HSD). The bold number highlights differences between soil treatment toward to the respective control.

3.2.3. Soil fungal communities

Analysis of the DGGE data of fungal communities (Figure 4 A)) showed significant differences between samples exposed to Cu(OH)₂ and the non-exposed soils (PERMANOVA analysis: $F=3.91$, $P=0.002$). Also, the structure of fungal communities exposed to different copper forms was significantly different (PERMANOVA analysis: $t=2.02$, $P=0.001$). Regarding the copper forms, the effect was dependent on the concentration (PERMANOVA analysis: $F=2.44$, $P=0.018$). The presence of *P. pruinosis* in soils (Figure 4 B)) did not change the trend of a spatial separation between exposed soils and the respective control (PERMANOVA analysis: $F= 3.37$, $P=0.001$). However, only at the season application rate the communities exposed to both copper formulations were significantly different from each other (PERMANOVA analysis: $t=2.04$, $P=0.008$).

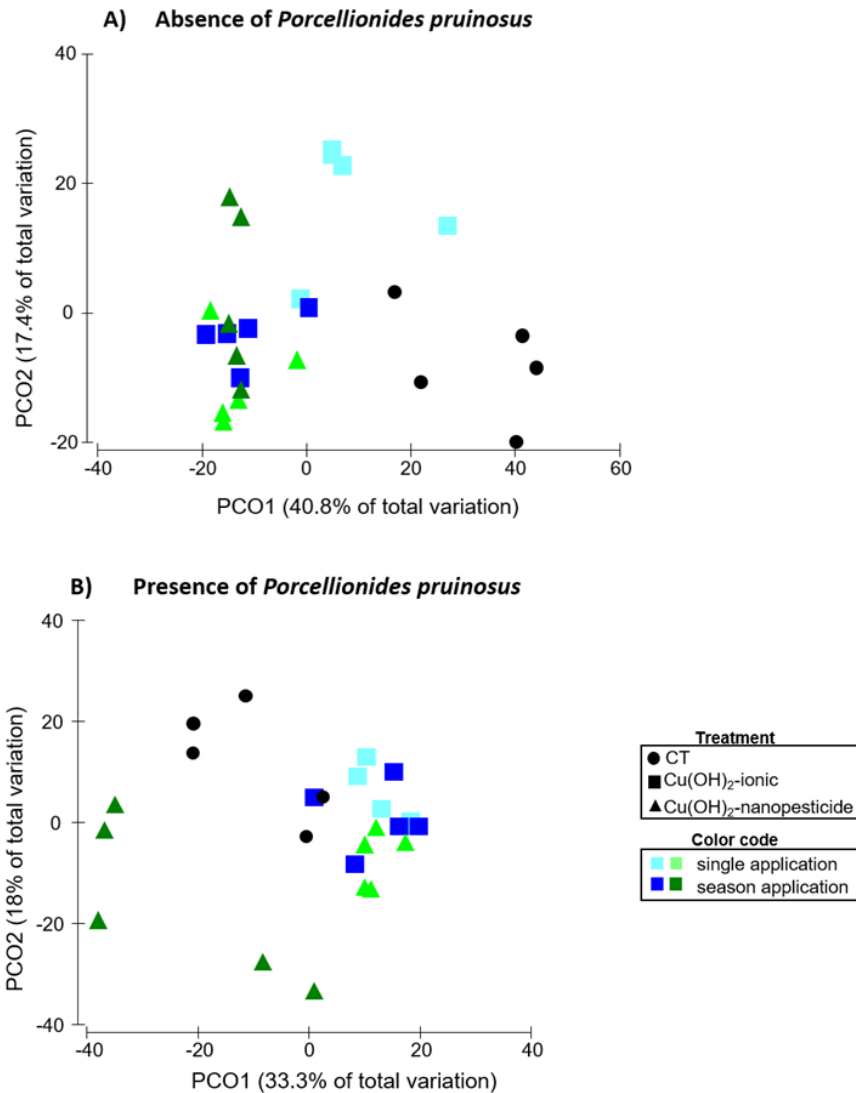


Figure 4. Principal Coordinates analysis (PCoA) of DGGE profiles representing the structural effects of the nanopesticide and of ionic Cu(OH)₂ on soil fungal communities in the absence (A)) or in the presence of *Porcellionides pruinosus* (B)). The PCoA was constructed based on Jaccard similarity from DGGE profiling at 90 days of exposure. Soil treatments included the non-exposed soil (CT), soil exposed to Cu(OH)₂-nanopesticide and to Cu(OH)₂-ionic, at two different application rates (single or season).

In the absence of the isopod, significant lower richness (Table 1) was detected only in exposed soils to Cu(OH)₂-nanopesticide, at the season application ($F=20.5$, $p<0.001$). The diversity and evenness of fungal communities were not significantly affected by the copper exposure regardless of the application rate (H' : $F=0.658$, $p=0.422$; J' : $F=0.28$, $p=0.868$). Although in the presence of *P. pruinosus* copper did not influence the richness of the fungal communities in soils ($F=2.85$, $p=0.099$), a significant decrease in

the diversity ($F=17.70$, $p<0.001$) and evenness ($F=17.29$, $p<0.001$) was detected, regardless of the copper form and the application rate.

3.3. Effects of Cu(OH)₂ nanopesticide on microbial activity

3.3.1. Community level physiological profiling (CLPP)

After 90 days of exposure, the microbial community from the control soil used most carbon sources present in Biolog[®]Ecoplate, except the α -cyclodextrin, α -ketobutyric and α -D-lactone substrates (Table S3). On the other hand, control soils with *P. pruinus* showed a microbial community capable of using all carbon sources (31) from the Biolog[®]Ecoplate.

Using repeated measures ANOVA, a significant increase in carbon consumption during the incubation time of the Biolog[®]Ecoplate was observed, being detected after 48 h to 120 h of incubation ($F=497.3$, $p<0.001$) (Figure 5 A)). After this 120h till 144h, in the absence of isopods, similar values were obtained suggesting a stabilization of carbon consumption (120 h=144 h: $F=497.3$; $p=0.075$). On the other hand, communities in the presence of *P. pruinus* (Figure 5 B)) presented a significant increase in carbon consumption after 48 h to 120 h and 144 h of Biolog[®]Ecoplate incubation ($F=750.9$, $p<0.001$).

Communities exposed to Cu(OH)₂-nanopesticide showed to be more metabolically active than communities from the control soil or exposed to Cu(OH)₂-ionic. Thus, a significant increase in carbon consumption was detected in communities exposed to Cu(OH)₂-nanopesticide ($F=40.3$; $p<0.001$) in comparison to the control and Cu(OH)₂-ionic, regardless of the application rate ($F=3.92$; $p=0.062$). Also, this distinct metabolic activity was observed during the incubation period, in which communities exposed to Cu(OH)₂-nanopesticide presented an earlier (at 48 h) utilization of different carbon substrates than control (72 h) and the Cu(OH)₂-ionic (72 h) ($F=23.15$, $p<0.001$) (Table S4).

Overall, the presence of *P. pruinus* in soils seems to mitigate the effects of the Cu(OH)₂-nanopesticide, showing a similar carbon consumption towards the control ($F=10.54$, $p=0.662$). However, punctual differences were detected when carbon consumption was analyzed for each incubation time. For instance, a significant increase of carbon consumption in Cu(OH)₂-nanopesticide treated soils was detected at 48h and a significant decrease in soils exposed to Cu(OH)₂-ionic was detected at 144h.

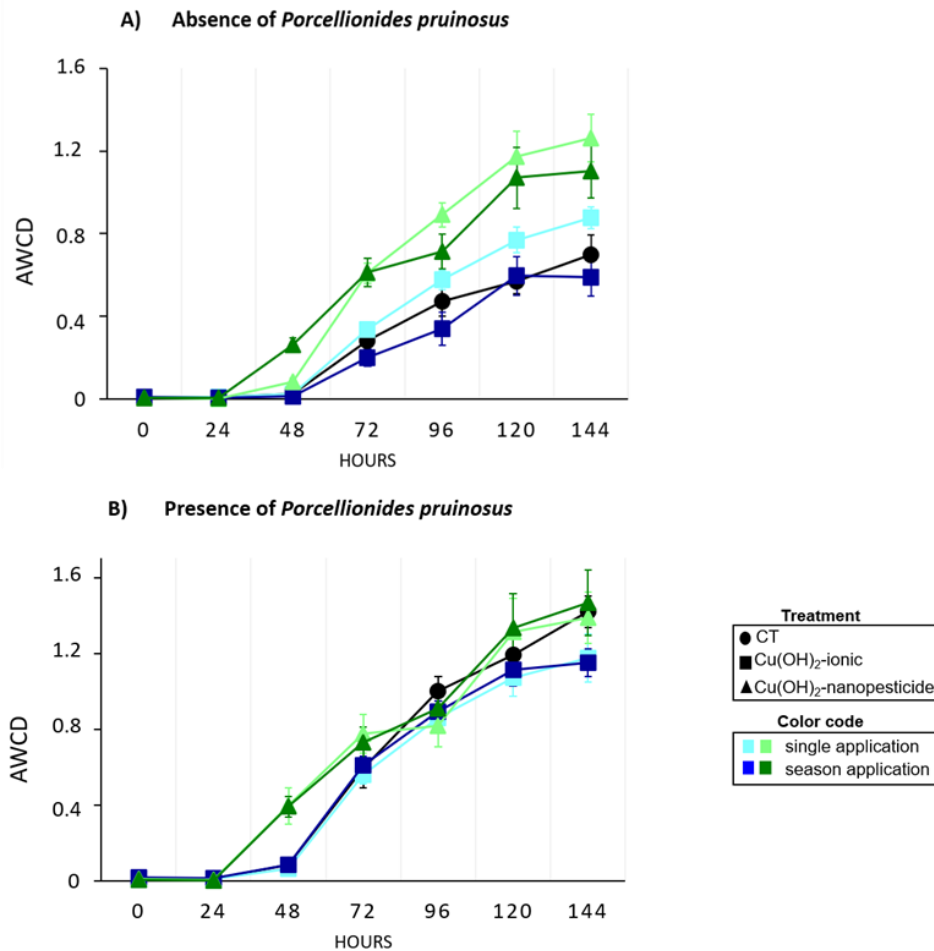


Figure 5. Average Well Color Development - AWCD representing the carbon consumption ($n=5 \pm$ standard deviation) of the soil community exposed to the nanopesticide and of ionic Cu(OH)₂, in the absence (A) or in the presence of *Porcellionides pruinosus* (B). The soil treatments included the non-exposed soil (CT), soil exposed to Cu(OH)₂-nanopesticide and to Cu(OH)₂-ionic, at two different application rates (single or season).

Due to relevant differences, among soil treatments, in AWCD after 144 hours of Biolog[®]Ecoplates incubation, the substrates classes (SAWCD) were examined (Figure 6), in the presence or absence of the *P. pruinosus*. For soil exposed to Cu(OH)₂-nanopesticide, 60% (single application) and 34% (season application) increase on tetrazoline reduction was detected for carbohydrates class (increasing the D-cellobiose, α -D-lactone, β -methyl-D-glucoside and i-erythritol utilization) towards to the control ($F=10.00$, $p=0.003$); 62% (single application) and 52% (season application) increase for carboxylic/acetic acid class (increasing the D-galactonic acid γ -lactone, D-malic acid, itaconic acid and α -ketobutyric acid utilization) towards to the control ($F=43.07$, $p<0.001$); 51% (single application) and 52% (season application) for amino acids class (increasing the Glycyl-L-glutamic acid and L-serine utilization) towards to the control

($F=37.02$, $p<0.001$). No significant effects of Cu(OH)₂-ionic were observed for SAWCD, in the absence of soil invertebrates. The application of Cu(OH)₂ (in both forms) in soils did not influence the consumption of the carbon substrates related to the polymers class ($F=0.472$, $p=0.496$). Regarding copper forms, a significant increase of utilization rate of carbohydrates, carboxylic/acetic acid, amino acid and amides/amines classes was observed in soil spiked with the Cu(OH)₂-nanopesticide.

In overall, the soil communities in the presence of *P. pruinosis* significantly increased the carbon consumption for each substrate classes by the microbial community, both in contaminated and control soils. In soils exposed to the highest concentration of the Cu(OH)₂-ionic a significant decrease on the utilization of carbon substrates related to amines/amides class ($F=6.76$, $p=0.013$), putrescine (52%) and phenylalanine (27%), was observed. Additionally, no effects of Cu(OH)₂-nanopesticide were observed in SAWCD, in the presence of these organisms.

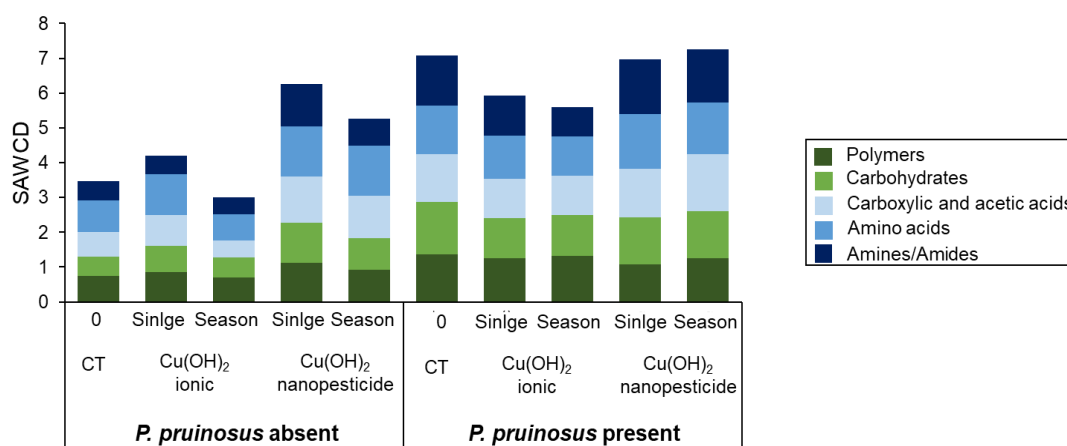


Figure 6. Substrate Average Well Color Development (SAWCD) index representing the functional effects of the nanopesticide and of ionic Cu(OH)₂ on soil microbiome in the absence (A) or in the presence of *Porcellionides pruinosus* (B). The SAWCD was calculated based on 144 h from Ecoplate incubate at 90 days of exposure. Values are presented per mean of 5 replicates per treatment. The soil treatments included the non-exposed soil (CT), soil exposed to Cu(OH)₂-nanopesticide and to Cu(OH)₂-ionic, two different application rates (single or season).

3.3.2. Enzymatic activity

Soil enzymatic activity was presented in a Principal Coordinate Analysis (PCoA) (Figure 7 A and B), after 90 days of exposure. As an initial analysis, a significant difference in the spatial distribution of enzymatic activities along the exposure time was verified in Figure S3, where two different groups were formed: (1) at day 2 and (2) at

day 90. However, only at day 90, a significant difference among soil treatments was observed.

At day 90, in absence of the *P. pruinosus* (Figure 7 A), a total variation of 77.1% was explained by the two axes (PCO1=49.2% and PCO2=27.7%). The spatial distribution of enzymatic activity only showed a significant difference between treatments [Cu(OH)₂ in nanopesticide vs. in ionic form], when the lowest concentration was applied in soils (PERMANOVA analysis: $t=1.73$, $P=0.009$).

Regarding the vectors plotted in PCoA, β G activity demonstrate to be the best correlated vector within the soil enzymatic activity distribution along to the PCO1 axis ($R=0.96$), suggesting the β G activity is negatively correlated with samples from Cu(OH)₂-nanopesticide and Cu(OH)₂-ionic at the season application and single application of nanopesticide. In fact, β G activity reductions of 44% (nanopesticide at season application), 29% (nanopesticide at single application), and 39% [Cu(OH)₂-ionic at season application] were observed, as shown in Figure S2. The urease activity vector presented a $R=0.90$ with PCO2 and seems to be positively correlated with contaminated samples, regardless of copper form. The other vectors presented weak correlation values, around 0.4 (Acid Phosphatase and Dehydrogenase activity), and 0.2 (Arylsulfatase activity) and no significant effects on these enzymatic activities were detected in contaminated soils (Figure S2).

In the presence of isopods (Figure 7 B), 75.8% of the total variation in distribution of soil enzymatic activity was explained by the two axes (PCO1=50.7% and PCO2=25.1%). A significant separation between control and contaminated samples with both Cu forms was detected (PERMANOVA analysis: $F=15.6$, $P=0.001$). Also, different spatial separation between samples exposed to distinct copper forms was observed, regardless the application rate (PERMANOVA analysis: single: $t=3.056$, $P=0.008$ and season $t=3.678$, $P=0.01$). As observed in soils in absence of *P. pruinosus*, the β G activity showed the highest correlation with PCO1 ($R=0.99$), in which a negative correlation with Cu(OH)₂-nanopesticide treatment was observed. Corroborating with β G measurements in Figure S2, being observed a significant decrease of these enzymatic activity (in 44%) in Cu(OH)₂-nanopesticide exposed soil at the season application.

The AP and UA showed to be the best correlated vectors with PCO2, presented a correlation values around of $R=0.74$ and $R=-0.86$, respectively. The AP seems to be negatively correlated with Cu(OH)₂-ionic treatment, resulting in a 28% decreasing of this activity (Figure S2). While, UA activity showed to be positively correlated with

soils from Cu(OH)₂-ionic, showing a significant increase of 68% (Figure S2). The other vectors presented lowest correlation values, around R=0.5 (Dehydrogenase activity), and R=0.4 (aryl-sulfatase activity).

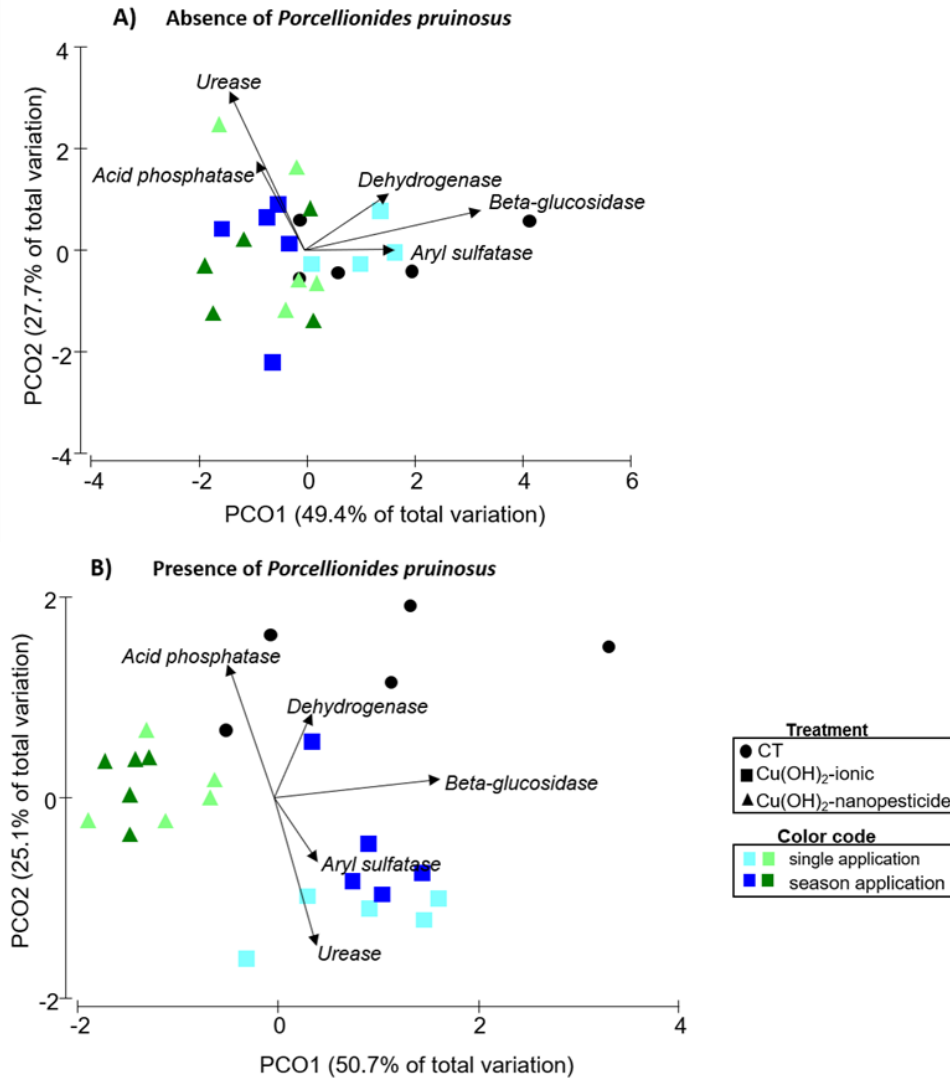


Figure 7. Principal Coordinates analysis (PCoA) of soil enzymatic activities representing the functional effects of the nanopesticide and of ionic Cu(OH)₂ on soil microbiome in the absence (A) or in the presence of *Porcellionides pruinosus* (B)). The PCoA was constructed based on Euclidean distance from soil enzymatic activities at 90 days of exposure. Soil treatments included the non-exposed soil (CT), soil exposed to Cu(OH)₂-nanopesticide and to Cu(OH)₂-ionic, at two different application rates (single or season). The vectors represent each enzymatic activity tested and were constructed based on Pearson correlation (R>0.2).

4. Discussion

The present study provides relevant information on the long-term effects of two different recommended application doses (single and season) of Cu(OH)₂-nanopesticide on soil microbial community. These effects were assessed in presence or absence of *P. pruinosus* and also compared to those obtained under Cu(OH)₂-ionic exposure. The presence of this soil invertebrate increases the realism in our experience, as representative of the invertebrate community that plays a crucial role in decomposition processes (Zimmer & Topp, 2002), with an intrinsic relation with soil microbial community (Bray *et al.*, 2019).

Overall, our study showed that long-term exposure to the nanopesticide has an impact on the structure and richness of soil bacterial and fungal communities, particularly at the season application dose, while affecting microbial functions related to carbon cycle, at both application rates. This agrees with previous studies, where negative effects on the microbial community were observed in different soils contaminated with Cu(OH)₂-nanopesticide (loamy soil, Zhang *et al.*, 2020; sandy-clay-loam soil, Simonin *et al.*, 2018b and Carley *et al.*, 2020; silt soil, Zhang *et al.*, 2019). Similarly, other copper-based nanomaterials (CuO NPs) and conventional pesticides (CuSO₄) showed a clear impact in the microbial communities from calcareous soils (*e.g.*, Lufa 2.1; pH=7.6) (Guan *et al.*, 2020).

Effects to soil (micro)organisms are often related to the porewater concentration of substances. Our study showed a higher Cu porewater concentration in soil exposed to Cu(OH)₂-nanopesticide when compared to soil exposed to the ionic form, at season application, which agrees with the reported by Neves (*et al.* 2019). This result may be related with the different rates of partitioning of Cu (in time), between soil particles and porewater, in both soils with nanoparticulate and ionic forms of Cu (Li *et al.*, 2019a, Tourinho *et al.*, 2012). Additionally, a decrease of Cu levels in porewater was observed in the nanopesticide-exposed soils over time (2 days > 90 days, but still higher than the ionic), suggesting a time-dependent Cu(OH)₂-nanopesticide particles aggregation (Liu *et al.*, 2019) or adsorption to the soil particles (Zhang *et al.*, 2019). In fact, the aggregation process can reduce the particle surface area in contact with the soil porewater, and consequently, decrease the dissolution rate of Cu (Liu *et al.*, 2019). The presence of *P. pruinosus* did not change the levels of Cu concentration in porewater.

After 90 days of exposure to the season application rate of the nanopesticide, the heterotrophic bacteria abundance in soil was negatively affected, while the Cu(OH)₂-ionic increased the number of CFU g⁻¹ soil. These differences might be related with Cu levels in porewater, since after 90 days the nanopesticide showed significantly higher copper level than the control and the Cu(OH)₂-ionic. Several studies demonstrated the toxic effect of Cu(OH)₂-nanopesticide in soil microbial community or in a specific bacterial group (Abbasi *et al.*, 2016), and multiple modes of action have been proposed. Generally, these toxic effects can occur due to dissolved Cu²⁺, Cu(OH)₂-specific effects, or oxidative stress due to the production of reactive oxygen species (ROS) (*i.e.* superoxide or hydroxyl radicals) (Keller *et al.*, 2017). The abundance of heterotrophic bacteria was significantly higher in soils with isopods compared to soils without isopods, irrespective of contamination, which may be due to the increased oxygen (*e.g.*, burrowing) and ammonia (*e.g.*, excretion) levels, deposition of nitrogen-enriched faeces, and gut-derived bacteria in fecal pellets (Zimmer & Topp, 2002; Bray *et al.*, 2019).

At the structural level, our results showed a significant impact on both communities, fungal and bacterial, regardless the dose and the Cu(OH)₂ form (nanopesticide or ionic form). Corroborating our results, structural changes on fungal communities (Keiblinger *et al.*, 2018) and bacterial communities (Zhang *et al.*, 2019) were already reported in soils exposed to Cu(OH)₂-nanopesticides. For instance, different copper concentrations [from 50 to 5000 mg (Cu) kg⁻¹ of Kocide[®]3000] were tested in two agricultural soils, during 3 months, and a significant decrease on fungal abundance was revealed, specifically for the Hypocreales order (Keiblinger *et al.*, 2018). A significant decrease on the number of bacterial genera was also observed by Zhang (*et al.*, 2019), after 2 days of direct soil application of Kocide[®]3000 (50 mg kg⁻¹). Also, the study by Zhang (*et al.*, 2020) noticed that the class Actinobacteria was significantly decreased after a 21 day foliar application of the Cu(OH)₂-nanopesticide and CuSO₄, compared to the control soil (Zhang *et al.*, 2020). In this line, our results also confirmed that the application of nanopesticide negatively affected the richness index of both bacterial and fungal communities (only at the season application dose). Additionally, the bacterial diversity and evenness increased, regardless of copper concentration and formulation, while these indexes did not change in the fungal community. The differences in effects observed for the bacterial and fungal communities may be due to their physiological differences. Accordingly, it is well known that the first mode of action of the metal NMs is through the interaction between Cu²⁺ ions, released from copper formulation,

and cell membrane/wall (Kaweeteerawat *et al.*, 2015). Thus, ergosterol present in fungal cells may confer protection against the copper ions. Also, the presence of fungal mycelia, spores and production of extra- and intra- enzymes (*e.g.*, ferric reductase) (Zabrieski *et al.*, 2015), might contribute to the distinct impact on fungal and bacterial communities. On the other hand, the fungal community can mobilize, sequester and/or transform the metal ions, consequently affecting the copper mobility in soils (Gadd, 2013).

In the soils treated with Cu(OH)₂-nanopesticide, the presence of isopods affected the microbial structure in soils, attenuating the impact of this nanopesticide, particularly the impact on richness of the fungal community. This attenuation effect may result from the soil oxygenation increased through the isopod's activities (mobility/behavior in soil) and to increasing nutrients (through the fecal pellets) on soils (Abd El-Wakeil, 2015), as briefly described in above. On the other hand, isopods may also induce Cu speciation (Adeleye *et al.*, 2014), precipitation or adsorption (Loureiro *et al.*, 2018), or cation exchange, resulting in the binding of copper to soil organic matter (Li *et al.*, 2019a). These processes reduce copper bioavailability, and consequently, the effect of Cu(OH)₂-nanopesticide on the soil microbial community.

Regarding the soil function, our study demonstrated that the Cu(OH)₂-nanopesticide affected microbial functions related to the carbon cycle, through reducing the β G activity and increasing the community-level physiological profiling (AWCD). β G activity has been considered the most sensitive enzyme to copper contamination, as well as an essential indicator of soil quality (Turner *et al.*, 2002). In accordance with our results, Simonin and their collaborators (2018b) also demonstrated that a 3 month foliar application of Cu(OH)₂-nanopesticide at 6.68 mg L⁻¹ reduced the β G activity in a sandy-clay-loam soil (pH=5.8). Regarding the AWCD, at short-term exposures, a decrease in soils exposed to metal nanoparticles has been reported (Kumar *et al.*, 2011; Sillen *et al.*, 2015). This is not in agreement with the observed in our study, where a significant increase of AWCD index for the soil exposed to Cu(OH)₂-nanopesticide was reported. This long-term effect may reflect a higher energy demand to fuel the activation of energy-dependent copper-tolerance mechanisms, such as those mediated by efflux pumps (Xing *et al.*, 2020). The carbon sources for which consumption was significantly increased were simple carbon sources (mono and di-saccharides), which indicates a preference for this type of simple C forms, already reported for stress scenarios by Kumar (*et al.* 2011). Also, the application of Cu(OH)₂-nanopesticide seems to increase

the abundance and/or activity of α -proteobacteria in soils, as is apparent from the increased use of erythritol (Geddes *et al.*, 2013). Erythritol is also an important nutrient for N₂-fixing plant endosymbionts (Barbier *et al.*, 2014), which may also be changed upon exposure to Cu(OH)₂-nanopesticide. Additionally, the group of substrates classified as carbohydrates, carboxylic/acetic acids, amino acids, and amines/amides, also presented a significant increase in utilization (SAWCD), but only in Cu(OH)₂-nanopesticide-treated soils. Only the polymers, namely Glycogen, Tween 80, Tween 40, and α -cyclodextrin, did not change significantly with any treatment applied [nanopesticide or ionic Cu(OH)₂]. For the Cu(OH)₂-ionic application, no change in carbon sources utilization was detected in comparison to the non-exposed soil, probably due to the lower concentration of copper in porewater as explained above.

Our study also evaluated soil enzymatic activities related with nutrient cycles, like nitrogen (UA activity), phosphorous (AP activity), sulfur (AS activity) and carbon (DHA activity). The positive and strong correlation of urease activity with Cu(OH)₂ exposure, in our experiment, suggests an increased NH₄-N rate in exposed soils. In fact, the study by Bogomolov (*et al.*, 1996) suggested that nitrogen released from dead microbial cells, by the copper contamination, resulted in increased dissolved organic N, and consequently, increased the NH₄-N rate through the activity of urease. However further studies are needed to confirm this hypothesis. On the other hand, the study by Zhang and their collaborators (2020) showed that urease activity was significantly lower in soils exposed to Cu(OH)₂-nanopesticide for 21 days, at concentrations of 5 and 50 mg kg⁻¹ soil. Distinct exposure times might explain these contrasting results. On the other hand, 90 days exposure to Cu(OH)₂-nanopesticide was weakly correlated with other enzymatic activities (DHA, AS, and AP), suggesting a lesser impact on other nutrient cycles. A similar result was observed in the study from Zhang *et al.* (2020), in which the AP activity was similar across the copper-treated (at 0.5, 5 and 50 mg kg⁻¹ soil) and control soils. Although short-term experiments may underestimate the risks posed by nanopesticides in agroecosystems, a study by Simonin (*et al.*, 2018b) demonstrated that short-term exposures might be more effective in detecting shifts on enzymatic activity related to C (α -glucosidase, β -glucosidase and cellulase), P (alkaline phosphatase), S (arylsulfatase) and N (chitinase – N-acetylglucosaminidase) cycles.

In terms of microbial activity, differences between control and contaminated soils were in part attenuated in the presence of isopods. For instance, the ability to use of carbon substrates (AWCD) was similar in control and contaminated soils. In fact, some studies

described increased carbon, nitrogen, potassium, ammonia, and phosphorous levels in soils when isopods are present (Yang *et al.*, 2020). Therefore, isopods might play a crucial role in balancing the microbiome of Cu contaminated soils, whose success was observed by the evaluation of some endpoints/soil functions. Other studies have also evaluated the influence of other organisms in copper contaminated soils, highlighting the importance of including biota in soil functioning. Keiblinger and collaborators (2018) indicated an increase of phenoloxidase and peroxidase, oxidative stress related enzymes, in two different vineyard soils (acid and alkaline pH) when alfafa was present, after 4 weeks of Cu application. Additionally, Gao and co-workers (2018) demonstrates that the plant presence changes de dissolution of CuO NPs-treated soils (in freshly spiked soils with 500 mg Cu/kg soil and in aged soils), and consequently, their toxicity in soils.

5. Conclusions

The current study provides evidence that recommended application rates of a Cu(OH)₂-nanopesticide affect soil microbial communities at structural and functional levels. This impact might imbalance the quality, fertility and functioning of the soil. This long-term assessment showed that effects were still observed 90 days after contamination. On the other hand, Cu(OH)₂ in ionic form exhibited a lower impact in the fungal community's structure. At the functional level, parameters related with the carbon cycle were impacted by this nanopesticide, through increasing the carbon substrates consumption (both application doses) and decreasing the β -glucosidase activity (season application dose). The presence of the soil invertebrate *P. pruinosus* seems to minimize the impact of the Cu(OH)₂-nanopesticide and Cu ionic form in soils, at both structural (fungal diversity) and functional levels (carbon consumption). This attenuation effect might result from the microbial growth stimulus resulting from soil oxygenation. Therefore, our results emphasize the importance of including the detritivores organisms, like *P. pruinosus*, in the risk assessment of these copper-based nanopesticides in the terrestrial compartment (*e.g.*, vineyard areas), and the crucial function of this invertebrates in soil functioning.

Further studies using several species of soil organisms should be conducted, under more realistic exposure scenarios (*e.g.*, using repeated applications, combined concentrations of copper-based nanopesticides, and/or using a realistic condition like indoor/outdoor

mesocosms experiments), during short- and long-term exposures, also to understand in more detail time-dependent effects the nanopesticide mechanism of action.

6. Acknowledgements

This work was supported by Nano-FARM - Fate and Effects of Agriculturally Relevant Materials (ERANET SIIN 2014, SIINN/0001/2014), supported by Fundação para a Ciência e a Tecnologia (FCT), under the frame of SIINN, the ERA-NET; and ECOCENE- Ecological Effects of Nanopesticides to Soil Ecosystems (PTDC/CTA-AMB/32471/2017), supported by FCT - Fundação para a Ciência e a Tecnologia, within the PT2020 Partnership Agreement and Compete 2020 co-funded by the FEDER - Fundo Europeu de Desenvolvimento Regional. Also, this work was supported by FCT through a PhD grant to Sara Peixoto (SFRH/BD/117738/2016). Thanks are due to CESAM for the financial support to (UIDP/50017/2020+UIDB/50017/2020), through national funds.

7. References

- Abbasi, A. R., Noori, N., Azadbakht, A., Bafarani, M. (2016). Dense coating of surface mounted Cu₂O nanoparticles upon silk fibers under ultrasound irradiation with antibacterial activity. *Journal of the Iranian Chemical Society*, 13(7), 1273-1281.
- Abd El-Wakeil, K. F. (2015). Effects of terrestrial isopods (Crustacea: Oniscidea) on leaf litter decomposition processes. *The Journal of Basic & Applied Zoology*, 69, 10-16.
- Adeleye, A. S., Conway, J. R., Perez, T., Rutten, P., Keller, A. A. (2014). Influence of extracellular polymeric substances on the long-term fate, dissolution, and speciation of copper-based nanoparticles. *Environmental Science & Technology*, 48(21), 12561-12568.
- Ballabio, C., Panagos, P., Lugato, E., Huang, J. H., Orgiazzi, A., Jones, A., Montanarella, L. (2018). Copper distribution in European topsoils: An assessment based on LUCAS soil survey. *Science of The Total Environment*, 636, 282-298.

- Barbier, T., Collard, F., Zúñiga-Ripa, A., Moriyón, I., Godard, T., Becker, J., Letesson, J. J. (2014). Erythritol feeds the pentose phosphate pathway via three new isomerases leading to D-erythrose-4-phosphate in *Brucella*. *Proceedings of the National Academy of Sciences*, 111(50), 17815-17820.
- Bogomolov, D. M., Chen, S. K., Parmelee, R. W., Subler, S., Edwards, C. A. (1996). An ecosystem approach to soil toxicity testing: a study of copper contamination in laboratory soil microcosms. *Applied Soil Ecology*, 4(2), 95-105.
- Bray, N., Kao-Kniffin, J., Frey, S. D., Fahey, T., Wickings, K. (2019). Soil macroinvertebrate presence alters microbial community composition and activity in the rhizosphere. *Frontiers in Microbiology*, 10, 256.
- Carley, L. N., Panchagavi, R., Song, X., Davenport, S., Bergemann, C. M., McCumber, A. W., Simonin, M. (2020). Long-term effects of copper nanopesticides on soil and sediment community diversity in two outdoor mesocosm experiments. *Environmental Science & Technology*, 54(14), 8878-8889.
- Dick, R. P., Breakwell, D. P., Turco, R. F. (1997). Soil enzyme activities and biodiversity measurements as integrative microbiological indicators. *In Methods for Assessing Soil Quality*, 49 (pp. 247-271).
- European Commission (2018). Commission implementing regulation (EU) 2018/1981 of 13 December 2018 renewing the approval of the active substances copper compounds, as candidates for substitution, in accordance with Regulation (EC) No 1107/2009 of the European Parliament and of the Council concerning the placing of plant protection products on the market, and amending the Annex to Commission Implementing Regulation (EU) No 540/201. Available at <https://eur-lex.europa.eu/legal-content/EN/TXT/PDF/?uri=CELEX:32018R1981&rid=3>
- Gao, X., Avellan, A., Laughton, S., Vaidya, R., Rodrigues, S. M., Casman, E. A., Lowry, G. V. (2018). CuO nanoparticle dissolution and toxicity to wheat (*Triticum aestivum*) in rhizosphere soil. *Environmental Science & Technology*, 52(5), 2888-2897.
- Gadd, G. M. (2013). Microbial roles in mineral transformations and metal cycling in the Earth's critical zone. *In Molecular Environmental Soil Science* (pp. 115-165). Springer, Dordrecht.

- Geddes, B. A., Hausner, G., Oresnik, I. J. (2013). Phylogenetic analysis of erythritol catabolic loci within the Rhizobiales and Proteobacteria. *BMC Microbiology*, 13(1), 46.
- Guan, X., Gao, X., Avellan, A., Spielman-Sun, E., Xu, J., Laughton, S., Yun, J., Zhang, Y., Bland, G.D., Zhang, Y., Zhang, R., Wang, X., Casman, E. A., Lowry, G. V. (2020). CuO nanoparticles alter the rhizospheric bacterial community and local nitrogen cycling for wheat grown in a Calcareous soil. *Environmental Science & Technology*, 54(14), 8699-8709.
- Kah, M. (2015). Nanopesticides and nanofertilizers: emerging contaminants or opportunities for risk mitigation?. *Frontiers in Chemistry*, 3, 64.
- Kah, M., Kookana, R. S., Gogos, A., Bucheli, T. D. (2018). A critical evaluation of nanopesticides and nanofertilizers against their conventional analogues. *Nature Nanotechnology*, 13(8), 677-684.
- Kandeler, E., Gerber, H. (1988). Short-term assay of soil urease activity using colorimetric determination of ammonium. *Biology and Fertility of Soils*, 6(1), 68-72.
- Kaweeteerawat, C., Chang, C. H., Roy, K. R., Liu, R., Li, R., Toso, D., Zhou, Z. H. (2015). Cu nanoparticles have different impacts in *Escherichia coli* and *Lactobacillus brevis* than their microsized and ionic analogues. *ACS nano*, 9(7), 7215-7225.
- Keiblinger, K. M., Schneider, M., Gorfer, M., Paumann, M., Deltedesco, E., Berger, H., Zehetner, F. (2018). Assessment of Cu applications in two contrasting soils-effects on soil microbial activity and the fungal community structure. *Ecotoxicology*, 27(2), 217-233.
- Keller, A. A., Adeleye, A. S., Conway, J. R., Garner, K. L., Zhao, L., Cherr, G. N., Ji, Z. (2017). Comparative environmental fate and toxicity of copper nanomaterials. *NanoImpact*, 7, 28-40.
- Kumar, N., Shah, V., Walker, V. K. (2011). Perturbation of an arctic soil microbial community by metal nanoparticles. *Journal of Hazardous Materials*, 190(1-3), 816-822.
- Li, J., Rodrigues, S., Tsyusko, O. V., Unrine, J. M. (2019a). Comparing plant–insect trophic transfer of Cu from lab-synthesised nano-Cu(OH)₂ with a commercial nano-Cu(OH)₂ fungicide formulation. *Environmental Chemistry*, 16(6), 411-418.

- Li, L., Xu, Z., Kah, M., Lin, D., Filser, J. (2019b). Nanopesticides: a comprehensive assessment of environmental risk is needed before widespread agricultural application. *Environmental Science & Technology*, 53 (14), 7923–7924.
- Liu, J., Williams, P. C., Goodson, B. M., Geisler-Lee, J., Fakharifar, M., Gemeinhardt, M. E. (2019). TiO₂ nanoparticles in irrigation water mitigate impacts of aged Ag nanoparticles on soil microorganisms, *Arabidopsis thaliana* plants, and *Eisenia fetida* earthworms. *Environmental Research*, 172, 202-215.
- Loureiro, S., Nogueira, A. J. A. and Soares, A. M. V. M. (2007) A microbial approach in soils from contaminated mine areas - the Jales mine (Portugal) study case. *Fresenius Environmental Bulletin*, 16(12b), 1648-1654.
- Loureiro, S., Tourinho, P. S., Cornelis, G., Van Den Brink, N. W., Díez-Ortiz, M., Vázquez-Campos, S., Van Gestel, C. A. (2018). Nanomaterials as soil pollutants. *In Soil Pollution* (pp. 161-190). Academic Press.
- Lowry, G. V., Avellan, A., Gilbertson, L. M. (2019). Opportunities and challenges for nanotechnology in the agri-tech revolution. *Nature Nanotechnology*, 14(6), 517–522.
- Muyzer, G., De Waal, E. C., Uitterlinden, A. G. (1993). Profiling of complex microbial populations by denaturing gradient gel electrophoresis analysis of polymerase chain reaction-amplified genes coding for 16S rRNA. *Applied and Environmental Microbiology*, 59(3), 695-700.
- Neves, J., Cardoso, D. N., Malheiro, C., Kah, M., Soares, A. M., Wrona, F. J., Loureiro, S. (2019). Copper toxicity to *Folsomia candida* in different soils: a comparison between nano and conventional formulations. *Environmental Chemistry*, 16(6), 419-429.
- Samarajeewa, A. D., Velicogna, J. R., Princz, J. I., Subasinghe, R. M., Scroggins, R. P., Beaudette, L. A. (2017). Effect of silver nano-particles on soil microbial growth, activity and community diversity in a sandy loam soil. *Environmental Pollution*, 220, 504-513.
- Sekhon, B. S. (2014). Nanotechnology in agri-food production: an overview. *Nanotechnology, Science and Applications*, 7, 31.
- Sillen, W. M., Thijs, S., Abbamondi, G. R., Janssen, J., Weyens, N., White, J. C., Vangronsveld, J. (2015). Effects of silver nanoparticles on soil microorganisms and maize biomass are linked in the rhizosphere. *Soil Biology and Biochemistry*, 91, 14-22.

- Simonin, M., Cantarel, A. A., Crouzet, A., Gervais, J., Martins, J. M., Richaume, A. (2018a). Negative effects of copper oxide nanoparticles on carbon and nitrogen cycle microbial activities in contrasting agricultural soils and in presence of plants. *Frontiers in Microbiology*, 9, 3102.
- Simonin, M., Colman, B. P., Tang, W., Judy, J. D., Anderson, S. M., Bergemann, C. M., Bernhardt, E. S. (2018b). Plant and microbial responses to repeated Cu(OH)₂ nanopesticide exposures under different fertilization levels in an agroecosystem. *Frontiers in Microbiology*, 9, 1769.
- Tabatabai, M. A. (1994). Soil enzymes. *Methods of Soil Analysis: Part 2 Microbiological and Biochemical Properties*, 5, 775-833.
- Tourinho, P. S., Van Gestel, C. A., Lofts, S., Svendsen, C., Soares, A. M., Loureiro, S. (2012). Metal-based nanoparticles in soil: Fate, behavior, and effects on soil invertebrates. *Environmental Toxicology and Chemistry*, 31(8), 1679-1692.
- Tourinho, P. S., van Gestel, C. A., Jurkschat, K., Soares, A. M., Loureiro, S. (2015). Effects of soil and dietary exposures to Ag nanoparticles and AgNO₃ in the terrestrial isopod *Porcellionides pruinosus*. *Environmental Pollution*, 205, 170-177.
- Turner, B. L., Hopkins, D. W., Haygarth, P. M., Ostle, N. (2002). β -Glucosidase activity in pasture soils. *Applied Soil Ecology*, 20(2), 157-162.
- van Gestel, C. A., Loureiro, S. (2018). Terrestrial isopods as model organisms in soil ecotoxicology: a review. *ZooKeys*, (801), 127.
- Xing, C., Chen, J., Zheng, X., Chen, L., Chen, M., Wang, L., Li, X. (2020). Functional metagenomic exploration identifies novel prokaryotic copper resistance genes from the soil microbiome. *Metallomics*, 12(3), 387-395.
- Yang, X., Li, T. (2020). Effects of terrestrial isopods on soil nutrients during litter decomposition. *Geoderma*, 376, 114546.
- Zabrieski, Z., Morrell, E., Hortin, J., Dimkpa, C., McLean, J., Britt, D., Anderson, A. (2015). Pesticidal activity of metal oxide nanoparticles on plant pathogenic isolates of *Pythium*. *Ecotoxicology*, 24(6), 1305-1314.
- Zhao, L., Huang, Y., Adeleye, A. S., Keller, A. A. (2017). Metabolomics reveals Cu(OH)₂ nanopesticide-activated anti-oxidative pathways and decreased beneficial antioxidants in spinach leaves. *Environmental Science & Technology*, 51(17), 10184-10194.

- Zhai, Y., Hunting, E. R., Wouterse, M., Peijnenburg, W. J., Vijver, M. G. (2017). Importance of exposure dynamics of metal-based nano-ZnO, -Cu and -Pb governing the metabolic potential of soil bacterial communities. *Ecotoxicology and Environmental Safety*, 145, 349-358.
- Zhang, X., Xu, Z., Wu, M., Qian, X., Lin, D., Zhang, H., Li, L. (2019). Potential environmental risks of nanopesticides: Application of Cu(OH)₂ nanopesticides to soil mitigates the degradation of neonicotinoid thiacloprid. *Environment International*, 129, 42-50.
- Zhang, X., Xu, Z., Qian, X., Lin, D., Zeng, T., Filser, J., Kah, M. (2020). Assessing the Impacts of Cu(OH)₂ nanopesticide and ionic copper on the soil enzyme activity and bacterial community. *Journal of Agricultural and Food Chemistry*, 68(11), 3372-3381.
- Zimmer, M., Topp, W. (2002). The role of coprophagy in nutrient release from feces of phytophagous insects. *Soil Biology and Biochemistry*, 34(8), 1093-1099.

8. Supplementary data

8.1. List of Figures

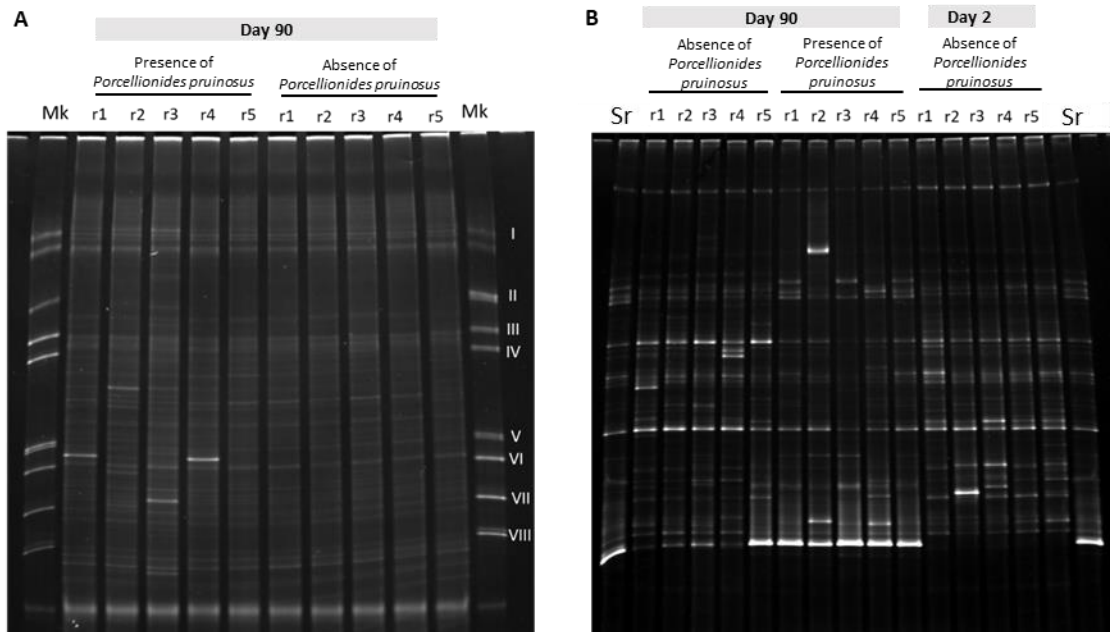


Figure S1. The electrophoresis of DGGE gel, of the non-exposed soil bacterial community (A) and fungal community (B) in the absence or in the presence of *Porcellionides pruinosus*, after 90 days of exposure or initial fungal community – day 2 (B). Lane Mk refers to DGGE marker for bacterial communities (A): I - RAI 70; II - RAN 60; III - RAI 3; IV - RAI 43; V - RAN 18; VI - RAN 12; VII - RAN 140; VIII - RAI 76 (Henriques *et al.*, 2004). Also, Lane Sr refers to sample r5 from non-exposed soils in the presence of *Porcellionides pruinosus*, used as a reference position on the DGGE gel (B).

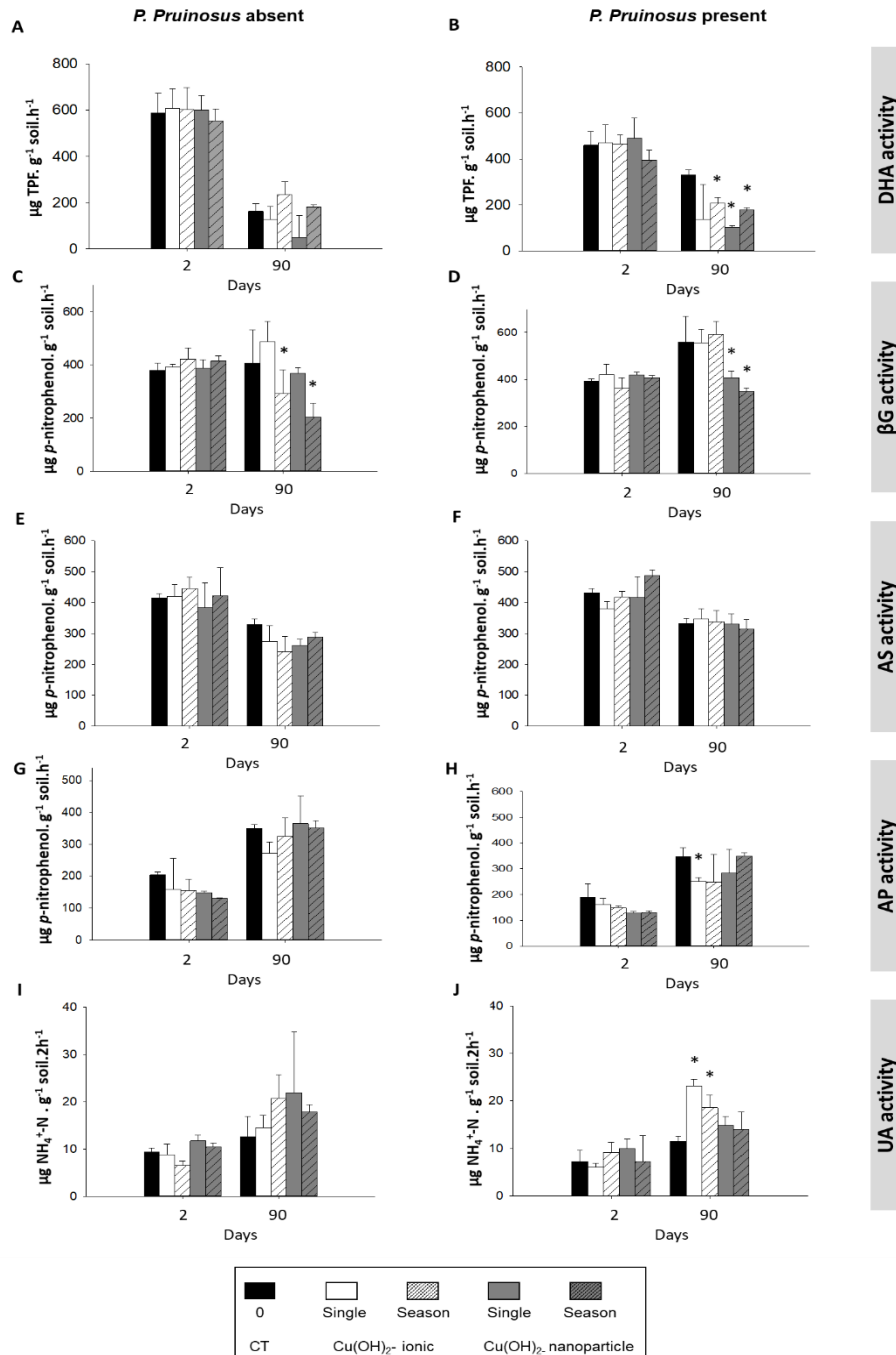


Figure S2. Soil enzymatic activities representing the functional effects of the Cu(OH)₂-nanopesticide and Cu(OH)₂-ionic, at two different application (single or season) [dehydrogenase - DHA (A and B), β -glucosidase - β G (C and D), arylsulfatase - AS (E and F), acid phosphatase -AP (G and H) and urease - UA activities (I and J)]. These effects were evaluated for soils in the absence (A C, E, G and I) or in the presence of *Porcellionides pruinosus* (B, D, F, H and J). The data is represented by the mean \pm standard deviation. The soil treatments included the non-exposed soil (CT), soil exposed to Cu(OH)₂ - nanopesticide and to Cu(OH)₂ - ionic, at two different concentrations (single or season application). Asterisks (*) indicate a statistically significant difference ($p < 0.05$) between nanopesticide or ionic Cu(OH)₂ treatments towards the respective control.

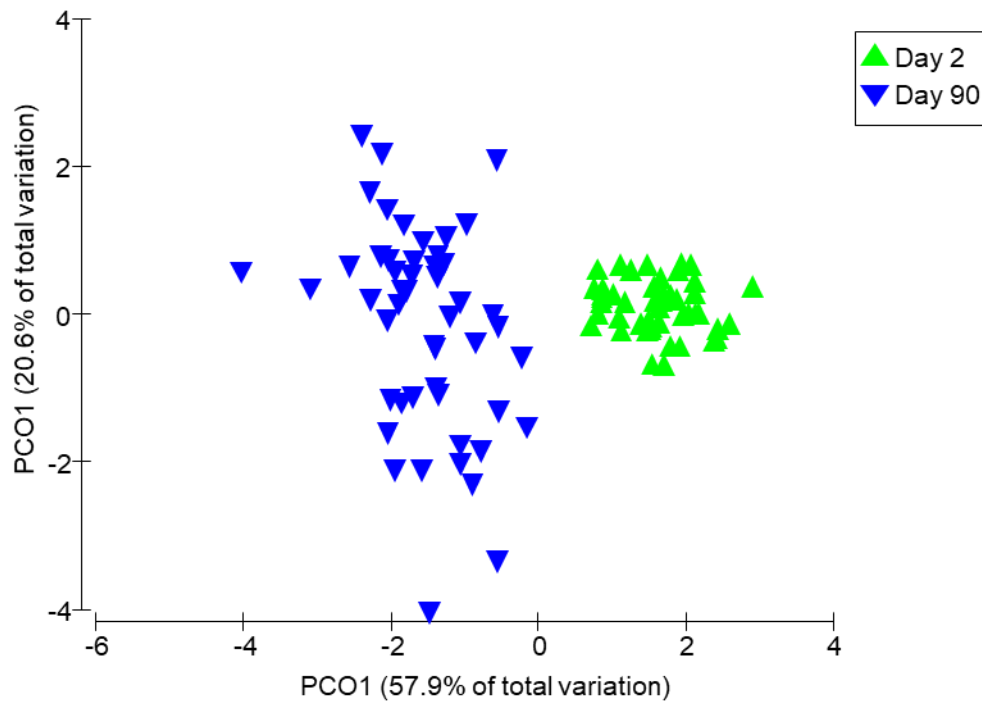


Figure S3. Principal Coordinates Analysis (PCoA) of soil enzymatic activities representing the functional effects of the nanopesticide and of ionic Cu(OH)₂ on soil microbiome. The PCoA was constructed based on Euclidean distance from soil enzymatic activities, at 90 days of exposure. Soil treatments included the non-exposed soil (CT), soil exposed to Cu(OH)₂-nanopesticide and to Cu(OH)₂-ionic, at two different concentrations (single or season application). These treatments also included the absence or in the presence of *P. pruinosis*.

8.2. List of Tables

Table S1. Number of invertebrates, *Porcellionides pruinosus*, per replicate in each soil treatment, at the beginning of the experiment (day 2) and after 90 days of soil exposure. Soil treatments included the non-exposed soil (CT), soil exposed to Cu(OH)₂-nanopesticide and to Cu(OH)₂-ionic, at two different concentrations, at two different application rates (single or season).

		Number of organisms				
		Non-exposed soil	Cu(OH) ₂ -ionic		Cu(OH) ₂ -nanopesticide	
Time of exposure	Replicates	0	Single	season	single	season
Day 2	R1	3	3	3	3	3
	R2	3	3	3	3	3
	R3	3	3	3	3	3
	R4	3	3	3	3	3
	R5	3	3	3	3	3
Day 90	R1	3	2	2	3	2
	R2	3	3	3	3	3
	R3	3	3	2	3	3
	R4	3	3	3	3	3
	R5	2	3	3	2	2

Table S2. Soil pH for each treatment, at the beginning of the experiment and after 90 days of soil exposure. Soil treatments included the non-exposed soil (CT), soil exposed to Cu(OH)₂-nanopesticide and to Cu(OH)₂-ionic, at two different concentrations, at two different application rates (single or season). Data was expressed as average and standard deviation (SD).

		Non-exposed soil	Cu(OH) ₂ - ionic		Cu(OH) ₂ - nanopesticide	
		0	Single	season	single	season
Day 2	Average	5.65	5.66	5.67	5.64	5.63
	SD	0.003	0.01	0.002	0.01	0.01
Day 90 in absent of <i>Porcellionides</i> <i>pruinus</i>	Average	5.55	5.53	5.53	5.54	5.55
	SD	0.01	0.02	0.02	0.08	0.01
Day 90 in the presence of <i>Porcellionides</i> <i>pruinus</i>	Average	5.57	5.55	5.56	5.56	5.53
	SD	0.03	0.01	0.04	0.01	0.02

Table S3. Heatmap for carbon sources utilization by the soil microbiome, non-exposed (CT), or exposed to Cu(OH)₂ nanopesticide or ionic form at two different application rates (single or season). These carbon utilizations were analyzed after 90 days of soil exposure. These effects were assessed in the absence or presence of *Porcellionides pruinosus*.

Nutrient Cycle	Classes	Carbon substrates	Absence of <i>Porcellionides pruinosus</i>					Presence of <i>Porcellionides pruinosus</i>				
			CT	Cu(OH) ₂ -ionic		Cu(OH) ₂ -nanopesticide		CT	Cu(OH) ₂ -ionic		Cu(OH) ₂ -nanopesticide	
			0	single	season	single	season	0	single	season	single	season
-	-	Water	0	0	0	0	0	0	0	0	0	0
C	Polymers	Tween 40	1,33	1,46	1,11	1,76	1,42	1,86	1,74	2,01	1,65	1,64
C + N	Polymers	Tween 80	1,42	1,78	1,46	1,73	1,47	2,12	1,88	2,13	1,77	1,69
C	Polymers	β-Cyclodextrin	0	0	0	0,35	0,36	0,82	0,69	0,30	0,44	0,80
C	Polymers	Glycogen	0,21	0,18	0,24	0,64	0,46	0,68	0,67	0,82	0,40	0,92
C + N	Carboxylic & acetic acids	N-Acetyl-D-Glucosamine	1,20	1,41	0,61	1,64	2,01	2,28	1,75	1,61	2,05	1,95
C	Carboxylic & acetic acids	D,L-7-Glycerol Phosphate	0,13	0,05	0,11	0,10	0,09	0,35	0,31	0,13	0,31	0,33
C + N	Carboxylic & acetic acids	D-Galactonic acid γ-Lactone	0,61	1,12	0,67	1,55	1,25	1,44	1,37	1,35	1,58	1,80
C + N	Carboxylic & acetic acids	D-Galacturonic Acid	1,52	2,19	1,26	2,05	2,38	1,81	1,90	1,49	1,81	1,98
C	Carboxylic & acetic acids	2-Hydroxy Benzoic Acid	0,12	0,11	0,04	0,48	0,25	0,35	0,48	0,05	0,69	0,73
C + P	Carboxylic & acetic acids	4-Hydroxy Benzoic Acid	1,36	1,72	1,34	1,82	1,80	2,12	1,75	2,10	2,07	3,70
C + P	Carboxylic & acetic acids	γ-Hydroxybutyric Acid	0,95	0,33	0,38	1,67	1,47	1,81	0,82	1,41	1,73	1,96
C	Carboxylic & acetic acids	Itaconic Acid	0,22	0,40	0	1,53	1,07	1,69	1,24	1,32	1,84	2,06
C	Carboxylic & acetic acids	γ-Ketobutyric Acid	0	0	0	0,52	0,30	0,41	0,16	0,34	0,46	0,43
C	Carboxylic & acetic acids	D-Malic Acid	0,82	1,57	0,39	1,82	1,52	1,50	1,43	1,48	1,40	1,46
C	Carbohydrates	Pyruvic Acid Methyl Ester	0,95	1,11	0,65	1,31	1,03	1,08	1,15	0,68	1,51	1,31
C + N	Carbohydrates	D-Cellobiose	0,27	0,24	0,42	1,05	0,66	2,06	0,90	1,70	1,72	1,54
C + N	Carbohydrates	β-D-Lactose	0	0,12	0,12	0,93	0,47	0,96	0,88	0,79	1,04	1,07
C + N	Carbohydrates	β-Methyl-D-Glucoside	0,21	0,39	0,09	1,11	0,57	1,53	0,91	0,93	1,32	1,38
C + N	Carbohydrates	D-xyllose	0,42	0,31	0,22	0,91	0,75	1,46	1,03	1,49	0,85	0,94
C + N	Carbohydrates	l-Erythritol	0,14	0,12	0,19	0,61	0,36	0,86	0,54	0,57	0,82	0,87
C + N	Carbohydrates	D-Mannitol	1,61	3,08	2,52	2,54	2,58	2,79	2,71	2,14	2,64	2,66
C	Carbohydrates	D-Glucosaminic Acid	1,33	1,38	1,05	1,43	1,58	1,79	1,81	1,62	1,45	1,57
C	Carbohydrates	Glucose-1-phosphate	0,14	0	0	0,58	0,18	1,01	0,56	0,74	0,83	0,76
C	Amines/amides	Phenylethyl-amine	0,36	0,07	0,11	0,25	0,49	1,70	1,45	0,81	2,01	1,87
C	Amines/amides	Putrescine	0,74	0,98	0,88	1,06	1,05	1,20	0,88	0,87	1,17	1,17
C	Amino acids	L-Arginine	1,11	1,64	1,27	2,02	2,14	2,12	1,81	1,54	1,95	1,93
C	Amino acids	L-Asparagine	2,63	2,58	1,37	2,45	2,52	2,38	2,19	2,20	2,50	2,33
C	Amino acids	L-Phenylalanine	0,27	0,36	0,13	0,83	0,68	0,90	0,77	0,53	1,30	1,27
C	Amino acids	L-Serine	1,33	2,28	1,59	2,47	2,43	2,47	2,12	1,78	2,32	2,26
C	Amino acids	L-Threonine	0,09	0,15	0	0,31	0,37	0,15	0,27	0,14	0,63	0,26
C	Amino acids	Glycyl-L-Glutamic Acid	0,07	0	0	0,51	0,49	0,32	0,24	0,59	0,71	0,82

Table S4. Carbon consumption of the soil communities measured during the 144 h of the Biolog[®]Ecoplate incubation. Data were expressed in terms of Confidence intervals, with a 95% of significance. Bold numbers indicates a significant difference between time of incubation for each soil treatment [non-exposed soil, Cu(OH)₂-ionic or Cu(OH)₂-nanopesticide]. Repeated measure ANOVA, Tukey HSD, p<0.05.

	Soil Treatment	Incubated plate (hours)	Mean	Std. Error	95% Confidence interval	
					Lower Bound	Upper Bound
Carbon consumption in absence of <i>Porcellionides pruinosus</i>	Non-exposed soil	0	0.01	0.00	0.00	0.01
		24	0.01	0.00	0.00	0.01
		48	0.03	0.02	-0.01	0.06
		72	0.28	0.05	0.19	0.34
		96	0.47	0.07	0.38	0.61
		120	0.57	0.08	0.40	0.74
		144	0.70	0.08	0.53	0.86
	Cu(OH) ₂ -ionic	0	0.01	0.00	0.01	0.01
		24	0.01	0.00	0.00	0.01
		48	0.02	0.01	0.00	0.04
		72	0.27	0.03	0.20	0.34
		96	0.46	0.05	0.36	0.55
		120	0.68	0.06	0.56	0.81
		144	0.73	0.06	0.62	0.85
	Cu(OH) ₂ -nanopesticide	0	0.01	0.00	0.00	0.01
		24	0.00	0.00	0.00	0.01
		48	0.17	0.01	0.15	0.20
		72	0.61	0.03	0.54	0.68
96		0.80	0.05	0.71	0.90	
120		1.12	0.06	1.00	1.24	
144		1.17	0.06	1.05	1.28	
Carbon consumption in presence of <i>Porcellionides pruinosus</i>	Non-exposed soil	0	0.01	0.00	0.00	0.02
		24	0.01	0.00	0.00	0.02
		48	0.09	0.04	0.00	0.18
		72	0.60	0.07	0.45	0.74
		96	1.00	0.07	0.86	1.14
		120	1.20	0.08	1.02	1.36
		144	1.42	0.08	1.25	1.59
	Cu(OH) ₂ -ionic	0	0.01	0.00	0.01	0.02
		24	0.01	0.00	0.01	0.02
		48	0.08	0.03	0.01	0.14
		72	0.59	0.05	0.49	0.68
		96	0.88	0.05	0.78	0.97
		120	1.09	0.06	0.97	1.21
		144	1.16	0.06	1.04	1.28
	Cu(OH) ₂ -nanopesticide	0	0.01	0.00	0.00	0.01
		24	0.00	0.00	0.00	0.01
		48	0.39	0.03	0.33	0.46
		72	0.75	0.05	0.65	0.85
96		0.86	0.05	0.77	0.96	
120		1.32	0.06	1.20	1.44	
144		1.43	0.06	1.31	1.55	

Chapter 4

Responses of soil microbiome to copper-based nanomaterials for
agricultural applications

Responses of soil microbiome to copper-based nanomaterials for agricultural applications

Peixoto, S.; Morgado, R. G.; Prodana, M.; Cardoso, D. N.; Malheiro, C.; Neves, J.; Santos, C.; Khodaparast, Z.; Pavlaki, M. D.; Rodrigues, S.; Rodrigues, S. M.; Henriques, I.; Loureiro, S.

Abstract

The foreseen increasing application of copper-based nanomaterials (Cu NMs), replacing or complementing existing Cu-agrochemicals, could result in a negative impact on soil microbiome. Thus, we studied the effects of Kocide[®]3000, nCu(OH)₂ and nCuO, at 50 mg(Cu)kg⁻¹ soil, on soil microbiome function and composition. For this, indoor mesocosms were set up, including biota, during 28 days of exposure. The Cu(OH)₂-i was also included as an ionic control. At day-28, we found a reduction in the dehydrogenase, arylsulfatase and urease activities (Cu-treatments); an increase in the utilization of carbon substrates (nCuO-treatment); and an increased abundance of culturable bacteria [nCu(OH)₂-treatment], towards the non-treated soil (CT). Concerning compositional level, Acidobacteria [Kocide[®]3000, nCuO and Cu(OH)₂-i treatments] and Flavobacteriia [nCu(OH)₂- treatment] classes were negatively affected by the Cu exposure. Classes including some Cu-tolerant bacterial members increased in Kocide[®]3000 (Clostridia) and nCu(OH)₂ (Gemmatimonadetes) treatments. A reduced abundance of genes involved in denitrification (e.g., *nosZ* and *nirS*) was predicted in Cu-treatments. A distinct pool of DTPA-extractable ionic Cu in treated soils was detected: Cu(OH)₂-i>Kocide[®]3000~nCuO>nCu(OH)₂, which helped to explain the distinct impact of NMs on the soil microbiome. Thus, our study highlights the importance to assess the impact of Cu-NMs using a dynamic and complex exposure scenario and the need for specific regulatory frameworks for (nano)materials.

Keywords: indoor-mesocosm, nanopesticide, microbial functionality, Illumina MiSeq.

1. Introduction

Due to growing global human population, the Food and Agriculture Organization of the United Nations estimated that global food production needs to be increased by about 70% by 2050 (FAO, 2020). In order to boost crop productivity and improve soil fertility, the application of fertilizers and pesticides has been increasing in agriculture (Li *et al.*, 2019a). Two million tonnes of pesticides are utilized annually worldwide, where China, USA and Argentina as major contributing countries (Zhang, 2018). Although pesticides can increase crop productivity, the frequent application may result in negative consequences at the ecosystem level, mainly due to their persistence and accumulation in soils and plant tissues (Sharma *et al.*, 2019). The accumulation of pesticide residues along food webs and loss of ecosystem services is expected to have consequences for human health and well-being. For these reasons, nanotechnology has focused on the development of safer pesticides with nano-formulations (Li *et al.*, 2019b; Lowry *et al.*, 2019). These (nano)pesticides are designed to release an active ingredient in a slow and/or targeted manner to increase its efficacy and reduce the environmental load, compared with conventional pesticides (Li *et al.*, 2019b). Despite the reported advantages of these (nano)pesticides, the environmental risk associated with their use must be assessed before being widely used in agriculture (Li *et al.*, 2019b, Grillo *et al.*, 2021). Currently, nanopesticides share the same regulatory process with conventional pesticides, in most countries, however additional considerations about their properties (nanoscale) should be taken in account (Grillo *et al.*, 2021). In this point of view, an additional physicochemical characterization, exposure methodologies, and ecotoxicology assays are suggested to be included in the risk assessment of these materials (Grillo *et al.*, 2021). In the last years, copper (Cu) -based inorganic nanopesticides, namely Kocide[®]3000, were made available in the USA market as an alternative to conventional CuSO₄, and are being used in organic farming (Li *et al.*, 2019b). Also, metal oxide nanoparticles (*e.g.*, nCuO) have been shown to have positive influences on agricultural crops by improving the bioavailability of micronutrients and protecting plants from pathogens (Simonin *et al.*, 2018a). Due to their potential benefit in crop production and agriculture sustainability, there has been great interest in assessing the environmental impact of these nanomaterials (NMs) [nano-Cu(OH)₂ and nCuO]. For that, there is a need to evaluate their fate in soils, their accumulation in soils

and organisms, and their effect on the soil microbiome (Zhang *et al.*, 2020, Guan *et al.*, 2020).

The microbiome is crucial for soil quality, fertility and health and is vulnerable to environmental stress induced by contaminants, like NMs (Holden *et al.*, 2014). The Cu-based NMs (from both dissolved ionic Cu^{2+} and Cu nanoparticles) has a toxic effect on microorganisms due to their multiple modes of action, such as the interaction with and alteration of the cell wall structure and composition, and/or oxidative stress (Sharma *et al.*, 2021; Vincent *et al.*, 2018). Thus, disturbances in microbial metabolic activity, composition and diversity may lead to disbalance in biogeochemical cycling (Shahsavari *et al.*, 2017). Recently, a few studies assessed microbial endpoints to understand the effects of Cu-based NMs in soil microbial communities and to evaluate environmental risks in the terrestrial compartment. Among these endpoints, the following stand out: soil enzymatic activity (Zhang *et al.*, 2020, Simonin *et al.*, 2018 a,b); microbial community structure and composition (Zhang *et al.*, 2020, Keiblinger *et al.*, 2018; Carley *et al.*, 2020), community-level physiological profiling (Samarajeewa *et al.*, 2020) and the abundance of genes involved in the nitrogen cycle (Guan *et al.*, 2020). However, the effects of Cu-based NMs on soil microbiome are challenging to predict. These studies used different NMs concentrations, soil types, and were conducted at different experimental designs. Even so, most studies showed a more substantial impact of the ionic Cu or conventional pesticides (*e.g.* CuSO_4) when compared to Kocide[®]3000 (Zhang *et al.*, 2020; Neves *et al.*, 2019). Also, a negative impact of nCuO on soil microbiome has been described in terms of denitrification, nitrification, and soil respiration processes (Simonin *et al.*, 2018a; Guan *et al.*, 2020). These adverse effects are generally associated with the ionic Cu dissolution and/or bound ionic Cu(II) in soil (Vincent *et al.*, 2018). Metal extraction protocols, such as the diethylenetriaminepentaacetic acid (DTPA) extraction method, have been often proposed as a proxy for predicting the bioavailability of metallic nanoparticles (*e.g.*, CuO, CeO_2 , ZnO NPs) in soil (Gao *et al.*, 2017; Peng *et al.*, 2020; Rodrigues *et al.*, 2021). The DTPA extracted-metal method assesses not only the dissolved Cu in soil porewater (Cu^{2+} free or complexed with soluble ligands in dissolved organic matter) but also the Cu^{2+} reversibly bound to solid phase (*e.g.*, in soil organic matter or clay particles) (Gao *et al.*, 2017). By extracting both the labile and the potentially available metal pools, this method is thought to describe more adequately the time-dependent

processes affecting metallic nanoparticles in soil, and has proved to be a better predictor for metal toxicity and bioaccumulation (Gao *et al.*, 2017).

Up to date, most studies about the impact of Cu-based NMs in the terrestrial compartment were conducted solely in the presence of target crops (Simonin *et al.*, 2018b; Carley *et al.*, 2020) or without soil organisms (Zhang *et al.*, 2019; Samarajeewa *et al.*, 2021). Little is known about the impact of these NMs on soil microbiome in the context of the interactions with key decomposer organisms and (non)target plants. In fact, the presence of these organisms in soils may change the diversity, structure and composition of soil microbiome, by increasing the oxygen and nutrient content in soils (Zimmer and Topp, 2002), which may influence the microbial responses to the NMs (Peixoto *et al.*, 2021). Our previous study revealed that the inclusion of different species of organisms was a useful strategy to detect the impact of silver sulfidized nanoparticles on soil microbiome (Peixoto *et al.*, 2020). Thus, the innovative approach of the current study was the inclusion of different soil organisms as essential edaphic elements in the terrestrial ecosystem and as potential drivers of the composition and structure of the soil microbiome.

Thus, our study aims to (1) investigate the effects of Cu-based NMs on soil microbiome at functional (by culture of functional bacterial groups, soil enzymatic activity and community-level physiological profiling) and structural level (metagenomic analysis), and (2) monitoring the ionic Cu(II) bound in soil from each Cu-treatment, using a DTPA extraction method. For this, indoor soil mesocosms were set up using an environmental-relevant concentration of contaminants, which was predicted for top soil in vineyard soil (Ballabio *et al.*, 2018) and represent at the same time the recommended dose for Kocide[®]3000 for several crops. The impact of different Cu-based NMs on soil microbiome was evaluated as a function of time [day -2 (spiking time), day 0 (day of input soil organisms), 14 and 28 days] and were compared to the non-treated soil (CT) and ionic Cu control [Cu(OH)₂-i].

2. Material and Methods

2.1. Copper-based nanoparticles characterization

The study was conducted with different Cu-based NMs: a) the commercial formulation - Kocide[®]3000 (DuPont Co.[™], Wilmington, DE, United States), b) nCu(OH)₂ (lab-synthesized as previously described by Li *et al.*, 2019), and c) nCuO (commercial,

Sigma-Aldrich; <50 nm particle size). Additionally, d) Cu(II) hydroxide [Cu(OH)₂-i] was purchased from Sigma-Aldrich (99 % purity, CAS 7761-88-8, Germany) and included as an ionic Cu control. Kocide[®]3000 and nCu(OH)₂ were characterized as previously reported by Li *et al.*, (2019) by Transmission electron micrograph (TEM) and presented the following characteristics: Kocide[®]3000 consisted qualitatively of nano-needles with 10–15 nm in diameter, 300–600 nm long, with a zeta potential of -38 ± 3.5 mV (mean \pm standard deviation, $n=3$); nCu(OH)₂ presented an average particle length of 1442 nm ($n=335$) and diameter of 16 nm ($n=32$), hydrodynamic diameters >2000 nm (in water, pH= 6.5) with aggregation, and a zeta potential of $+13 \pm 4.7$ mV (mean \pm standard deviation, $n=3$).

2.2. Copper exposure

The Lufa 2.2 soil (LUFA-Speyer 2.2, Speyer, Germany) was spiked by adding each Cu formulation directly into the soils (with solid addition) to a final concentration of 50 mg (Cu) kg⁻¹ soil. The water holding capacity (WHC) was adjusted at 55 %, using ultrapure water. Soils (spiked and watered) were mixed manually during few minutes and left for two days to equilibrate, as previous reported by Peixoto *et al.*, (2020). For each column mesocosm (20 cm long columns with 11 cm of diameter), half of the column (bottom layer) was filled with 1.3 kg of CT, and the other half was filled with either 1.3 kg of CT or spiked soil with Cu-forms [*i.e.*, Kocide[®]3000, nCu(OH)₂, nCuO or Cu(OH)₂-i] (upper layer: 1-8 cm). Additionally, a PVP nylon mesh (1 mm) was used to settle the column and a funnel with a 50 mL tube was located to collect the leachate during the exposure period. A total of six replicates/columns per treatment were established in indoor conditions [temperature 20 ° C \pm 2 and photoperiod 16h : 8h (light : dark)]. The 16 ml of artificial rainwater was daily distributed in each mesocosm column [NaCl (0.01mM), (NH₄)₄ SO₄.H₂O (0.0053 mM), NaNO₃ (0.0059 mM), and CaCl₂.H₂O (0.0039 mM); (pH=5.1) as described in (Peixoto *et al.*, 2020)] to maintain the water content in soil. The day 0 of the experiment refers to the date of inclusion of plants and soil invertebrates into the mesocosm columns after two days of soil equilibration, as previously described in Peixoto *et al.*, (2020). *Triticum estivum* L. plants were germinated from seeds in multi-welled germinator plates, using Cu-treated or CT soil according to the respective treatment. Five specimens were transplanted to each column at day 0 (*i.e.*, plant age was six days old). Regarding soil invertebrates, ten individuals of *Eisenia andrei* (adults, clitellate, 300-600 mg fresh weight), *Porcellionides pruinosus*

(adults, 15-25 mg fresh weight, no gender distinction but no pregnant individuals), and *Tenebrio molitor* (larvae, 30-40 mg fresh weight, no gender distinction), were sequentially included on the top of each mesocosm column at day 0.

Soil samples were collected at day -2 (spiking day), day 0 (input of organisms into the mesocosm column), days 14 and 28. In each sampling time, three replicates (per treatment) were destructively sampled to collect top-soil (surface: 0-2 cm) for chemical analysis and microbiome analysis. A comprehensive array of additional endpoints related to plant and animal performance, soil ecosystem functioning, Cu bioaccumulation, and physicochemical measurements were also assessed but not included in this work.

2.3. Chemical extraction test to assess soil-bound ionic Cu

The concentration of ionic Cu(II) bound to soil from each treatment [Kocide[®]3000, nCu(OH)₂, nCuO and Cu(OH)₂-i] was measured using a DTPA extraction method, as previously described by Gao *et al.* (2017). The soil-bound DTPA-extractable Cu was observed to increase proportionally as the nano-forms of Cu dissolve in soil and has been used as proxy measure for the variation of dissolved Cu in soil along time upon soil treatment and to characterize dissolution profiles of Cu-based NMs in dosed soil (Gao *et al.*, 2017; Rodrigues *et al.*, 2021). Briefly, for each Cu treatment, two grams of air-dried soil were extracted with four mL of DTPA [0.005 M DTPA (> 99%, Sigma-Aldrich), 0.01 M CaCl₂ (≥ 99.0%, ACS grade, Fischer Scientific) and 0.1 M TEA (≥ 99.0% (GC), Sigma-Aldrich) at ~pH 7.6], during 2 h at 180 rpm. After extraction, samples were centrifuged in a reciprocal shaker at 3000 rpm for 10 minutes (GFL-3016 horizontal back and forth shaker) and filtered with 0.45 µm PTFE filters. These filtered samples were acidified with 20% HNO₃ (PanReac AppliChem, trace metal grade 65%) (final HNO₃ concentration, 2%) kept at 4 °C, and analyzed for Cu by ICP-MS (Agilent 7700 Series) within 4 d after collection. A quality control program was implemented for the determination of Cu, including method blanks, and three replicate samples. The Cu detection limit was 0.5 mg L⁻¹.

2.4. Culture-dependent analysis of soil microbiome

To assess the effects of Cu-based formulations on the culturable fraction of the soil microbiome, Colony Forming Units (CFU's) of heterotrophic bacteria and of bacteria able to solubilize phosphate (P-SB) were counted in the Nutrient Agar (NA) (Merck,

Darmstadt, Germany) and the National Botanical Research Institute's phosphate (NBRIP) medium (Nautiyal, 1999), respectively. The procedure was done as previously described in Peixoto *et al.* (2020).

2.5. Enzymatic activity

Five soil enzymatic activities were tested during the time of exposure. The urease activity (UA) was measured based on Kandeler & Gerber (1988); and the dehydrogenase (DHA), beta-glucosidase (β G), arylsulfatase (AS) and acid phosphatase (AP) activities were determined adapted from protocols described by Dick *et al.* (1997). The adaptations were previously described in Peixoto *et al.* (2021).

2.6. Community level physiological profiling

Community-level physiological profiling was performed using 96-well Biolog[®]Ecoplates (Biolog, Hayward, CA, USA) as described by Peixoto *et al.* (2020). The color development was measured by reading optical density at a wavelength of 590 nm at 24 h intervals during 186 h of plates incubation, using a microplate spectrophotometer (Biolog, MicroStation TM, USA). The area under curve (AUC) was calculated using the trapezoidal integration function, as previously described in Peixoto *et al.* (2020). After 186 h of Biolog[®]Ecoplate incubation, substrate well-averaged color development (SAWCD) index was calculated, for each soil treatment. The 31 carbon substrates from Biolog[®]Ecoplate were divided into six guilds (*i.e.*, carbohydrates, carboxylic acids, amines and amides, amino acids, polymers, and phenolic acids) following the classification described in Sala *et al.* (2006).

2.7. Microbiome analysis

After day 0 and day 28 of exposure, the total DNA was extracted (from 0.25 g of soil) using the UltraClean[®]Power Soil DNA Isolation Kit (MoBio Laboratories, Inc., Carlsbad, CA). Sequencing was performed by Eurofins Genomic (Ebersberg, Germany). The amplification of the 16S rRNA gene (V3-V4 region) was performed on Illumina MiSeq[®]sequencer (Illumina, San Diego, CA, USA), using the primers 357F (TACGGGAGGCAGCAG) and 800R (CCAGGGTATCTAATCC) (Turner *et al.*, 1999; Kisand *et al.*, 2002), following the manufacturer's protocols (Illumina, San Diego, CA, USA). Concerning the sequencing processing, raw reads less than 285 bp and average quality lower than Q30 were removed the analysis. Only the high-quality reads were

assigned to Operational Taxonomic Units (OTU), using the Minimum Entropy Decomposition method (Eren *et al.*, 2015). The DC-MEGABLAST alignments – NCBI database was used to the taxonomy assignment. Additionally, the lineage-specific 16S rRNA gene copy numbers were used to normalized the abundance estimations (Angly *et al.*, 2014).

To obtained the functional profile, OTU sequences were matched against the Kyoto Encyclopedia of Genes and Genomes, using the Piphillin tool (Iwai *et al.*, 2016; Narayan *et al.*, 2020).

2.8. Statistical analysis

The homogeneity of variance (Levene's test) and normality (Shapiro-Wilk's test) were always verified ($p < 0.05$), using the SPSS version 12.5. Two-way ANOVA was conducted to assess the effect among the soil treatments [CT, Kocide[®]3000, nCu(OH)₂, nCuO, and Cu(OH)₂-i], and the exposure time (days: -2, 0, 14 and 28). When a single sampling time was considered (*e.g.*, sequencing at day 28), a one-way ANOVA was conducted to assess differences among the soil treatments [CT, Kocide[®]3000, nCu(OH)₂, nCuO and Cu(OH)₂-i]. Additionally, three-way ANOVA was performed for bacterial counts data analysis, considering the following factors: Cu-treatments, time of exposure and culture media. Tukey's HSD (Honestly Significant Difference) post-hoc analysis was always performed to obtained multiple comparisons between soil treatments.

The clustering analysis of soil microbiome analysis was constructed based on Bray-Curtis distance after the data square root transformed, using the Primer 6+permanova software (Primer-E Ltd., Plymouth, UK). Additionally, a PERMANOVA analysis was performed (999 permutations) to obtain the statistical significances between soil treatments and exposure time.

3. Results

3.1. General trends in extractable Cu for amended soil

The analysis DTPA-extractable ionic Cu suggests a distinct pool ionic Cu(II) from treated soil along exposure time (Figure 1). Since the first time of exposure, Cu(OH)₂-i showed a significantly higher DTPA-extractable pool of ionic Cu(II) in soil compared to the other materials, presenting bound ionic Cu(II) levels of 90.4% (day -2) and 94.8%

(day 0) (Table S1). Over time, this formulation also showed a significantly higher bioavailability than the other materials (Table S1). For instance, at both 14 and 28 days, the pool of ionic Cu(II) bound in soil significantly decreased in order: $\text{Cu}(\text{OH})_2\text{-i}$ (92.7 - 88.7%) > Kocide[®]3000 (85.3 - 74.5%) ~ nCuO (85.5 - 68.9%) > nCu(OH)₂ (63.5 - 50.4%). Concerning the nano-formulations, nCuO showed a significantly lower pool of ionic Cu(II) compared to the other materials in the first sampling times, presenting of 33.1% (day -2) and 41.8% (day 0) (Table S1). At these exposure times, a similar ionic Cu (II) level was detected for both Kocide[®]3000 and nCu(OH)₂ treated soils [nCu(OH)₂: 63.0 – 70.8 % and Kocide[®]3000: 63.9 – 81.3 %; Table S1]. At later times of exposure (days 14 and 28), the pool of ionic Cu(II) in nCuO-treated soil increased to similar levels to those detected in Kocide[®]3000-treated soil (Table S1). On the other hand, the pool of ionic Cu(II) of nCu(OH)₂ slightly decreased over time, to values of 63.5% (day 14) and 50.4% (day 28), making it the less bioavailable form of Cu in soil compared to other NMs (Table S1).

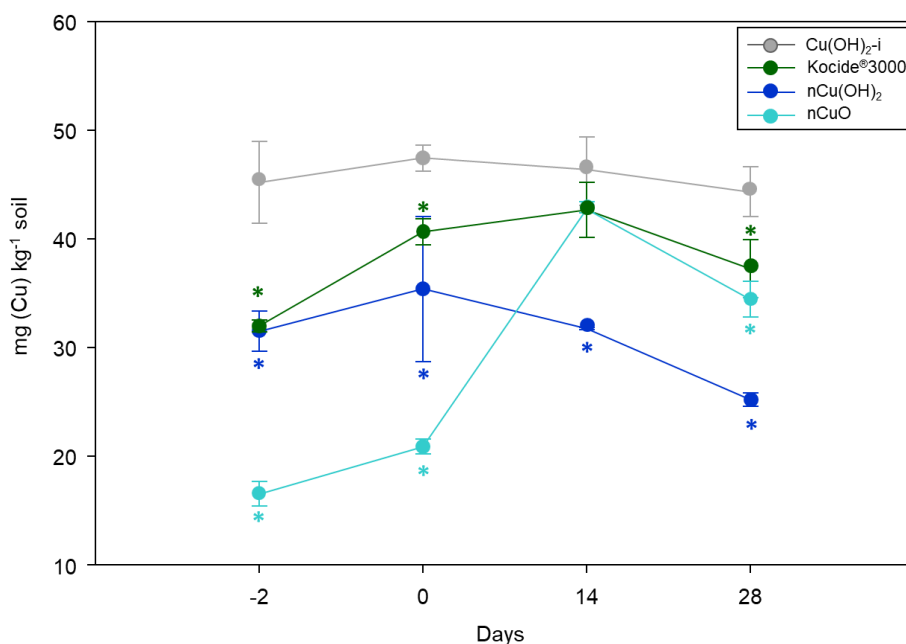


Figure 1. Diethylenetriaminepentaacetic acid (DTPA) extractable Cu in Lufa 2.2 treated with $\text{Cu}(\text{OH})_2\text{-i}$, Kocide[®]3000, nCu(OH)₂, or nCuO, after day -2 (soil-spiking), day 0 (input soil organisms), day 14 and day 28. The data was expressed as mg (Cu) kg⁻¹ of soil [average (n = 3) ± standard deviation]. The DTPA extractable Cu in non-treated soil (CT) was measured in all soil treatments and presented values below the detection level (<LOD). Asterisks (*) indicate significant differences between Cu-treated soil towards the $\text{Cu}(\text{OH})_2\text{-i}$ treated soil (one-way ANOVA, Tukey HSD method; p<0.05), for each sampling time.

3.2. Effects on culturable bacteria

The abundance of viable heterotrophic bacteria (HB) and of bacteria able to solubilize phosphate (P-SB), significantly increased in soils over time (Figure 2), regardless of Cu contamination ($F=76.3$; $p<0.001$). The $\text{Cu}(\text{OH})_2\text{-i}$, Kocide[®]3000 and nCuO treatments resulted in a slight, non-significant, decrease of CFUs in both media after 28 days. For HB, the decrease was 0.3%, 16.5% and 17.5% for $\text{Cu}(\text{OH})_2\text{-i}$, Kocide[®]3000 and nCuO, respectively. For P-SB, the decrease was 5.9%, 13.8% and 16.7% for $\text{Cu}(\text{OH})_2\text{-i}$, Kocide[®]3000 and nCuO, respectively, towards the CT. In contrast, nCu(OH)₂-exposure resulted in a significant ($F=3.19$; $p=0.023$) increase of 75% and 69% of the CFUs counted in NA and NBRIP medium, respectively, after 28 days.

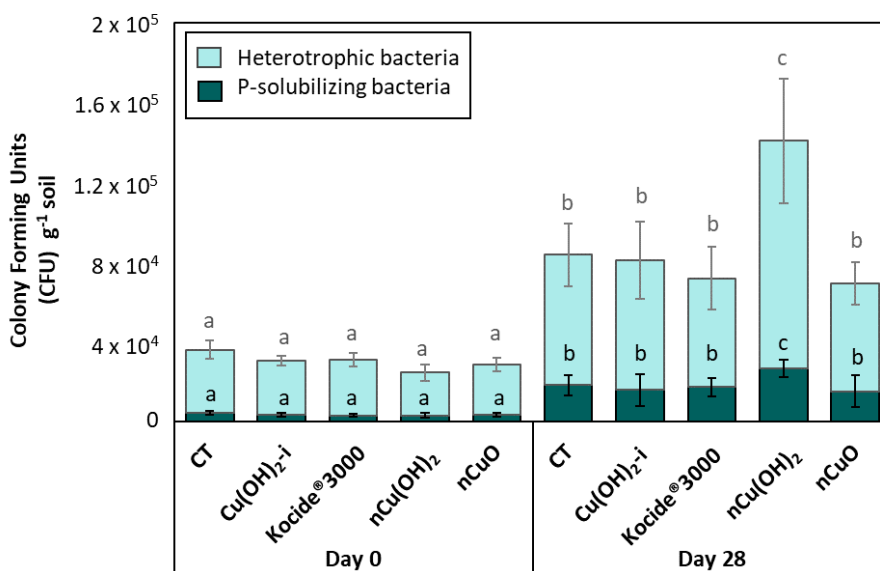


Figure 2. Average colony forming units (CFUs) in non-treated Lufa 2.2 soil (CT) and in soil spiked with $\text{Cu}(\text{OH})_2\text{-i}$, Kocide[®]3000, nCu(OH)₂, or nCuO, sampled at day 0 and 28. Heterotrophic bacteria (HB) were counted in nutrient agar medium and P-solubilizing bacteria in National Botanical Research Institute Phosphate (NBRIP) medium (B). Different letters (^{a,b,c}) indicate significant differences regarding the time of exposure and treatments for each culture media, using the three-way ANOVA (Tukey HSD method; $p<0.05$).

3.3. Treatment effects on enzymatic activity

The impact of Cu (nano)formulations on soil enzymatic activities (DHA, βG , AP, AS, and UA) are represented in Figure 3 (A-E). The DHA and AS (Figure 3 A and 3 B) showed the greatest sensitivity after 28 days to all Cu materials tested, resulting in a significant activity decrease ($p<0.05$; Table S2). For DHA activity, the reduction was 92%, 95%, 86%, and 68% relative to the CT, in soils exposed to $\text{Cu}(\text{OH})_2\text{-i}$,

Kocide[®]3000, nCuO and nCu(OH)₂, respectively. For AS activity, a reduction of 41%, 27%, 44% and 32% was observed in soils exposed to Cu(OH)₂-i, Kocide[®]3000, nCuO and nCu(OH)₂, respectively. During the exposure time, the microbial communities exposed to all Cu-treatments regardless of its formulation [Cu(OH)₂-i, Kocide[®]3000, nCu(OH)₂ and nCuO] also displayed a significant reduction in UA activity (Figure 3 E), showing a decreased activity between ~20% and ~40% for all sampling points (p<0.05; Table S2). In opposite, Cu-treatments did not affect AP and βG activities (Figure 3 C and D).

Additionally, differences among treatments were observed for the AP activity at day 14, in which nCuO-treated soils presented a higher AP activity (10%) than soils treated with nCu(OH)₂, while at 28 days AP activity was lower in soils spiked with Cu(OH)₂-i (15%) or nCuO (13%) in comparison to the activity in nCu(OH)₂-treated soils (Table S2).

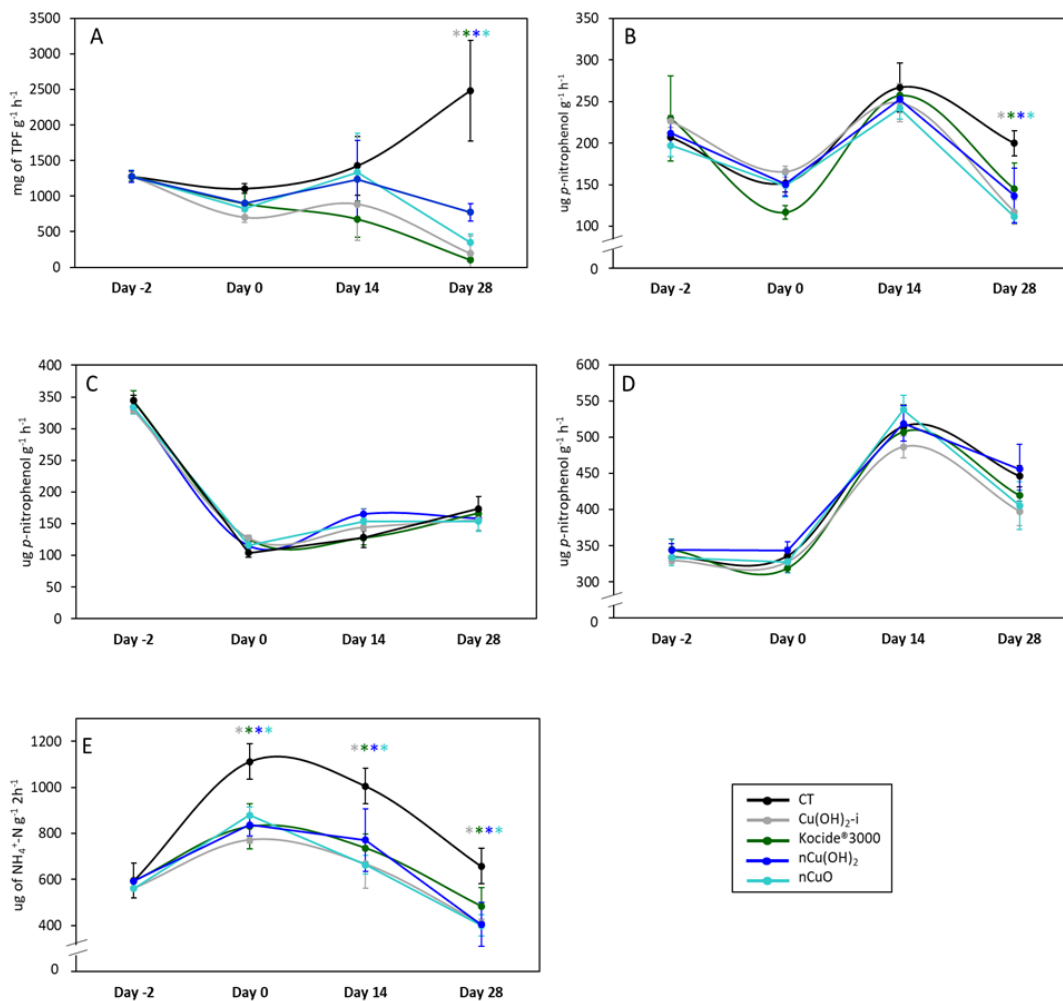


Figure 3. Enzymatic activity measured in Lufa 2.2 non-treated soil (CT) and soil spiked with Cu(OH)₂-i, Kocide[®]3000, nCu(OH)₂ or nCuO, and sampled at day -2, 0, 14 and 28. The data represent the average enzymatic activity ($n=3 \pm$ standard deviation) of dehydrogenase (A), arylsulfatase (B), β -glucosidase (C), acid phosphatase (D), and urease (E). Asterisks (*) indicate significant differences between Cu-treated samples towards the CT soil (two-way ANOVA, Tukey HSD method; $p < 0.05$), for each sampling time.

3.4. Effects on carbon substrates utilization

Over time, the carbon substrate utilization significantly increased irrespective of the treatment ($F=51.51$; $p < 0.001$) (Figure 4). Regarding the Cu-treatments, only the microbial community from nCuO-exposed soils exhibited a significantly higher carbon utilization toward the CT or soil exposed to Kocide[®]3000 (based on AUC; Figure 4), after 28 days of exposure ($F=51.51$; $p < 0.001$).

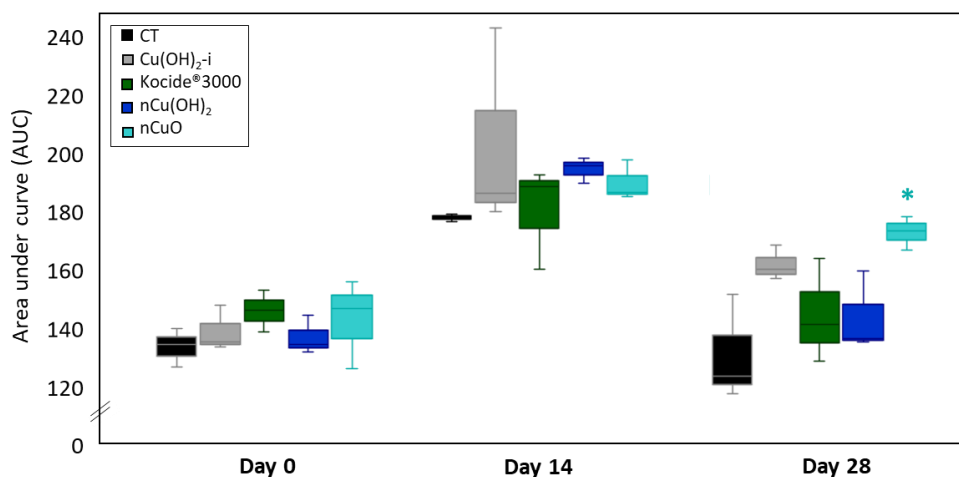


Figure 4. Community-level physiological profiles (CLPP) measured in non-treated Lufa 2.2 soil (CT) or spiked with Cu(OH)₂-i, Kocide[®]3000, nCu(OH)₂ or nCuO, sampled at day 0, 14 and 28. The data represent the mean ($n=3 \pm$ standard deviation) of area under curve (AUC). The AUC was calculated based on the trapezoidal integration function. Asterisks (*) indicate significant differences ($p < 0.05$) between Cu-treated soils and CT soil (two-way ANOVA, Tukey HSD test), for each sampling time.

Analysing the substrate classes, the use of phenolic compounds and amines/amides was significantly affected by exposure to all Cu-formulations (Figure 5, Table S3). Regarding the phenolic compounds, a significant lower utilization was measured in soils spiked with Kocide[®]3000 (18% at day 14 and 38% at day 28), Cu(OH)₂-i (26% at day 28), nCu(OH)₂ (21% at day 28) and nCuO (25% at day 28), towards the respective CT (Table S4). On the other hand, significantly higher utilization of amides/amines was detected in soils exposed to Kocide[®]3000 (34% at day 28), Cu(OH)₂-i (33% at day 14 and 31% at day 28), nCu(OH)₂ (30% at day 14 and 17% at day 28) and nCuO (29% at day 14 and 32% at day 28) (Table S3). In addition, changes were detected in the utilization of specific substrates grouped in amides/amines class: the putrescine use increased in soils spiked with Kocide[®]3000 (82%; at day 14); Cu(OH)₂-i (104% at day 14); nCu(OH)₂ (111% at day 14), nCuO (98% at day 14, and 77% at day 28) compared with CT soils; while the phenylethylamine use was higher in soils exposed to Kocide[®]3000 when compared to other contaminants, namely Cu(OH)₂-i (115% at day 14), nCu(OH)₂ (95% at day 14) and nCuO (102% at day 14) (Table S4). Also, the use of 4-hydroxybenzoic acid, grouped in the class of phenolic compounds, decreased significantly in Kocide[®]3000-treated soils (152%) compared to CT (Table S4). Differences in the utilization rate of specific substrates were registered between Cu forms, during the experiment (Table S4). For instance, these differences were detected

at day 0 for glycogen [43 to 52 % decrease in nCuO-treated soil towards soils treated with other Cu forms] and D-glucosaminic acid [77% decrease in nCuO towards the nCu(OH)₂ and Cu(OH)₂-i-treated soils]; at day 14 for Tween 40 [26 to 28% decrease in nCuO towards the Cu(OH)₂-i and Kocide[®]3000-treated soils], and Phenylethylamine [3 to 5% increase in Kocide[®]3000-treated soil towards other Cu treatments]; and at day 28 for Y-hydroxybutiric acid, L-threonine and L-arginine [increase in nCuO-treated soil towards the nCu(OH)₂-treated soil: 56%, 146%, and 53%, respectively], L-phenylalanine [increase in nCuO-treated soil towards the nCu(OH)₂ (53%) and Kocide[®]3000 (64%) treated soils; and increase in Cu(OH)₂-i towards the nCu(OH)₂-treated soil (56%)], L-serine [increased use in nCuO-tread soil towards the nCu(OH)₂ and Kocide[®]3000-treated soils (66% and 48%, respectively)].

Moreover, exposure to nCuO, Cu(OH)₂-i, and nCu(OH)₂ significantly increased the diversity/type of carbon substrates utilized (Shannon-Wiener index) towards the CT, after 28 days of exposure (Figure S1). Regarding Cu-formulations, the carbon substrates' diversity was similar in soils exposed to Kocide[®]3000, nCu(OH)₂ and CT. However, it was lower in Kocide[®]3000-exposed soil than the soil exposed to ionic Cu(OH)₂ and nCuO.

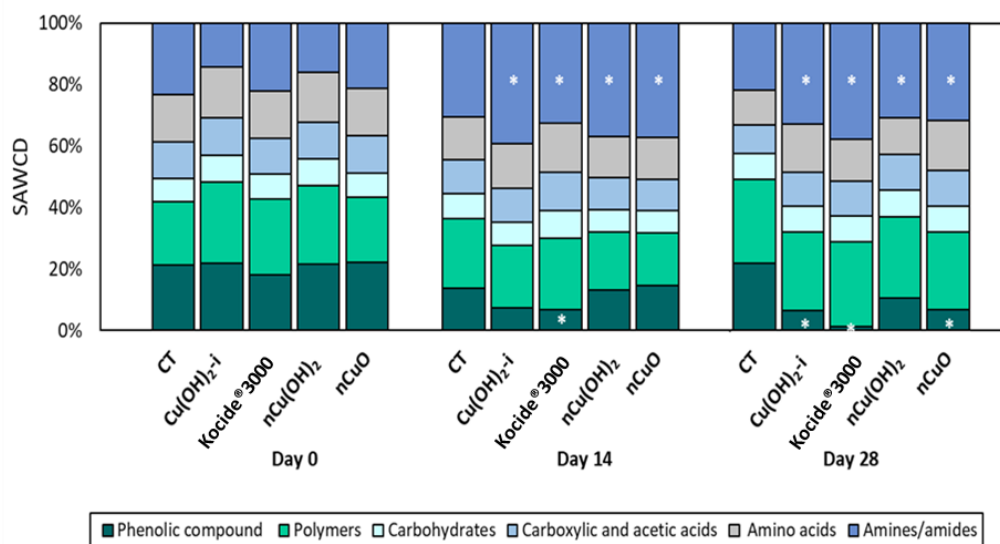


Figure 5. Substrate average well colour development (SAWCD) measured in Lufa 2.2 soil spiked with Cu(OH)₂-i, Kocide[®]3000, nCu(OH)₂ or nCuO, sampled at days 0, 14 and 28. Non-treated soil (CT) was included. The data represent the mean (n=3) of SAWCD index. Asterisks (*) indicate significant differences (p<0.05) between treated soils and respective CT soil (two-way ANOVA, Tukey HSD method), for each sampling time.

3.5. Metagenomic analysis

A total of 2 653 984 sequence reads (after quality-filtering) were included in this analysis (Table S5). The saturation in the rarefaction curves presented in Figure S2 suggested an adequate sampling for this analysis. Based on OTUs composition and abundance, a significant shift in soil bacterial community was detected from day 0 to day 28 (PERMANOVA: $F=39.39$, $P=0.001$). As observed in Figure 6 A, the similarity between soil treatments decreased over time (day 0: ~80% and day 28: ~60% of similarity). On day 0 (2 days after the addition of the contaminants), there was no clear separation from the CT. However, significant differences between Cu-formulations were detected across the following treatments: nCuO, nCu(OH)₂ and Cu(OH)₂-i [PERMANOVA: nCuO x nCu(OH)₂: $t=1.23$; $P=0.05$; nCuO x Cu(OH)₂-i: $t=1.23$; $P=0.049$; and nCu(OH)₂ x Cu(OH)₂-i: $t=1.85$; $P=0.027$]. On the other hand, a significant impact of Cu exposure in the bacterial community structure was observed at day 28, regardless of Cu-formulation (Figure 6 A and PERMANOVA: $F=2.18$, $P=0.022$). The principal coordinate analysis corroborates with the clustering analysis (Figure 6 B and C).

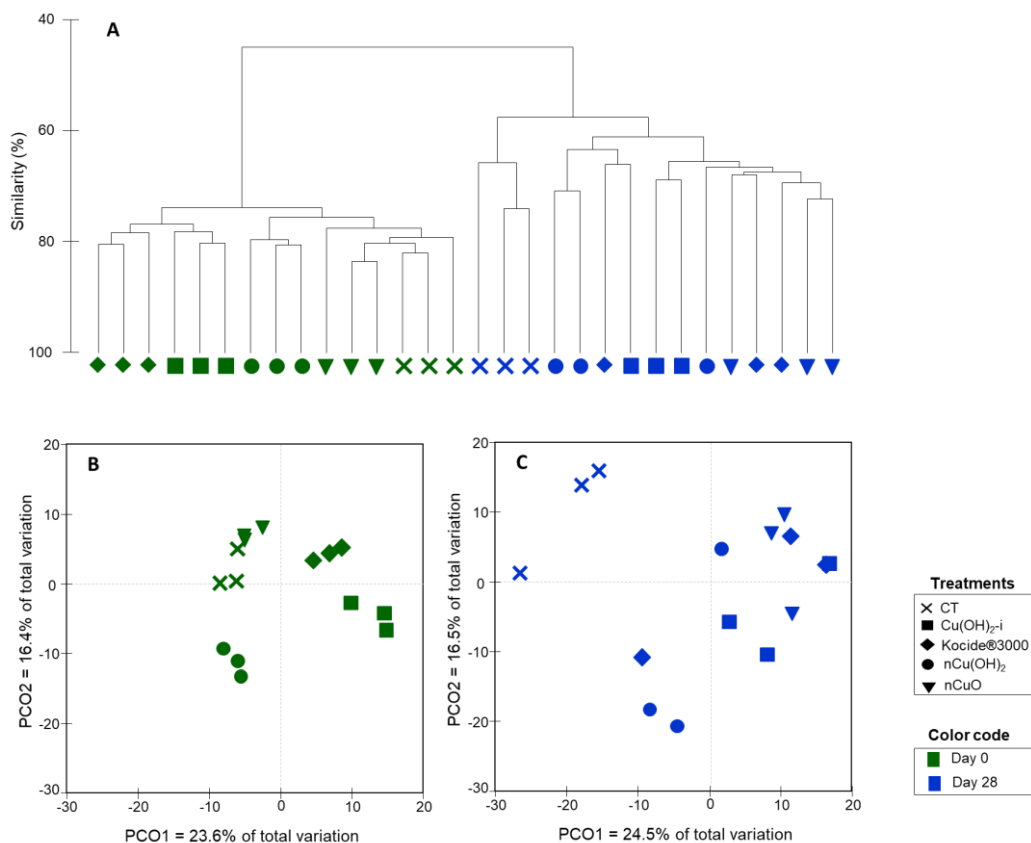


Figure 6. Soil microbiome structure from non-treated soil (CT) and soil treated to $\text{Cu}(\text{OH})_2\text{-i}$, Kocide[®]3000, $\text{nCu}(\text{OH})_2$, or nCuO , after 0 and 28 days of exposure. Cluster analysis (A) and principal coordinate analysis (B - day 0 and C - day 28) were constructed based on Bray-Curtis similarity after square root transformation on OTU abundance.

Regarding alpha-diversity, no significant changes were observed on the richness, Shannon-wiener and Pielou's indexes of soil bacterial communities, regardless of the Cu addition (Table S6).

At the class level, the most abundant classes at day 0 were Acidobacteria ($33\% \pm 3$), Alphaproteobacteria ($23\% \pm 1$), Rubrobacteria ($11\% \pm 2$), and Actinobacteria ($11\% \pm 1$), irrespective of soil treatments (Figure 7 A). At day 28, these abundances were significantly decreased for Acidobacteria (-16% ; $F=240$; $p<0.001$), and Rubrobacteria (-5% ; $F= 61$, $p<0.001$) in CT soils, when compared with day 0. At the end of the experiment (28 days, Figure 7 B), a significant increase of the relative abundance for Gemmatimonadetes [1.3% in the $\text{nCu}(\text{OH})_2$ -treated soil vs. 0.2% in CT] and Clostridia (0.3% in the soil spiked with Kocide[®]3000-treated soil vs. 0.1% in CT) were detected in soils spiked with Cu in comparison to the respective CT (Table S7). On the other hand, a significant decrease in the relative abundance of both classes Acidobacteria [16.6% in CT vs. 13.0% in $\text{Cu}(\text{OH})_2\text{-i}$; 9.0% in Kocide[®]3000; 13.2% in nCuO treated soils], and

Flavobacteriia [4% in nCu(OH)₂ vs. 6% in CT] was observed in Cu -treated soil towards the CT (Table S7). The effects significantly differed among Cu-forms for Gemmatimonadetes [0.14% in Kocide®3000 vs. 1.3% in nCu(OH)₂] and Flavobacteriia [8.20% in Kocide®3000 vs. 3.70% in nCu(OH)₂] (Table S7).

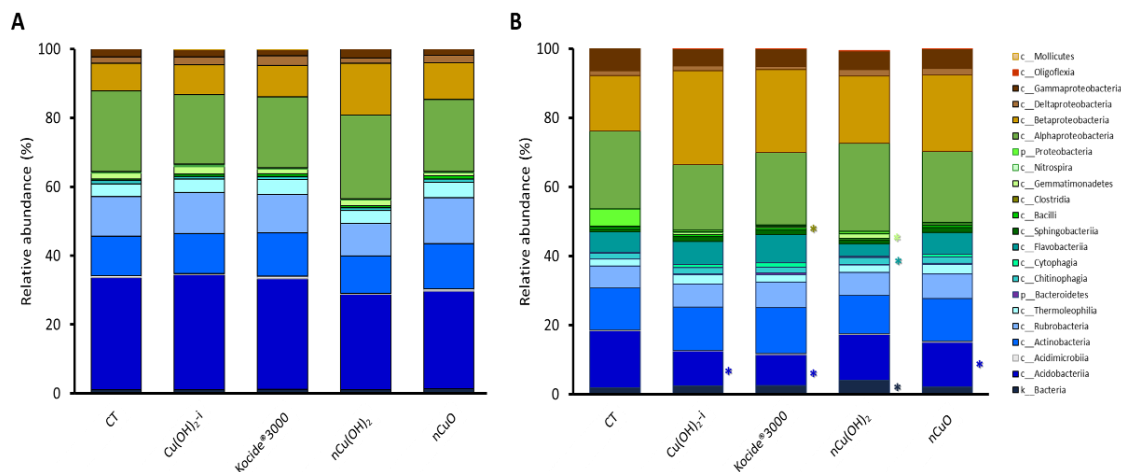


Figure 7. Relative abundance (%) of classes and unidentified classes affiliated with phylum or kingdom in non-treated Lufa 2.2. soil (CT) or in spiked soil with 50 mg (Cu) kg⁻¹ soil of Cu(OH)₂-i, Kocide®3000, nCu(OH)₂, or nCuO, after 0 (A) and 28 (B) days of exposure. Data represent the average of three replicates per treatment. Asterisks (*) indicate significant differences between copper-treated samples and the respective control (CT) ($p < 0.05$; Tukey HSD).

At the genus level (Figure 8), a total of 9 and 24 genera were significantly affected by the Cu contamination, in both nano and ionic formulations, towards the CT, after 2 days of Cu addition in soil (day 0) and 28 days of exposure, respectively. At day 0 (Figure 8), a total of five, two, four and three genera were changed by the Cu(OH)₂-i, Kocide®3000, nCu(OH)₂ and nCuO exposure, respectively, in comparison to the CT soil ($p < 0.05$, Table S8). At the end of the experiment (day 28), the Cu(OH)₂-i, Kocide®3000, nCu(OH)₂, and nCuO exposure influenced the abundance of 10, 11, 14 and 15 genera, respectively, in comparison to the CT (Figure 8 and Table S8).

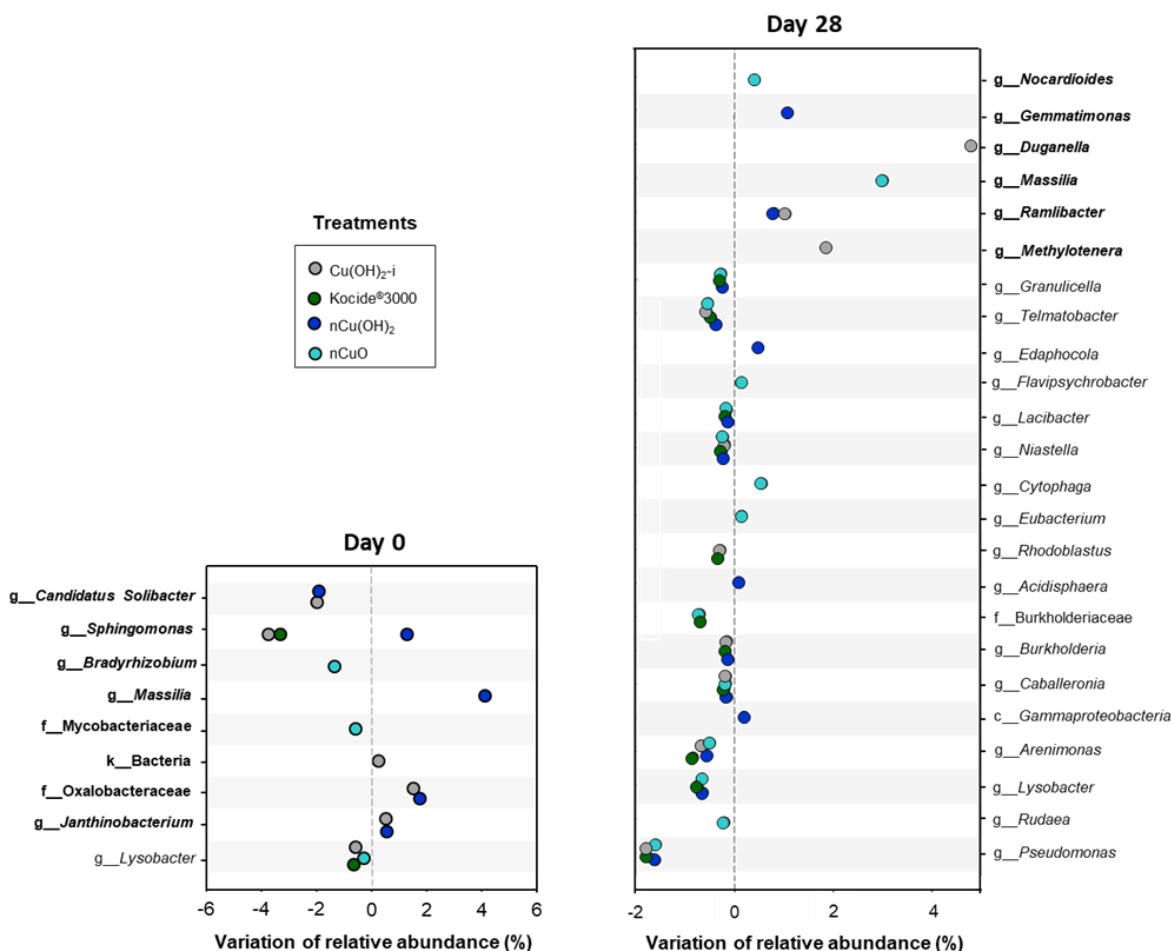
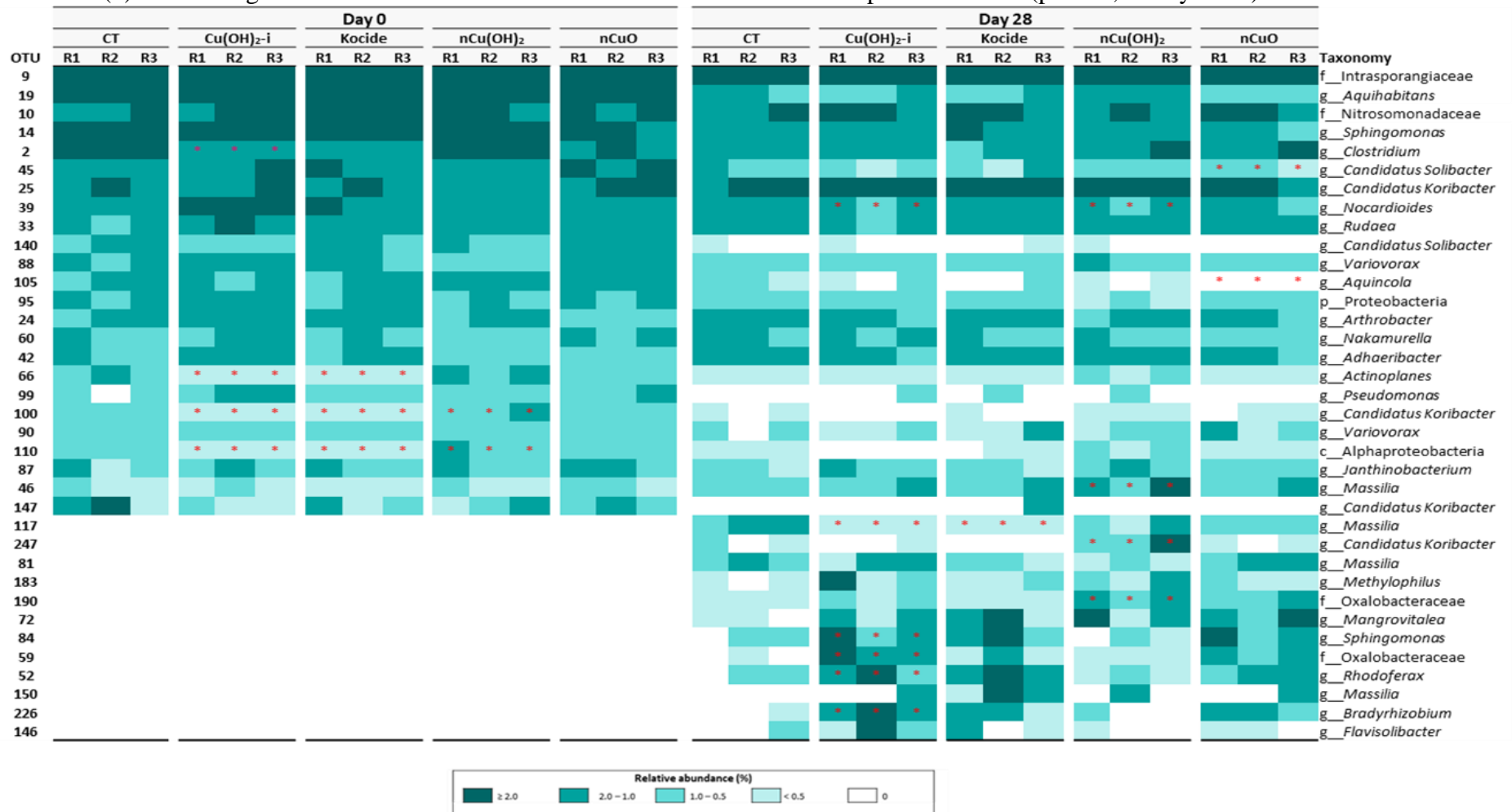


Figure 8. Genera and unidentified genera affiliated with family, class or kingdom significantly affected by 50 mg (Cu) kg⁻¹ soil of copper formulations [Cu(OH)₂-i, Kocide®3000, nCu(OH)₂, or nCuO] (one-way ANOVA; p<0.05), after day 0 and 28 of exposure. The direction (positive or negative variation) and the magnitude of the responses are indicated on the x-axis, which shows the percentage of variation to the control (CT). Data represent the average of three replicates per treatment. Bold letters indicate the most abundant genera (relative abundance >1%).

The top 15 most abundant OTUs from soil samples, after both 0 and 28 days of exposure, are represented in the Heatmap presented in Table 1. After 2 days of soil spiking (day 0), the Cu-formulations significantly affected the relative abundance of four OTUs, namely OTU 66 [Cu(OH)₂-i: -71%; and Kocide®3000: -64%], OTU 100 [Cu(OH)₂-i: -46%; Kocide®3000: -43%; and nCu(OH)₂: +46%], and OTU 110 [nCu(OH)₂-i: -70%; and Kocide®3000: -67%, and nCu(OH)₂: +45%] and OTU 2 [Cu(OH)₂-i: -45%], towards the respective CT (Table S9). At the end of the experiment, the Cu contamination significantly affected the relative abundance of 11 OTUs towards the CT (Table S9). For instance, Kocide®3000-treated soil only exhibited a significant decrease in OTU 117 (-72%); nCuO treatment changed the abundance of OTU 45 (-

52%) and OTU 105 (-100%); and soil spiked with $n\text{Cu}(\text{OH})_2$ presented a significant change in relative abundance of four OTUs [OTU 190 (+67%), OTU 46 (+ 65%), OTU 247 (+84%), and OTU 39 (+58%)]; while the $\text{Cu}(\text{OH})_2\text{-i}$ treated soil exhibited a significant change in the abundance of six OTUs [OTU 39 (-37%), OTU 84 (-71%), OTU 117 (-71%), OTU 52 (+94%), OTU 59 (+83%), OTU 226 (+91%)]. Additionally, fourteen OTUs showed to be distinctly affected by NMs, regarding the Cu-formulation, as described in Table S9.

Table 1. Relative abundance of the 15 most abundant OTUs per treatment in control soil and soil spiked with different copper formulations. Asterisks (*) indicate significant differences in relative abundances towards the respective control ($p < 0.05$; Tukey HSD).



3.6. Functional prediction

The function inference analysis (Table 2) predicted a significant influence of Cu-based NMs in the relative abundance of sequences related to different metabolic pathways (*e.g.*, carbon, nitrogen, sulfur metabolisms) towards the CT, only after 28 days of exposure. For instance, a significant increase of sequences encoding phosphoadenosine phosphosulfate reductase (sulfur metabolism; +0.26%) was inferred for soils exposed to nCu(OH)₂. For nitrogen cycle was predicted a significant change in the abundance of sequences encoding nitrous-oxide reductase (-0.05% of *nosZ* in all Cu-treated soils); nitrate reductase (-0.40% of *napA* and *napB* in nCuO-treated soil); nitric oxide reductase subunit B (-0.27% of *norB* in nCuO-treated soil); nitrite reductase [-0.46% of *nirS* in Kocide[®]3000, -0.45% in nCuO, and -0.56% in Cu(OH)₂-i-treated soil]; nitrite reductase [-0.42% of *nirB* in nCu(OH)₂]; and nitrite reductase - cytochrome c-552 [+0.079% of *nrfA* and *nrfH* in Cu(OH)₂-i]. Carbon related metabolism sequences/genes were also affected, like the ones encoding phosphoribulokinase [-0.45% in soils spiked with Cu(OH)₂-i and nCuO], and glyceraldehyde 3-phosphate dehydrogenase [+0.62% in soils spiked with Cu(OH)₂-i and +0.74% with nCuO]. Additionally, a significant change of genes associated with metal resistance mechanisms was inferred in Cu-treated soils in comparison to the CT, including efflux pumps [+0.01% of *cusC* in soil spiked with nCu(OH)₂, and -0.30% of *cusR*, and *copR* (regulation of CusR system) in nCuO-treated soil], transcriptional factors [-2.30% of *rnk*; regulator of nucleoside diphosphate kinase in nCuO-treated soil], translation [+1.98% aminoacyl-tRNA biosynthesis in nCu(OH)₂-treated soil], *Quorum Sensing* [-4.78% the *ddpD*; peptide/nickel transport system ATP-binding protein], and signalling and cellular processes [+0.47% of *pcoB*, *copB* genes]. Additionally, genes related to the ABC transporters were predicted to decrease in Cu - treated soils (-14% of *livK*: branched-chain amino acid transport system substrate-binding protein). However, a strong impact was inferred for soil spiked with Cu(OH)₂-i and nCuO, in which was observed a decrease of *e. g.*, *livK*, *livH*, *livM*, *livF*, *livG*, and ABC.PE.P. Also, a significant decrease (-0.02%) in the relative abundance of *scsB* genes, related to the suppressor for Cu -sensitivity B, was predicted in nCuO-treated soil. Regarding the energy metabolism, only the soils spiked with the ionic form of Cu(OH)₂-i showed a significant increase in the sequences related to different NADH-quinone oxidoreductase subunits (*e.g.*, A, C, D).

Table 2. Inference of pathways affected by exposure to 50 mg (Cu) kg⁻¹ soil, as different formulation of copper [Cu(OH)₂-i, Kocide[®]3000, nCu(OH)₂, nCuO]. The soil sampling was done at day 28. The significative decrease (■) and increase (■) of the relative abundance of function-related sequences towards the non-treated soil (CT) are highlighted (Tukey HSD; p<0.05). White colour represents no statistically significant effects towards the CT.

	Pathways	KEGG	CT	Cu(OH) ₂ -i	Kocide [®] 3000	nCu(OH) ₂	nCuO	
Sulfur metabolism	<i>cysH</i> ; Phosphoadenosine phosphosulfate reductase	K00390	0.036	0.038	0.037	0.038	0.038	
	<i>napA</i> ; Nitrate reductase (cytochrome)	K02567	0.016	0.013	0.014	0.014	0.012	
	<i>napB</i> ; Nitrate reductase (cytochrome), electron transfer subunit	K02568	0.016	0.013	0.014	0.014	0.012	
	<i>nirB</i> ; Nitrite reductase (NADH) large subunit	K00362	0.055	0.054	0.054	0.051	0.053	
Nitrogen metabolism	<i>nrfA</i> ; Nitrite reductase (cytochrome c-552)	K03385	0.000	0.001	0	0.001	0.001	
	<i>nrfH</i> ; Cytochrome c nitrite reductase small subunit	K15876	0.000	0.001	0	0.001	0.001	
	<i>nirS</i> ; Nitrite reductase (NO-forming)/hydroxylamine reductase	K15864	0.001	0	0	0.001	0	
	<i>norB</i> ; Nitric oxide reductase subunit B	K04561	0.019	0.018	0.018	0.017	0.017	
	<i>nosZ</i> ; Nitrous-oxide reductase	K00376	0.002	0.001	0.001	0.002	0.001	
	PRK, <i>prkB</i> ; Phosphoribulokinase	K00855	0.018	0.013	0.015	0.015	0.013	
	<i>rbcL</i> , <i>cbbl</i> ; Ribulose-bisphosphate carboxylase large chain	K01601	0.021	0.016	0.018	0.019	0.017	
Carbon metabolism	<i>rbcS</i> , <i>cbbs</i> ; Ribulose-bisphosphate carboxylase small chain	K01602	0.016	0.013	0.014	0.014	0.012	
	GAPDH, <i>gapA</i> ; Glyceraldehyde 3-phosphate dehydrogenase	K00134	0.043	0.049	0.047	0.046	0.050	
	ALDO; Fructose-bisphosphate aldolase, class I	K01623	0.021	0.016	0.018	0.019	0.017	
	<i>rpiA</i> ; Ribose 5-phosphate isomerase A	K01807	0.016	0.013	0.014	0.014	0.012	
	<i>rpiB</i> ; Ribose 5-phosphate isomerase B	K01808	0.043	0.049	0.047	0.046	0.050	
	GAPDH, <i>gapA</i> ; Glyceraldehyde 3-phosphate dehydrogenase	K00134	0.028	0.031	0.029	0.027	0.029	
	ACAT, <i>atoB</i> ; acetyl-CoA C-acetyltransferase	K00626	0.324	0.277	0.299	0.309	0.287	
	Translation	tRNA-Ala; Aminoacyl-tRNA biosynthesis	K14218	0.134	0.148	0.134	0.153	0.144
	Transcription factors	<i>rnk</i> ; Regulator of nucleoside diphosphate kinase	K06140	0.117	0.097	0.107	0.103	0.094
	Energy metabolism	<i>nuoA</i> ; NADH-quinone oxidoreductase subunit A	K00330	0.040	0.044	0.040	0.042	0.042
<i>nuoC</i> ; NADH-quinone oxidoreductase subunit C		K00332	0.039	0.043	0.040	0.041	0.042	
<i>nuoD</i> ; NADH-quinone oxidoreductase subunit D		K00333	0.039	0.043	0.040	0.041	0.042	
Two-component system	<i>cusC</i> , <i>silC</i> ; outer membrane protein, copper/silver efflux system	K07796	0	0	0	0.0001	0	
	<i>cusR</i> , <i>copR</i> , <i>silR</i> ; two-component system, OmpR family, copper resistance phosphate regulon response regulator CusR	K07665	0.022	0.027	0.026	0.021	0.019	
Other	<i>pcoB</i> , <i>copB</i> ; copper resistance protein B	K07233	0.005	0.006	0.006	0.010	0.007	
Transporters, signalling and cellular processes	<i>scsB</i> ; Suppressor for copper-sensitivity B	K08344	0.0004	0.0002	0.0003	0.0004	0.0002	
ABC transporters and <i>Quorum sensing</i>	<i>livK</i> ; branched-chain amino acid transport system substrate-binding protein	K01999	0.732	0.602	0.651	0.636	0.592	
	<i>livH</i> ; branched-chain amino acid transport system permease protein	K01997	0.572	0.469	0.509	0.496	0.461	
	<i>livM</i> ; branched-chain amino acid transport system permease protein	K01998	0.566	0.464	0.504	0.490	0.457	

4| Responses of soil microbiome to copper-based nanomaterials for agricultural applications

	<i>livF</i> ; branched-chain amino acid transport system ATP-binding protein	K01996	0.542	0.446	0.482	0.471	0.440
	<i>livG</i> ; branched-chain amino acid transport system ATP-binding protein	K01995	0.540	0.445	0.480	0.470	0.438
	ABC.PE.S; peptide/nickel transport system substrate-binding protein	K02035	0.363	0.295	0.324	0.319	0.288
	ABC.PE.P1; peptide/nickel transport system permease protein	K02034	0.278	0.230	0.250	0.245	0.224
	ABC.PE.P; peptide/nickel transport system permease protein	K02033	0.264	0.220	0.238	0.233	0.214
<i>Quorum sensing</i>	<i>ddpD</i> ; peptide/nickel transport system ATP-binding protein	K02031	0.251	0.208	0.225	0.222	0.203

4. Discussion

Currently, a dynamic model ecosystem, including key decomposer organisms (invertebrates: *Porcellionides pruinosus*, *Eisenia andrei* and *Tenebrio molitor*) and plants (wheat: *Triticum aestivum* L.), allowed a more accurate assessment of effects of Cu-based NMs on the soil microbiome structure/composition and function, during the 28 days of exposure. The ionic Cu(II) bound in soils was also monitored during 28 days of exposure, which allowed us to explain some distinct effects of Cu-formulations on the soil microbiome.

4.1. Pattern of bound ionic Cu in soil

Our study showed distinct pattern of DTPA-extracted pool of Cu(II) in treated soils, which depended on the exposure time and Cu-forms. The ionic control Cu(OH)₂-i was the most bioavailable form over time, and accordingly, it was often the treatment eliciting more effects on the soil microbiome (*e.g.*, at OTU level). In fact, this ionic form of Cu quickly reacts with porewater and/or bounds to the soil particles, while the nano-forms release a smaller amount of Cu(II) ions in a more controlled manner along time (Zhang *et al.*, 2020). Concerning the Cu nano-forms, an increased DTPA-extracted pool of ionic Cu(II) in soil treated with nCuO in comparison to the Cu(NO₃)₂ have been reported, over time (Gao *et al.*, 2017). This suggested that nCuO had a slower dissolution, which also agrees with our results. Although a similar pattern of pool of Cu(II) in soil was observed in Kocide[®]3000 and nCuO treatments at day 28, some distinct effects on soil microbiome structure and function were detected, suggesting a potential nanoparticle-specific effect. Contrarily to our results, previous studies reported a higher Cu dissolution rate in soil spiked to Kocide[®]3000 compared to Cu(OH)₂-i (Neves *et al.*, 2019; Peixoto *et al.*, 2021), which may result from the use of distinct Cu concentration, time of exposure or Cu-extraction methods. Concerning the Cu-extraction method, the ionic Cu linked to soil organic matter or soil particles measured in DTPA analysis is not measured by the method used by Neves (*et al.*, 2019) and Peixoto (*et al.*, 2021).

4.2. Copper exposure affects the soil microbiome activity and function

As a fast response to metal contamination, bacterial colony counts are a good estimation for measuring NMs effects on the abundance of viable soil microorganisms (Vasileiadis

et al., 2015). In our study, only the $n\text{Cu}(\text{OH})_2$ treatment significantly increased the counts of culturable heterotrophic and P-SB bacteria, after 28 days of exposure. The lower pool of ionic $\text{Cu}(\text{II})$ detected in $n\text{Cu}(\text{OH})_2$ -treatment towards the other Cu-materials may explain the distinct effect on bacterial counts.

Soil enzymatic activities and utilization of carbon substrates have been suggested as good endpoints in assessing the impact of NMs in terrestrial ecosystem functioning (Samarajeeva *et al.*, 2020). In our experiment, enzymatic activity related to microbial activity (DHA), sulphur (AS) and nitrogen (UA) cycles showed to be the most affected enzymes by Cu contamination, regardless of formulation, which significantly reduced their activities. Also, this impact was mainly observed after 28 days of exposure, except for UA activity. In agreement with our results, several studies reported a negative impact of the nanosized Cu in different soil enzymatic activities, like DHA (Xu *et al.*, 2015; Samarajeeva *et al.*, 2020), βG (Simonin *et al.*, 2018; Peixoto *et al.*, 2021), phosphatase (acid and/or alkaline) (Xu *et al.*, 2015; Simonin *et al.*, 2018; Samarajeeva *et al.*, 2020) and UA (Xu *et al.*, 2015; Zhang *et al.*, 2020) activities. Particularly for DHA activity, this activity showed a stronger inhibition in Cu-treated soil. Since this enzyme can be associated with the microbial biomass, the abundance decreased of class Flavobacteriia [$n\text{Cu}(\text{OH})_2$ -treated soil] and Acidobacteria [Kocide[®]3000, $n\text{CuO}$, and $\text{Cu}(\text{OH})_2$ -i -treated soils] in Cu-treated soils may explain this inhibition. In our study, significant differences between Cu-formulations were not detected for these enzymatic activities. This suggests that the Cu addition *per se*, resulting in DTPA concentrations higher than 25 mg L^{-1} (at day 28), seems to inhibit the DHA, AS and UA activities. Additionally, the βG and AP activities were not affected by the Cu-exposure. Corroborating our results, the study of Samarajeeva (*et al.*, 2020) also reported similar βG activity in $n\text{CuO}$ -treated soil and CT soil. Concerning the functional profile, a slight effect of Cu-based NMs was detected in carbon substrate utilization. In fact, only the soil microbiome exposed to $n\text{CuO}$ showed a significant increase in AUC compared to the CT. In this treatment was registered a significant increase in the relative abundance of genus *Massilia*. This bacterium was described as copiotrophic, being highly competitive in utilizing carbon substrates (like saccharose, fructose and amino acids) (Su *et al.*, 2020b). Thus, its increased abundance may contribute to the higher carbon utilization. Accordingly, the study by Samarajeeva and collaborators (2020) also demonstrated that the $n\text{CuO}$ treatment slightly stimulated the carbon utilization index, at 54 to $123 \text{ mg (Cu) kg}^{-1}$ soil after 28 days of exposure. Regarding specific groups of

carbon substrates, a significant increase in the utilization of amines/amides and a decrease in the utilization of phenolic compounds [Kocide[®]3000, nCuO and Cu(OH)₂-i] were detected in exposed soils. The promoted utilization of amines/amides in Cu-treated soils may result from the increased abundance of some members of Betaproteobacteria, (R=0.44); Cytophaga (R=0.54) and Flavobacteriia (R=0.32). In fact, a study by Su *et al.* (2020a) showed a positive correlation between the class Betaproteobacteria and utilization of amines, carbohydrates, and carboxylic acids. The increased utilization of these compounds by the community exposed to Cu, resulting in their depletion from the soil, may negatively affect the plant growth and its responses to the abiotic and biotic stresses, as described in Bouchereau *et al.* (1999). In terms of phenolic compounds, only a decrease in the utilization of 4-hydroxybenzoic acid was registered. This substrate was described as a carbon source for *Pseudomonas* spp. (Bertani *et al.*, 2001). Thus, the observed decrease in the relative abundance of *Pseudomonas* (Proteobacteria class) in all Cu-treatments (Figure 8) may partly explain this result. Our work also reveals that the decrease in the abundance of Proteobacteria was positively correlated (R=+0.63) with the use of this carbon group, and it was the strongest correlation compared to the other classes. This decreased utilisation of phenolic compounds may result in their soil accumulation, with consequent detrimental effects on plants and microorganisms. In fact, the accumulation of these compounds in agricultural soils was previously related to plant diseases (*e.g.*, apple replant disease) (Radl *et al.*, 2019).

4.3. Copper exposure affects the soil microbiome structure and composition

Lufa soil is usually characterized by the dominance of phylum Proteobacteria (Alphaproteobacteria, Betaproteobacteria classes), Actinobacteria and Acidobacteria classes, which constitute their core microbiome (Fajardo *et al.*, 2019). The variability observed within the control group in terms of the microbiome structure may be related to slight differences in the invertebrate's weight, root biomass and the soil pH and conductivity (data not shown). Cu in nano- and ionic-form induced a shift in the bacterial community structure/composition, and different bacterial taxa responded differently to Cu contaminantion. Flavobacteriia [nCu(OH)₂] and Acidobacteria [Kocide[®]3000, nCuO, and Cu(OH)₂-i] were the most sensitive classes to the Cu exposure. A decreased abundance of these classes may negatively affect the nitrogen cycle since they influence the growth of plants and cellulose degradation (*e.g.*,

Flavobacteriia), decomposition of organic matter (e.g., Acidobacteria); and play a key role in nitrogen fixation, nitrification, or denitrification processes (Kielak *et al.*, 2016; Pankratov *et al.*, 2008). Although Acidobacteria includes metal-tolerant bacteria (Campbell, 2014), in our study a significant decrease in its abundance was detected in soils exposed to Kocide[®]3000, nCuO and Cu(OH)₂-i. For instance, a significant decrease in the relative abundance of genera *Telmatobacter* and *Granulicella* was detected in all Cu-treatments in comparison to the CT. Generally, the abundance of members of these genera was stimulated in soils with acidic pH and lower oxygen levels or anoxic conditions (Campbell, 2014). In our experiment, the inclusion of soil organisms (e.g., invertebrates and plants) and daily watering might promote soil oxygenation, which may explain the decreased abundance of these genera. On the other hand, the classes Gemmatimonadetes [nCu(OH)₂], and Clostridia [Kocide[®]3000] showed to be tolerant to Cu exposure, potentially due to the expression of resistance mechanisms (like sporulation, efflux pumps and *Quorum Sensing*, among others) (Chater *et al.*, 2010; Berg *et al.*, 2012; Kou *et al.*, 2018). Particularly, the members of Clostridia are able to form endospores, a resistant structure produced under stress conditions, like a metal contaminated soil (Fajardo *et al.*, 2019). Additionally, *Clostridium* spp. were described as producers of Cu NPs, when Cu²⁺ were available in soil and/or soil porewater (Hofacker *et al.*, 2015). Since the toxicity is mainly related to the ionic fraction of Cu, such conversion of Cu²⁺, nanoparticle form may reduce the Cu toxicity for the soil microbiome. However, Clostridia increase was only observed in Kocide[®]3000-treated soil, suggesting that the Cu-formulation is crucial to the toxicity. Differently to the other Cu-treatments, the formulation of Kocide[®]3000 contained 73.5% of excipients (quantified dry mass of the product), like C, O, Na, Al, Si, P, S, and Zn (Simonin *et al.*, 2018b), which may have some impact on soil microbiome.

Several studies reported that Cu in nanoscale induces changes in the nitrogen cycle, potentially representing an ecological impact in agroecosystem (Park *et al.*, 2017; Guan *et al.*, 2020). Accordingly, our study predicted a negative impact on the denitrification process [conversion of nitrate (NO₃⁻) to nitrite (NO₂⁻), nitric oxide (NO), nitrous oxide (N₂O) and nitrogen gas (N₂)]. The impact was stronger in soil spiked with nCuO. Following our results, Guan and collaborators (2020) also reported a negative impact on denitrification in soil spiked with 50 mg kg⁻¹ of nCuO and in the presence of wheat. Besides, these authors reported an increased abundance of genes related to nitrogen-fixation (*nifH* gene) and nitrification (*amoA* and *nxrA* genes). In our study, nitrogen-

fixation and nitrification were similar across treatments, possibly due to the presence of soil invertebrates in mesocosms columns, which may increase the ammonia, oxygen, and nitrogen content in soils (Thakur and Geisen, 2019; Bouchon *et al.*, 2016), promoting the abundance of bacteria involved in these steps of the nitrogen cycle. Notwithstanding, the increased abundance of these classes in Cu-treated soils may also be influenced by the decrease in the abundance of other classes (like Acidobacteria and Flavobacteriia).

In our study, the predicted functional analysis revealed that metal detoxification mechanisms might decrease in Cu-treated soils through the decreased abundance of genes related to the ABC transporters activity (*e.g.*, *livK* gene). So, the reduced efficacy of this mechanism may lead to the increased of Cu inside the bacterial cell, disturbing their homeostasis (Vincent *et al.*, 2018). This result also suggests that the bacterial communities in Cu-treated soil may use other tolerance mechanisms to survive in metal contaminated soils. A similar result was reported in Cd-contaminated soils (Lee *et al.*, 2014). However, a stronger impact on this mechanism was mainly predicted in soil spiked with $\text{Cu}(\text{OH})_2$ -i and nCuO, which may be explained by the ionic Cu bound in these soils (as shown in Figure 1). Additionally, our study also suggested the activation of the efflux system (*e.g.*, mediated by *cusC* genes) and the increasing abundance of Cu-resistance genes (*e.g.*, *pcoB* and *copB* genes) in nCu(OH)₂-treated soils, which may promote the tolerance of bacterial community to this material. Accordingly, the study by Huang *et al.* (2019) predicted an increase of sequences related to efflux systems (*e.g.*, CusA and CusB systems) and metal resistance genes (*e.g.*, *copA*, *copC*, *copR*, *copS* and *cutO* genes) after exposure to metallic nanoparticles in sludge (CuO and Zn NPs; 5 and 20 mg g⁻¹). Contrary, our study projected the inactivation of the metal efflux in nCuO-treated soil (*e.g.*, by reducing the abundance of sequences encoding the transcriptional regulator CusR), which reduce the efficacy of this resistance mechanism (Banoee *et al.*, 2010; Outten *et al.*, 2001). Compared to our study, the higher Cu concentration used by Huang *et al.* (2019) may explain the contradictory influence of nCuO treatment in the efflux activity. Although this predicted analysis contributes to increased understanding of these NMs' mode of action and the bacterial strategies used against the Cu materials, methodologies like qPCR should be further explored to confirm this potential impact.

5. Conclusions

The present study showed that Cu-based NMs exposure significantly alters soil microbiome function, structure, and composition under a realistic exposure scenario and using an environmentally relevant concentration. At the functional level, Cu-based NMs exposure may stimulate specific processes related to the carbon cycle [*i.e.*, utilization of carbon substrates in nCuO-treated soil; and bacterial abundance (HB and P-SB) in nCu(OH)₂-treated soil], after 28 days of exposure. However, the overall microbial activity (DHA) and the enzymatic activities associated with the nitrogen (UA) and sulfur cycle (AS) were negatively affected, regardless of Cu form. Concerning community structure and composition, after day 28, classes involved in the decomposition of organic matter and cellulose degradation were the most susceptible to the Cu-exposure, such as Acidobacteria [in Kocide[®]3000, nCuO and Cu(OH)₂-i-treated soils] and Flavobacteriia [in nCu(OH)₂-treated soil]. On the other hand, classes involved in nitrogen cycling, Gemmatimonadetes [in nCu(OH)₂-treated soil] and Clostridia (in Kocide[®]3000-treated soil), were tolerant to Cu exposure, possibly due to the activation of resistance mechanisms. Predicted functional analysis indicates that the Cu-based NMs may negatively influence the denitrification process. Concerning Cu forms, nCuO is suggested to have a stronger negative impact on this process. In opposite, the ionic form was predicted to stimulate the dissimilatory nitrate ammonification and decline the denitrification. Additionally, a decreased pool of ionic Cu(II) in soil was detected concerning the distinct Cu-formulations: Cu(OH)₂-i > Kocide[®]3000 ~ nCuO > nCu(OH)₂, suggesting a higher bioavailability of Cu(OH)₂-i in soil. This result supports the stronger impact of Cu(OH)₂-i on the soil microbiome composition (*e.g.*, metagenomic and predicted functional analysis). The current study highlights the usefulness of the indoor mesocosm (which including non-target soil invertebrates and target-plants) based approach to evaluate the effects of Cu- NMs on microbial parameters. Due to the observed later effects (at day 28), further studies should address long-term responses of soil microbiome to Cu- NMs (*e.g.*, potential resilience effect). Moreover, the possible effects of excipients used in the commercial formulations (*e.g.*, Kocide[®]3000) or dispersed agents used in lab-synthesized NMs should be assessed in future studies.

6. Acknowledgements

The mesocosm experiment was run under the: (1) ECOCENE-Ecological Effects of Nanopesticides to Soil Ecosystems (PTDC/CTA-AMB/32471/2017), supported by FCT - Fundação para a Ciência e a Tecnologia, within the PT2020 Partnership Agreement and Compete 2020 co-funded by the FEDER - Fundo Europeu de Desenvolvimento Regional; (2) Nano-FARM - Fate and Effects of Agriculturally Relevant Materials (ERANET SIIN 2014, SIINN/0001/2014), supported by Fundação para a Ciência e a Tecnologia (FCT), under the frame of SIINN, the ERA-NET; and (3) AgriTarget (PTDC/BAA-AGR/ 29258/2017) funded by FEDER, through COMPETE2020 - Programa Operacional Competitividade e Internacionalização (POCI), and by national funds (Portuguese OE), through FCT/MCTES. All the authors received additional financial support from FCT/MCTES, through national funds, to CESAM (UIDP/50017/2020+UIDB/50017/2020). Also, this work was supported by FCT through: (1) a PhD grant to Peixoto, S. (SFRH/BD/117738/2016), Malheiro, C. (PD/BD/135577/2018), and Sandra Rodrigues (SFRH/BD/143646/2019); (2) a post-doctoral grant to Morgado, G. R. (SFRH/BPD/123384/2016) and (3) a contract under the Scientific Employment Stimulus—Individual Call (CEECIND/01190/2018) to Cardoso, N. D.

7. References

- Angly, F. E., Dennis, P. G., Skarshewski, A., Vanwonderghem, I., Hugenholtz, P., Tyson, G. W. (2014). CopyRighter: a rapid tool for improving the accuracy of microbial community profiles through lineage-specific gene copy number correction. *Microbiome*, 2(1), 1-13.
- Ballabio, C., Panagos, P., Lugato, E., Huang, J. H., Orgiazzi, A., Jones, A., Montanarella, L. (2018). Copper distribution in European topsoils: An assessment based on LUCAS soil survey. *Science of The Total Environment*, 636, 282-298.
- Banoee, M., Seif, S., Nazari, Z. E., Jafari-Fesharaki, P., Shahverdi, H. R., Moballegh, A., Shahverdi, A. R. (2010). ZnO nanoparticles enhanced antibacterial activity of ciprofloxacin against *Staphylococcus aureus* and *Escherichia coli*. *Journal of Biomedical Materials Research Part B: Applied Biomaterials*, 93(2), 557-561.

- Berg, J., Brandt, K. K., Al-Soud, W. A., Holm, P. E., Hansen, L. H., Sørensen, S. J., Nybroe, O. (2012). Selection for Cu-tolerant bacterial communities with altered composition, but unaltered richness, via long-term Cu exposure. *Applied and Environmental Microbiology*, 78(20), 7438-7446.
- Bertani I, Kojic M, Venturi V (2001) Regulation of the p-hydroxybenzoic acid hydroxylase gene (*pobA*) in plant-growth-promoting *Pseudomonas putida* WCS358. *Microbiology* (SGM) 147:1611–1620.
- Bouchereau, A., Aziz, A., Larher, F., Martin-Tanguy, J. (1999). Polyamines and environmental challenges: recent development. *Plant science*, 140(2), 103-125.
- Bouchon, D., Zimmer, M. Dittmer, J. (2016). The terrestrial isopod microbiome: An all-in-one toolbox for animal-microbe interactions of ecological relevance, *Frontiers in Microbiology*, 7, 1–19.
- Campbell B.J. (2014) The Family Acidobacteriaceae. *In: The Prokaryotes*. Springer, Berlin, Heidelberg. Rosenberg E., DeLong E.F., Lory S., Stackebrandt E., Thompson F. (eds).
- Carley, L. N., Panchagavi, R., Song, X., Davenport, S., Bergemann, C. M., McCumber, A. W., Simonin, M. (2020). Long-term effects of copper nanopesticides on soil and sediment community diversity in two outdoor mesocosm experiments. *Environmental Science & Technology*, 54(14), 8878-8889.
- Chater, K. F., Biro, S., Lee, K. J., Palmer, T., Schrempf, H. (2010). The complex extracellular biology of *Streptomyces*. *FEMS microbiology reviews*, 34(2), 171-198.
- Dick, R. P., Breakwell, D. P., Turco, R. F. (1997). Soil enzyme activities and biodiversity measurements as integrative microbiological indicators. *In Methods for Assessing Soil Quality*, 49 (pp. 247-271).
- Eren, A. M., Morrison, H. G., Lescault, P. J., Reveillaud, J., Vineis, J. H., Sogin, M. L. (2015). Minimum entropy decomposition: unsupervised oligotyping for sensitive partitioning of high-throughput marker gene sequences. *The ISME Journal*, 9(4), 968-979.
- Fajardo, C., Costa, G., Nande, M., Botías, P., García-Cantalejo, J., Martín, M. (2019). Pb, Cd, and Zn soil contamination: Monitoring functional and structural impacts on the microbiome. *Applied Soil Ecology*, 135, 56-64.

- FAO. (2020). How to Feed the World in 2050, site assessed in October 2020 <http://www.fao.org/wsfs/forum2050/wsfs-background-documents/issues-briefs/en/>
- Gao, X.; Spielman-Sun, E.; Rodrigues, S. M.; Casman, E. A.; Lowry, G. V. (2017). Time and nanoparticle concentration affect the extractability of Cu from CuO NP amended soil. *Environmental Science & Technology*. 51 (4), 2226– 2234.
- Grillo, R., Fraceto, L. F., Amorim, M. J., Scott-Fordsmand, J. J., Schoonjans, R., Chaudhry, Q. (2020). Ecotoxicological and regulatory aspects of environmental sustainability of nanopesticides. *Journal of Hazardous Materials*, 124148.
- Guan, X., Gao, X., Avellan, A., Spielman-Sun, E., Xu, J., Laughton, S., Lowry, G. V. (2020). CuO nanoparticles alter the rhizospheric bacterial community and local nitrogen cycling for wheat grown in a Calcareous soil. *Environmental Science & Technology*, 54(14), 8699-8709.
- Hofacker, A. F., Behrens, S., Voegelin, A., Kaegi, R., Lösekann-Behrens, T., Kappler, A., Kretzschmar, R. (2015). *Clostridium* species as metallic copper-forming bacteria in soil under reducing conditions. *Geomicrobiology Journal*, 32(2), 130-139.
- Holden, P. A., Klaessig, F., Turco, R. F., Priester, J. H., Rico, C. M., Avila-Arias, H., Gardea-Torresdey, J. L. (2014). Evaluation of exposure concentrations used in assessing manufactured nanomaterial environmental hazards: Are they relevant?, *Environmental Science & Technology*, 48(18), 10541–10551.
- Huang, H., Chen, Y., Yang, S., Zheng, X. (2019). CuO and ZnO nanoparticles drive the propagation of antibiotic resistance genes during sludge anaerobic digestion: possible role of stimulated signal transduction. *Environmental Science: Nano*, 6(2), 528-539.
- Iwai, S., Weinmaier, T., Schmidt, B. L., Albertson, D. G., Poloso, N. J., Dabbagh, K., DeSantis, T. Z. (2016). Piphillin: improved prediction of metagenomic content by direct inference from human microbiomes. *PloS one*, 11(11), e0166104.
- Kandeler, E., Gerber, H. (1988). Short-term assay of soil urease activity using colorimetric determination of ammonium. *Biology and Fertility of Soils*, 6(1), 68-72.
- Keiblinger, K. M., Schneider, M., Gorfer, M., Paumann, M., Deltedesco, E., Berger, H., Zehetner, F. (2018). Assessment of Cu applications in two contrasting soils-

- effects on soil microbial activity and the fungal community structure. *Ecotoxicology*, 27(2), 217-233.
- Kielak, A. M., Barreto, C. C., Kowalchuk, G. A., van Veen, J. A., Kuramae, E. E. (2016). The ecology of Acidobacteria: moving beyond genes and genomes. *Frontiers in Microbiology*, 7, 744.
- Kou, S., Vincent, G., Gonzalez, E., Pitre, F. E., Labrecque, M., Brereton, N. J. (2018). The response of a 16S ribosomal RNA gene fragment amplified community to lead, zinc, and copper pollution in a Shanghai field trial. *Frontiers in Microbiology*, 9, 366.
- Lee, J., Yang, J., Zhitnitsky, D., Lewinson, O., Rees, D. (2014). Structural and functional characterization of a heavy metal detoxifying ABC transporter (997.2). *The FASEB Journal*, 28, 997-2.
- Li, J., Rodrigues, S., Tsyusko, O. V., Unrine, J. M. (2019a). Comparing plant–insect trophic transfer of Cu from lab-synthesised nano-Cu (OH)₂ with a commercial nano-Cu (OH)₂ fungicide formulation. *Environmental Chemistry*, 16(6), 411-418.
- Li, L., Xu, Z., Kah, M., Lin, D., Filser, J. (2019b). Nanopesticides: A Comprehensive Assessment of Environmental Risk Is Needed before Widespread Agricultural Application. *Environmental Science & Technology*, 7923-7924.
- Lowry, G. V., Avellan, A., Gilbertson, L. M. (2019). Opportunities and challenges for nanotechnology in the agri-tech revolution. *Nature Nanotechnology*, 14(6), 517–522.
- Narayan, N. R., Weinmaier, T., Laserna-Mendieta, E. J., Claesson, M. J., Shanahan, F., Dabbagh, K., DeSantis, T. Z. (2020). Piphillin predicts metagenomic composition and dynamics from DADA2-corrected 16S rDNA sequences. *BMC genomics*, 21(1), 1-12.
- Nautiyal, S. C. (1999). An efficient microbiological growth medium for screening phosphate solubilizing microorganisms. *FEMS Microbiology Letters*, 170(436), 265–270.
- Neves, J., Cardoso, D. N., Malheiro, C., Kah, M., Soares, A. M., Wrona, F. J., Loureiro, S. (2019). Copper toxicity to *Folsomia candida* in different soils: a comparison between nano and conventional formulations. *Environmental Chemistry*, 16(6), 419-429.

- Outten, F. W., Huffman, D. L., Hale, J. A., O'Halloran, T. V. (2001). The independent cue and cues confer copper tolerance during aerobic and anaerobic growth in *Escherichia coli*. *Journal of Biological Chemistry*, 276(33), 30670-30677.
- Pankratov, T. A., Serkebaeva, Y. M., Kulichevskaya, I. S., Liesack, W., Dedysh, S. N. (2008). Substrate-induced growth and isolation of Acidobacteria from acidic Sphagnum peat. *The ISME Journal*, 2(5), 551-560.
- Park, H. D., Noguera, D. R. (2008). Nitrospira community composition in nitrifying reactors operated with two different dissolved oxygen levels. *Journal Microbiol Biotechnol*, 18(8), 1470-1474.
- Peixoto, S., Henriques, I., Loureiro, S. (2021). Long-term effects of Cu(OH)₂ nanopesticide exposure on soil microbial communities. *Environmental Pollution*, 269, 116113.
- Peixoto, S., Khodaparast, Z., Cornelis, G., Lahive, E., Etxabe, A. G., Baccaro, M., Henriques, I. (2020). Impact of Ag₂S NPs on soil bacterial community—A terrestrial mesocosm approach. *Ecotoxicology and environmental safety*, 206, 111405.
- Peng, C., Tong, H., Shen, C., Sun, L., Yuan, P., He, M., Shi, J. (2020). Bioavailability and translocation of metal oxide nanoparticles in the soil-rice plant system. *Science of The Total Environment*, 713, 136662.
- Radl, V., Winkler, J. B., Kublik, S., Yang, L., Winkelmann, T., Vestergaard, G., Schloter, M. (2019). Reduced microbial potential for the degradation of phenolic compounds in the rhizosphere of apple plantlets grown in soils affected by replant disease. *Environmental Microbiome*, 14(1), 1-12.
- Rodrigues, S., Bland, G. D., Gao, X., Rodrigues, S. M., Lowry, G. V. (2021). Investigation of pore water and soil extraction tests for characterizing the fate of poorly soluble metal-oxide nanoparticles. *Chemosphere*, 267, 128885.
- Sala, M. M., Pinhassi, J., Gasol, J. M. (2006). Estimation of bacterial use of dissolved organic nitrogen compounds in aquatic ecosystems using Biolog plates. *Aquatic Microbial Ecology*, 42(1), 1-5.
- Samarajeewa, A. D., Velicogna, J. R., Schwertfeger, D. M., Princz, J. I., Subasinghe, R. M., Scroggins, R. P., Beaudette, L. A. (2021). Ecotoxicological effects of copper oxide nanoparticles (nCuO) on the soil microbial community in a biosolids-amended soil. *Science of The Total Environment*, 763, 143037.

- Shahsavari, E., Aburto-Medina, A., Khudur, L. S., Taha, M., Ball, A. S. (2017). From microbial ecology to microbial ecotoxicology. *In* *Microbial Ecotoxicology* (pp. 17-38). Springer, Cham.
- Sharma, A., Kumar, V., Shahzad, B., Tanveer, M., Sidhu, G. P. S., Handa, N., Thukral, A. K. (2019). Worldwide pesticide usage and its impacts on ecosystem. *SN Applied Sciences*, 1(11), 1-16.
- Sharma, P., Goyal, D., Chudasama, B. (2021). Ecotoxicity of as-synthesised copper nanoparticles on soil bacteria. *IET Nanobiotechnology*, 15(2), 236-245.
- Simonin, M., Cantarel, A. A., Crouzet, A., Gervais, J., Martins, J. M., Richaume, A. (2018a). Negative effects of copper oxide nanoparticles on carbon and nitrogen cycle microbial activities in contrasting agricultural soils and in presence of plants. *Frontiers in microbiology*, 9, 3102.
- Simonin, M., Colman, B. P., Tang, W., Judy, J. D., Anderson, S. M., Bergemann, C. M., Bernhardt, E. S. (2018b). Plant and microbial responses to repeated $\text{Cu}(\text{OH})_2$ nanopesticide exposures under different fertilization levels in an agroecosystem. *Frontiers in microbiology*, 9, 1769.
- Spielman-Sun, E., Lombi, E., Donner, E., Avellan, A., Etschmann, B., Howard, D., Lowry, G. V. (2018). Temporal evolution of copper distribution and speciation in roots of *Triticum aestivum* exposed to CuO , $\text{Cu}(\text{OH})_2$, and CuS nanoparticles. *Environmental science & technology*, 52(17), 9777-9784.
- Su, X., Su, X., Yang, S., Zhou, G., Ni, M., Wang, C., Deng, J. (2020a). Drought changed soil organic carbon composition and bacterial carbon metabolizing patterns in a subtropical evergreen forest. *Science of the Total Environment*, 736, 139568.
- Su, Y., He, Z., Yang, Y., Jia, S., Yu, M., Chen, X., Shen, A. (2020b). Linking soil microbial community dynamics to straw-carbon distribution in soil organic carbon. *Scientific reports*, 10(1), 1-12.
- Thakur, M. P., Geisen, S. (2019). Trophic regulations of the soil microbiome. *Trends in microbiology*, 27(9), 771-780.
- Vasileiadis, S., Puglisi, E., Trevisan, M., Scheckel, K. G., Langdon, K. A., McLaughlin, M. J., Donner, E. (2015). Changes in soil bacterial communities and diversity in response to long-term silver exposure. *FEMS microbiology ecology*, 91(10), fiv114.

- Vincent, M., Duval, R. E., Hartemann, P., Engels-Deutsch, M. (2018). Contact killing and antimicrobial properties of copper. *Journal of applied microbiology*, 124(5), 1032-1046.
- Xu, C., Peng, C., Sun, L., Zhang, S., Huang, H., Chen, Y., Shi, J. (2015). Distinctive effects of TiO₂ and CuO nanoparticles on soil microbes and their community structures in flooded paddy soil. *Soil Biology and Biochemistry*, 86, 24-33.
- Zhang, W. (2018). Global pesticide use: Profile, trend, cost/benefit and more. *Proceedings of the International Academy of Ecology and Environmental Sciences*, 8(1), 1.
- Zhang, X., Xu, Z., Qian, X., Lin, D., Zeng, T., Filser, J., Kah, M. (2020). Assessing the Impacts of Cu(OH)₂ nanopesticide and ionic copper on the soil enzyme activity and bacterial community. *Journal of Agricultural and Food Chemistry*, 68(11), 3372-3381.
- Zimmer, M., Topp, W. (2002). The role of coprophagy in nutrient release from feces of phytophagous insects. *Soil Biology and Biochemistry*, 34(8), 1093-1099.

8. Supplementary material

8.1. List of Figures

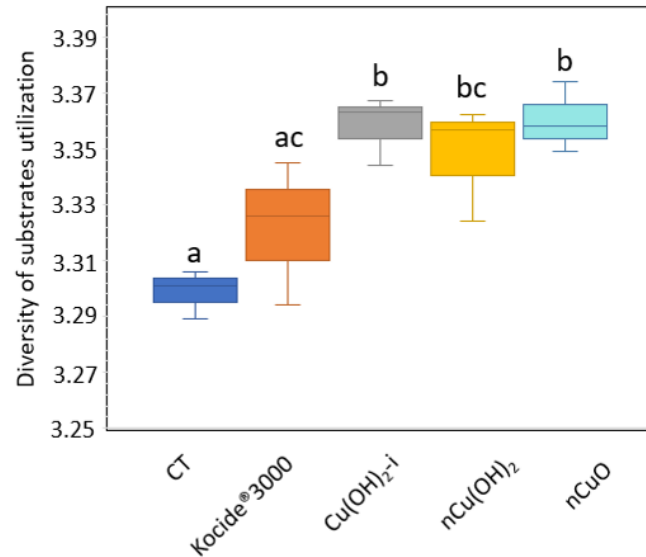


Figure S1. Diversity of carbon substrates used by the microbial community. Soil treatments included the non-treated soils (CT) and spiked soils with Cu(OH)₂-i, Kocide®3000, nCu(OH)₂, or nCuO, based on optical density (570 nm, read=168h) of Biolog®Ecoplate data after 28 days of exposure. Different letters (^{a,b,c}) indicate significant differences ($p < 0.05$) regarding the soil treatments, using the one-way ANOVA (Tukey HSD).

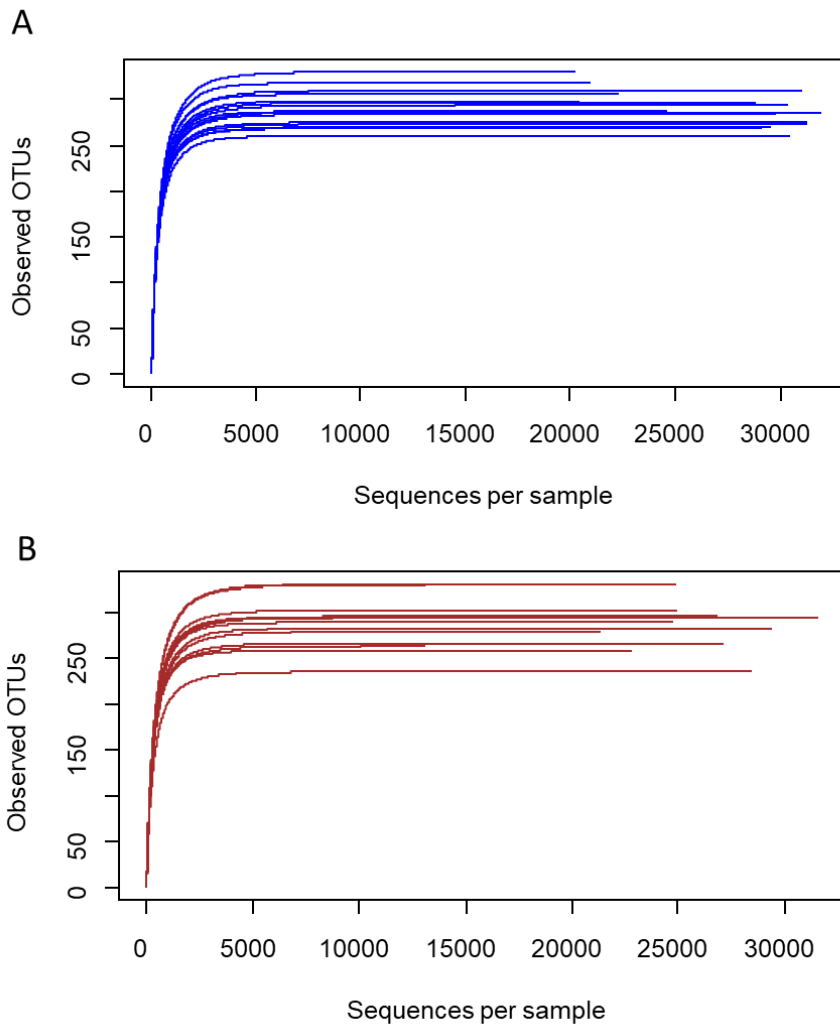


Figure S2. Rarefaction curves of observed OTUs as function of the number of reads (sequences per sample). Results of three replicates are presented for control soil (CT) and copper-treated soil [50 mg (Cu) kg⁻¹ soil of Kocide[®]3000, nCuO, nCu(OH)₂ and Cu(OH)₂·i]. The soil sampling was done at day 0 (A) and day 28 (B).

8.2. List of Tables

Table S1. Statistical significance ($p < 0.05$), using the two-way ANOVA (Tukey HSD test), for the copper dissolution in spiked soil with copper-based (nano)materials [$\text{Cu}(\text{OH})_2\text{-i}$, Kocide[®]3000, $\text{nCu}(\text{OH})_2$, or nCuO]. The table represents the copper formulations for each sampling time (day -2, 0, 14 and 28).

Sampling time (days)	Multiple comparisons (Treatments)	F	p
-2	$\text{Cu}(\text{OH})_2\text{-i}$ x nCuO	86.47	<0.001
	$\text{Cu}(\text{OH})_2\text{-i}$ x $\text{nCu}(\text{OH})_2$	86.47	<0.001
	$\text{Cu}(\text{OH})_2\text{-i}$ x Kocide [®] 3000	86.47	<0.001
	Kocide [®] 3000 x nCuO	86.47	<0.001
	$\text{nCu}(\text{OH})_2$ x nCuO	86.47	<0.001
0	$\text{Cu}(\text{OH})_2\text{-i}$ x nCuO	31.75	<0.001
	$\text{Cu}(\text{OH})_2\text{-i}$ x $\text{nCu}(\text{OH})_2$	31.75	0.012
	Kocide [®] 3000 x nCuO	31.75	<0.001
	$\text{nCu}(\text{OH})_2$ x nCuO	31.75	0.004
14	$\text{Cu}(\text{OH})_2\text{-i}$ x $\text{nCu}(\text{OH})_2$	31.24	<0.001
	nCuO x $\text{nCu}(\text{OH})_2$	31.24	<0.001
	Kocide [®] 3000 x $\text{nCu}(\text{OH})_2$	31.24	<0.001
28	$\text{Cu}(\text{OH})_2\text{-i}$ x $\text{nCu}(\text{OH})_2$	31.24	<0.001
	$\text{Cu}(\text{OH})_2\text{-i}$ x nCuO	31.24	0.001
	$\text{Cu}(\text{OH})_2\text{-i}$ x Kocide [®] 3000	31.24	0.009
	Kocide [®] 3000 x $\text{nCu}(\text{OH})_2$	31.24	<0.001
	nCuO x $\text{nCu}(\text{OH})_2$	31.24	0.002

Table S2. Statistical significance ($p < 0.05$), using the two-way ANOVA (Tukey HSD test), for the enzymatic activity from non-treated soil (CT) and spiked soil with copper (nano)materials [$\text{Cu}(\text{OH})_2\text{-i}$, Kocide[®]3000, $\text{nCu}(\text{OH})_2$, or nCuO]. In the table are represented two factors: (1) copper formulations and (2) sampling time (day 0, 14 and 28).

Soil enzymatic activity	Sampling time (days)	Treatments	F	p
DHA	28	CT x Kocide [®] 3000	5.322	<0.001
		CT x $\text{Cu}(\text{OH})_2\text{-i}$	5.322	<0.001
		CT x nCuO	5.322	<0.001
		CT x $\text{Cu}(\text{OH})_2\text{-s}$	5.322	<0.001
βG	14	CT x Kocide [®] 3000	2.775	0.006
		CT x $\text{Cu}(\text{OH})_2\text{-s}$	2.775	0.007
AS	28	CT x nCuO	2.466	<0.001
		CT x $\text{Cu}(\text{OH})_2\text{-i}$	2.466	<0.001
		CT x $\text{nCu}(\text{OH})_2$	2.466	0.015
		CT x Kocide [®] 3000	2.466	0.044
AP	14	nCuO x $\text{Cu}(\text{OH})_2\text{-i}$	1.357	0.037
	28	$\text{nCu}(\text{OH})_2$ x $\text{Cu}(\text{OH})_2\text{-i}$	1.357	0.014
		$\text{nCu}(\text{OH})_2$ x nCuO	1.357	0.042
UA	0	CT x $\text{Cu}(\text{OH})_2\text{-i}$	1.469	<0.001
		CT x Kocide [®] 3000	1.469	0.006
		CT x $\text{nCu}(\text{OH})_2$	1.469	0.008
		CT x nCuO	1.469	0.033
	14	CT x $\text{Cu}(\text{OH})_2\text{-i}$	1.469	<0.001
		CT x Kocide [®] 3000	1.469	0.009
		CT x $\text{nCu}(\text{OH})_2$	1.469	0.031
		CT x nCuO	1.469	0.014
	28	CT x $\text{nCu}(\text{OH})_2$	1.469	0.016
		CT x $\text{Cu}(\text{OH})_2\text{-i}$	1.469	0.019
		CT x Kocide [®] 3000	1.469	0.047

Table S3 – Statistical significance, using the two-way ANOVA (Tukey HSD test), for the substrate well colour development (SAWCD). In the table are represented the two factors considered to the analysis: (1) copper formulation [Kocide[®]3000, nCu(OH)₂, nCuO and Cu(OH)₂-i] and (2) sampling time (day 0, 14 and 28).

Carbon classes	Sampling time (days)	Treatments	F	p
Amides/amines	14	Cu(OH) ₂ -i x CT	2.679	<0.001
		nCuO x CT	2.679	<0.001
		nCu(OH) ₂ x CT	2.679	<0.001
		nCuO x Kocide [®] 3000	2.679	<0.001
		nCu(OH) ₂ x Kocide [®] 3000	2.679	<0.001
		Cu(OH) ₂ -i x Kocide [®] 3000	2.679	<0.001
	28	Kocide [®] 3000 x CT	2.679	<0.001
		nCu(OH) ₂ x CT	2.679	0.05
		nCuO x CT	2.679	<0.001
		Cu(OH) ₂ -i x CT	2.679	<0.001
Phenolic compounds	14	CT x Kocide [®] 3000	2.679	0.036
		nCuO x Kocide [®] 3000	2.679	<0.001
		nCuO x Cu(OH) ₂ -i	2.679	0.011
	28	nCu(OH) ₂ x Kocide [®] 3000	2.679	0.005
		CT x Kocide [®] 3000	2.679	<0.001
		CT x Cu(OH) ₂ -i	2.679	<0.001
		CT x nCuO	2.679	<0.001

Table S4. Statistical significance, using the two-way ANOVA (Tukey HSD test, $p < 0.05$), for each carbon substrate utilized (from Biolog[®]Ecoplate) by the microbial community from non-treated (CT) and spiked soil with copper [Cu(OH)₂-i, Kocide[®]3000, nCu(OH)₂, or nCuO]. Data was based on the optical density (590 nm). In this analysis was considered two factors: (1) soil treatments and (2) sampling time (days 0, 14 and 28).

Sampling time (days)	Carbon Substrates	Multiple comparisons (Treatments)	F	P
0	Cyclodextrin	nCuO x CT	2.082	0.002
		Kocide [®] 3000 x CT	2.082	0.018
		Kocide [®] 3000 x nCuO	5.957	<0.001
	Glycogen	Kocide [®] 3000 x CT	5.957	<0.001
		Cu(OH) ₂ -i x nCuO	5.957	0.001
		Cu(OH) ₂ -i x CT	5.957	0.005
		nCu(OH) ₂ x nCuO	5.957	0.001
	α-D-lactone	nCu(OH) ₂ x CT	5.957	0.005
		nCuO x CT	1.481	0.03
	D-Glucosaminic acid	nCuO x nCu(OH) ₂	2.194	0.021
nCuO x Cu(OH) ₂ -i		2.194	0.021	
14	L-arginine	Kocide [®] 3000 x CT	2.099	0.004
		Cu(OH) ₂ -i x nCuO	2.843	0.003
	Tween 40	Kocide [®] 3000 x nCuO	2.843	0.015
		CT x nCuO	2.843	0.01
	i-erythritol	nCu(OH) ₂ x CT	1.365	0.016
		Cu(OH) ₂ -i x Kocide [®] 3000	3.387	0.01
	Phenylethylamine	nCuO x Kocide [®] 3000	3.387	0.027
		nCu(OH) ₂ x Kocide [®] 3000	3.387	0.044
		nCu(OH) ₂ x CT	1.751	0.001
		Cu(OH) ₂ -i x CT	1.751	0.003
Putrescine	nCuO x CT	1.751	0.005	
	Kocide [®] 3000 x CT	1.751	0.023	
	nCuO x CT	1.481	0.018	
28	A-d-lactone	nCuO x CT	1.365	0.01
		Cu(OH) ₂ -i x CT	1.365	0.023
	i-erythritol	nCu(OH) ₂ x CT	1.365	0.043
		Kocide [®] 3000 x CT	1.726	0.001
		Cu(OH) ₂ -i x CT	1.726	0.002
	D-xylose	nCu(OH) ₂ x CT	1.726	0.02
		nCuO x CT	1.726	0.045
	4-hydroxy benzoic acid	CT x Kocide [®] 3000	1.644	0.007
		nCuO x CT	1.357	0.003
	Y-hydroxybutiric acid	nCuO x nCu(OH) ₂	1.357	0.017
Cu(OH) ₂ -i x CT		1.357	0.05	
Itaconic acid	Kocide [®] 3000 x CT	2.599	0.01	
	Cu(OH) ₂ -i x CT	2.599	0.012	
A-ketobutiric acid	nCuO x CT	0.76	0.005	
	nCuO x CT	1.701	0.003	
D-malic acid	nCuO x nCu(OH) ₂	2.099	0.043	
	nCuO x nCu(OH) ₂	1.847	0.002	
L-arginine	nCuO x CT	1.847	0.005	
	nCuO x CT	1.847	0.005	
L-phenylalanine	nCuO x Kocide [®] 3000	1.847	0.045	
	Cu(OH) ₂ -i x nCu(OH) ₂	1.847	0.002	
	Cu(OH) ₂ -i x CT	1.847	0.006	
	nCuO x CT	3.559	<0.001	
L-serine	nCuO x nCu(OH) ₂	3.559	<0.001	
	nCuO x Kocide [®] 3000	3.559	0.005	
L-threonine	Cu(OH) ₂ -i x CT	3.559	0.017	
	nCuO x CT	2.028	0.001	
Putrescine	nCuO x nCu(OH) ₂	2.028	0.014	
	Cu(OH) ₂ -i x CT	2.028	0.023	
Pyruvic acid methyl ester	nCuO x CT	1.751	0.036	
	nCuO x CT	1.649	0.043	

Table S5. Number of reads and OTUs per sample after each sequence data processing step.

Treatment	Sampling point	Replicate	Input sequences	Sequences after pre-processing	Sequences after chimera removal	Sequences assigned to OTU	Sequences assigned to taxa	Count after lineage-specific copy-number correction	Median sequence length after pre-processing
CT	0	1	98129	98122	97996	49285	49285	31328	404
		2	96418	96414	96277	47382	47382	29115	404
		3	93173	93172	93046	47111	47111	29806	404
Cu(OH) ₂ -i	0	1	101368	101363	101253	51195	51195	31112	404
		2	66529	66527	66451	33820	33820	20453	404
		3	101929	101922	101808	49173	49173	30499	404
nCuO	0	1	98424	98416	98210	50048	50048	31277	404
		2	92249	92244	92183	46781	46781	29620	404
		3	83331	83322	83287	39280	39280	24659	404
Kocide	0	1	91961	91957	91831	46515	46515	28854	404
		2	101348	101343	101130	50498	50498	31998	404
		3	64269	64267	64157	32926	32926	20271	404
nCu(OH) ₂	0	1	72787	72783	72694	37196	37196	22263	404
		2	68402	68399	68340	35476	35476	20965	404
		3	98966	98960	98800	51690	51690	30413	404
CT	28	1	111436	111431	111197	57940	57940	28471	422
		2	95212	95206	95035	54754	54754	26841	422
		3	84173	84167	84005	49787	49787	23643	422
Cu(OH) ₂ -i	28	1	76859	76854	76653	42683	42683	21337	422
		2	98953	98948	98741	61667	61667	29396	422
		3	82374	82373	82158	46027	46027	22802	422
nCuO	28	1	97797	97792	97625	55740	55740	27151	422
		2	110940	110935	110688	66606	66606	31576	422
		3	91769	91766	91593	52836	52836	24749	422
Kocide	28	1	83570	83570	83322	48351	48351	23264	422
		2	84559	84557	84434	52286	52286	24580	422
		3	87823	87819	87722	48247	48247	25892	422
nCu(OH) ₂	28	1	91261	91256	91109	49412	49412	24996	422
		2	84845	84842	84643	49043	49043	24921	422
		3	47677	47675	47596	26766	26766	13122	422

Table S6. Diversity indexes calculated based on metagenomic analysis from non-treated soil (CT) and spiked soil with Cu(OH)₂-i, Kocide[®]3000, nCu(OH)₂, or nCuO, after day 0 and 28. Average values (n=3 ± standard deviation) for each soil treatment.

Sampling time (days)	Treatments	Richness (S)	Pielou (<i>J'</i>)	Shannon-wiener (<i>H'</i>)
0	CT	276 ± 8	0.920 ± 0.001	5.170 ± 0.029
	Cu(OH) ₂ -i	289 ± 25	0.917 ± 0.002	5.195 ± 0.071
	Kocide [®] 3000	304 ± 23	0.917 ± 0.004	5.240 ± 0.085
	nCu(OH) ₂	306 ± 12	0.923 ± 0.002	5.281 ± 0.047
	nCuO	277 ± 9	0.922 ± 0.002	5.186 ± 0.032
28	CT	286 ± 48	0.904 ± 0.035	5.105 ± 0.344
	Cu(OH) ₂ -i	272 ± 13	0.918 ± 0.014	5.143 ± 0.040
	Kocide [®] 3000	293 ± 1	0.921 ± 0.002	5.231 ± 0.012
	nCu(OH) ₂	297 ± 33	0.923 ± 0.003	5.251 ± 0.119
	nCuO	281 ± 15	0.930 ± 0.008	5.244 ± 0.090

Table S7. Statistical significance ($p < 0.05$) for each class in the soil treatments from non-treated soil or spiked soil with copper [Cu(OH)₂-i, Kocide[®]3000, nCu(OH)₂, or nCuO]. Two factors were considered (two-way ANOVA; Tukey HSD method, $p < 0.05$): (1) soil treatments and (2) sampling time (day 0 and 28) for each class.

Classes	Multiple comparisons (Treatments)	F	p
Gemmatimonadetes	nCu(OH) ₂ x CT	5.79	0.019
	Kocide [®] 3000 x nCu(OH) ₂	5.79	0.010
Clostridia	Kocide [®] 3000 x CT	4.28	0.001
	Cu(OH) ₂ -i x CT	5.28	0.010
Acidobacteriia	Kocide [®] 3000 x CT	5.28	0.015
	nCuO x CT	5.28	0.021
Flavobacteriia	Kocide [®] 3000 x CT	2.01	0.034
	Kocide [®] 3000 x nCu(OH) ₂	2.01	0.021

Table S8. Statistical significance ($p < 0.05$) for each genus affiliated across the soil treatments [CT, soil spiked with $\text{Cu}(\text{OH})_2$ -i, Kocide[®]3000, $\text{nCu}(\text{OH})_2$, or nCuO] after 0, and 28 days of exposure, using the one-way ANOVA for each sampling time (Tukey HSD method; $p < 0.05$).

Sampling time (days)	Genus	F	p
0	<i>Bradyrhizobium</i>	10.65	<0.001
	<i>Candidatus Solibacter</i>	4.00	0.034
	<i>Janthinobacterium</i>	21.15	<0.001
	<i>Lysobacter</i>	64.23	<0.001
	<i>Massilia</i>	32.09	<0.001
	<i>Sphingomonas</i>	88.23	<0.001
	Mycobacteriaceae	8.34	0.003
	Bacteria	5.05	0.017
	Oxalobacteraceae	25.85	<0.001
28	<i>Telmatobacter</i>	6.32	0.008
	<i>Niastella</i>	9.76	0.002
	<i>Arenimonas</i>	10.22	0.001
	<i>Pseudomonas</i>	29.99	0.001
	<i>Granulicella</i>	139.66	<0.001
	<i>Lacibacter</i>	125.56	<0.001
	<i>Caballeronia</i>	91.38	<0.001
	<i>Burkholderia</i>	5.99	<0.001
	<i>Nocardioiodes</i>	3.54	0.048
	<i>Massilia</i>	0.53	0.030
	<i>Gemmatimonas</i>	4.12	0.048
	<i>Ramlibacter</i>	7.65	0.024
	<i>Duganella</i>	4.82	0.012
	<i>Methylotenera</i>	4.01	0.042

Table S9. Statistical significance ($p < 0.05$) for the 15 most abundant OTU from non-treated soil or spiked soil with copper [Cu(OH)₂-i, Kocide[®]3000, nCu(OH)₂, or nCuO]. Two factors were considered (two-way ANOVA; Tukey HSD method, $p < 0.05$): (1) soil treatments and (2) sampling time (day 0 and 28) for each OTU.

OTU	Sampling time (days)	Multiple comparisons (Treatments)	F	p
39	28	CT x nCuO	3.652	0.007
		Cu(OH) ₂ -i x nCuO		0.019
		Kocide [®] 3000 x nCuO		0.044
2	28	nCu(OH) ₂ x Cu(OH) ₂ -i	64.572	0.001
		nCu(OH) ₂ x Kocide [®] 3000		0.003
		CT x Cu(OH) ₂ -i		0.017
45	0	CT x Kocide [®] 3000	167.979	0.039
	28	nCuO x nCu(OH) ₂		0.038
46	28	CT x nCuO	18.24	0.046
52	28	nCu(OH) ₂ x CT	23.312	0.02
59	28	Cu(OH) ₂ -i x CT	22.72	0.003
		Cu(OH) ₂ -i x nCu(OH) ₂		0.025
66	0	nCu(OH) ₂ x Cu(OH) ₂ -i	47.058	<0.001
		nCu(OH) ₂ x Kocide [®] 3000		<0.001
		nCu(OH) ₂ x nCuO		0.005
		CT x Cu(OH) ₂ -i		<0.001
		CT x Kocide [®] 3000		<0.001
		nCuO x Cu(OH) ₂ -i		0.007
81	28	nCuO x Kocide [®] 3000	77.215	0.023
		nCuO x nCu(OH) ₂		0.039
84	28	Cu(OH) ₂ -i x nCu(OH) ₂	47.060	0.014
		Cu(OH) ₂ -i x CT		0.033
		Kocide [®] 3000 x nCu(OH) ₂		0.032
95	0	nCuO x nCu(OH) ₂	119.915	0.035
		Cu(OH) ₂ -i x nCu(OH) ₂		0.026
100	0	nCu(OH) ₂ x Cu(OH) ₂ -i	185.443	<0.001
		nCu(OH) ₂ x Kocide [®] 3000		<0.001
		nCu(OH) ₂ x nCuO		<0.001
		nCu(OH) ₂ x CT		0.006
		CT x Cu(OH) ₂ -i		0.006
105	28	CT x Kocide [®] 3000	124.078	0.012
		CT x nCuO		0.021
110	0	nCu(OH) ₂ x Cu(OH) ₂ -i	63.348	<0.001
		nCu(OH) ₂ x Kocide [®] 3000		<0.001
		nCu(OH) ₂ x nCuO		0.004
		nCu(OH) ₂ x CT		0.015
		CT x Cu(OH) ₂ -i		<0.001
	28	CT x Kocide [®] 3000		<0.001
		nCuO x Cu(OH) ₂ -i		<0.001
		nCuO x Kocide [®] 3000		0.001
		nCu(OH) ₂ x Cu(OH) ₂ -i		<0.001
		nCu(OH) ₂ x Kocide [®] 3000		0.004
117	28	nCuO x Cu(OH) ₂ -i	68.982	0.008
		CT x Cu(OH) ₂ -i		0.025
190	28	CT x Kocide [®] 3000	45.869	0.001
		CT x Cu(OH) ₂ -i		0.001
226	28	nCu(OH) ₂ x CT	34.398	0.025
		nCu(OH) ₂ x Kocide [®] 3000		0.046
		Cu(OH) ₂ -i x CT		<0.001
247	28	Cu(OH) ₂ -i x nCu(OH) ₂	4.667	<0.001
		nCu(OH) ₂ x Kocide [®] 3000		0.012
		nCu(OH) ₂ x Cu(OH) ₂ -i		0.015
		nCu(OH) ₂ x nCuO		0.031
		nCu(OH) ₂ x CT		0.042

Chapter 5

Copper-based nanomaterials alter the rhizosphere bacterial
community

Copper-based nanomaterials alter the rhizosphere bacterial community

Peixoto, S.; Morgado, R. G.; Prodana, M.; Cardoso, D. N.; Malheiro, C.; Loureiro, S. Henriques, I.

Abstract

The application of nanopesticides in agriculture might lead to the exposure of rhizosphere to copper-based nanomaterials, possibly affecting several bacterial-mediated processes. Thus, we investigated the effects of copper-based compounds [Kocide[®]3000, nCu(OH)₂, nCuO and Cu(OH)₂-i (as an ionic control), at 50 mg kg⁻¹ soil] on the function and structure of rhizosphere bacterial communities, using indoor mesocosms which included soil organisms, during 28 days of exposure. The soil located outside the rhizosphere (bulk soil), was also included in this study for comparison purposes. Overall, the structure and function of the rhizosphere bacterial community were affected by copper exposure, mainly at day-14. At this exposure time, enzymatic activity related to the nitrogen, phosphorous, and sulfur cycles significantly decreased in copper-treated rhizosphere soil. At the structural level, a reduction of alpha-diversity was observed in nCu(OH)₂-treated rhizosphere soils, at day-28. Additionally, the structure and function of bulk soil bacterial community were affected by copper only at day-28, suggesting a stimulation of copper dissolution by the root exudates. In general, the ionic Cu(OH)₂-i exerted a similar impact compared to the nano-formulations. Concerning nanomaterials, nCu(OH)₂ (structure) and nCuO (enzymatic activity) presented a stronger effect on the rhizosphere bacterial community. This work highlights the relevance to study the rhizosphere soil to assess the impact of copper-based nanomaterials in terrestrial compartment. Further studies should clarify the role of exudates as a driver of the rhizosphere microbiome composition and as a determinant of copper dissolution in soil.

Keywords: soil bacterial community, nanomaterials, nanopesticides, soil enzymatic activity, denaturing gradient gel electrophoresis.

1. Introduction

Soil microbiome is key in terrestrial functioning, mainly due to its mediation in nutrient acquisition and regulation of biogeochemical cycles (Yang *et al.*, 2014; Jansson and Hofmockel, 2018). Generally, soil microbiome is defined as the microbial community living together in the rhizosphere (adjacent to roots) and the bulk (outside the rhizosphere) soil, comprising the Bacteria, Fungi, Archaea, Protists and Virus (Philippot *et al.*, 2013; Lladó *et al.*, 2017; Thakur and Geisen, 2019). Nevertheless, distinct microbial abundance and diversity have been described for bulk versus rhizosphere soil (Whalley *et al.*, 2005; Lladó *et al.*, 2017). In fact, the microbial community structure, composition and diversity from rhizosphere soil can be shaped by the type and developmental stages of plants, root deposition and activity (*e.g.*, exudates) (Philippot *et al.*, 2013). For instance, the roots' deposition and extension may increase the porosity of soil, water and oxygen content and soil aggregates (Whalley *et al.*, 2005), which may influence the richness and composition of rhizosphere microbial community (Praeg *et al.*, 2019). Additionally, nutrient-rich root exudates can influence the soil pH, increasing the microbial activity, richness and diversity (Lladó *et al.*, 2017; Praeg *et al.*, 2019). The rhizosphere soil provides a dynamic and complex interaction between plant roots and microorganisms, which is crucial for plant growth, nutrition and health in agroecosystems (Philippot *et al.*, 2013). For example, plant growth-beneficial rhizosphere microorganisms (PGPR) can be recruited by root exudates and/or phytohormones to protect the plants against phytopathogens (Philippot *et al.*, 2013; Yuan *et al.*, 2018). For instance, a study by Yuan *et al.*, (2018) demonstrated that the inoculation of plants (*A. thaliana*) with *Pseudomonas syringae* *pv.* *tomato* altered the root exudates composition, stimulating the abundance of beneficial rhizosphere bacteria (*e.g.*, *Roseiflexus*) and fostering plant defence mechanisms.

Currently, the development of new agrochemicals aims at a better efficacy on pathogen control, but decreasing their application rates and therefore decreasing the foreseen hazards and risks (Kah *et al.*, 2018). For instance, the commercial fungicide/bactericide Kocide®3000, which contains nano-Cu(OH)₂ particles as active ingredients, is applied in both organic and conventional agroecosystems to protect several crops against pathogens, in USA (Lowry *et al.*, 2019). Additionally, the application of nCuO in agroecosystems was reported to stimulate plant growth, promoting the bioavailability of micronutrients and protecting plants from pathogens (Simonin *et al.*, 2018a). Despite

these potential advantages, the environmental risks associated with these nano-agrochemicals are not fully known and are difficult to predict. For instance, depending on the application method (usually sprayed), around 10-75% of the active ingredient of pesticides can reach the terrestrial compartment (Kah *et al.*, 2018). To try to understand the impact of these nanomaterials (NMs) in agroecosystems, some studies concerning the fate, dissolution, transformation and toxicity to non-target organisms and microorganisms have been carried out in the last few years (Carley *et al.*, 2020; Zhang *et al.*, 2020; Simonin *et al.*, 2018b). Some studies on the soil microbiome reported a toxic effect of copper-based NMs on bulk soil bacterial communities, decreasing the enzymatic activity, gene abundance related to the nitrogen cycle and affecting microbial community composition, structure and diversity (Zhang *et al.*, 2020; Peixoto *et al.*, 2021; Chapter 4). Nevertheless, the impact of these copper-based NMs on rhizosphere bacterial community was infrequently investigated. Up to now, it was reported that the exposure to nCuO (at 50 mg kg⁻¹ soil) influenced the plants biomass, rhizosphere bacterial community structure and composition, and increased the abundance of nitrogen cycle-related genes (Guan *et al.*, 2020). Also, a detrimental effect on the activity of rhizosphere soil enzymes was shown in nCuO-treated soils, under concentrations of 0.1, 1, and 100 mg kg⁻¹ soil (Simonin *et al.*, 2018a). On the other hand, the function and composition of soil microbial community were slightly affected by the sequential application of Kocide®3000 in crops using an outdoor mesocosm for one year (Carley *et al.*, 2020; Simonin *et al.*, 2018b). Detected impacts were mainly linked to changes in root exudates, which change the soil properties, and/or the copper speciation and bioavailability (Guan *et al.*, 2020). Nevertheless, little is still known about the impact of these NMs on soil rhizosphere microbiome accounting the interactions with key edaphic organisms. To bridge this knowledge gap, the current study assesses the impact of copper-based NMs in soil bacterial rhizosphere soil using indoor mesocosms and including soil invertebrates and plants as 1) essential elements in soil functioning and 2) potential drivers of soil microbiome composition.

Accordingly, we hypothesized that the rhizosphere bacterial community is affected by exposure to NMs, and this community will be distinct from the observed in the bulk soil. Due to its importance in plant productivity and soil fertility, changes in the bacterial community of the rhizosphere might negatively impact the agronomic sector. In the current study, we tested these hypotheses by analyzing the rhizosphere bacterial community, at the structural and functional level, using the denaturing gradient gel

electrophoresis (DGGE) and soil enzymatic activity. For that, indoor mesocosms, which included target-plants (wheat) and non-target invertebrates (mealworms, isopods and earthworms) to simulate realistic ecosystem conditions, were deployed using an environmental-relevant concentration of copper (50 mg kg^{-1} soil), used as the maximum dose applied to several plant-crops (*e.g.*, as Kocide[®]3000). Effects were evaluated after 14 and 28 days of exposure and compared to effects on bulk soil bacterial community. Exposure to $\text{Cu}(\text{OH})_2\text{-i}$ was also included in this experiment, as an ionic control.

2. Material and Methods

2.1. Copper-based nanoparticles exposure

Three copper-based NMs were used in this work: (1) the commercial pesticide Kocide[®]3000 (DuPont Co.TM, Wilmington, DE, United States; fully characterized in Li *et al.*, 2019) which contains the nano $\text{Cu}(\text{OH})_2$ as the active ingredient; (2) the lab-synthesized $\text{nCu}(\text{OH})_2$ (fully characterized by Li *et al.*, 2019); and (3) nCuO (Sigma-Aldrich; $<50 \text{ nm}$ particle size). In addition, our study included a negative control (CT, non-treated soil) and an ionic control [spiked soil with ionic copper hydroxide - $\text{Cu}(\text{OH})_2\text{-i}$] (Sigma-Aldrich, 99 % purity, CAS 7761-88-8, Germany).

The experimental design and procedure were previously described in (Chapter 4). Briefly, the natural Lufa 2.2 soil (LUFASpeyer 2.2, Speyer, Germany), recommended for testing the toxicity of NMs/nanoparticles (NPs) by Geitner (*et al.*, 2020), was spiked with each copper formulation to a nominal concentration of $50 \text{ mg (Cu) kg}^{-1}$ soil. The compounds were directly applied in soils, which were watered to reach 55 % of water holding capacity (WHC), and then mixed manually for several minutes. To non-treated soils (CT) only water was added to adjust the WHC. Then, soils were transferred to mesocosms columns (20 cm long columns with 11 cm of diameter). For each column, a 1.3 kg of non-treated soil were added in the bottom of the column (8-16 cm), and the first layer (1-8 cm) was filled with 1.3 kg of CT or spiked soil with Kocide[®]3000, $\text{nCu}(\text{OH})_2$, nCuO or $\text{Cu}(\text{OH})_2\text{-i}$. A total of 6 replicates/columns per treatment were established in indoor conditions [temperature $20 \pm 2 \text{ }^\circ\text{C}$ and photoperiod 16h:8h (light:dark)]. Additionally, 16 ml of artificial rainwater was daily added in each column (as previously described in Peixoto *et al.*, 2020).

Two days after soil spiking (herein designated day 0) different organisms' species were included in the surface of the mesocosm column: five plants (*Triticum aestivum L.*;

plants with six days old; these plants were germinated from seeds in multi-welled germinator plates, using CT or copper-treated soil according to the respective treatment), ten isopods (*Porcellionides pruinosus*; adults with 15-25 mg fresh weight), ten mealworms (*Tenebrio molitor*; larvae with 30-40 mg fresh weight) and six earthworms (*Eisenia andrei*; adults with 300-600 mg fresh weight). Two sampling times were considered in this study: day 14 and day 28. In each sampling time, three replicates (per treatment) were destructively sampled to collect bulk (soil not close to the roots, soil depth around of 2 cm) and rhizosphere soil (soil attached to the roots) for microbial analysis. To collect rhizosphere soil, the whole root system of two plants from mesocosms was gently shaken to remove excess soil adhered to the root system. For DNA extraction, soil samples were collected (0.25 g) and frozen in liquid nitrogen and kept at -80°C until the DNA extraction.

2.2. PCR-DGGE analysis

The UltraClean[®]Power Soil DNA Isolation Kit (MoBio Laboratories, Inc., Carlsbad, CA) was used to extract total DNA from each soil sample. Then, the V3-V4 region of 16S rRNA gene was amplified using the universal primers 338f-GC (5'-GACTCCTACGGGAGGCAGCAG-3') and 518r (5'-ATTACCGCGGCTGCTGG-3') with a GC clamp attached to the forward primer (Muyzer *et al.*, 1993). Nuclease-free water (16.25 µL), NZYTaQ 2x Green Master Mix (6.25 µL; 2.5 mM MgCl₂; 200 mM dNTPs; 0.2 U/µL DNA polymerase) (NZYTech, Portugal), 0.75 µL of each primer (from a 10 mM solution), and DNA (1 µL) were used to prepare the PCR mixture. The amplification conditions were performed as described in (Peixoto *et al.*, 2021). The obtained PCR products were loaded onto polyacrylamide [8% (w/v); 37.5:1, acrylamide:bisacrylamide] gels with denaturing gradient ranging from 35% to 62.5% [100% denaturant corresponded to 7 M urea and 40% (v/v) formamide]. Electrophoresis and image gel capture were performed as previously described in Peixoto *et al.*, 2021.

2.3. Enzymatic activity

The activity of dehydrogenase (DHA), as a microbial viability indicator, was determined based on protocol from Dick *et al.* (1997). Also, the beta-glucosidase (βG), arylsulfatase (AS) and acid phosphatase (AP) activities were determined based on Dick *et al.* (1997), to obtain information about the regulation of the carbon, sulfur and phosphorus cycling. The protocol from Kandeler and Gerber (1988) was used to test the

urease activity (UA), which is related to the nitrogen cycle. Some adaptations were included as previously described in Peixoto *et al.*, (2021).

2.4. Statistical analysis

DGGE profiles were analyzed by cluster and Principal coordinate analysis, based on Jaccard coefficient, using PRIMER v6 software (Primer-E Ltd., Plymouth, UK). Additionally, a Permanova analysis was performed, using a 999 permutations, to test significant differences among soil treatments [CT, Cu(OH)₂-i, Kocide[®]3000, nCu(OH)₂, or nCuO] in each exposure time.

The enzymatic activity and alpha-diversity indexes were analyzed using the IBM SPSS software, version 21. After verifying the normal distribution (Shapiro-Wilk's test) and homogeneity of variances (Levene's test), a two-way ANOVA followed by the Tukey method were used to test differences between soil treatments and exposure time (day 14 and 28). When normality failed, data were squared-root transformed.

3. Results

3.1. Effects of copper on soil bacterial community structure and diversity

The effect of copper-based NMs on the bacterial community structure was assessed in rhizosphere and bulk soil, using the DGGE analysis (Figure 1 A - F). Clustering analysis (Figure 1 A) revealed a temporal effect, in which samples from day-14 were significantly separated from those at day-28, sharing a similarity lower than 50% (Permanova: $F = 14.4$, $P < 0.05$). For each sampling time, clustering analysis revealed a significant impact of copper treatments on the structure of rhizosphere bacterial community compared to the respective CT (Permanova: $F = 14.4$, $P < 0.05$). Concerning day-14, the nCu(OH)₂ and nCuO distinctly affect the bacterial community structure in comparison to the other copper formulations and the CT soil, sharing a 54.6% of similarity (Figure 1 A). The PCoA analysis corroborates the clustering analysis results. In this analysis, the first axis represents 40.3% of the total variation in the sample distribution, and the second axis indicates 19.4% of the total variation (Figure 1 B). At the end of experiment (day-28), all copper formulations significantly impacted the bacterial community compared to the non-exposed communities (Permanova < 0.05 ; Table S1). Comparing copper forms, the nCu(OH)₂-treated soil exhibited a distinct

bacterial structure from those of soils exposed to Kocide[®]3000, nCuO or Cu(OH)₂-i, or even in non-treated soil (Permanova < 0.05; Table S1). PCoA analysis revealed that nCu(OH)₂ and CT treatments had a distinct bacterial community structure in comparison to the other copper formulations, which may explain 38% of the total variation along the first axis (PCO1 axis, Figure 1 C). While copper exposure (regardless of formulation) may explain 24.9% of the total variation along the second axis (PCO2 axis, Figure 1 C). The Permanova analysis also corroborates this result (P < 0.05; Table S1).

Concerning the bulk soil (Figure 1 D, 1 E and 1 F), a significant separation between samples from day 14 and day 28 were observed, which shared a similarity of 42.6% (Permanova: F=14.77; P=0.001). For each sampling time, the copper-treated soil samples and non-treated soil samples was also observed (Permanova: F=2.80; P < 0.001; Table S1). Concerning the day 14, only the most soluble copper formulations, Cu(OH)₂-i and nCu(OH)₂, exhibited a significant impact on the structure of bacterial community compared to respective CT (Permanova: F = 3.64; P < 0.05; Table S1). In opposite, the bacterial communities exposed to Kocide[®]3000 and nCuO showed a similar structure than those from control soil (Permanova: Kocide[®]3000: F = 3.64; P = 0.095; nCuO: F=3.64; P=0.058). Concerning copper formulation, the bacterial communities exposed for 14 days to Cu(OH)₂-i were significantly different from those exposed to nCu(OH)₂ (Permanova: F = 3.64; P < 0.05; Table S1). Also, the Kocide[®]3000-treated soil presented a distinct bacterial community structure in comparison to soils treated with nCuO and nCu(OH)₂ (Permanova: F = 3.64; P < 0.05; Table S1). Additionally, the PCoA analysis corroborates the clustering analysis.

After 28 days of exposure, all copper formulations exerted a significant impact on the bacterial community structure, sharing 55.2% of similarity with the CT group. The PCoA analysis revealed that copper exposure (regardless of form) may explain 44.1% of the total variation along the first axis (PCO1, Figure 1 F), while the nCuO and nCu(OH)₂ treatments may explain 27.9% of the total variation along the second axis (PCO2, Figure 1 F). Comparing copper formulations, only the nCu(OH)₂-treated soil showed a distinct effect on the soil bacterial community compared to the Cu(OH)₂-i, Kocide[®]3000, and nCuO treated soils (Permanova: F= 6.27; P< 0.05; Table S1).

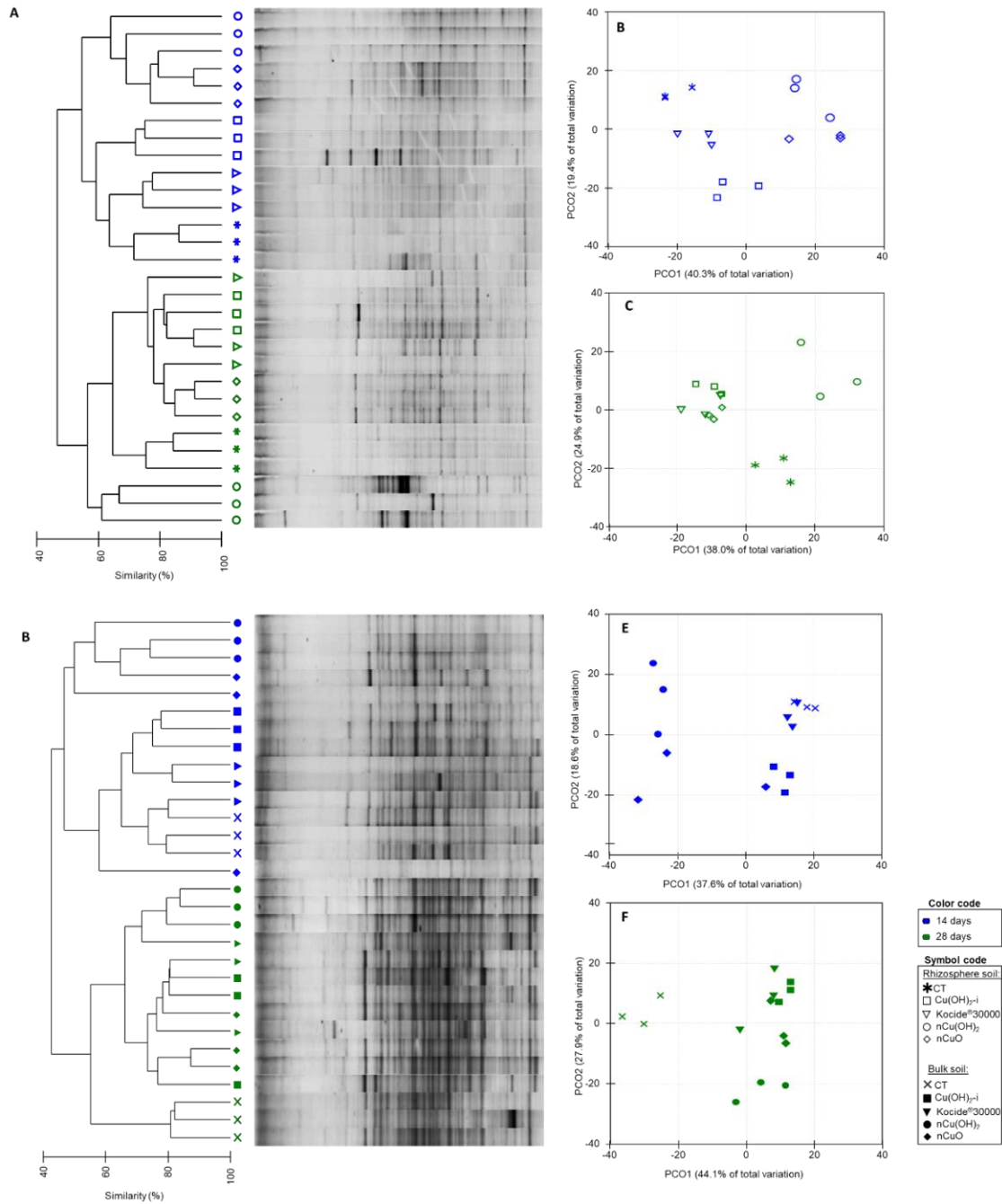


Figure 1. Denaturing gradient gel electrophoresis (DGGE) analysis, targeting the bacterial community (16S rRNA gene) from rhizosphere (A, B, and C) or bulk (D, E, and F) soil. Soil treatments included: non-treated soil (CT), and soil treated with 50 mg (Cu) kg⁻¹ soil as Cu(OH)₂-i, Kocide®30000, nCu(OH)₂, or nCuO, after 14 (■ blue symbols) and 28 (■ green symbols) days of exposure. Clustering analysis (A and D) and Principal coordinate analysis (PCoA) (B, C, E, and F), were constructed based on Jaccard similarity of DGGE relative abundance data (n=3).

Regarding diversity indexes (Figure 2), rhizosphere bacterial community showed a significant reduction of richness (-5%), diversity (-54%) and evenness (-12%) in

nCu(OH)₂-treated soils compared to the respective CT, after day-28 ($p < 0.05$; Table S2).

Regarding diversity indexes (Figure 2), rhizosphere bacterial community showed a significant reduction of diversity (-54%) and evenness (-12%) in nCu(OH)₂-treated soils compared to the respective CT, after day-28 ($p < 0.05$; Table S2). In addition, nCu(OH)₂-treated soil exhibited a decreased diversity (-43%) and evenness (-10%) compared to nCuO-treated soil ($p < 0.05$; Table S2). On the other hand, a significant decrease in richness [nCuO: -8% and Cu(OH)₂-i -6%] and diversity (nCuO: -8%) was observed in bulk soil treated with these Cu-formulations compared to the respective CT, at day-14 ($p < 0.05$; Table S2). Also, the Cu(OH)₂-i treated soil presented a significant increased bulk bacterial richness compared to the nCuO (+6%) and nCu(OH)₂ (+5%) treated soil, at day-14. After 28 days of exposure, a significant increase in the bulk bacterial richness was detected in Kocide®3000-treated soil compared to the respective CT (+3%), the nCu(OH)₂-treated soil (+4%) and the Cu(OH)₂-i treated soil (+4%) ($p < 0.05$; Table S2).

Additionally, the non-treated rhizosphere soil presented a significantly higher diversity (Shannon-Wiener) and evenness indexes (Pielou's index) compared to the non-treated bulk soil, after 28 days of exposure (Shannon-Wiener: $F=7.791$, $p=0.49$; Pielou: $F=8.155$, $p=0.46$), suggesting a distinct community from soil location.

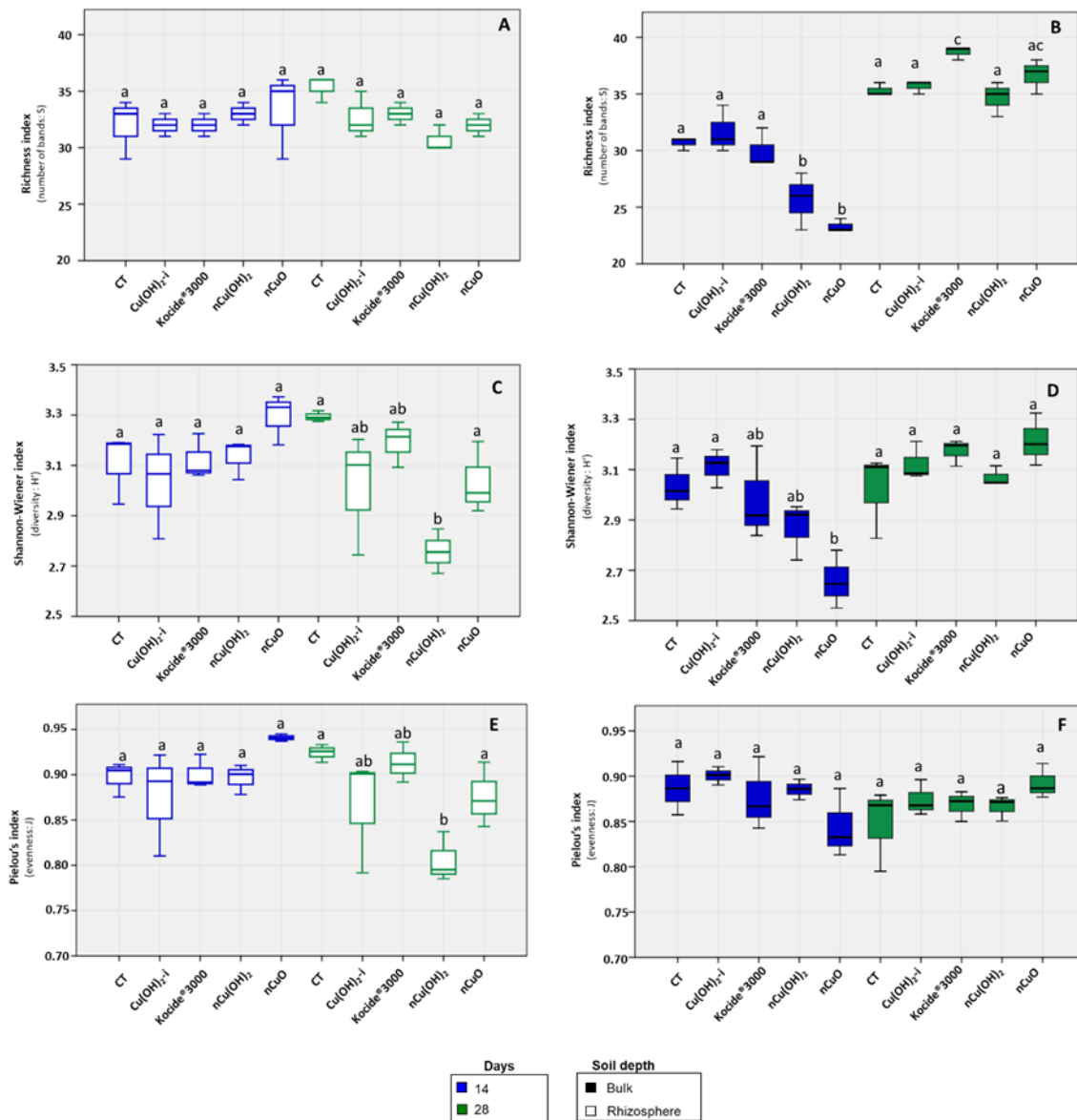


Figure 2. Richness (number of bands; S), Shannon-Wiener (diversity index; H') and Pielou's (evenness index; J') indexes calculated for bacterial communities from rhizosphere (A, C and E) or bulk soil (B, D, and F). Soil treatments included the non-exposed or exposed to $\text{Cu}(\text{OH})_2\text{-i}$, or Kocide®3000, or nCuO or nCu(OH)₂, after day 14 (■ blue symbols) or 28 (■ green symbols). Values are presented per mean \pm standard deviation. Values are presented per mean \pm standard deviation. Different letters (^{a,b,c}) indicates a significant difference between soil treatments and exposure time (two-way ANOVA, $p < 0.05$; Tukey HSD).

3.2. Effects of copper on enzymatic activity

The activities of DHA, βG , AP, AS, and UA were measured in rhizosphere soil treated with copper-based NMs (Figure 3 A - E). Significant effects, which depended on the contaminant, were only observed after 14 days for enzymes AS, AP and UA (Figure 3 C, 3 D and 3 E). Concerning the AS activity, a significant decreased activity (-38%) was detected in nCuO-treated soils, compared to the respective CT soil ($p < 0.05$, Table

S3). Concerning the AP activity, the reduction was of -13%, -7%, -16%, and -8% relative to the CT, in rhizosphere soil treated with $\text{Cu}(\text{OH})_2\text{-i}$, Kocide[®]3000, nCuO and $\text{nCu}(\text{OH})_2$, respectively ($p < 0.05$, Table S3). The UA activity was the enzyme most affected in copper-treated soils, resulting in a significant reduction of -48%, -43% and -42% in soils treated with $\text{Cu}(\text{OH})_2\text{-i}$, nCuO and $\text{nCu}(\text{OH})_2$, respectively, compared to the respective CT ($p < 0.05$, Table S3). On the other hand, copper treatments did not affect the DHA and BG activities (Figure 3 A and 3 B), irrespective of the sampling time. Regarding copper formulations, significant differences among treatments were observed for the AP activity (at day 14) in which nCuO-treated soils exhibited a lower AP activity than soils treated with $\text{nCu}(\text{OH})_2$ (-8%) or Kocide[®]3000 (-9%) ($p < 0.05$, Table S3).

These enzymatic activities were previously analyzed in bulk soil and results are shown in Figure 3 (in Chapter 4). In overall, the activity of DHA, AS, and UA was significantly reduced in copper-treated soil, mainly after 28 days. For instance, after 28 days of exposure, DHA activity showed a reduction of 95% (Kocide[®]3000), 92% [$\text{Cu}(\text{OH})_2\text{-i}$], 86% (nCuO) and 68% [$\text{nCu}(\text{OH})_2$] compared to the CT. Regarding the AS activity (day-28), soils treated with Kocide[®]3000, $\text{Cu}(\text{OH})_2\text{-i}$, nCuO and $\text{nCu}(\text{OH})_2$ presented a decreased activity of 27%, 41%, 44% and 32%, respectively. For UA activity, a reduction between of 20% and 40% were detected in copper-treated soils, after both 14 and 28 days of exposure. The activity of AP and βG were similar in copper-treated soils and CT soil.

For comparison purposes, Figure S1 was also constructed using both rhizosphere and bulk soil enzymatic data, over-time. In this figure, the enzymatic activity profile of the rhizosphere was distinct from that observed in the bulk soil (Permanova: $F=119.75$; $P=0.001$), over-time (Permanova: $F=83.43$; $P=0.001$). For instance, significant differences between non-treated bulk and rhizosphere soil enzymatic activity were detected in DHA (-9% in rhizosphere soil; $F=21.69$, $p=0.011$), βG (+0.5% in rhizosphere soil; $F=165.50$, $p=0.004$), AS (-1% in rhizosphere soil; $F=129.25$, $p=0.04$), and UA (-7% in rhizosphere soil; $F=374.98$; $p < 0.001$), after day-14.

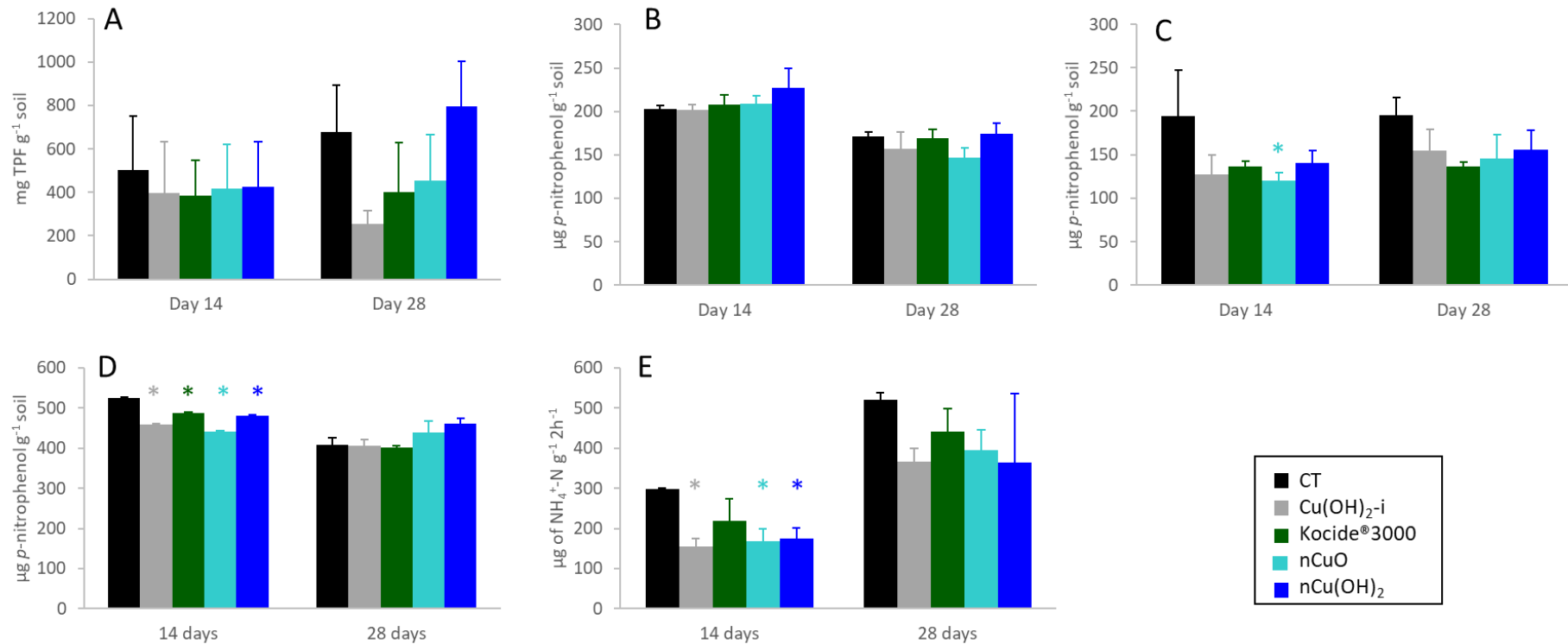


Figure 3. Enzymatic activity measured in Lufa 2.2 non-exposed soil (CT) and in soil spiked with Cu(OH)₂-i, Kocide®3000, nCu(OH)₂, or nCuO, and sampled from rhizosphere at day 14 and 28. The data represent the average enzymatic activity (n=3 ± standard deviation) of dehydrogenase (A), β-glucosidase (B), arylsulfatase (C), acid phosphatase (D) and urease (E). Asterisks (*) indicate significant differences between exposed samples towards the respective control (two-way ANOVA, Tukey HSD method; p<0.05), for each sampling point.

4. Discussion

The impact of copper-based NMs in the rhizosphere bacterial community, under a complex exposure scenario and in the presence of biota, is still poorly understood. Additionally, a distinct response of bacterial communities from rhizosphere and bulk soil to the copper NMs exposure is expected, which may be due to distinct soil microbiome composition in these soils. Thus, this work provides relevant information about the impact of environmental relevant concentration of copper-based NMs [Kocide[®]3000, nCu(OH)₂, nCuO, and ionic Cu(OH)₂] in the rhizosphere and bulk soil bacterial community structure and function.

4.1. Effects of copper-based nanomaterials on soil bacterial rhizosphere

Copper-based NMs significantly affected the rhizosphere bacterial community structure, diversity and function, depending on the exposure time and the copper formulation. For instance, the earlier (at day 14) alteration on the rhizosphere bacterial communities' structure was detected in treated soils with nCu(OH)₂ and nCuO, suggesting a distinct mode of action of these NMs compared to the other formulations. After 28 days, all copper formulations affected the rhizosphere bacterial communities' structure compared to the CT. However, the alpha-diversity was significantly reduced only for the community exposed to nCu(OH)₂ (day-28). Accordingly, nCuO have been reported to affect the soil bacterial community's structure, composition and alpha-diversity, in the presence of plants (Fernandes *et al.*, 2017; Guan *et al.*, 2020). In opposite, the sequential application of Kocide[®]3000 did not affect the structure, composition and diversity of soil bacterial communities, in the presence of several crops and under outdoor mesocosms (Carley *et al.*, 2020). On the contrary, our study showed that Kocide[®]3000 influences the bacterial communities' structure/composition, which may result from the distinct experimental design, application procedure, and copper concentration tested.

At functional level, soil enzymatic activity is a relevant microbial indicator for soil quality/function, plant growth and used to assess the impact of NMs exposure in contaminated soils (Nannipieri *et al.*, 2018; Holden *et al.*, 2014). Thus, the activity of five enzymes related to different nutrient cycles (carbon, sulfur, nitrogen, and phosphorous) was analyzed in our study. Results demonstrated a significant reduction of enzymatic activities related to nitrogen (UA), phosphorous (AP), and sulfur (AS)

cycles in rhizosphere soil treated with copper, but only at day-14. This result suggests a potential disruption in microbial-mediated nutrient cycling, with consequences in plant nutrition and soil fertility (Nannipieri *et al.*, 2018). Although all copper formulations slightly decrease AS activity, only nCuO significantly affects this enzymatic activity, suggesting a distinct mode of action for this formulation (*e.g.*, a potential nanoparticle-specific effect or a disruption of ABC transporters and *Quorum Sensing* as shown in Chapter 4). In accordance with our results, the inhibition of AP and UA activities has already been reported in rhizosphere soils (*Oryza sativa L.*) treated with nCuO (20 nm), at concentrations of 100, 500 and 1000 mg kg⁻¹ soil (Xu *et al.*, 2015). Also, the single application of Kocide®3000 (6.68 mg/L) reduced the activity of AP and AS after 15 days of exposure, in the presence of several crops and under an outdoor mesocosms (Simonin *et al.*, 2018b). However, after two and three applications of this nanoproduct in plants, its effect was no longer detected in these soil enzymatic activities (Simonin *et al.*, 2018b). On the other hand, our study demonstrated that the activity of enzymes related to the carbon cycle and cellular viability (β -glucosidase and dehydrogenase, respectively) did not significantly change in copper-treated soils, which may be due to an increased carbon mobilization by root exudates (Canarini *et al.*, 2019). In opposite, the reduction of the activity of enzymes involved in this nutrient cycle has been reported in rhizosphere soil treated with nCuO (Xu *et al.*, 2015; DHA) or with Kocide®3000 (Simonin *et al.*, 2018b; α -glucosidase, β -glucosidase, and cellulase). This distinct observation may result from the distinct experimental designs, copper concentrations and plant species.

Recent studies suggest that root exudates stimulate the dissolution of copper NMs in soil (Cervantes-Avilés *et al.*, 2021; Guan *et al.*, 2020; Zhang *et al.*, 2020; Spielman-Sun *et al.*, 2018; Gao *et al.*, 2018), which may explain the earlier structural and functional effects detected in our study. Additionally, the particle-effect of these NMs mainly explain the structural effect, because the other NMs did not show a significant effect. On the other hand, the increased bioavailable Cu in the root system (*i.e.*, uptake) was observed mainly at day-14, regardless of the copper form (data not shown), which may support our observations in soil enzymatic assays.

At a longer exposure period, the impact of copper exposure on soil enzymatic activities was attenuated, suggesting a recover of the soil functionality. This recovery has been described in soils with a high diversity of microorganisms, and related to the replacement of the microorganisms originally present in the community by others

tolerant to copper and capable of performing the same function (Allison and Martiny, 2008). However, we cannot exclude the possibility of a recovery of the affected microorganisms due to a change in the bioavailability of the contaminant. Even so, this last hypothesis is not supported by the structural analysis data, since the effects on the structure were not attenuated.

4.2. Distinct effects of copper-based nanomaterials on soil bacterial rhizosphere and bulk

Distinct alpha-diversity and soil enzymatic activities among non-treated rhizosphere and bulk soil were observed in our study, supporting the evidence of distinct bacterial communities in these soils. For instance, our study showed higher diversity and evenness indexes in the rhizosphere bacterial community compared to the bulk soil, after 28 days of exposure. In accordance, higher abundance of bacterial communities was also reported in the rhizosphere soil in comparison to the bulk soil (Lopes *et al.*, 2016; Guan *et al.*, 2020). The alteration of soil properties (decreased pH, or increased oxygen level or nutrient available) promoted by the root elongation and the exudates released by the roots, may shape the composition and activity of soil bacterial community in rhizosphere area (Knauff *et al.*, 2003). The protons (H^+) released from roots exudates not only reduce the pH in soil (which increases the metal bioavailability) but also can stimulate the activity of AS and AP (Knauff *et al.*, 2003; Sun *et al.*, 2020). However, our study showed a decreased activity of AS in non-treated rhizosphere soil compared to the non-treated bulk soil. This decreased activity may result from the slight differences between soil depth between rhizosphere and bulk collected samples (for example, the root system may have expanded more than 2 cm into the soil, which was the collection depth for the bulk soil that we use).

Due to the distinct bacterial community in both rhizosphere and bulk soil, a dissimilar response of these communities to copper exposure is hypothesized in our study. In fact, copper-based NMs affected the function of rhizosphere bacterial community but only after 14 days of exposure, while a later effect was observed in the bulk soil (at day-28). As described above, the root exudates may promote a faster dissolution of copper-based NMs and decrease their aggregation in soil (Cervantes-Avilés *et al.*, 2021; Guan *et al.*, 2020; Zhang *et al.*, 2020; Spielman-Sun *et al.*, 2018), explaining this earlier effect of copper in rhizosphere soil. At the functional level, a distinct impact of these copper NMs in the rhizosphere and bulk soil communities was detected, which depended on the

enzyme tested. For instance, the activity of the enzyme related to the cellular viability and C cycle, namely dehydrogenase activity, was only reduced in the bulk soil treated with copper, after day-28. On the other hand, this alteration was not detected in the rhizosphere soil, which may be due to the mobilization of nutrients, *e.g.*, carbon, by the root exudates. The mobilization of this nutrient may promote the abundance of the symbiotic microorganisms in this area (Canarini *et al.*, 2019), which may enhance the plant defence in metal contaminated soils, by the regulation of several enzymes (*e.g.*, catalase, glutathione reductase, ascorbate peroxidase) and genes involved in ROS homeostasis (Vilela *et al.*, 2018). Concerning acid phosphatase, the activity of this enzyme was only reduced in the copper-treated soil from rhizosphere, suggesting a decrease amount and/or form of phosphorus available for plants (Sun *et al.*, 2020). The study by Zhang and their collaborators (2019) reported that this enzyme activity is dependent on the composition of root exudates, and any change in that composition alter the AP activity. In fact, our previous study (Chapter 4) showed that copper-based NMs exposure changes the utilization of phenolic acid and amines/amides by soil microbiome, which were already described as elements in the root exudate composition (Canarini *et al.*, 2019).

Additionally, a distinct impact on the bacterial richness from rhizosphere and bulk soil was also detected in copper-treated soil. For instance, the bacterial richness increased in Kocide®3000-treated bulk soil (day-28), while a significant decrease in this index was detected in the nCu(OH)₂-treated rhizosphere soil (day-28). Although a contradictory impact of the copper-based NMs was reported in alpha-diversity from both rhizosphere and bulk soil (Zhang *et al.*, 2020; Carley *et al.*, 2020), the increased richness in Kocide®3000 may result from its distinct formulation. Actually, Kocide®3000 includes a high percentage of excipients (73.5%) composed by metal and non-metal elements (*e.g.*, C, O, Na, Al, Si, P, S, and Zn) (Simonin *et al.*, 2018b), which may be utilized as substrate/micronutrients by several microorganisms.

4.3. The environmental and agronomic relevance

Overall, this work highlighted the importance to investigate the soil bacterial community associated to the rhizosphere soil to assess the impact of copper-based NMs in terrestrial compartment, under a complex exposure scenario. The initial soil microbiome (composition, abundance, diversity and activity), from bulk and rhizosphere soil, can be a decisive factor in its response to the copper NMs exposure, as

we observed in our study. At the ecological and agronomic perspective, the presence of plants in soils is a key factor in shaping the soil microbiome structure and functions, essentially due to the chemical composition of plant residues (*e.g.*, exudates) and/or rhizodeposition (Whalley *et al.*, 2005; Lladó *et al.*, 2017). Thus, in future studies, the analysis of soil exudates should be conducted to clarify the potential effect on copper dissolution, and on soil bacterial community composition and function. On the other hand, the application of copper NMs in soil, under complex scenarios, may impair the regulation of the P cycle (*e.g.*, by the reduced AP activity), which can represent a negative impact on soil fertility and growth/quality of plants (Wei *et al.*, 2019). Also, the application of nCuO suggested a stronger impact on the sulfur cycle, potentially due to a distinct mode of action compared to the other copper formulations. However, over-time, an attenuated impact of these NMs on functional parameters, suggests a potential recover or a redundancy of the rhizosphere microbiome functionality. Thus, to clarify this potential impact, longer exposure times should be considered in the presence/absence of plants.

5. Conclusion

The current work provides relevant information on the impact of copper-based NMs on rhizosphere soil bacterial communities, which can be a starting point to understand the potential impact of these NMs in the soil fertility. Due to the distinct bacterial diversity and enzymatic activities observed in both non-treated rhizosphere and bulk soil, a distinct soil microbiome was suggested in these soils. Also, distinct microbial response to the copper exposure was detected between rhizosphere and bulk soil, depending on the time of exposure and the copper formulation. Concerning the functional level, the copper exposure rapidly affected the enzymatic activity in the rhizosphere soil (at day-14), while late effects were detected in the bulk soil (day-28), suggesting a faster copper dissolution in the rhizosphere soil. Also, the regulation of P cycle suggested to be negatively affected only in rhizosphere soil, probably due to the root exudates activity. Comparing copper formulations, Cu(OH)₂-i showed a similar impact to NMs on the structure and function of bacterial community from the rhizosphere soil. On the other hand, nCuO and nCu(OH)₂ exerts a stronger impact in the rhizosphere soil enzymatic activity or in alpha-diversity, respectively. Future studies are needed to confirm the potential negative impact of these nano-formulations on soil fertility, and a rhizobox

setup should be a good design to assess this impact (Wei *et al.*, 2019). Additionally, future studies should also consider a deeper analysis of soil microbiome, *e.g.*, using next-generation sequencing and qPCR methodologies, to identify changes in specific microbial phylotypes (*e.g.*, bacterial and fungal) and functional genes (*e.g.*, related to nitrogen, phosphorus, and sulfur cycles), respectively.

6. Acknowledgements

The mesocosm experiment was run under the ECOCENE-Ecological Effects of Nanopesticides to Soil Ecosystems (PTDC/CTA-AMB/32471/2017), supported by FCT - Fundação para a Ciência e a Tecnologia, within the PT2020 Partnership Agreement and Compete 2020 co-funded by the FEDER - Fundo Europeu de Desenvolvimento Regional; and Nano-FARM - Fate and Effects of Agriculturally Relevant Materials (ERANET SIIN 2014, SIINN/0001/2014), supported by Fundação para a Ciência e a Tecnologia (FCT), under the frame of SIINN, the ERA-NET. All the authors received additional financial support from FCT/MCTES, through national funds, to CESAM (UIDP/50017/2020+UIDB/50017/2020). This work was supported by FCT through a PhD grant to Peixoto, S. (SFRH/BD/117738/2016). The authors also would to thanks to Marta Alves for the extraction of the biological matrix from DGGE data.

7. References

- Allison, S. D., Martiny, J. B. (2008). Resistance, resilience, and redundancy in microbial communities. *Proceedings of the National Academy of Sciences*, 105, 11512-11519.
- Canarini, A., Kaiser, C., Merchant, A., Richter, A., Wanek, W. (2019). Root exudation of primary metabolites: mechanisms and their roles in plant responses to environmental stimuli. *Frontiers in Plant Science*, 10, 157.
- Carley, L. N., Panchagavi, R., Song, X., Davenport, S., Bergemann, C. M., McCumber, A. W., Simonin, M. (2020). Long-term effects of copper nanopesticides on soil and sediment community diversity in two outdoor mesocosm experiments. *Environmental Science & Technology*, 54(14), 8878-8889.

- Cervantes-Avilés, P., Huang, X., Keller, A. A. (2021). Dissolution and aggregation of metal oxide nanoparticles in root exudates and soil leachate: implications for nanoagrochemical application. *Environmental Science & Technology*.
- Dick, R. P., Breakwell, D. P., Turco, R. F. (1997). Soil enzyme activities and biodiversity measurements as integrative microbiological indicators. *In Methods for Assessing Soil Quality*, 49 (pp. 247-271).
- Fernandes, J. P., Almeida, C. M. R., Andreotti, F., Barros, L., Almeida, T., Mucha, A. P. (2017). Response of microbial communities colonizing salt marsh plants rhizosphere to copper oxide nanoparticles contamination and its implications for phytoremediation processes. *Science of The Total Environment*, 581, 801-810.
- Gao, X., Avellan, A., Laughton, S., Vaidya, R., Rodrigues, S. M., Casman, E. A., Lowry, G. V. (2018). CuO nanoparticle dissolution and toxicity to wheat (*Triticum aestivum*) in rhizosphere soil. *Environmental Science & Technology*, 52(5), 2888-2897.
- Geitner, N.; Hendren, C.; Cornelis, G.; Kaegi, R.; Lead, J.; Lowry, G.; Lynch, I.; Nowack, B.; Petersen, E.; Bernhardt, E.; Brown, S.; Chen, W.; de Garidel-Thoron, C.; Hanson, J.; Harper, S.; Jones, K.; von der Kammer, F.; Kennedy, A.; Kidd, J.; Matson, C.; Metcalfe, C.; Pedersen, J.; Peijnenburg, W.; Quik, J.; Rodrigues, S. M.; Rose, J.; Sayre, P.; Simonin, M.; Svendsen, C.; Tanguay, R.; Tufenkji, N.; van Teunenbroek, T.; Thies, G.; Tian, Y.; Rice, J.; Turner, A.; Liu, J.; Unrine, J.; Vance, M.; White, J.; Wiesner, M. (2020). Harmonizing across environmental nanomaterial testing media for increased comparability of nanomaterial datasets. *Environmental Science: Nano*, 7(1), 13-36.
- Guan, X., Gao, X., Avellan, A., Spielman-Sun, E., Xu, J., Laughton, S., Lowry, G. V. (2020). CuO nanoparticles alter the rhizospheric bacterial community and local nitrogen cycling for wheat grown in a Calcareous soil. *Environmental Science & Technology*, 54(14), 8699-8709.
- Holden, P. A., Klaessig, F., Turco, R. F., Priester, J. H., Rico, C. M., Avila-Arias, H., Gardea-Torresdey, J. L. (2014). Evaluation of exposure concentrations used in assessing manufactured nanomaterial environmental hazards: are they relevant?. *Environmental Science & Technology*, 48(18), 10541-10551.
- Jansson, J. K., Hofmockel, K. S. (2018). The soil microbiome—from metagenomics to metaphenomics. *Current opinion in microbiology*, 43, 162-168.

- Kah, M., Kookana, R. S., Gogos, A., Bucheli, T. D. (2018). A critical evaluation of nanopesticides and nanofertilizers against their conventional analogues. *Nature Nanotechnology*, 13(8), 677-684.
- Kandeler, E., Gerber, H. (1988). Short-term assay of soil urease activity using colorimetric determination of ammonium. *Biology and Fertility of Soils*, 6(1), 68-72.
- Knauff, U., Schulz, M., Scherer, H. W. (2003). Arylsulfatase activity in the rhizosphere and roots of different crop species. *European Journal of Agronomy*, 19(2), 215-223.
- Li, J., Rodrigues, S., Tsyusko, O. V., Unrine, J. M. (2019 a). Comparing plant–insect trophic transfer of Cu from lab-synthesised nano-Cu(OH)₂ with a commercial nano-Cu(OH)₂ fungicide formulation. *Environmental Chemistry*, 16(6), 411-418.
- Lladó, S., López-Mondéjar, R., Baldrian, P. (2017). Forest soil bacteria: diversity, involvement in ecosystem processes, and response to global change. *Microbiology and Molecular Biology Reviews*, 81(2), e00063-16.
- Lopes, L. D., Pereira e Silva, M. D. C., Andreote, F. D. (2016). Bacterial abilities and adaptation toward the rhizosphere colonization. *Frontiers in Microbiology*, 7, 1341.
- Lowry, G. V., Avellan, A., Gilbertson, L. M. (2019). Opportunities and challenges for nanotechnology in the agri-tech revolution. *Nature Nanotechnology*, 14(6), 517–522.
- Muyzer, G., Waal, E., C. and Uitterlinden, A., G. (1993). profiling of complex microbial populations by denaturing gradient gel electrophoresis analysis of polymerase chain reaction-amplified genes coding for 16S rRNA, *Applied and Environmental Microbiology*, 59(3), 695–700.
- Nannipieri, P., Trasar-Cepeda, C., Dick, R. P. (2018). Soil enzyme activity: a brief history and biochemistry as a basis for appropriate interpretations and meta-analysis. *Biology and Fertility of Soils*, 54(1), 11-19.
- Peixoto, S., Henriques, I., Loureiro, S. (2021). Long-term effects of Cu(OH)₂ nanopesticide exposure on soil microbial communities. *Environmental Pollution*, 116113.

- Peixoto, S., Khodaparast, Z., Cornelis, G., Lahive, E., Etxabe, A. G., Baccaro, M., Henriques, I. (2020). Impact of Ag₂S NPs on soil bacterial community—A terrestrial mesocosm approach. *Ecotoxicology and environmental safety*, 206, 111405.
- Philippot, L., Raaijmakers, J. M., Lemanceau, P., Van Der Putten, W. H. (2013). Going back to the roots: the microbial ecology of the rhizosphere. *Nature Reviews Microbiology*, 11(11), 789-799.
- Praeg, N., Pauli, H., Illmer, P. (2019). Microbial diversity in bulk and rhizosphere soil of *Ranunculus glacialis* along a high-alpine altitudinal gradient. *Frontiers in Microbiology*, 10, 1429
- Simonin, M., Cantarel, A. A., Crouzet, A., Gervais, J., Martins, J. M., Richaume, A. (2018a). Negative effects of copper oxide nanoparticles on carbon and nitrogen cycle microbial activities in contrasting agricultural soils and in presence of plants. *Frontiers in Microbiology*, 9, 3102.
- Simonin, M., Colman, B. P., Tang, W., Judy, J. D., Anderson, S. M., Bergemann, C. M., Bernhardt, E. S. (2018b). Plant and microbial responses to repeated Cu(OH)₂ nanopesticide exposures under different fertilization levels in an agro-ecosystem. *Frontiers in Microbiology*, 9, 1769.
- Spielman-Sun, E., Lombi, E., Donner, E., Avellan, A., Etschmann, B., Howard, D., Lowry, G. V. (2018). Temporal evolution of copper distribution and speciation in roots of *Triticum aestivum* exposed to CuO, Cu(OH)₂, and CuS nanoparticles. *Environmental Science & Technology*, 52(17), 9777-9784.
- Sun B.R., Gao Y.Z., Wu X., Ma H.M., Zheng C.C., Wang X.Y., Zhang H.L., Li Z.J., Yang H.J. (2020). The relative contributions of pH, organic anions, and phosphatase to rhizosphere soil phosphorus mobilization and crop phosphorus uptake in maize/alfalfa polyculture. *Plant and Soil*, 447(1), 117-133.
- Thakur, M. P., Geisen, S. (2019). Trophic regulations of the soil microbiome. *Trends in Microbiology*, 27(9), 771-780.
- Vilela, L. A., Teixeira, A. F., Lourenço, F. M., Souza, M. D. (2018). Symbiotic microorganisms enhance antioxidant defense in plants exposed to metal/metalloid-contaminated soils. In *Plants Under Metal and Metalloid Stress* (pp. 337-366). Springer, Singapore.

- Wei, Z., Gu, Y., Friman, V. P., Kowalchuk, G. A., Xu, Y., Shen, Q., Jousset, A. (2019). Initial soil microbiome composition and functioning predetermine future plant health. *Science Advances*, 5(9), eaaw0759.
- Whalley, W. R., Riseley, B., Leeds-Harrison, P. B., Bird, N. R., Leech, P. K., Adderley, W. P. (2005). Structural differences between bulk and rhizosphere soil. *European Journal of Soil Science*, 56(3), 353-360.
- Xu, C., Peng, C., Sun, L., Zhang, S., Huang, H., Chen, Y., Shi, J. (2015). Distinctive effects of TiO₂ and CuO nanoparticles on soil microbes and their community structures in flooded paddy soil. *Soil Biology and Biochemistry*, 86, 24-33.
- Yang, Y., Quensen, J., Mathieu, J., Wang, Q., Wang, J., Li, M., Alvarez, P. J. (2014). Pyrosequencing reveals higher impact of silver nanoparticles than Ag⁺ on the microbial community structure of activated sludge. *Water Research*, 48, 317-325.
- Yuan, J., Zhao, J., Wen, T., Zhao, M., Li, R., Goossens, P., Shen, Q. (2018). Root exudates drive the soil-borne legacy of aboveground pathogen infection. *Microbiome*, 6(1), 1-12.
- Zhang, X., Xu, Z., Qian, X., Lin, D., Zeng, T., Filser, J., Kah, M. (2020). Assessing the Impacts of Cu(OH)₂ Nanopesticide and Ionic Copper on the Soil Enzyme Activity and Bacterial Community. *Journal of Agricultural and Food Chemistry*, 68(11), 3372-3381.
- Zhang, X., Dippold, M. A., Kuzyakov, Y., Razavi, B. S. (2019). Spatial pattern of enzyme activities depends on root exudate composition. *Soil Biology and Biochemistry*, 133, 83-93.

8. Supplementary material

8.1. List of Figures

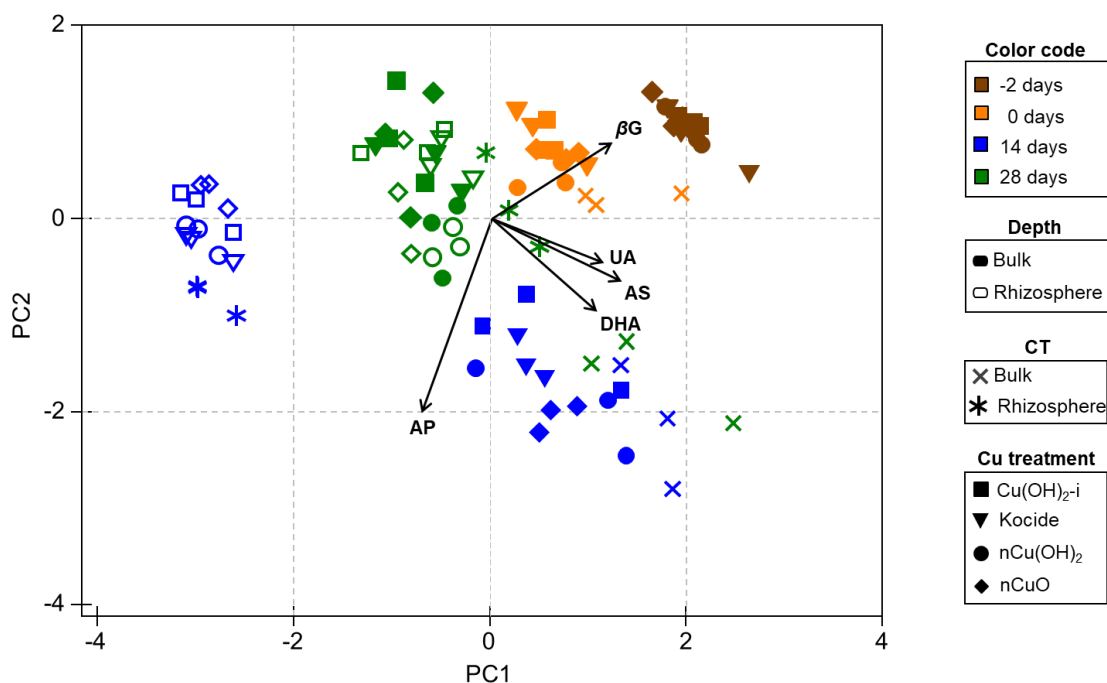


Figure S1. Soil enzymatic activity measured in rhizosphere and bulk soil, sampled at day -2, 0, 14 and 28. Soil treatments included the non-exposed soil (CT) and soil spiked with $\text{Cu}(\text{OH})_2\text{-i}$, or Kocide[®]3000, or $\text{nCu}(\text{OH})_2$, or nCuO . The data represent the average of enzymatic activity ($n=3 \pm$ standard deviation) of dehydrogenase (DHA), arylsulfatase (AS), β -glucosidase (βG) acid phosphatase (AP) and urease (UA) activities. The vectors represent each enzymatic activity tested.

8.2. List of Tables

Table S1. Permanova analysis regarding the bacterial community structure, by DGGE analysis, from rhizosphere and bulk soil. Treatments included: the non-exposed soil or exposed soil to 50 mg (Cu) kg⁻¹ soil of Cu(OH)₂-i, or Kocide®3000, or nCuO or nCu(OH)₂, after 14 and 28 days of exposure. Data was paired-wised test based on 999 permutations.

Soil	Sampling time (days)	Multiple comparison (treatments)	Permanova (Monte Carlo)
Rhizosphere	14	CT x Cu(OH) ₂ -i	0.018
		CT x nCuO	0.006
		CT x Kocide®3000	0.035
		CT x nCu(OH) ₂	0.017
		Cu(OH) ₂ -i x nCuO	0.013
		Cu(OH) ₂ -i x Kocide®3000	0.027
		Cu(OH) ₂ -i x nCu(OH) ₂	0.024
	28	nCuO x Kocide®3000	0.013
		Kocide®3000 x nCu(OH) ₂	0.016
		CT x Cu(OH) ₂ -i	0.007
		CT x nCuO	0.021
		CT x Kocide®3000	0.028
		CT x nCu(OH) ₂	0.025
		Cu(OH) ₂ -i x nCu(OH) ₂	0.031
Bulk	14	nCuO x nCu(OH) ₂	0.031
		Kocide®3000 x nCu(OH) ₂	0.030
		CT x Cu(OH) ₂ -i	0.021
		CT x nCu(OH) ₂	0.021
	28	Cu(OH) ₂ -i x nCu(OH) ₂	0.021
		nCuO x Kocide®3000	0.07
		Kocide®3000 x nCu(OH) ₂	0.023
Bulk	14	CT x Cu(OH) ₂ -i	0.003
		CT x nCuO	0.005
		CT x Kocide®3000	0.009
	28	CT x nCu(OH) ₂	0.005
		Cu(OH) ₂ -i x nCu(OH) ₂	0.017
		nCuO x nCu(OH) ₂	0.033
		Kocide®3000 x nCu(OH) ₂	0.025

Table S2. Statistical significance ($p < 0.05$) for diversity indexes in non-exposed soil or exposed soil to 50 mg (Cu) kg^{-1} soil of $\text{Cu}(\text{OH})_2\text{-i}$, Kocide[®]3000, nCuO or nCu(OH)₂. using the two-way ANOVA (Tukey HSD test).

Soil	Time (days)	Diversity index	Multiple comparison (Treatments)	F	p	
Rhizosphere	28	J'	CT x nCu(OH) ₂	4.90	0.018	
			nCu(OH) ₂ x nCuO	4.90	0.031	
		H'	CT x nCu(OH) ₂	6.55	0.005	
			nCu(OH) ₂ x nCuO	6.55	0.021	
Bulk	14	S	CT x nCuO	13.45	0.003	
			CT x nCu(OH) ₂	13.45	0.030	
			nCuO x nCu(OH) ₂ -i	13.45	0.001	
		nCu(OH) ₂ x nCu(OH) ₂ -i	13.45	0.01		
		nCuO x Kocide [®] 3000	13.45	0.005		
		nCu(OH) ₂ x Kocide [®] 3000	13.45	0.008		
	H'	nCuO x Cu(OH) ₂ -i	5.98	0.008		
		nCuO x CT	5.99	0.027		
		28	S	CT x Kocide [®] 3000	6.412	0.22
				Kocide [®] 3000 x nCu(OH) ₂	6.412	0.007
Kocide [®] 3000 x Cu(OH) ₂ -i	6.412			0.39		

Table S3. Statistical significance ($p < 0.05$) for enzymatic activity in non-exposed rhizosphere soil or exposed rhizosphere soil to 50 mg (Cu) kg^{-1} soil of $\text{Cu}(\text{OH})_2\text{-i}$, Kocide[®]3000, nCuO or nCu(OH)₂, using the two-way ANOVA (Tukey HSD test).

Soil	Sampling time (days)	Enzyme	Multiple comparison (Treatments)	F	p
Rhizosphere	14	UA	CT x $\text{Cu}(\text{OH})_2\text{-i}$	6.942	0.030
			CT x nCuO		0.026
			CT x nCu(OH) ₂		0.018
		AP	CT x nCuO	826.523	<0.001
			CT x $\text{Cu}(\text{OH})_2\text{-i}$		<0.001
			CT x nCu(OH) ₂		<0.001
			CT x Kocide [®] 3000		<0.001
			Kocide [®] 3000 x nCuO		<0.001
			nCu(OH) ₂ x nCuO		<0.001
		AS	CT x nCuO	4.055	0.044

Chapter 6

Impact of Ag₂S NPs on soil bacterial community – a terrestrial mesocosm approach

Impact of Ag₂S NPs on soil bacterial community – a terrestrial mesocosm approach

Peixoto, S., Khodaparast, Z., Cornelis, G., Lahive, E., Green Etxabe, A., Baccaro M., Papadiamantis, A.G., Gonçalves, S.F., Lynch, I., Busquets-Fite, M, Puntas V., Loureiro, S., Henriques, I.

Ecotoxicology and Environmental Safety, 206, 111405, doi.org/10.1016/j.ecoenv.2020.111405

Abstract

Soils might be a final sink for Ag₂S nanoparticles (NPs). Still, there are limited data on their effects on soil bacterial communities (SBC). To bridge this gap, we investigated the effects of Ag₂S NPs (10 mg kg⁻¹ soil) on the structure and function of SBC in a terrestrial indoor mesocosm, using a multi-species design. During 28 days of exposure, the SBC function-related parameters were analysed in terms of enzymatic activity, community level physiological profile, culture of functional bacterial groups [phosphorous-solubilizing bacteria (P-SB) and heterotrophic bacteria (HB)], and SBC structure was analysed by 16S rRNA gene-targeted denaturing gradient gel electrophoresis. The SBC exposed to Ag₂S NPs showed a significative decrease of functional parameters, such as β-glucosidase activity and L-arginine consumption, and increase of the acid phosphatase activity. At the structural level, significantly lower richness and diversity were detected, but at later exposure times compared to the AgNO₃ treatment, likely because of a low dissolution rate of Ag₂S NPs. In fact, stronger effects were observed in soils spiked with AgNO₃, in both functional and structural parameters. Changes in SBC structure seem to negatively correlate with parameters related to phosphorous (acid phosphatase activity) and carbon cycling (abundance of HB, P-SB, and β-glucosidase activity). Our results indicate a significant effect of Ag₂S NPs on SBC, specifically on parameters related to carbon and phosphorous cycling, at doses as low as 10 mg kg⁻¹ soil. These effects were only observed after 28 days, highlighting the importance of long-term exposure experiments for slowly dissolving NPs.

Keywords: silver sulfide nanoparticle; soil bacterial community; denaturing gradient gel electrophoresis; soil enzymatic activity; community-level physiological profile; indoor-mesocosm.

1. Introduction

Silver nanoparticles (AgNPs) are broadly used in many applications and products, due to their anti-microbial, anti-inflammatory, and anti-cancer properties (McGillicuddy *et al.*, 2017). The global production of AgNP-based products has been estimated at 450 tons per year (McGillicuddy *et al.*, 2017), whereas the market of AgNP-based antimicrobials has been predicted to grow from 0.79 billion dollars in 2014 to 2.54 billion dollars in 2022 (Pachapur *et al.*, 2016). The increasing application and consumption of AgNPs-containing products results in AgNPs release into wastewater treatment plants (WWTPs) (European Commission Science for Environment Policy, 2017). In these plants, it has been shown that most of the AgNPs are captured and settled in the sludge (Kaegi *et al.*, 2011), where the estimated AgNPs concentration ranges between 1 to 6 mg kg⁻¹ (Gottschalk *et al.*, 2009). During wastewater treatment, the majority of AgNPs (79% as estimated by Wang *et al.*, 2016) are transformed to Ag sulfide NPs (Ag₂S NPs), which are then incorporated into biosolids. Additionally, this sulfidation process also was suggested to occur for silver in ionic form (Ag⁺) as a means to reduce silver toxicity (Kent *et al.*, 2014).

In many countries, these biosolids are amended to agricultural soils to improve soil fertility (Doolette *et al.*, 2016). In the United Kingdom for example, of the 1.05 million tons of dry biosolids produced per year, 85% on average are applied on land (European Commission Science for Environment Policy, 2017). Agricultural soils are often considered a sink for Ag₂S NPs, characterized by a low dissolution rate of these Ag₂S in biosolids and most likely also in soils. For instance, Wang *et al.*, (2016) demonstrated that the ≥ 87% of Ag₂S NPs from biosolids remained in this form at least up to 400 days after soil spiking. The dissolution rate of Ag₂S NPs depends on the degree of sulfidation (Reinsch *et al.*, 2012) and a higher degree of sulfidation of silver results in lower dissolution and a lower toxic effect on soil organisms (Starnes *et al.*, 2015, Wang *et al.*, 2017) and microorganisms (Reinsch *et al.*, 2012, Doolette *et al.*, 2015). Indeed, the toxicity of AgNPs strongly depends on its speciation (Doolette *et al.*, 2015), and

insoluble Ag₂S NPs ($K_{sp} = 8 \times 10^{-51}$) are less toxic and less bioavailable compared to non-sulfidated AgNPs (Doolette *et al.*, 2015).

Only a limited number of studies have thus far explored the toxic effects of Ag₂S NPs on terrestrial organisms. Wang and their co-workers (2017) showed that Ag₂S NPs were bioavailable to some extent and caused toxic effects in *planta*. A substantial increase of Ag accumulation on leaves (3.8 to 5.8 $\mu\text{g Ag g}^{-1}$ dry mass) was demonstrated when wheat (*Cucumis sativus*) and cucumber (*Triticum aestivum* L.) plants were exposed to 10 mg (Ag) L⁻¹ as Ag₂S NPs for one week (Wang *et al.*, 2017). However, Ag₂S NPs fate and toxicity to plants are still a matter of debate since different studies have used different plant species and different silver concentrations (Wang *et al.*, 2017), obtaining conflicting results. A study by Starnes and their collaborators suggests that the exposure to Ag₂S NPs (at 10 mg Ag L⁻¹) resulted in a 20% increase in mortality rate of *Caenorhabditis elegans* (Starnes *et al.*, 2015). However, this observed toxic effect is mainly due to the solubilization of Ag⁺ (released from Ag₂S particles) in soils.

Although a few studies have investigated the stability (Reinsch *et al.*, 2012), toxicity, fate (Schlich *et al.*, 2018), and (bio)availability (Wang *et al.*, 2016) of Ag₂S NPs in soils, the impact on soil bacterial communities (SBC) and microbiological processes is still unknown. SBC play a vital role in soil ecological functions and have been considered a sensitive target for assessing the impact of manufactured nanomaterials on terrestrial compartments (Doolette *et al.*, 2016). Some microbial endpoints have been used to infer on these effects such as soil enzyme activities (Samarajeewa *et al.*, 2017), biological nitrification, microbial respiration rates and organic matter decomposition (Samarajeewa *et al.*, 2017), community level physiological profiling (Samarajeewa *et al.*, 2017) and microbiome structure and diversity (Doolette *et al.*, 2016). Currently, the effects of Ag₂S NPs on SBC are difficult to assess, since the few reported studies used different NP concentrations, exposure times, soil types, and were conducted at different scales (*e.g.*, microcosms, mesocosms). Even so, most studies showed a stronger impact of the ionic silver when compared to AgNPs and Ag₂S NPs (Doolette *et al.*, 2016). Although Ag₂S NPs were the least toxic form, impacts on the structure (Judy *et al.*, 2015) and composition (Doolette *et al.*, 2016) of SBC were confirmed. In terms of function-related parameters, a decrease in the abundance of the genes *nirK*, encoding nitrite reductase, and *amoA*, encoding ammonia oxidizing bacteria, was demonstrated as well as a reduction of the nitrification rate (Doolette *et al.*, 2016). Studies with single

microbial species also reported toxic effects, *e.g.*, on *Escherichia coli* (*E. coli*) (Reinsch *et al.*, 2012) and *Arthrobacter globiformis* (Schultz *et al.*, 2018).

In a terrestrial ecosystem, the presence of different organisms might change the bioavailability of contaminants in soils, in some localized spots, as well as their toxicity to soil microorganisms. In fact, changes in oxygenation levels and soil pH might occur due to the organism's behaviour (burrowing, ingestion and egestion, among other activities) (Abd El-Wakeil, 2015), promoting changes in microbial communities' abundance and structure. Thus, microbial responses to the contaminants can be altered and pose a risk for the terrestrial ecosystem functions.

Our study aims to investigate the effects of Ag₂S NPs on SBC at structural (Denaturing Gradient Gel Electrophoresis - DGGE) and functional (culture of functional bacterial groups, soil enzymatic activity, and Community Level Physiological Profiling - CLPP) levels, using a more realistic exposure scenario than has been reported previously, in order to obtain relevant information at the ecosystem level. Thus, indoor terrestrial mesocosms experiments were performed in which a 1000x predicted environmental concentration estimated for 2050 (10 µg kg⁻¹ - sludge treated soils) (Giese *et al.*, 2018) was tested in the presence of biota, simulating a worst-case scenario. Besides SBC, wheat plants (*Triticum aestivum* L.) and terrestrial organisms, such as isopods (*Porcellio scaber*), mealworms (*Tenebrio molitor*), and earthworms (*Lumbricus rubellus*) were also included in the mesocosms to simulate a real edaphic scenario. The impact of Ag₂S NPs on SBC was evaluated as a function of time (0, 14 and 28 days) and the impact was compared with that of the ionic Ag form (AgNO₃) and an unexposed control.

2. Material and methods

2.1. Silver exposure

The study was conducted with sulfidized silver nanoparticles (Ag₂S NPs) and AgNO₃ (Sigma-Aldrich, 99% purity, CAS 7761-88-8, Germany). AgNO₃ was used as a Ag control for comparing the toxicity of the NPs with the toxicity of the ionic Ag form. The polyvinylpyrrolidone (PVP) coated Ag₂S NPs colloids were synthesized and characterized by Applied Nanoparticles (Barcelona, Spain). These particles were used in this work as a model of sulphidized Ag₂S NPs, in which no degree of sulfidation was demonstrated. These particles were supplied in suspension with a stock concentration of 1320±48 mg L⁻¹. These particles presented an average diameter of 20.4 ± 11.9 nm

[mean (n=3) ± standard deviation] (Figure S1), a ζ-potential of -23.8 ± 4.5 mV in miliQ water (16.12 mg Ag₂S NPs ml⁻¹, conductivity 0.174 mS cm⁻¹, pH 8.72). Additionally, Ag₂S NPs colloids, measured by ICP-MS (fully described in in supplemental materials S1), showed high stability in ultrapure water over-time, and a very low proportion of dissolved Ag during the 48h (<0.1 %, Table S1).

The Lufa 2.2 soil (LUFA-Speyer 2.2, LUFA Speyer, Speyer, Germany) was used as a natural and standard soil, because this soil is suggested as a reference soil for testing NPs toxicity (Geitner *et al.*, 2020). This soil was spiked with Ag₂S NPs or AgNO₃ to a final concentration of 10 mg Ag kg⁻¹ soil. For this, an Ag₂S NPs stock suspension and an AgNO₃ stock solution were prepared, using deionized water, with a final concentration of 1150 mg Ag L⁻¹ and 1148 mg Ag L⁻¹, respectively. These stock solutions were added to the soil, to maximize homogeneity by mixing thoroughly, and the soil was brought to 55 % of the water holding capacity (WHC) using de-ionised water. Spiked and watered soils were mixed manually which has been shown to result in a homogeneous exposure throughout replicates. Once prepared, soils were transferred to each replicate (column) and incubated for two days at 20° C ± 2, to achieve a chemical equilibrium stage of the soil. This is a common procedure for equilibrium in soil for metal exposure in ecotoxicological tests and it has also been tested for nanomaterials (see Neves *et al.*, 2019). Indeed, silver transportation, speciation, and availability might change in soils due to silver exchange between the solid (soil) and liquid phase (pore water). Each mesocosm column was watered daily with artificial rainwater (16 ml per day; NaCl (0.01mM), (NH₄)₄ SO₄. H₂O (0.0053 mM), NaNO₃ (0.0059 mM), and CaCl₂.H₂O (0.0039 mM); pH=5.1) dripping/distributing the water volume over the whole core surface by a syringe avoiding the edges. The soil pH was measured at sampling times (day 0, 14 and 28); five grams of soil were shaken with 25 ml of a 0.01 M CaCl₂ solution, and pH measured after a 2 h settling period. Soil pH did not change with Ag₂S NPs or AgNO₃ exposure in time (Table S2).

2.2. Mesocosm setup

The terrestrial mesocosm was established in indoor conditions [(temperature 20±2 °C and photoperiod 16h (light):8h (dark))] and three soil treatments were used: non-exposed soil, as the negative control (CT), soil spiked with Ag₂S NPs and soil spiked with AgNO₃ (as the ionic control, Ag⁺). For each treatment, 10 replicates were made. Each mesocosm replicate (column = 20 cm long and 11 cm diameter) was filled with 2.6 kg

of Lufa 2.2 soils: 1.3 kg (wet soil) of control or spiked soil (with Ag₂S NPs or AgNO₃) in the upper layer (1-8 cm); and 1.3 kg of non-treated soil in the bottom layer (8-16 cm). Total soil height for the two layers was 16 cm.

The bottom of the core was closed with a PVP nylon mesh (1 mm) and a funnel was placed underneath with a 50 ml tube to collect leachate. To the upper layer of each replicate ten isopods (*Porcellio scaber*), ten mealworms (*Tenebrio molitor*), six earthworms (*Lumbricus rubellus*) and four plants (*Triticum aestivum L.*) were included. A destructive sampling approach was used at each sampling time. At day 0 (after 2 days of spiking equilibrium), 14 and 28 (after organisms were introduced), several replicates were removed from the design (three, three and four, respectively at each sampling time and from each treatment) and the 0-4 cm, 4-6 cm, 10-14 cm, and 14-16 cm mesocosm layers were destructively sampled for all invertebrates, plants, soil chemical analysis and SBC (Figure 1).

During the experiment, organisms' mortality (isopods, mealworms, and earthworms) was recorded and was reported to be similar among treatments (data not shown).

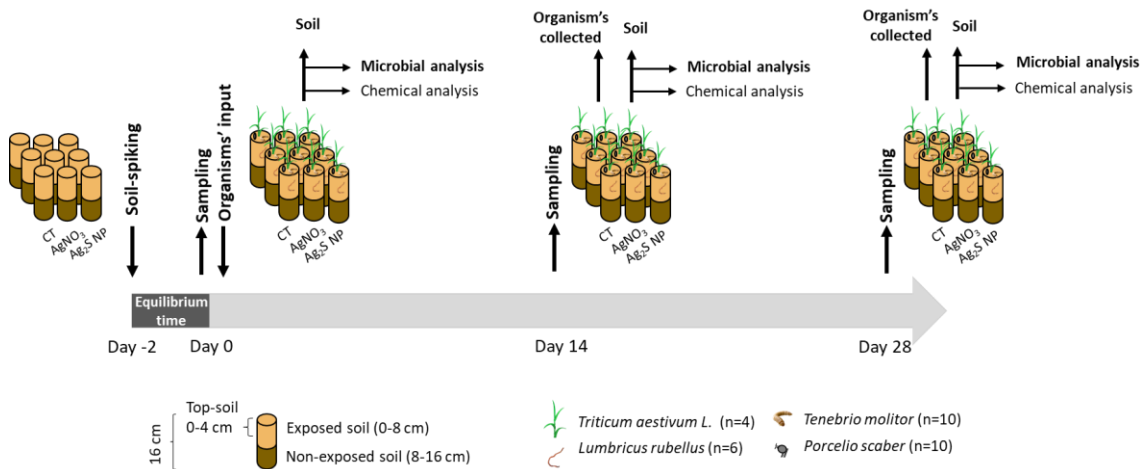


Figure 1. Scheme of the temporal procedures during the 28 days of the mesocosm experiment.

2.3. Soil chemical analysis

The total soil Ag concentration was determined using an *aqua regia* digestion (3:1 HCl:HNO₃) using a microwave (Milestone) (US-EPA, 1996). Digests were diluted to an acid concentration of ca. 3 % and measured using Inductively Coupled Plasma-Mass Spectrometry (ICP-MS) (Perkin Elmer Nexion 350 D). Calibration procedures used known Ag concentrations matrix-matched in 3 % HCl solutions, and only the correlation coefficient greater than 0.999 was considered. ¹⁰³Rh was applied in all

samples as internal standard quality control. The ICP-MS instrument detection limit for Ag was 0.028 µg l⁻¹ (mean blank + 3σ reagent blank, n=22) and the instrument method had a precision of 0.28% (n=22).

To analyse Ag concentration (total and soluble) in soil pore water, the procedure was adapted from Lahive *et al.* (2017). After sampling, the soil was moistened (to 100% of its water holding capacity) to achieve an extractable aqueous sample volume, and incubated overnight at 20°C. The soils (35 g) were then transferred to inserts with 0.02 g glass wool and 0.45 µm PVDF filters, previously soaked with a Cu solution (0.1M CuSO₄) to minimize Ag⁺ adsorption (Cornelis *et al.*, 2010), and the pore water was removed by 1 h centrifugation at 2000 g. Part of this pore water extract was sampled for total metal analysis and the remaining water was centrifuged in a Cu soaked 10 kDa ultra-filtration tube at 4000 g for 30 min to measure the soluble Ag concentration. Ag analyses were completed as described above by ICP-MS.

2.4. Culture-dependent analysis of SBC

To assess Ag₂S NPs effects on the culturable fraction of the SBC, Colony Forming Units (CFUs) were counted in Nutrient Agar (NA) (Merck, Darmstadt, Germany), which is a general purpose medium for heterotrophic bacteria, and in the National Botanical Research Institute's phosphate (NBRIP) medium (Nautiyal, 1999), which was designed to count bacteria able to solubilize phosphate (P-SB). Media were sterilized at 121° C for 20 min and supplemented with 0.2 mg L⁻¹ cycloheximide (95% purity, Acros organics, New Jersey) to prevent the growth of fungi.

From samples collected at 0 and 28 days, three grams of soil were suspended in 25 mL of phosphate saline buffer (PBS, pH=7.4), in triplicate. Soil samples were shaken at 304 g with twenty sterile glass beads (4 mm) for 10 min at 20 °C, followed by fold serial dilutions (10⁻² dilution) in PBS. From each suspension, 100 µl was plated on NA or NBRIP (three replicates, with four technical replicates per medium), and the plates were incubated at 20°C, for three days. Colony counts were reported as % of the variation of Log₁₀ [colony forming units (CFU) per gram of soil].

To assess the usefulness of the medium in the context of this study, the identity of a randomly selected colony from NBRIP was confirmed by 16S rRNA gene sequencing (data not shown).

2.5. Enzymatic activity

Dehydrogenase (DHA), β -glucosidase (β G), acid phosphatase (AP), and arylsulfatase (AS) activities were determined according to the methods described by Dick *et al.* (1996), with some modifications. The DHA activity was evaluated by suspending soil (2.5 g) in a 3% triphenyl tetrazolium chloride (TTC; Sigma-Aldrich, 98%) solution (1 mL), followed by 24 h incubation at 37°C, in darkness (Dick *et al.*, 1996). The triphenyl formazan (TPF) produced was extracted with methanol. Then, soil samples were centrifuged (3000 rpm for 15 min) and the supernatant was measured photometrically at a wavelength of 546 nm. The results were expressed as μg of TPF g^{-1} 24 h^{-1} . The β G, AS and AP activities were measured using specific substrate solutions: 4-nitrophenyl β -D-glucopyranoside substrate (0.05 M) (Acros organics, 99%); 4-nitrophenyl sulfate (0.05 M) (Acros organics, 99%); and *p*-nitrophenyl phosphate (0.05 M) (Sigma-Aldrich), respectively (Dick *et al.*, 1996; Tabatabai 1994). The soil samples (0.5 g) were incubated at 37°C for 1 h with 0.5 mL of substrate solution and 2 mL of the modified universal buffer (MUB) with pH 6.5 (β G) and pH 6.0 (AP); or acetate buffer (0.5 M; pH=5.8) for AS activity (Tabatabai, 1994). The reaction was stopped with 0.5 M CaCl₂ (0.5 mL) and 0.5 M NaOH (2 mL) and the soil samples were centrifuged at 4562 g for 15 minutes. The supernatant was subsequently measured spectrophotometrically at wavelengths of 400 nm (β G) and 410 nm (AP, AS).

All enzymatic activities were measured in 96 wells microplates, in three replicates (with four technical replicates) using a microplate spectrophotometer (Thermo Scientific Multiskan Spectrum, USA).

2.6. Community level physiological profiling (CLPP)

Community-level physiological profiling (CLPP) was performed using 96-well Biolog[®] Ecoplates that contained 31 different carbon sources (Biolog, Hayward, CA, USA). The rate of utilization of these carbon sources was verified by the reduction of tetrazolium violet redox dye, which changed from colourless to purple as a function of microbial activity (Garland 1997). Following the method by Samarajeewa *et al.*, (2017), three grams of soil were collected and added to 27 mL of sterile water with 20 sterile glass beads. This soil suspension was shaken at 304 g for 10 min, at 20°C and then left for 45 min. The suspension was diluted 100-fold to attain a cellular density of approximately 10^7 cell mL^{-1} . One hundred microliters of the suspension were then inoculated into each well, and plates incubated at 20 ° C. The colour development was measured by reading

optical density at a wavelength of 590 nm at 24 h intervals over 192 h of plates incubation, using a microplate spectrophotometer (Biolog, MicroStation™, USA).

Measurements were calibrated against blank wells (water) (Garland 1997), and the optical density values below 0.06 were set as 0. Optical density curves of CLPP were constructed for each technical replicate (n=3). The total area under the curve (AUC) was calculated using the trapezoidal integration function, included in the `trapz` {pracma} package (version 2.2.2) in R program (version 3.5.1).

Additionally, the 31 carbon substrates from Biolog®Ecoplate were divided into six groups following the method of Sala *et al.* (2006): (1) carbohydrates, (2) carboxylic acids, (3) amines and amides, (4) amino acids, (5) polymers, and (6) phenolic acids. Thus, the substrate well averaged colour development (SAWCD) index was calculated based on optical density values obtained after 192 h of Biolog®Ecoplate incubation for each soil treatment.

2.7. PCR-DGGE

Soil (0.25 g) was collected from each core, and the total DNA was extracted using the UltraClean®Power Soil DNA Isolation Kit (MoBio Laboratories, Inc., Carlsbad, CA) following the instructions of the manufacturer.

The V3 region of the 16S rRNA gene was amplified using a nested PCR strategy. First, the 16S rRNA gene was amplified using the universal primers 27F (5'-AGAGTTTGATCCTGGCTCAG-3') and 1492R (5'-GGTTACCTTGTTACGACTT-3'). The PCR mixture (25 µL) contained: nuclease-free water (16.25 µL), NZYTaQ 2x Green Master Mix (6.25 µL; 2.5 mM MgCl₂; 200 mM dNTPs; 0.2 U/µL DNA polymerase) (NZYTech, Portugal), each primer (0.75 µL of a 10 mM solution), and a DNA sample (1 µL). The amplification conditions consisted of an initial denaturation step (94°C for 3 min), followed by 30 cycles comprising the following steps: denaturation (94°C for 1 min), annealing (52°C for 1 min) and extension (72°C for 2 min), and a final extension step (72°C for 10 min). The second PCR was conducted as described above, using 1 µL of the first PCR product as template, and the universal primers [338f-GC (5'-GACTCCTACGGGAGGCAGCAG-3') and 518r (5'-ATTACCGCGGCTGCTGG-3')], (Muyzer *et al.* 1993), and the amplification conditions were: denaturation (94°C for 5 min), annealing (52°C for 30 sec) and extension (72°C for 30 sec), and a final extension step (72°C for 30 min). Positive and negative controls were included, consisting of identical reactions but using purified

bacterial DNA from *Escherichia coli* ATCC 25922 and nuclease-free water as templates, respectively. Amplification was confirmed by electrophoresis (1.5% agarose).

PCR products were loaded into 8% (w/v) polyacrylamide (37.5:1, acrylamide:bisacrylamide) gels with denaturing gradient ranging from 35% to 62.5% [100% denaturant corresponded to 7 M urea and 40% (v/v) formamide]. A DGGE marker composed of 8 bands (Henriques *et al.*, 2004) was included in the extremities of each gel. The electrophoresis was performed on a D-Code™ System (Bio-Rad, Hercules, CA, USA) with 1X TAE buffer (Sigma-Aldrich, Germany) at 60°C in two steps, (1) for 15 min at 20 V and (2) for 16 h at 70 V. Gels were stained in a solution of ethidium bromide (0.5 µg mL⁻¹) for 5 minutes and rinsed in distilled water (20 min). Images were captured by the Molecular Imager® Gel Doc™ XR+ System (BioRad Laboratories, Hercules, California, USA).

DGGE patterns were analyzed using Bionumerics Software (Applied Maths, Belgium).

2.8. Statistical analysis

All microbial endpoints [CFU counts, enzymatic activity, and CLPP] were analyzed using Sigma plot V.12.5 (SysStat software Inc., CA, USA). Assumptions of homogeneity of variance and test for normality of distributions were verified using Levene's test and Shapiro-Wilk's test, respectively. When the normality test failed, a Kruskal-Wallis test followed by the appropriate post-hoc (Holm-Sidak) test was used. A level of $p=0.05$ was considered to assume statistical significance. A two-way ANOVA analysis was conducted to assess the effect of the two factors (soil treatments *vs.* time of exposure). Additionally, the Tukey's HSD (honestly significant difference) and Dunnett's method test was applied for the post-hoc analysis, to obtain multiple comparisons between treatments or toward the respective control, respectively.

DGGE band matrix was analysed in PRIMER v6 software (Primer-E Ltd., Plymouth, UK). Band position and intensity was used to calculate the richness, the Shannon-Wiener diversity and Pielou's indexes. A one-way ANOVA followed by the Dunnett's method was used to discriminate differences in diversity indices. Further, two-dimensional Principal Coordinate Analysis (PCoA) was performed based on the Bray-Curtis similarity after the matrix was square root transformed. Additionally, a PCoA analysis was performed as described above for DGGE patterns of samples obtained after 28 days of exposure. Functional variables that presented a good correlation ($R \geq 0.6$

based on Pearson correlation) with SBC structure were represented as vectors in the PCoA plot.

Differences in SBC structure between treatments were evaluated through PERMANOVA based on 999 permutations.

3. Results

The effects of Ag₂S NPs on SBC were assessed in different layers (0-4 cm, 4-6 cm, 10-14 cm, and 14-16 cm) of the mesocosm core. As expected, effects were clearer in the top-soil layer (0-4 cm), for which significant differences were observed between SBC subjected to different treatments [non-exposed soil - CT and soil exposed to Ag₂S NPs or AgNO₃] (Figure S2 A-D). Moreover, a significant decrease in Shannon-Wiener and richness indexes was observed for soils exposed to Ag₂S NPs, in comparison to the CT, exclusively for top-soil samples (Table S1). Based on these results and given that all the main biota groups (that were part of the mesocosms) were also in this layer, subsequent analyses were focused on the top-soil layer (0-4 cm).

Soil analysis of the top 0-4 cm of the soil corer confirmed the accurate soil spiking procedures (Figure 2 A), with the control soil presenting a basal value of 0.051 mg Ag kg⁻¹, while the AgNO₃ and Ag₂S NPs spiked soils presenting 9.97 and 12.20 mg Ag kg⁻¹, respectively. At day 28, the spiked soils still presented similar concentrations, with average values of 10.7 ± 0.5 (AgNO₃ addition) and 13 ± 1 mg Ag kg⁻¹ (Ag₂S addition). The control soil maintained a similar basal concentration (0.045 mg Ag kg⁻¹).

Porewater analysis from top-soil (Figure 2 B) showed similar average values for non-exposed soil [0.03 ± 0.008 µg Ag L⁻¹] and soil exposed to Ag₂S NPs [0.10 ± 0.08 µg Ag L⁻¹], at day 0. Soil spiked with AgNO₃ showed an initial Ag dissolution and presented an average value of 2.47 ± 1.64 µg Ag L⁻¹.

After 28 days of exposure, a similar Ag content in porewater samples was verified for CT and Ag₂S NPs, although a slight increase in Ag dissolution was detected when compared with day 0, presenting an average concentration of 0.33 ± 0.08 µg Ag L⁻¹ and 0.67 ± 0.02 µg Ag L⁻¹, respectively. Soils spiked with AgNO₃ revealed a significant (Tukey test: F=35.474; p<0.001) free Ag⁺ concentration, when compared with other treatments, presenting an average value of 1.74±0.22 µg Ag L⁻¹.

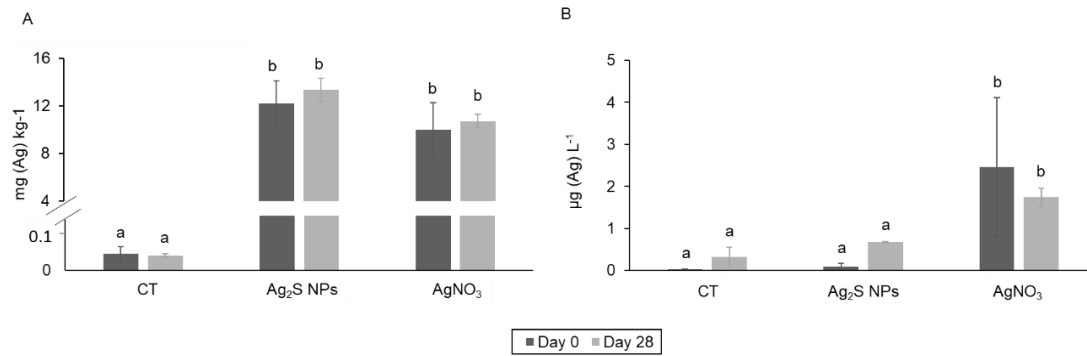


Figure 2. Silver content in soils (A) and silver dissolution into soil porewater (B), after 0 (2 days after soil spiking) and 28 days of exposure. The data was expressed as mg (Ag) kg⁻¹ of soil (A) and as µg (Ag) L⁻¹ of porewater [average (n=3) ± standard deviation]. The treatments included: the non-exposed soil (CT), soil exposed to Ag₂S NPs and soil exposed to AgNO₃. Different letters (a,b) indicate statistical significance (p<0.05) between soil treatments and the time of exposure, using the two-way ANOVA (Tukey post-hoc test, p<0.05).

3.1. Effects on culturable bacteria

The abundance of heterotrophic bacteria and of bacteria able to solubilize phosphate was determined using a culture-based method (Figure 3 A and B).

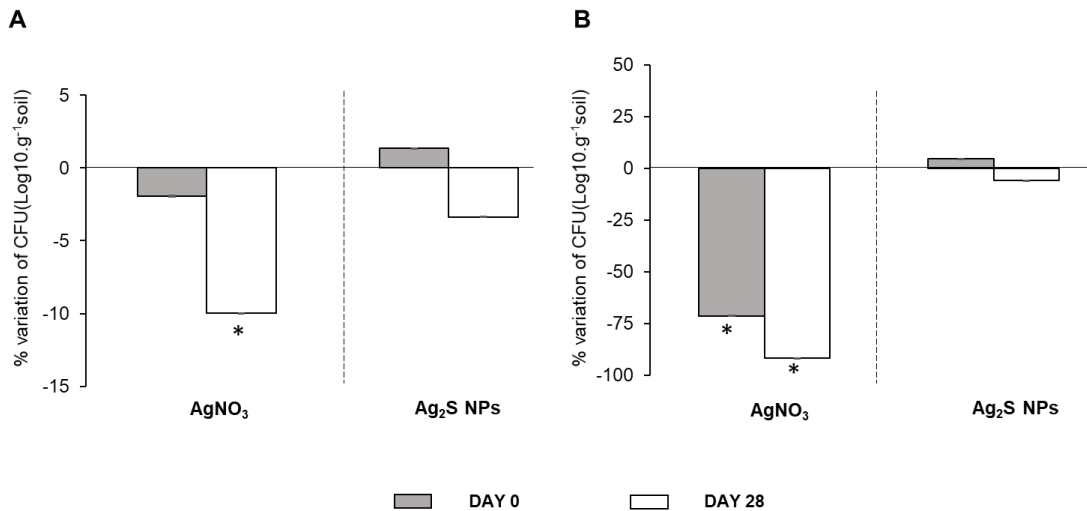


Figure 3. Soil colony forming units (CFUs) measured in Lufa 2.2 soil, sampled at day 0 and 28 from the mesocosm experiment, previously spiked with AgNO₃ and Ag₂S NPs. CFUs are presented as % of variation on CFUs (Log₁₀ g⁻¹ soil) (± standard deviation) from the respective control (non-exposed soil), n=3. Heterotrophic bacteria in nutrient agar (NA) medium (A); and P-solubilizing bacteria in National Botanical Research Institute Phosphate (NBRIP) medium (B). The grey bars represent the soil samples collected at the beginning of the mesocosm soil experiment (day 0), and the white bars represent samples after 28 days. Asterisks (*) indicate significant differences using two-way ANOVA (Dunnnett's post-hoc test), p<0.05) relative to the respective control.

The Ag₂S NPs treatment did not significantly affect the CFUs counts, in either culture medium, although, a slight reduction was observed after 28 days of exposure [less 3.4% and 5.9% of Log₁₀(CFU.g⁻¹soil) for NA and NBRIP culture media, respectively]. In contrast, the AgNO₃ treatment resulted in a significant (Dunnett's Method: df=0.1; q=6.363; p<0.001) reduction of 10% of the CFUs counted in NA medium after 28 days (Figure 3 A). For P-SB an even stronger impact of AgNO₃ was observed (Figure 3 B), corresponding to a significant reduction of 71.3% (Dunnett's Method: df=0.66; q=10.7; p<0.001) and 91.8% of Log₁₀ (CFU g⁻¹ soil) (Dunnett's Method: df=0.918; q=14.691; p<0.001), at sampling day 0 and 28 after the beginning of the mesocosm trial, respectively.

3.2. Treatment effects on enzymatic activity

The effects of Ag₂S NPs treatment on soil enzymatic activities (DHA, βG, AP, and AS) were assessed over time and are represented in Figure 4 (A-D).

The DHA activity (Figure 4 A) showed the greatest sensitivity to AgNO₃ treatment resulting in significant activity decrease in the three sampling times. For this enzyme, an activity reduction of 72.8% was observed after 28 days of exposure (Tukey HSD: CT vs. AgNO₃: p<0.001). No significant effect from Ag₂S NPs exposure was observed (Tukey HSD: CT vs. Ag₂S NPs: p=0.852). Accordingly, significant differences between AgNO₃ and Ag₂S NPs treatments were observed (Tukey HSD: AgNO₃ vs. Ag₂S NPs: p<0.001).

A time-dependent effect was verified for βG activity (Figure 4 B). Thus, at an earlier time of exposure, the AgNO₃ treatment resulted in a significant (Tukey HSD: CT vs. AgNO₃: p=0.020) activity reduction (AgNO₃ 0 day vs. CT 0 day: 75.3%). Despite an apparent recovery after 14 days for the AgNO₃ exposure, a significant reduction on βG activity was again observed after 28 days, but now for both treatments [Tukey HSD: (CT > AgNO₃: p<0.001); (CT > Ag₂S NPs: p=0.001)].

Moreover, the level of inhibition on βG activity observed for soils exposed to Ag₂S NPs was lower than for soils exposed to AgNO₃ (Tukey HSD: AgNO₃ < Ag₂S NPs: p=0.019).

After day 28, AP activity (Figure 4 C) significantly increased in soils exposed to Ag₂S NPs (Tukey HSD: CT < Ag₂S NPs: p=0.007), while no significant effect was observed for soils exposed to AgNO₃.

The activity of AS significantly decreased after 14 days in soils spiked with AgNO₃ (Tukey HSD: CT > AgNO₃: p=0.047), recovering to levels similar to the control at day 28 (Figure 4 D). No significant effects were observed on the AS activity from Ag₂S NPs exposure.

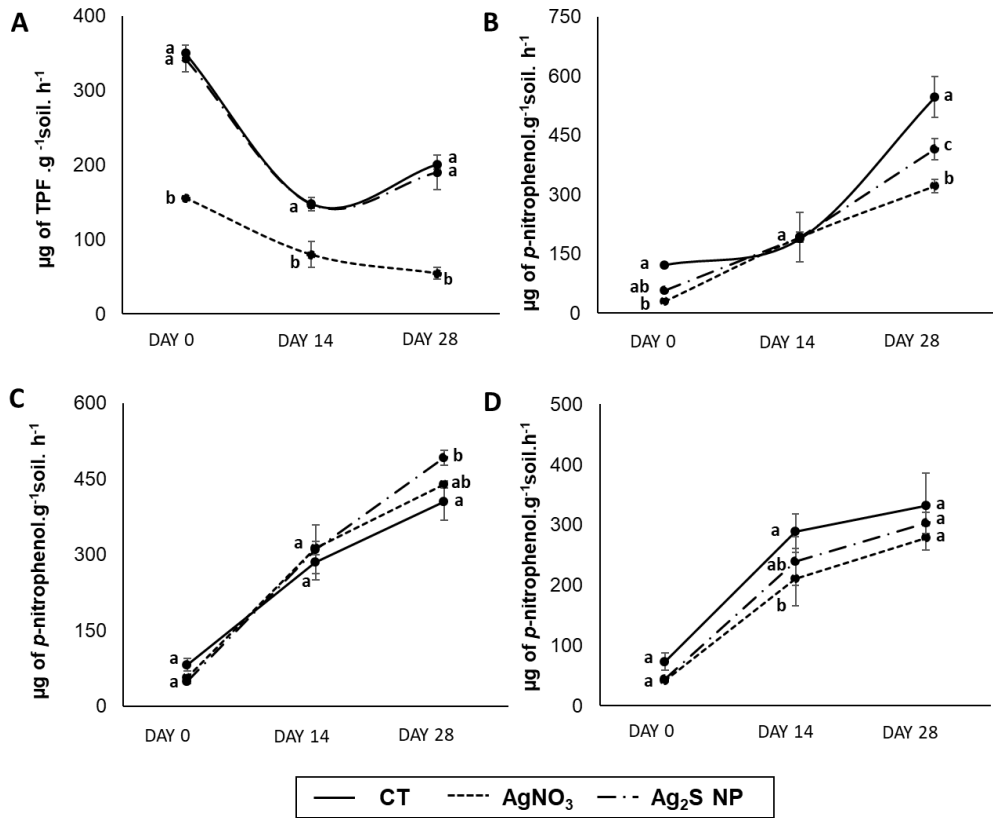


Figure 4. Soil enzymatic activity measured in Lufa 2.2 soil, sampled at days 0, 14 and 28 from the mesocosm experiment, previously spiked with AgNO₃ and Ag₂S NPs. Also, the non-exposed soil was included in this experiment (CT). The data represent the mean (n=3) of enzymatic activity (\pm standard deviation) of dehydrogenase (A), β -glucosidase (B), acid phosphatase (C) and arylsulfatase (D) activities. Different letters (a, b) indicate a significant difference using two-way ANOVA (Tukey post-hoc test, p<0.05), among treatments.

3.3. Effects on carbon source consumption

The Ag₂S NPs effects on carbon substrate utilization were assessed using the Biolog[®] Ecoplate and are shown in Figure 5 (A-C). The analysis of AUC (Figure 5 A) revealed an over-time significant increase on substrate consumption for non-exposed soils (AUC: CT 0 days < CT 14 days; Tukey HSD: F=554.985, p<0.001) until 14 days, and a slight decrease between 14 and 28 days of incubation (AUC: CT 14 days > CT 28 days; Tukey HSD: F=554.985, p=0.915).

Time-dependent effects on AUC calculated for soils exposed to silver were observed. A significant inhibitory effect of Ag₂S NPs on L-arginine consumption (Figure 5 B) was observed after 28 days ($p < 0.05$, Table S2). On the other hand, after 14 days the AgNO₃ treatment caused a significant reduction ($p < 0.05$, Table S2) of the consumption of the following substrates: tween 80, L-erythritol, D-glucosaminic acid and L-serine. At day 28 AgNO₃ treatment resulted in a significant decrease of the consumption of pyruvic acid methyl ester, β -methyl-D-glucoside, and L-arginine ($p < 0.05$, Table S4).

In terms of SAWCD analysis, a significant effect was observed between sampling times but not between treatments *versus* control. Considering exposure time, SAWCD results were in accordance with AUC, with the pattern of substrate utilization being 0 days > 14 days > 28 days of exposure, for phenolic acid and amides/amines classes. For the other classes (Figure 5 C) a significant difference over time was not observed.

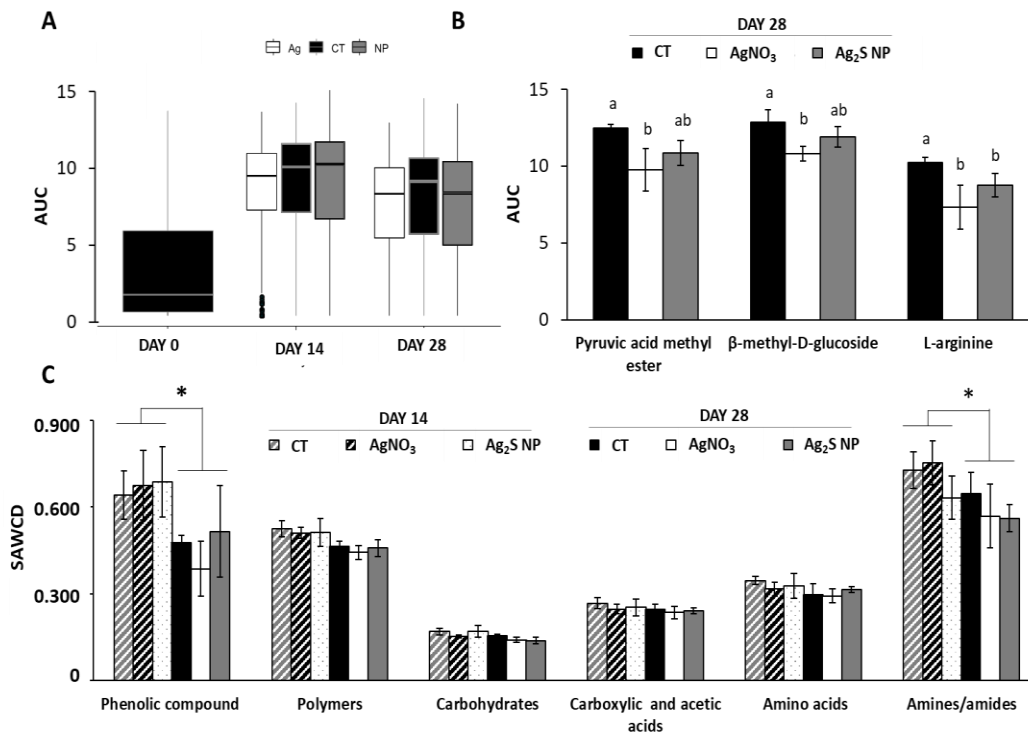


Figure 5. Community level and physiological profile (CLPP) measured in Lufa 2.2 soil, sampled at days 0, 14 and 28 from the mesocosm experiment, previously spiked with AgNO₃ and Ag₂S NPs. For further comparison the non-exposed soil (CT) was included. The area under the curve (AUC) was calculated based on a trapezoidal integration function (A) over time; (B) after day 28, the Pyruvic acid methyl ester, β -methyl-D-glucoside, and L-arginine consumption; and (C) substrate average well colour development (SAWCD) after 14 and 28 days of exposure. The data represent the mean ($n=3$) of AUC (\pm standard deviation). Letters (^{a, b}) represent significant differences using two-way ANOVA (Tukey HSD, $p < 0.05$) between treatments.

3.4. Effects on SBC structure and diversity

The impact of Ag₂S NPs and AgNO₃ on the SBC structure was assessed over time and results are presented in Figure 6 (A-B). The cluster analysis (Figure 6 A) showed a temporal effect among soil treatments, in which the Ag₂S NPs treatment was completely separated from the other treatments only at day 28. The soil treated with AgNO₃ conversely revealed a strong impact on SBC from the experiment start onwards.

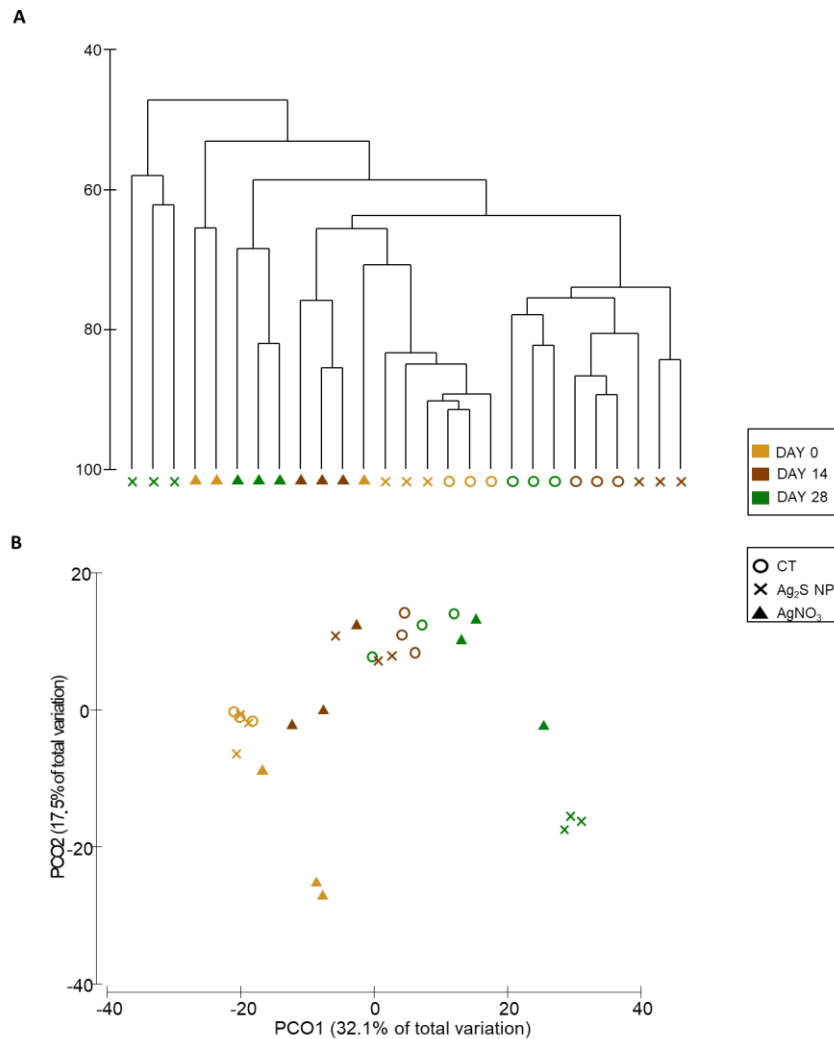


Figure 6. Denaturing gradient gel electrophoresis (DGGE) analysis of the V3 region of the 16S rRNA gene amplified from SBC from non-exposed soil (CT), soil exposed to Ag₂S NPs and AgNO₃, after 0, 14 and 28 days of exposure. Cluster analysis (A); and Principal component analysis (PCoA) (B), were constructed based on Bray-Curtis similarity after square root transformation of DGGE relative abundance data (n=3).

The first two axis of the principal coordinate analysis (PCoA) explained 49.6% of the total variation in the data: PCO1 axis (32.1%) and PCO2 axis (17.5%) (Figure 6 B). Along the PCO1 axis, samples tend to cluster as a function of exposure time while

along the PCO2 axis separation seems to be influenced by treatment. At 28 days of exposure, a clear separation between soil exposed to Ag₂S NPs from the other treatments was observed.

The Permanova analysis confirmed a significant spatial separation between soil treatments (CT, AgNO₃ and Ag₂S NPs) according to the time of exposure (day 0, 14, 28) (PERMANOVA: F=4.76; P=0.001), except for non-exposed soils that did not show a significant difference, in spatial separation, between day 14 and 28 (PERMANOVA: CT14 vs. CT28: t= 1.93; P=0.052).

In terms of diversity indices, a significant decrease in richness and Shannon-Wiener diversity was induced by exposure to Ag₂S NPs after 28 days (p<0.05; Table 1). On the other hand, significant effects of AgNO₃ were only observed in richness after 48 h of soil spiking (Table 1), which corresponds to the day 0 of mesocosm experiment (Figure 1), suggesting binding of the Ag⁺ to soil and thus lowered bioavailability.

Table 1. Diversity indexes from SBC structure analysis were analysed over time and considering the following soil treatments: CT (non-exposed soil), and spiked soil with AgNO₃ and Ag₂S NPs. The diversity indexes included: the richness (S), Pielou (J') and Shannon-Wiener index (H'). The data represent the mean of each diversity index (n=3± standard deviation). Different letters (^a, ^b) indicate statistical difference using two-way ANOVA (Tukey post-hoc test, p<0.05) among treatments and within exposure time.

Diversity indexes						
Soil Treatment	Sampling time (day)	S	J'	H'		
CT	0	44 ± 1 ^a	0.922 ± 0.003 ^a	3.483 ± 0.022 ^a		
AgNO ₃	0	41 ± 2 ^a	0.897 ± 0.006 ^a	3.321 ± 0.051 ^b		
Ag ₂ S NPs	0	44 ± 1 ^a	0.919 ± 0.004 ^a	3.469 ± 0.030 ^a		
CT	14	48 ± 1 ^a	0.911 ± 0.006 ^a	3.527 ± 0.038 ^a		
AgNO ₃	14	45 ± 1 ^{ab}	0.903 ± 0.005 ^a	3.431 ± 0.020 ^a		
Ag ₂ S NPs	14	44 ± 2 ^b	0.898 ± 0.013 ^a	3.403 ± 0.076 ^a		
CT	28	45 ± 1 ^a	0.888 ± 0.028 ^a	3.380 ± 0.091 ^a		
AgNO ₃	28	43 ± 1 ^a	0.911 ± 0.014 ^a	3.428 ± 0.070 ^a		
Ag ₂ S NPs	28	37 ± 2 ^b	0.885 ± 0.018 ^a	3.193 ± 0.042 ^b		

3.5. Relationship between structure and functions of SBC

Due to late-term effects of Ag₂S NPs on SBC, at structural level, the PCoA based on relative band intensity from DGGE profiles (Figure 6) was performed only considering the 28 days of exposure (Figure 7). Moreover, different functional parameters were imposed as a vector, to obtain the correlation between both levels (structural and functional). Thus, the association between SBC structure and functional variables was assessed for samples collected at 28 days of exposure and results are shown in Figure 7. As explained above, a significant difference among treatments was revealed. The two main PCoA axes (Figure 7) explained 65.1% of the total variation [PCO1 axis (42.5%) and PCO2 axis (22.6%)]. The PCO1 axis separated soil samples according to treatment. The highest negative correlation with axis 1 was determined for AP activity (Pearson correlation: $R=-0.79$, $p=0.023$), consistent with a significantly increased AP activity in soils exposed to Ag₂S NPs in comparison to other treatments (Figure 4 C). On the other hand, the axis 2 separated the soils exposed to AgNO₃ from the other treatments, and the highest negative correlations with this axis were observed for β G, heterotrophic bacteria and P-SB (Pearson correlation: $R=-0.67$, $p=0.144$; $R=-0.74$, $p=0.796$; $R=-0.87$, $p=0.864$, respectively). The other functional variable assessed correlated with both axes, namely L-arginine (PCO1: $R=0.35$ and PCO2: $R=-0.50$; $p=0.949$).

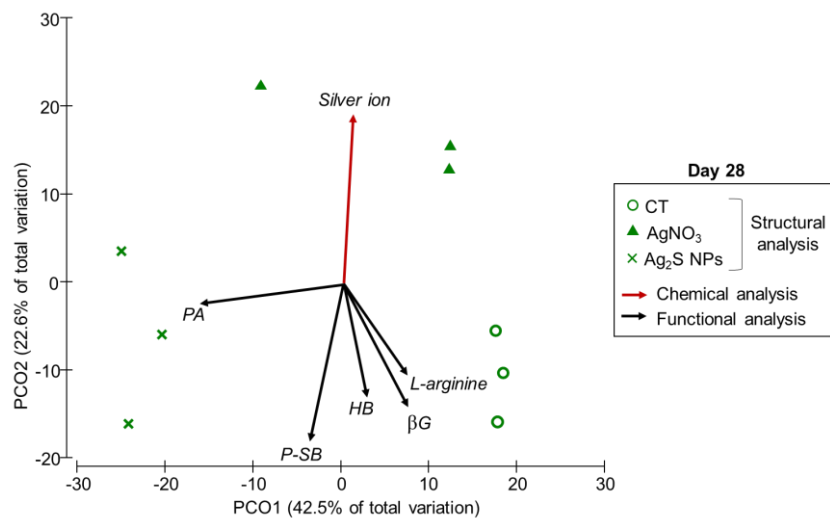


Figure 7. Principal coordinates analysis (PCoA) ordinations based on Bray-Curtis similarity showing the spatial distribution of SBC structures among the different soil treatments: non-exposed soil (CT) and exposed soil to Ag₂S NPs or AgNO₃ (n=3), after 28 days of exposure. The vectors represent a functional variable (Black: enzymatic activity and CLPP) or a chemical variable (Red: silver ion presence (Figure 2) in soil pore-water) that presented a correlation ≥ 0.6 with SBC structure: AP - Acid Phosphatase; β G - β -Glucosidase; HB - Heterotrophic bacteria; P-SB - Phosphatase-Solubilizing Bacteria.

4. Discussion

Currently, there is a lack of research data indicating the potential effects of Ag₂S NPs on SBC, under realistic scenarios. There is also insufficient knowledge on the effects of Ag₂S NPs compared to those of Ag ionic forms. To address these knowledge gaps, we conducted an indoor mesocosm experiment to evaluate the impact of Ag₂S NPs on SBC during 28 days, at a nominal exposure concentration of 10 mg Ag kg⁻¹ soil. Structure and function of AgNO₃- and Ag₂S NPs-exposed SBC were compared to those of communities in the control soil and related to the content/dissolution of Ag⁺ in the soil pore water over time.

4.1. Effects of silver on SBC function

Colony bacterial counts are considered a suitable indicator for measuring Ag₂S NPs effects on SBC, as they usually present a fast response to metal contamination (Vasileiadis *et al.*, 2015). Our study demonstrated that Ag₂S NPs did not significantly affect counts of heterotrophic bacteria and P-SB, albeit after 28 days of exposure a slight reduction was observed. Prior studies demonstrated that Ag₂S NPs are sparingly soluble in soils over a long period (> 1 year) (Wang *et al.*, 2016), which may justify our results. However, the toxic effect of Ag₂S NPs on specific bacterial groups was detected in previous studies and related to their sulfidation degree (Schultz *et al.*, 2018). For instance, a lower degree of sulfidation of Ag₂S NPs was reported to result in faster dissolution and release of Ag⁺, thus enhancing the toxic effects of Ag₂S NPs on SBC (Wang *et al.*, 2017; Schlich *et al.*, 2018). A similar trend was also documented for *Escherichia coli* (Reinsch *et al.*, 2012); *Arthrobacter globiformis* and *Pseudomonas putida* (Schultz *et al.*, 2018). The study by Schultz *et al.*, (2018) confirmed that the AgNO₃ treatment caused a higher toxic effect on bacterial counts (*Arthrobacter globiformis* and *Pseudomonas putida*) when compared to exposures to several NPs: Ag₂S (36 nm), Ag-PVP (49 nm) or Ag citrate (58 nm). These distinct toxic effects on SBC might be related with different free Ag⁺ concentrations, in which a higher free Ag⁺ concentrations resulting from AgNO₃ was documented that that arising from AgNPs dissolution in soil. In accordance, our study demonstrated this distinct toxic effect, considering the silver form present, on bacterial counts. The effect of AgNO₃ on P-SB

may indicate an impairment of phosphorous solubilization in soils, with consequences for crop production and soil fertility (Richardson & Simpson, 2011).

To assess the impact of nanomaterials on soil functions it is essential to evaluate the enzymatic activities related to nutrient cycling (Samarajeewa *et al.*, 2017). DHA is one of the most sensitive enzymes to metal contamination (Samarajeewa *et al.*, 2017). In our study, only the AgNO₃ treatment caused a strong inhibition of DHA activity over time, a result once again probably related with distinct free Ag⁺ concentrations. The investigation conducted by Shin *et al.* (2012), found a high sensitivity of DHA in soils exposed to citrate-coated AgNPs at different concentrations (0, 1, 10, 100, and 1000 µg g⁻¹). Also, McGee *et al.*, (2017), using a lower Ag concentration (1 mg kg⁻¹soil) and a non-sulfidized form of silver [AgNPs (20-30 nm and 0.5-1 µm)], observed a similar sensitivity of DHA. Although these studies demonstrated a significant impact of AgNPs on DHA activity, our study used the AgNPs in sulfidized form (Ag₂S NPs), which presents distinct physical and chemical properties. Consequently, the Ag⁺ dissolution is also different; for instance, Ag₂S NPs were shown to be more stable than AgNPs (Wang *et al.*, 2016). Additionally, Ag₂S NPs particles can be aggregated in soils, resulting in increased particle sizes (micro-particles) (Liu *et al.*, 2019), with less surface area for oxidative dissolution and consequently decreased toxicity (Liu *et al.*, 2019). The study by Liu *et al.*, (2019) reported that hetero-aggregation, tested by combining the exposure of TiO₂ and AgNPs in soils, exhibit a higher toxic effect than the homo-aggregation of each of the single TiO₂ or Ag NPs. Although this was discussed based on the size of aggregates, the joint toxicity of a binary combination of metals cannot be disregarded.

Besides, DHA is only expressed in intact cells and does not accumulate extracellularly in the soils (Dick, 1996), so its activity has been related with microbial biomass, respiratory activity, microbial oxidative activity, and microbial viability (Dick, 1996; McGee *et al.*, 2017; Samarajeewa *et al.*, 2017). Accordingly, in our study the lower abundance of heterotrophic bacteria (NA medium) in AgNO₃-exposed soils may explain at least in part the decreased DHA activity.

βG activity has been also considered as an indicator of soil quality (Turner *et al.*, 2002), related to carbon cycling in soils. Thus, the hydrolysis products resulting from βG activity are an essential energy source for microorganisms in soils (Dick, 1996). In accordance, studies from Kim *et al.*, (2018) showed that exposure to silver-graphene oxide (0.1–1 mg g⁻¹ soil) decreased the βG activity up to 80% in soils. Similarly, Samarajeewa *et al.*, (2017) showed a significant decrease of this enzyme's activity upon

exposure to 49 mg of AgNPs per kg of soil. In our study, a decrease on β G activity was observed for both treatments after 28 days of exposure, with approximately 56% and 33% decrease for the AgNO₃ and Ag₂S NPs treatments, respectively. Ag⁺ dissolution did not explain the effect of Ag₂S NPs, and some specific-particle effects might occur, as suggested Starnes *et al.*, (2015). In fact, the ratio between the silver total content in soil (Figure 2A) and the dissolved/dissociated Ag⁺ in the pore water (Figure 2B) showed the highest value for Ag₂S NPs (19.8) than for AgNO₃ (6.15), suggesting a specific-particle effect for the Ag₂S NPs treatment. Although previous studies reported a decrease of AP activity in soil exposed to AgNPs, regardless of the concentrations tested (Colman *et al.* 2013; Samarajeewa *et al.*, 2017), our study showed a significant increase in this enzymatic activity, after 28 days of exposure to 10 mg kg⁻¹ of Ag₂S NPs. Although our study did not evaluate the root biomass, we hypothesize that root growth and proliferation in soils may contribute to the increased AP activity in our experiment. On the other hand, the presence of different invertebrates possibly contributes to the complexation of the Ag₂S NPs in soils (*e.g.*, ligation with organic matter or with clay), and therefore, protected/stimulate the activity of extracellular enzymes (Shin *et al.*, 2012).

Although study from Vasileiadis *et al.*, (2018) demonstrated that the AS enzyme is more sensitive to Ag⁺ exposure (from AgNO₃ or acetate, respectively), our results corroborate this AS sensitivity to the AgNO₃ treatment but only after 14 days. After this period this enzymatic activity recovered, becoming similar to that in the non-exposed soil. This time-dependent effect might have been directly related to a rapid flux of free Ag⁺ from AgNO₃ in the first days (short period) or by directly affecting the sulfatase producer microorganisms (Vasileiadis *et al.*, 2018) followed by a gradually stronger adsorption of Ag⁺ to organic S groups or even a reduction to metallic Ag⁰ making Ag⁺ less available (Settimio *et al.*, 2014).

Some fluctuation in soil enzymatic activity was observed, even in non-exposed soil (CT), over time. The SBC is dynamic, and the soil conditions (*e.g.*, daily watering) and the invertebrates and plants (root growth) presence in our experiment might influence this fluctuation. Soil water content influences the SBC composition, resulting in an impact on oxygen concentrations and nutrient availability. The watering might reduce soil oxygen levels and promote anaerobic microorganisms (facultative and obligate) growth, whilst decreasing the total microbial activity (Sylvia *et al.*, 1999). On the contrary, the presence of invertebrates can promote soil aeration (Abd El-Wakeil, 2015),

which indirectly influences the proliferation of different bacteria/fungi, ultimately resulting in a structural and composition change of the SBC. Moreover, these organisms have a crucial role in the decomposition of the organic matter. Soil and organic matter are also ingested, digested and excreted by invertebrates, producing a substrate that is more accessible to SBC but that may also contain Ag (as free Ag⁺, and/or Ag₂S depending on the treatment plus some or all of the range of speciation forms noted above), inducing different microbial mobilizations. Indirectly, this can induce bacterial community adjustments, in terms of abundance and composition, according to the bacteria nutrient/metabolic requirements. Besides, plants and associated microorganisms alter the physicochemical properties of the root-soil interface, such as pH and redox conditions (Liu *et al.*, 2019).

The physiological profiles were used to assess the impact of both Ag forms on bacteria consortia. The significant reduction in L-arginine consumption (amino acid class) for both silver forms, indicates a potential effect on carbon and nitrogen cycles that are closely related to plant fertility success. L-arginine plays a key role in nitrogen distribution and recycling in plants (Slocum, 2005), and consequently, might be related to the plant homeostasis. The study by Yang *et al.*, (2018) demonstrated that AgNPs decreased the arginine and histidine content in wheat (*Triticum aestivum L.*), during 4 months in 2000 mg kg⁻¹ amended soil. On the other hand, the decrease of L-arginine consumption might be partially explained by the decreased bacterial counts observed in our results, at least for AgNO₃, because heterotrophic bacteria are able to catabolize the soil arginine, involved with ammonification processes (nitrogen and carbon cycles) (Alef & Kleiner, 1986). Other studies reported a significant decrease of general carbon substrate utilization (AWCD) by the microbial community from soils exposed to AgNPs (uncoated, 20 nm) (Sillen *et al.*, 2015) or decreased utilization of specific substrates such as amino acids and carbohydrates (Kumar *et al.*, 2011), for soils exposed to metal NPs. Our results did not indicate a significant impairment of SBC activity and the effects attenuation may be related to the presence of different soil invertebrates and plants in this mesocosms approach. Plants may change the availability of metals on soils and may release exudates that can directly change the soil conditions (pH, for instance) (Liu *et al.*, 2019), affecting the toxicity of AgNO₃ and Ag₂S NPs on SBC. Also, invertebrates may alter soil conditions, essentially through their behaviour in soils (Tourinho *et al.*, 2015), contributing to the microbial composition/abundance (decreasing, for instance) changes, as a result of the inhibition of oxygenation level.

4.2. Effects of silver on SBC structure and diversity

The effects of Ag₂S NPs on the structure, composition, and diversity of SBC were previously assessed in only a limited number of studies (Judy *et al.*, 2015; Doolette *et al.*, 2016). The present study is a considerable contribution given its higher tier approach, using an indoor mesocosm including several species of invertebrates and a plant species making them more representative of field conditions. Furthermore, our study revealed a distinct impact of Ag₂S NPs and AgNO₃ on the SBC structure, in a time-dependent manner. During the exposure, a faster increase of Ag⁺ concentration in the soil pore water from the AgNO₃ treatment was observed and might be responsible for an early structural change, as previously explained. Although Ag⁺ dissolution from Ag₂S NPs was detected in very low amounts at 28 days of exposure, this Ag⁺ dissolution wasn't enough to explain the latter's effects on SBC structure.

The impact of Ag₂S NPs on SBC structure has been already evaluated on natural soils after 28 days using metagenomics (Doolette *et al.*, 2016) and phospholipid fatty acids (PLFAs) analysis (Judy *et al.*, 2015). In this regard, Doolette *et al.*, (2016) observed that the impact of Ag₂S NPs (152 nm) on the number of operational taxonomic units (OTUs) was lower compared to non-sulfidized AgNPs (44 nm) and AgNO₃, when using the toxicity threshold hazardous concentrations (HC20) approach [5.9 (Ag₂S NPs); 1.4 (AgNPs) and 1.4 (AgNO₃) mg Ag kg⁻¹]. On the other hand, the study by Judy *et al.*, (2015) demonstrated that microbial biomass (inferred from PFLA analysis) decreased when Ag₂S NPs (30.1 nm) was applied in sandy loam soils (pH=6.8), at 1 and 100 mg kg⁻¹soil, however, the silver in sulfidized form was less toxic compared to the other silver NP (PVP-Ag - 20.6 nm) and ionic silver (AgNO₃). Although Ag toxicity is strongly dependent on soil characteristics (*e.g.*, pH, soil type), nanomaterials characteristics (*e.g.*, size, coating), and the specific microbial methodologies (Samarajeewa *et al.*, 2017; Vasileiadis *et al.*, 2018), both studies showed a similar toxicity pattern (Ag₂S NPs < AgNPs < AgNO₃) on microbial structure.

Moreover, a reduction of the alpha diversity of the bacterial community exposed to AgNPs has already been reported (Samarajeewa *et al.*, 2017). Regardless of silver form, our study revealed a significant reduction in diversity and richness, after 14 days of exposure. In fact, the free Ag⁺ concentration might explain the AgNO₃ impact on these indexes, as above mentioned. The negative impact of Ag₂S NPs on diversity indexes may result from the Ag⁺ released (from these particles); or the accumulation of

sulfidized particles in the plant tissues (Wang *et al.*, 2017). In fact, this accumulation (at 10 mg kg⁻¹) reduces plant growth (Wang *et al.*, 2017), changing the interaction between root exudates and microbes, which can result in an indirect change in the abundance of microorganisms in the soil. After day 28, the effect of AgNO₃ on SBC diversity and richness was gradually attenuated to values similar to the control, suggesting SBC resilience to this silver form or/and a decrease in Ag bioavailability. This pattern has been observed before for invertebrate species, where Ag⁺ from AgNO₃ decreased significantly over time in porewater, reflecting a decrease of Ag bioavailability. Due to the increased silver adsorption to soils, the free Ag⁺ concentration decreases in less than 14 days (Settimio *et al.*, 2014).

4.3. Environmental relevance and integrative analysis between structure and functional levels of SBC

Shifts of SBC structure may lead to a change in the biological function, albeit the functional redundancy reported for SBC (Vasileiadis *et al.*, 2015). The relationship between the SBC structure and soil function is not easy to predict and is poorly documented. Our results demonstrated that Ag₂S NPs change the SBC structure and this structural change may affect, for instance, the phosphorous cycle, resulting in an increased AP activity. Also, the P-SB counts showed a good correlation (R>0.6) with the SBC structure from soils exposed to Ag₂S NPs. In accordance with these findings, the study by Fanin *et al.*, (2015) showed a significant correlation (Mantel test) between CLPPs and SBC structure from different fertilization levels (N and P input) in undisturbed tropical forests.

Few studies are available that relate the N cycle with the SBC structure exposed to metal contamination (Kumar *et al.*, 2014, Doolette *et al.*, 2016), and other nutrient cycles are even less explored. Nevertheless, the effects of AgNPs (at 10 and 100 mg kg⁻¹) on SBC structure might impact the carbon cycle, through a decrease in microbial biomass (carbon) (Kumar *et al.*, 2014), soil enzymatic activity (*e.g.*, β-glucosidase) and/or soil microbial respiration.

5. Conclusions

This study provided evidence that Ag₂S NPs affect the SBC and that these effects become more pronounced over-time. Ag₂S NPs effects on the SBC are expected to

potentially imbalance soil functions, namely those related to the carbon (L-arginine consumption and β -glucosidase activity) and phosphorus cycles (P-SB and PA). The structure of SBC and diversity indexes were significantly impacted by Ag₂S NPs, after 28 days of exposure.

Function and structure of SBC were also impacted by AgNO₃, predominantly at earlier times of exposure due to the initial high concentration of free Ag⁺, with the expected decrease of Ag bioavailability over time, as a result of binding to lignin and clay particles, being a likely cause for the weakening of effects.

This study emphasizes the usefulness of the terrestrial mesocosm approach to evaluate the effects of sulfidation state of AgNPs on microbial parameters. Moreover, the observed temporal effects (28-days) from both ionic Ag and Ag₂S NPs highlight the importance of long-term exposure experiments under realistic environmental conditions.

6. Acknowledgements

All the authors were funded by the EU H2020 project Nano-FASE (Nanomaterial Fate and Speciation in the Environment; grant no. 646002). SL, IH, SP and ZK received additional financial support from FCT/MCTES, through national funds, to CESAM (UIDP/50017/2020+UIDB/50017/2020). Also, this work was supported by FCT through a PhD grant to Sara Peixoto (SFRH/BD/117738/2016).

7. References

- Abd El-Wakeil, K. F. A. (2015). Effects of terrestrial isopods (Crustacea: *Oniscidea*) on leaf litter decomposition processes. *The Journal of Basic & Applied Zoology*, 69, 10-16.
- Alef, K., Kleiner, D. (1986). Arginine ammonification, a simple method to estimate microbial activity potentials in soils. *Soil Biology and Biochemistry*, 18(2), 233-235.
- Colman, B. P., Arnaout, C. L., Anciaux, S., Gunsch, C. K., Hochella Jr, M. F., Kim, B., Unrine, J.M., (2013). Low concentrations of silver nanoparticles in biosolids cause adverse ecosystem responses under realistic field scenario. *PloS One* 8 (2), e57189.

- Cornelis, G., Kirby, J. K., Beak, D., Chittleborough, D., McLaughlin, M. J. (2010). A method for determination of retention of silver and cerium oxide manufactured nanoparticles in soils. *Environmental Chemistry*, 7(3), 298-308.
- Dick, R. P., Breakwell, D. P. and Turco, R. F. (1996). Soil enzyme activities and biodiversity measurements as integrative microbiological indicators. *In Methods for assessing soil quality*, SSSA. 49th, Madison, USA, 247–271.
- Doolette, C. L. Gupta, V. V., Lu, Y., Payne, J. L., Batstone, D. J., Kirby, J. K., McLaughlin, M. J. (2016). Quantifying the sensitivity of soil microbial communities to silver sulfide nanoparticles using metagenome sequencing. *PLoS ONE*, 11(8), 1–20.
- Doolette, C. L., McLaughlin, M. J., Kirby, J. K., Navarro, D. A. (2015). Bioavailability of silver and silver sulfide nanoparticles to lettuce (*Lactuca sativa*): Effect of agricultural amendments on plant uptake. *Journal of Hazardous Materials*, 300, 788–795.
- European Commission Science for Environment Policy (2017) IN-DEPTH REPORT 14 Assessing the environmental safety of manufactured nanomaterials Science for Environment Policy Environment.
- Fanin, N., Hättenschwiler, S., Schimann, H., Fromin, N. (2015). Interactive effects of C, N and P fertilization on soil microbial community structure and function in an Amazonian rain forest. *Functional Ecology*, 29(1), 140-150.
- Garland, J. L. (1997). Analysis and interpretation of community-level physiological profiles in microbial ecology. *FEMS Microbiology Ecology*, 24(4), 289-300.
- Geitner, N.; Hendren, C.; Cornelis, G.; Kaegi, R.; Lead, J.; Lowry, G.; Lynch, I.; Nowack, B.; Petersen, E.; Bernhardt, E.; Brown, S.; Chen, W.; de Garidel-Thoron, C.; Hanson, J.; Harper, S.; Jones, K.; von der Kammer, F.; Kennedy, A.; Kidd, J.; Matson, C.; Metcalfe, C.; Pedersen, J.; Peijnenburg, W.; Quik, J.; Rodrigues, S. M.; Rose, J.; Sayre, P.; Simonin, M.; Svendsen, C.; Tanguay, R.; Tufenkji, N.; van Teunenbroek, T.; Thies, G.; Tian, Y.; Rice, J.; Turner, A.; Liu, J.; Unrine, J.; Vance, M.; White, J.; Wiesner, M. (2020). Harmonizing. Across Environmental Nanomaterial Testing Media for Increased Comparability of Nanomaterial Datasets. *Environmental Science: Nano*, 7(1), 13-36.
- Giese, B., Klaessig, F., Park, B., Kaegi, R., Steinfeldt, M., Wigger, H., Gottschalk, F. (2018). Risks, release and concentrations of engineered nanomaterial in the environment. *Scientific Reports*, 8(1), 1-18.

- Gottschalk, F., Sonderer, T., Scholz, R. W., Nowack, B. (2009). Modeled environmental concentrations of engineered nanomaterials (TiO₂, ZnO, Ag, CNT, fullerenes) for different regions. *Environmental Science & Technology*, 43(24), 9216–9222.
- Henriques, I. S., Almeida, A., Cunha, Â., Correia, A. (2004). Molecular sequence analysis of prokaryotic diversity in the middle and outer sections of the Portuguese estuary Ria de Aveiro. *FEMS Microbiology Ecology*, 49(2), 269-279.
- Judy, J. D., Kirby, J. K., Creamer, C., McLaughlin, M. J., Fiebiger, C., Wright, C., Bertsch, P. M. (2015). Effects of silver sulfide nanomaterials on mycorrhizal colonization of tomato plants and soil microbial communities in biosolid-amended soil. *Environmental Pollution*, 206, 256–263.
- Kaegi, R., Voegelin, A., Sinnert, B., Zuleeg, S., Hagendorfer, H., Burkhardt, M., Siegrist, H. (2011). Behavior of metallic silver nanoparticles in a pilot wastewater treatment plant. *Environmental Science & Technology*, 45(9), 3902-3908.
- Kent, R. D., Oser, J. G., Vikesland, P. J. (2014). Controlled evaluation of silver nanoparticle sulfidation in a full-scale wastewater treatment plant. *Environmental Science & Technology*, 48(15), 8564-8572.
- Kim, M. J., Ko, D., Ko, K., Kim, D., Lee, J. Y., Woo, S. M., Chung, H. (2018). Effects of silver-graphene oxide nanocomposites on soil microbial communities. *Journal of Hazardous Materials*, 346, 93-102.
- Kumar, N., Palmer, G. R., Shah, V., Walker, V. K. (2014). The effect of silver nanoparticles on seasonal change in arctic tundra bacterial and fungal assemblages. *PLoS One*, 9(6).
- Kumar, N., Shah, V., Walker, V. K. (2011). Influence of a nanoparticle mixture on an arctic soil community. *Environmental Toxicology and Chemistry*, 31(1), 131–135.
- Lahive, E., Matzke, M., Durenkamp, M., Lawlor, A. J., Thacker, S. A., Pereira, M. G., Lofts, S. (2017). Sewage sludge treated with metal nanomaterials inhibits earthworm reproduction more strongly than sludge treated with metal metals in bulk/salt forms. *Environmental Science: Nano*, 4(1), 78-88.
- Liu, J., Williams, P. C., Goodson, B. M., Geisler-Lee, J., Fakharifar, M., & Gemeinhardt, M. E. (2019). TiO₂ nanoparticles in irrigation water mitigate

- impacts of aged Ag nanoparticles on soil microorganisms, *Arabidopsis thaliana* plants, and *Eisenia fetida* earthworms. *Environmental Research*, 172, 202-215.
- McGee, C. F., Storey, S., Clipson, N., Doyle, E. (2017). Soil microbial community responses to contamination with silver, aluminium oxide and silicon dioxide nanoparticles. *Ecotoxicology*, 26(3), 449–458.
- McGillicuddy, E., Murray, I., Kavanagh, S., Morrison, L., Fogarty, A., Cormican, M., Morris, D. (2017). Silver nanoparticles in the environment: Sources, detection and ecotoxicology. *Science of the Total Environment*, 575, 231-246.
- Muyzer, G., Waal, E., C. and Uitterlinden, A., G. (1993). Profiling of Complex Microbial Populations by Denaturing Gradient Gel Electrophoresis Analysis of Polymerase Chain Reaction-Amplified Genes Coding for 16S rRNA. *Applied and Environmental Microbiology*, 59(3), 695–700.
- Nautiyal, S. C. (1999). An efficient microbiological growth medium for screening phosphate solubilizing microorganisms. *FEMS Microbiology Letters*, 170(436), 265–270.
- Neves, J., Cardoso, D. N., Malheiro, C., Kah, M., Soares, A. M., Wrona, F. J., Loureiro, S. (2019). Copper toxicity to *Folsomia candida* in different soils: a comparison between nano and conventional formulations. *Environmental Chemistry*, 16(6), 419-429.
- Pachapur, V. L., Larios, A. D., Cledón, M., Brar, S. K., Verma, M., Surampalli, R. Y. (2016). Behaviour and characterization of titanium dioxide and silver nanoparticles in soils. *Science of the Total Environment*. 563, 933–943.
- Reinsch, B., Levard, C., Li, Z., Ma, R., Wise, A., Gregory, K. B., Lowry, G. V. (2012). Sulfidation of silver nanoparticles decreases *Escherichia coli* growth inhibition, *Environmental Science & Technology*, 46(13), 6992–7000.
- Richardson, A.E., Simpson, R.J., 2011. Soil microorganisms mediating phosphorus availability update on microbial phosphorus. *Plant Physiology* 156 (3), 989–996.
- Sala, M. M., Pinhassi, J., Gasol, J. M. (2006). Estimation of bacterial use of dissolved organic nitrogen compounds in aquatic ecosystems using Biolog plates. *Aquatic Microbial Ecology*, 42(1), 1-5.
- Samarajeewa, A. D., Velicogna, J. R., Princz, J. I., Subasinghe, R. M., Scroggins, R. P., Beaudette, L. A. (2017). Effect of silver nano-particles on soil microbial growth, activity and community diversity in a sandy loam soil. *Environmental Pollution*, 220, 504–513.

- Schlich, K., Hoppe, M., Kraas, M., Schubert, J., Chanana, M., Hund-Rinke, K. (2018). Long-term effects of three different silver sulfide nanomaterials, silver nitrate and bulk silver sulfide on soil microorganisms and plants. *Environmental Pollution*, 242, 1850–1859.
- Schultz, C. L., Gray, J., Verweij, R. A., Busquets-Fité, M., Puentes, V., Svendsen, C., Matzke, M. (2018). Aging reduces the toxicity of pristine but not sulphidised silver nanoparticles to soil bacteria. *Environmental Science: Nano*, 5(11), 2618–2630.
- Settimio, L., McLaughlin, M. J.; Kirby, J. K.; Langdon, K. A., Lombi, E., Donner, E., Scheckel, K. G. (2014). Fate and lability of silver in soils: effect of ageing. *Environmental Pollution*, 191, 151-157.
- Shin, Y. J., Kwak, J. I., An, Y. J. (2012). Evidence for the inhibitory effects of silver nanoparticles on the activities of soil exoenzymes. *Chemosphere*, 88(4), 524-529.
- Sillen, W. M., Thijs, S., Abbamondi, G. R., Janssen, J., Weyens, N., White, J. C., Vangronsveld, J. (2015). Effects of silver nanoparticles on soil microorganisms and maize biomass are linked in the rhizosphere. *Soil Biology and Biochemistry*, 91, 14-22.
- Slocum, R.D., 2005. Genes, enzymes and regulation of arginine biosynthesis in plants. *Plant Physiology and Biochemistry*. 43 (8), 729–745.
- Starnes, D. L., Unrine, J. M., Starnes, C. P., Collin, B. E., Oostveen, E. K., Ma, R., Tsyusko, O. V. (2015). Impact of sulfidation on the bioavailability and toxicity of silver nanoparticles to *Caenorhabditis elegans*. *Environmental Pollution*. 196, 239–246.
- Sylvia, D. M., Fuhrmann, J. J., Hartel, P. G., Zuberer, D. A. (2005). Principles and applications of soil microbiology (No. QR111 S674 2005). Pearson.
- Tabatabai, M. A. (1994). Methods of soil analysis: microbiological and biochemical properties. *In Soil enzymes*. SSSA Book series, 775–883.
- Tourinho, P. S., van Gestel, C. A., Jurkschat, K., Soares, A. M., Loureiro, S. (2015). Effects of soil and dietary exposures to Ag nanoparticles and AgNO₃ in the terrestrial isopod *Porcellionides pruinosus*. *Environmental Pollution*, 205, 170–177.
- Turner, B.L., Hopkins, D.W., Haygarth, P.M., Ostle, N., (2002). β-Glucosidase activity in pasture soils. *Applied Soil Ecology*, 20 (2), 157–162.

- US-EPA (1996). Method 3052: Microwave assisted digestion of siliceous and organically based matrices. United States Environmental Protection Agency, Washington.
- Vasileiadis, S., Brunetti, G., Marzouk, E., Wakelin, S., Kowalchuk, G. A., Lombi, E., Donner, E. (2018). Silver toxicity thresholds for multiple soil microbial biomarkers. *Environmental Science & Technology*, 52(15), 8745–8755.
- Vasileiadis, S., Puglisi, E., Trevisan, M., Scheckel, K. G., Langdon, K. A., McLaughlin, M. J., Donner, E. (2015). Changes in soil bacterial communities and diversity in response to long-term silver exposure. *FEMS Microbiology Ecology*, 91(10), 1–11.
- Wang, P., Lombi, E., Sun, S., Scheckel, K. G., Malysheva, A., McKenna, B. A., Kopittke, P. M. (2017). Characterizing the uptake, accumulation and toxicity of silver sulfide nanoparticles in plants. *Environmental Science: Nano*, 4(2), 448–460.
- Wang, P., Menzies, N. W., Dennis, P. G., Guo, J., Forstner, C., Sekine, R., Kopittke, P. M. (2016). Silver nanoparticles entering soils via the wastewater-sludge-soil pathway pose low risk to plants but elevated Cl concentrations increase Ag bioavailability. *Environmental Science & Technology*, 50(15), 8274–8281.
- Yang, J., Jiang, F., Ma, C., Rui, Y., Rui, M., Adeel, M., Xing, B. (2018). Alteration of crop yield and quality of wheat upon exposure to silver nanoparticles in a life cycle study. *Journal of Agricultural and Food Chemistry*, 66(11), 2589-2597.

8. Supplementary material

8.1. Nanoparticle's characterization

Dissolution of Ag₂S NPs colloids (stock solution) by ICP-MS

The dissolution of Ag₂S NPs colloids, in stock solution, was determined using the ICP-MS analysis (PerkinElmer, Nexion 3000), based on the protocol previously described by (Avramescu *et al.*, 2019). Prior to ICP-MS analysis, each sample (Ag₂S NPs-UPW, at 1 mg L⁻¹) was filtered [0.02 μm pore-diameter syringe filters (Anotop™, Whatman)], and acidified with pure ICP-grade HNO₃ (Sigma Aldrich; CAS Number 7697-37-2), to a final concentration of 2%. Five consecutive measurements per sample were measured during 2, 4, 24 and 48 hours, at 20°C after 2 minutes equilibration time. ICP-grade standards were used to generate the calibration curves, and only the correlation coefficient greater than 0.999 was considered. ¹⁰³Rh was applied in all samples as internal standard quality control. Samples failing the QC thresholds were re-calibrated and re-analyzed.

8.2. List of Figures

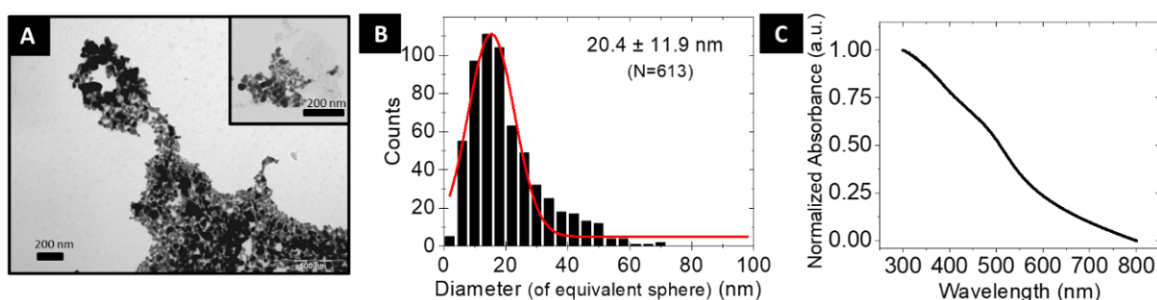


Figure S1. Characterization of Ag₂S NPs colloids, A) TEM image with scale bar 200 nm); B) size distribution by analysis of the TEM images (20.4 ± 11.9 nm; 613 nanoparticles analyzed); C) normalized UV-vis spectra in colloidal dispersion (mili-Q water).

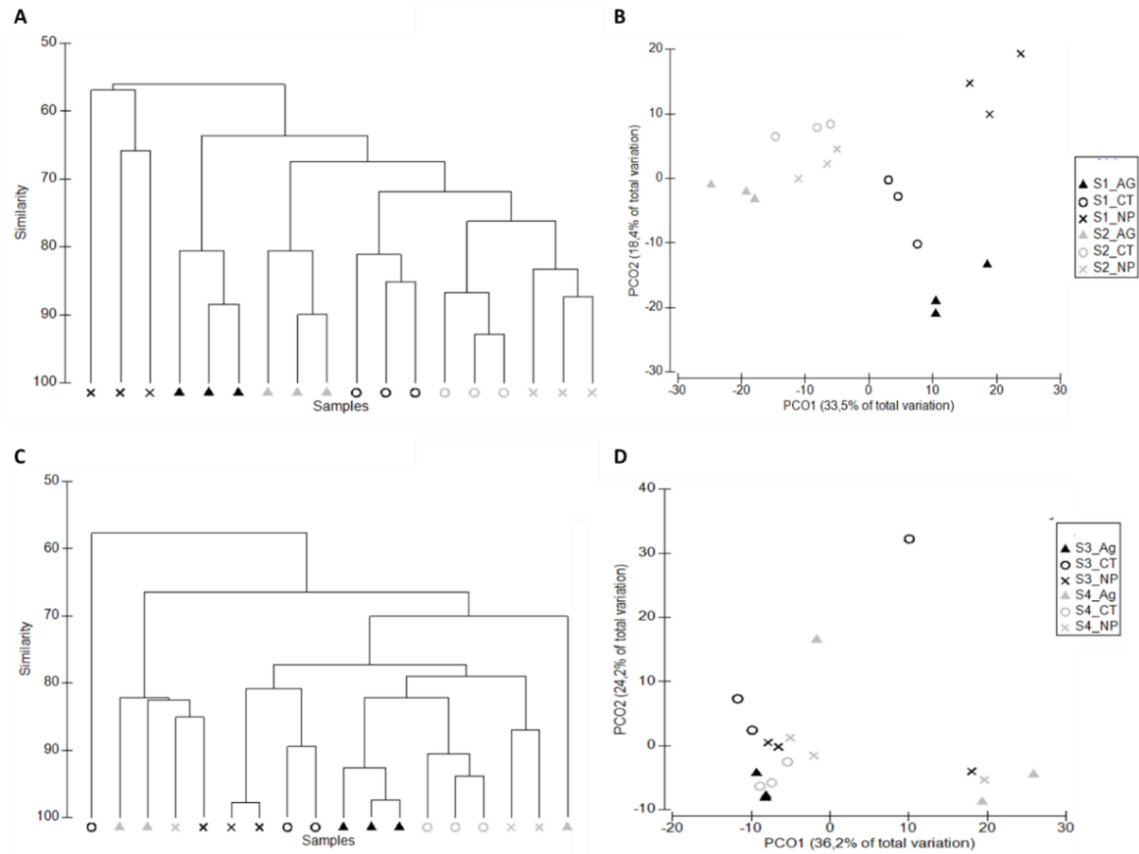


Figure S2. Clustering analysis (A and C) and Principal Coordinate Analysis (PCoA) (B and D) of SBC from upper layers [S1 (0-4 cm) and S2 (4-6 cm)] and bottom layers [S3 (10-12 cm) and S4 (12-16 cm)] of mesocosm columns with control soil (CT), soil spiked with Ag₂S NPs and soil spiked with AgNO₃.

8.3. List of Tables

Table S1. Percentage of dissolution measured by ICP-MS of Ag₂S NPs measured in ultrapure water (UPW) stock solution at a nominal concentration of 1 mg (Ag) L⁻¹. Data was expressed by mean and standard deviation (mean ± SD).

	2 h	4 h	24 h	48 h
% Ag dissolution	0.04 ± 0.02	0.01 ± 0.002	0.01 ± 0.001	0.01 ± 0.003

Table S2. Soil pH(CaCl₂) measured of mesocosm columns, Top-soil (0-4 cm), with control soil (CT), soil spiked with Ag₂S NPs and soil spiked with AgNO₃. Data was expressed by mean and standard deviation (mean ± SD).

Day	Treatment	Average	SD
0	CT	6.49	-
14	CT	6.08	0.07
14	Ag ₂ S NPs	6.08	0.06
14	AgNO ₃	5.92	0.06
28	CT	6.05	0.10
28	Ag ₂ S NPs	5.98	0.12
28	AgNO ₃	5.69	0.10

Table S3. Diversity indexes calculated based on DGGE analysis among soil treatments and soil depth in mesocosm core. The soil treatments consist in: CT (non-exposed soil), spiked soil with AgNO₃ and Ag₂S NPs were analysed for each soil layers (S1, S2, S3, and S4) after 28 days. Different letters (a, b) correspond to significant differences ($p < 0.05$) between soil treatments (CT vs. Ag₂S NP vs. AgNO₃) for each layers, after 28 days of exposure.

Layers/Depth	Treatment	<i>S</i>			<i>J'</i>			<i>H'</i>		
S1 (0-4 cm)	CT	45	± 1	a	0.888	± 0.028	a	3.380	± 0.091	a
	AgNO ₃	43	± 1	a	0.911	± 0.014	a	3.428	± 0.070	a
	Ag ₂ S NPs	37	± 2	b	0.885	± 0.018	a	3.193	± 0.042	b
S2 (4-6 cm)	CT	50	± 1	a	0.934	± 0.008	a	3.660	± 0.023	a
	AgNO ₃	49	± 1	a	0.938	± 0.006	a	3.656	± 0.041	a
	Ag ₂ S NP	52	± 1	a	0.935	± 0.003	a	3.694	± 0.005	a
S3 (10 -12 cm)	CT	56	± 1	a	0.935	± 0.004	a	3.025	± 1.062	a
	AgNO ₃	58	± 0	a	0.939	± 0.004	a	2.634	± 1.110	a
	Ag ₂ S NPs	74	± 7	a	0.880	± 0.004	a	3.025	± 1.062	a
S4 (10 - 14cm)	CT	64	± 1	a	0.942	± 0.006	a	3.797	± 0.040	a
	AgNO ₃	76	± 11	a	0.749	± 0.005	a	3.807	± 0.028	a
	Ag ₂ S NPs	74	± 12	a	0.926	± 0.005	a	3.808	± 0.028	a

Table S4. Statistical significance (using the Two-way ANOVA) for the area under curve (AUC) values for each substrate tested in Biolog[®] Ecoplate. In the table are represented the two factors considered to the analysis: (1) silver treatment (Ag₂S NP or AgNO₃) and (2) sampling time (Day 14 and 28). (*) Asterisks indicate significant changes in AUC using Tukey HSD (p<0.05), for each substrate, comparing the silver treatment towards the CT (non-exposed soil).

Classes	Substrate ID	Day 14						Day 28					
		AgNO ₃ vs. CT			Ag ₂ S NPs vs. CT			AgNO ₃ vs. CT			Ag ₂ S NPs vs. CT		
		AUC	F	P	AUC	F	P	AUC	F	P	AUC	F	P
Carboxylic acids	Pyruvic acid methyl ester	↓	0.296	0.862	↓	0.296	0.862	↓*	3.914	0.027	↓	3.914	0.239
Polymers	Tween 40	↓	2.369	0.115	↑	2.369	0.115	↓	3.276	0.055	↑	3.276	0.055
Polymers	Tween 80	↓*	5.248	0.027	↑	5.248	0.998	↓	4.279	0.118	↑	4.279	0.118
Polymers	Alpha-cyclodextrin	↓	1.852	0.396	↓	1.852	0.396	↑	1.453	0.484	↑	1.453	0.484
Polymers	Glycogen	↓	1.03	0.598	↑	1.03	0.598	↓	1.14	0.337	↓	1.14	0.337
Carbohydrates	D-cellobiose	↑	1.234	0.309	↑	1.234	0.309	↓	0.721	0.497	↓	0.721	0.497
Carbohydrates	Alpha-D-lactose	↑	1.215	0.314	↑	1.215	0.314	↑	0.321	0.852	↓	0.321	0.852
Carbohydrates	β-methyl-D-glucoside	↓	4.088	0.129	↑	4.088	0.129	↓*	5.169	0.010	↓	5.169	0.303
Carbohydrates	D-xylose	↓	0.148	0.863	↑	0.148	0.863	↓	3.347	0.188	↓	3.347	0.188
Carbohydrates	i-erythritol	↓*	6.265	0.04	↓	6.265	0.3	↓	0.0801	0.923	↓	0.0801	0.923
Carbohydrates	D-mannitol	↑	2.424	0.11	↑	2.424	0.11	↑	1.848	0.179	↑	1.848	0.179
Carbohydrates	N-acetyl-D-glucosamine	↓	5.972	0.051	↑	5.972	0.057	↓	1.083	0.582	↓	1.083	0.582
Carboxylic acids	D-glucosaminic acid	↓*	9.788	0.007	↓	9.788	0.52	↓	0.731	0.492	↑	0.731	0.492
Carbohydrates	Glucose-1-phosphate	↓	1.685	0.207	↓	1.685	0.207	↓	1.207	0.317	↓	1.207	0.317
Carbohydrates	D,L-alpha-glycerol phosphate	↓	1.9	0.171	↑	1.9	0.171	↑	3.623	0.167	↑	3.623	0.167
Carbohydrates	D-galactonic acid-gamma-lactone	↓	1.756	0.194	↓	1.756	0.194	↓	3.623	0.163	↓	3.623	0.163
Carboxylic acids	D-galacturonic acid	↓	9.824	0.3	↑	9.824	0.053	↓	1.146	0.564	↓	1.146	0.564
Phenolic acids	2-Hydroxy benzoic acid	↑	1.295	0.523	↑	1.295	0.523	↓	0.391	0.822	↑	0.391	0.822
Phenolic acids	4-Hydroxy benzoic acid	↑	1.852	0.396	↑	1.852	0.396	↓	1.757	0.194	↓	1.757	0.194
Carboxylic acids	Gamma-hydroxybutyric acid	↓	0.982	0.389	↓	0.982	0.389	↓	0.00353	0.998	↓	0.00353	0.998
Carboxylic acids	Itaconic acid	↓	1.564	0.23	↓	1.564	0.23	↓	2.234	0.129	↓	2.234	0.129
Carboxylic acids	Alpha-ketobutyric acid	↓	0.605	0.554	↑	0.605	0.554	↑	0.638	0.727	↑	0.638	0.727
Carboxylic acids	D-malic acid	↑	3.654	0.161	↑	3.654	0.161	↑	0.522	0.77	↓	0.522	0.77
Amino acids	L-arginine	↓	1.338	0.281	↑	1.338	0.281	↓*	9.75	0.008	↓*	9.75	0.008
Amino acids	L-asparagine	↓	3.75	0.153	↓	3.75	0.153	↓	2.294	0.123	↓	2.294	0.123
Amino acids	L-phenylalanine	↑	1.796	0.188	↓	1.796	0.188	↑	3.069	0.065	↓	3.069	0.065
Amino acids	L-serine	↓*	7.063	0.003	↓	7.063	0.256	↓	3.069	0.065	↑	3.069	0.065
Amino acids	L-threonine	↑	0.578	0.569	↓	0.578	0.569	↑	1.329	0.284	↑	1.329	0.284
Amino acids	Glycyl-L-glutamic acid	↓	0.985	0.388	↑	0.985	0.388	↑	0.222	0.803	↑	0.222	0.803
Amines/amides	Phenylethylamine	↑	5.331	0.414	↓	5.331	0.146	↓	1.383	0.27	↓	1.383	0.27
Amines/amides	Putrescine	↓	0.426	0.658	↑	0.426	0.658	↓	1.383	0.27	↓	1.383	0.27

Chapter 7

The impact of silver sulfide nanoparticles and silver ions in soil
microbiome

The impact of silver sulfide nanoparticles and silver ions in soil microbiome

Peixoto, S., Henriques, I., Loureiro, S.

Journal of Hazardous Materials, 422, 126793, doi.org/10.1016/j.jhazmat.2021.126793

Abstract

The use of biosolids as fertilizers in agriculture can lead to the exposure of soil biota to sulfidized silver nanoparticles (Ag₂S NPs), generated during the wastewater treatment procedures. Considering the crucial role of microorganisms on soil functions, we aimed to study the effects of 10 mg kg⁻¹ soil of Ag₂S NPs or AgNO₃ on the soil microbiome, using an indoor mesocosm. After 28 days of exposure, Ag₂S NPs induced a significant change in the soil microbiome structure, at class, genera and OTU levels. For instance, a significantly higher abundance of Chitinophagia, known for its lignocellulose-degrading activity, was observed in Ag₂S NPs-treated soil toward the control. Nevertheless, stronger effects were observed in AgNO₃-treated soil, over time, due to its higher silver dissolution rate in porewater. Additionally, only the AgNO₃-treated soil stimulates the abundance of ammonia-oxidizing (AOB; *amoA* gene) and nitrite-oxidizing (NOB; *nxrB* gene) bacteria, which are involved in the nitrification process. Distinct variants of *amoA* and *nxrB* genes emerged in silver-treated soils, suggesting a potential succession of AOB and NOB with different degree of silver-tolerance. Our study highlights the latter effects of Ag₂S NPs on the soil microbiome composition, while AgNO₃ exerted a stronger effect in both composition and functional parameters.

Keywords: soil microbiome; Piphillin; ammonia-oxidizing bacteria; nitrite-oxidizing bacteria; gene variants.

1. Introduction

Soil is the habitat of an abundant and diverse microbial community referred to as the soil microbiome (Jansson and Hofmockel, 2018). The abundance and diversity of this microbiome are fundamental to support the ecosystem functions and services, such as primary production, carbon sequestration, and nutrient acquisition (Yang *et al.*, 2014). Several abiotic (*e.g.*, pH, temperature) and biotic factors (*e.g.*, soil invertebrates and plants) have been reported to influence the structure, composition and functional diversity of soil microbiome (Thakur and Geisen, 2019). For instance, soil invertebrates and plants can increase the organic matter input and oxygen levels in soils, which might alter the soil pH and promote the abundance of the aerobic microorganisms (Thakur and Geisen, 2019; Bouchon *et al.*, 2016).

Anthropogenic activities may negatively impact the abundance, diversity and function of the soil microbiome, reducing also its capacity to recover from disturbances (Fajardo *et al.*, 2019). In the last years, the large production and use of AgNPs in consume products resulted in their inevitable release and deposition in sewage sludge in wastewater treatment plants (WWTP) (McGillicuddy *et al.*, 2017). As a result, AgNPs are considered pollutants of emerging environmental concern, and were estimated in a range of 1.24 – 103.79 ng L⁻¹ in sewage (Giese *et al.*, 2018). Recent studies demonstrated that silver, regardless of the form, is retained in the solid matrix (sludge) and converted to Ag-sulfides in the nanometer size range (*i.e.*, Ag₂S NPs) (Kaegi *et al.*, 2011; Wang *et al.*, 2017). The application of sewage sludge as a fertilizer is a common practice in agriculture, regulated by the European Union (Directive 86/278/EEC). In 2017, 5.7 million tons of sludge were used for this propose (Martín-Pozo *et al.*, 2019). The presence of Ag₂S NPs in the sludge may represent a potential hazard to soil, affecting the microbiome, and consequently, several biological processes in the terrestrial ecosystem. In fact, decreased microbial biomass and diversity were already reported in soil and/or sediments exposed to Ag₂S NPs and/or AgNPs (Doolette *et al.*, 2016; Liu *et al.*, 2018; Forstner *et al.*, 2020). Additionally, bacterial communities have shown to be more susceptible to silver exposure than fungal communities regarding the biomass (Montes de Oca-Vásquez *et al.*, 2020) and composition (at the OTU level; Forstner *et al.*, 2020). Additionally, the Ag₂S NPs can alter the abundance of genes (g⁻¹ soil) involved in nitrogen metabolism, including *amoA* encoding the α -subunit of ammonia monooxygenase (nitrification), *nirK* encoding nitrite reductase

(denitrification), *nxB* encoding β -subunit of nitrite oxidoreductase (nitrification), *narG* encoding nitrate reductase (nitrate-reduction), *napA* encoding periplasmic nitrate reductase (nitrate-reduction), *nirS* encoding nitrite reductase (denitrification), and *nosZ* encoding nitrous oxide reductase (denitrification) (Doolette *et al.*, 2016, Liu *et al.*, 2018; Wu *et al.*, 2020). These observed shifts may disrupt the regulation of nitrogen cycling, which is essential for all living organisms (Nelson *et al.*, 2016). Particularly for nitrification, the microbiome involved in the transformation of ammonia into nitrate plays a key role in agricultural soils, making nitrogen available (e.g., as nitrite) for plants (Nelson *et al.*, 2020). On the other hand, microbial denitrification mediates the reduction of nitrate into atmospheric nitrogen gas (N₂) or N oxides (NO, N₂O), which comprise the respiration process, as an important loss pathway of N in agricultural soils (Martens, 2005).

Most of these toxic effects were related to the broad antimicrobial spectrum, which depends on the ionic silver dissolution rate (released from the NPs), and/or on the Ag₂S NPs particle-interaction (Doolette *et al.*, 2016; Starnes *et al.*, 2015). The degree of sulfidation of silver is a key factor in determining the toxicity effect (Reinsch *et al.*, 2012), with a higher degree of sulfidation resulting in a much lower ionic silver dissolution rate, and consequently, in a lower toxic effect (Reinsch *et al.*, 2012; Schlich *et al.*, 2018; Doolette *et al.*, 2016). Additionally, this toxic effect is not only observed in soil microbiome composition but also in the reproduction of terrestrial invertebrates (Starnes *et al.*, 2015) and the plant biomass (Wang *et al.*, 2017; Zhang *et al.*, 2020).

Most of the studies evaluating the effects of Ag₂S NPs in soil microbiome have used a simple experimental design (e.g., microcosms) (Doolette *et al.*, 2016; Wu *et al.*, 2020), failing to reflect the real effects at the ecosystem level (Bour *et al.*, 2015). For this reason, in a previous study (Peixoto *et al.*, 2020) we evaluated the impact of Ag₂S NPs [at 10 mg (Ag) kg⁻¹ soil] on soil microbiome, using a multi-species mesocosm (mimicking a real edaphic scenario). Significant changes in soil microbiome structure were demonstrated using a 16S rRNA-based denaturing gradient gel electrophoresis (DGGE) approach. However, this approach can only detect the dominant members of the microbial community and is not suitable to establish the phylogenetic affiliation of the affected microorganisms. In the last years, next-generation DNA-sequencing technologies (NGS) have been used to analyze in detail the phylogenetic composition of complex microbial communities and were proved useful to assess the nanomaterials

effects in these communities (Nkongolo *et al.*, 2020). In addition, our previous study did not evaluate effects at the level of community functions.

In view of the above, we hypothesized that: 1) sulfidized silver nanoparticles and silver ions affect the soil bacterial community structure and composition; and 2) sulfidized silver nanoparticles and silver ions affect the functions of the soil microbiome (*e.g.*, those related with the nitrogen cycle). Thus, to confirm these hypotheses, the main objectives of our investigation were to i) study the effect of 10 mg (Ag) kg⁻¹ soil of Ag₂S NPs and AgNO₃ on soil microbiome using a 16S rRNA-based NGS analysis; and ii) determine if Ag₂S NPs or AgNO₃ influence the abundance of bacterial phylogenetic groups involved in the nitrification processes (N cycle).

2. Materials and Methods

2.1. Experimental design

The indoor mesocosms [temperature 20 °C ± 2, 16h(light):8h(dark)] were set up as previously described in Peixoto *et al.* (2020), using unexposed soil (control - CT), soil spiked with AgNO₃ (ionic control) and soil spiked with Ag₂S NPs. For this, we used the standard and natural Lufa 2.2 soil (LUFASpeyer 2.2, Speyer, Germany), which has been suggested as a reference soil for testing NPs toxicity (Geitner *et al.*, 2020), presenting a pH of 5.5 ± 0.2 (0.01 M CaCl₂), 1.61 ± 0.2% organic carbon, 0.17 ± 0.02% nitrogen, 7.3 ± 1.2% clay, 13.8 ± 2.7% silt and 78.9 ± 3.5% sand. This soil was spiked with Ag₂S NPs [lab-synthesized colloids nanoparticles (stock solution 1320 ± 48 mg L⁻¹), 100% sulfidized; polyvinylpyrrolidone (PVP) coated; particle size of 20.4 ± 11 nm; Applied Nanoparticles (Barcelona, Spain)] or with AgNO₃ (Sigma-Aldrich, 99 % purity, CAS 7761-88-8, Germany) to a nominal concentration of 10 mg kg⁻¹ soil. This concentration is 25 times higher than predicted environmental concentration (PEC) estimated for 2050 in sludge soils by (Giese *et al.*, 2018), and was selected to simulate a worst-case scenario of AgNPs exposure. For each silver formulation, a stock suspension was prepared with a final concentration of 1150 mg Ag L⁻¹ (Ag₂S NPs) or 1148 mg Ag L⁻¹ (AgNO₃), as previously described in (Peixoto *et al.*, 2020). Stock solutions were added to the soil, and a manual mixing was done thoroughly to guarantee the homogeneous exposure throughout replicates. Then, each core (20 cm long x 11 cm diameter), was loaded with 1.3 kg of control soil in the bottom layer and 1.3 kg of control or spiked soil in the upper part of the core (1-8 cm). The PVP nylon mesh (1 mm) and a high-density

polyethylene plate were used to close the bottom of the core. The columns were incubated for two days, at $20\text{ }^{\circ}\text{C} \pm 2$, to achieve the chemical equilibrium stage in soil (*i.e.*, the partitioning of the different silver forms between soil and pore water). After this period, isopods (10 individuals of *Porcellio scaber*), mealworms (10 individuals of *Tenebrio molitor*), earthworms (6 individuals of *Lumbricus rubellus*) and plants (10 individuals of *Triticum aestivum* L.) were allocated in the upper part of each core. After 14 and 28 days of exposure, soil samples (0.25 g of soil) were collected from the top-soil (core depth = 0-4 cm) of three cores per condition [non-treated soils (CT), and Ag₂S NPs-treated or AgNO₃-treated soils], following a destructive sampling approach.

2.2. Molecular analysis of soil microbiome

2.2.1. DNA extraction and Illumina high-throughput sequencing

The commercial kit Power Soil[®]DNA isolation kit (MOBIO laboratories, CA, USA) was used to extract the total DNA from soil samples, as previously described in Peixoto *et al.*, (2020). Sequencing of the V3-V4 region of 16S rRNA gene, using the Illumina MiSeq[®] sequencer (Illumina, San Diego, CA, USA), was performed by Eurofins Genomic (Ebersberg, Germany) using a SequalPrep 96-well plate kit (ThermoFisher Scientific, Waltham, USA). The primers used to amplify the V3-V4 region were 357F: TACGGGAGGCAGCAG (Turner *et al.*, 1999) and 800R: CCAGGGTATCTAATCC (Kisand *et al.*, 2002). PCR products were purified and normalized, pooled and paired-end sequenced according to manufacturer's instructions (Illumina, San Diego, CA, USA). Reads were processed as described in Almeida *et al.* (2020), to remove reads with less than 285 bp or containing ambiguous bases ("N"), and with an average quality lower than Q30). High-quality reads were assigned to Operational Taxonomic Units (OTU) using Minimum Entropy Decomposition method (Eren *et al.* 2015). Taxonomy assignment was conducted using DC-MEGABLAST alignments - NCBI database. In order to improve estimations, abundances were normalized using lineage-specific 16S rRNA gene copy number (Angly *et al.*, 2014).

2.2.1.1. *In silico* metagenome analysis

The predicted functional profile was analyzed using the Piphillin software (Iwai *et al.*, 2016). The OTU sequences (obtained in 2.2.1) were submitted to the Kyoto Encyclopedia of Genes and Genomes database of phylogenetically referenced prokaryotic genomes, as described in (Almeida *et al.*, 2020). This database using an

identity cut-off of 97% to obtain the KEGG orthologs list and their estimated abundance for each sample.

2.2.2. Real-time polymerase chain reaction (qPCR)

The abundance of total bacteria, ammonia-oxidizing (AOB) and nitrite-oxidizing (NOB) bacteria was assessed by qPCR, using primer sets described in Table S1. The PCR mixtures [NZYSpeedy qPCR Green Master Mix (2X) (NZYTech, Portugal), each primer (10 pmol/ μ L), DNA template and nuclease-free water] were made as previously described by (Tavares *et al.*, 2020). Standard curves and PCR amplifications were performed in triplicate and as described in Amorim *et al.*, (2018), using a CFX96 Touch Real-Time PCR Detection System (Bio-Rad, USA). Particularly for standard curves, the pNZY28 vector (NZYTech, Portugal) was used for cloning and was transformed into *Escherichia coli* NZYStar Competent Cells (NZYTech, Portugal). The correct insert was confirmed by Sanger sequencing. Plasmid DNA was purified using the NZYMiniprep Kit (NZYTech, Portugal), and residual chromosomal DNA was digested using the Plasmid-Safe-ATP-Dependent DNase (Epicentre). Finally, the plasmid DNA was quantified with the NanoDrop spectrophotometer (NanoDrop Technologies, USA), and converted to DNA copies as described in Kim *et al.*, (2013). The copies number of each target gene in each sample were interpolated from the standard curve, as described in Amorim *et al.*, (2018).

2.2.3. Diversity of *amoA* and *nxrB* gene variants

Gene fragments amplification was performed using the *amoA*-1F/*amoA*-2R (for the *amoA* gene) and *nxrB*-169F/*nxrB*-638R (for the *nxrB* gene) (Rotthauwe *et al.*, 1997; Pester *et al.*, 2014), as described in Table S1. For both target-genes, *amoA* and *nxrB* genes, few samples were selected from day-14 (AgNO₃-treated soil) and day-28 [CT (only for *amoA* gene) and Ag₂S NPs-treated soil], based on melting curve results (Figure S3 and S4). Clone libraries were constructed from these amplicons using the pNZY28 vector and *Escherichia coli* NZYStar competent cells (NZYTech). Clones were screened by PCR for the presence of fragments with the expected size and amplicons were sequenced. Sequences were edited and aligned to identify distinct gene variants. Gene diversity was further analyzed through DGGE profiling of *amoA* and *nxrB* gene amplicons obtained using the primers described in Table S1. The PCR mixture was made as previously described in Peixoto *et al.*, (2020). After amplification

(conditions described in Table S1), PCR products were loaded into a polyacrylamide [8% (w/v); 37.5:1, acrylamide:bisacrylamide] gels. The denaturing gradient ranged from 35% to 65% (for NOB) and 50% to 65% (for AOB), where a 100% denaturing solution is defined as 7 M urea and 40% (v/v) formamide. The electrophoresis was performed on a D-Code™ System (Bio-Rad, Hercules, CA, USA), as previously described in Peixoto *et al.*, (2020).

2.3. Statistical analysis

Cluster and principal coordinate analysis (PCoA), using a Bray-Curtis distance matrix constructed from a rarefied and transformed (Log $x+1$) OTU abundance table, were performed using the PRIMER v6 + Permanova software (Primer-E Ltd., Plymouth, UK). Species richness (number of OTU - S), diversity (Shannon-Wiener index - H') and evenness (Pielou's evenness index - J') indexes were calculated based on OTU abundance data. The rarefaction curves were obtained through the function *rarecurve* of *vegan* package from the R software (R Core Team, 2016).

The Levene's and Shapiro-Wilk's tests were performed to verify the homogeneity of variance and normality of distributions, respectively. To assume statistical significance, a p -value <0.05 was considered, using the SPSS version 12.5. When normality or homogeneity of variance was not confirmed the data was Log_{10} transformed. Two-way ANOVA was performed to identified differences among the treatments [CT, Ag₂ NPs and AgNO₃], and exposure time (day 14 and 28). Additionally, one-way ANOVA was conducted to assess the effect among the soil treatments [CT, Ag₂ NPs and AgNO₃], for specific sampling point. For the multiple comparisons between soil treatments, the Tukey's HSD test was applied.

Permanova analysis, based in 999 permutations, was conducted to test differences in soil microbiome structure among treatments.

DGGE patterns were analyzed using Gel ComparII Software (Applied Maths, Belgium), and used in cluster analysis obtained by UPGMA method (group average method) applying Dice coefficient.

3. Results

3.1. Effects of Ag₂S NPs and AgNO₃ on soil microbiome

In the current study, the impact of Ag₂S NPs and AgNO₃, at 10 mg kg⁻¹ soil, in the soil microbiome structure was assessed through Illumina sequencing analysis. After quality-filtering, a total of 2418.484 sequence reads were included in the analysis (Table S2). The obtained rarefaction curves tended to saturation, suggesting that the OTUs detected in each sample were a good estimation of the community richness (Figure S1).

3.1.1. Effect on soil microbiome after 14 days of exposure

After 14 days of exposure, cluster analysis showed that the microbiome from soil exposed to AgNO₃ clustered in a different branch from the other treatments (Figure 1A), sharing with them 53% of similarity. The same spatial separation was observed in PCoA, in which, 72.3% of the total variation were explained by the sum of the two axes (PCO1=54.3% and PCO2=18%) (Figure 1 C). Along the first axis (PCO1) samples corresponding to AgNO₃ treatment were separated from the remaining. In agreement, the Permanova analysis revealed that the AgNO₃-treated soil presented a significant difference in its microbiome structure (PERMANOVA: $t=2.29$; $P=0.001$), while there was no significant difference between the microbiome of the Ag₂S NPs-treated soil and the respective control (PERMANOVA: $t=0.71$, $P=0.713$). Differences between silver forms were also detected (PERMANOVA: $t=2.56$, $P=0.001$).

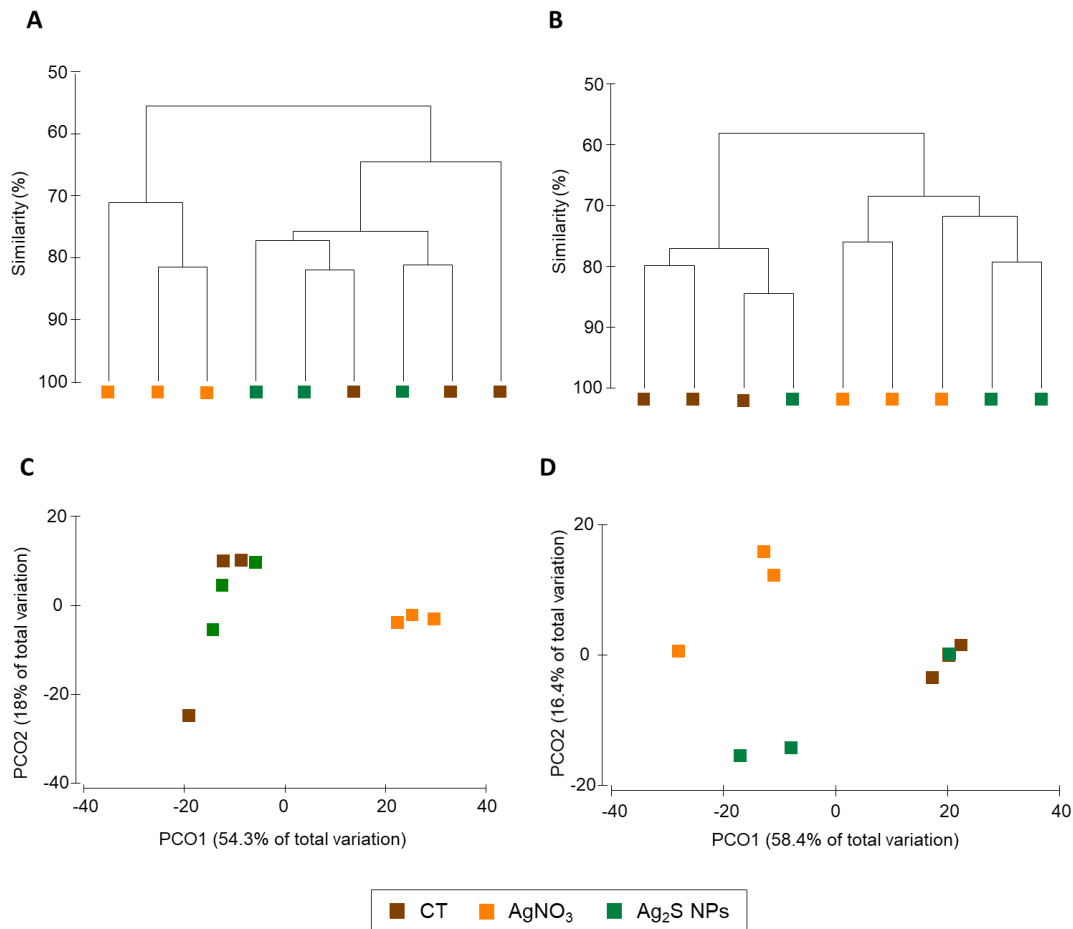


Figure 1. Structural changes in soil microbiome exposed to Ag₂S NPs or AgNO₃, represented in cluster analysis [A and B] and Principal Coordinate analysis (PCoA) [C and D]. Results of three replicates (n=3) are presented for non-exposed soil (CT) and for each treatment [10 mg (Ag) kg⁻¹ soil of AgNO₃ and Ag₂S NPs]. The soil sampling was done at day 14 [A and C] and day 28 [B and D].

In terms of alpha diversity (Table 1), the richness (S), Pielou's (J') and Shannon-wiener (H') indexes were similar among treatments (S : $F= 4.16$, $p= 0.139$; J' : $F= 1.20$, $p=0.334$; H' : $F=6.12$, $p=0.154$).

Table 1. Species richness (number of OTU; S), diversity (Shannon-Wiener index; H') and evenness (Pielou's evenness index; J') index of the soil bacterial communities exposed to Ag₂S NPs and AgNO₃ or non-exposed soil (CT) (OTU based profile). Values presented are mean \pm standard deviation. Asterisks (*) indicate significant differences between silver treatments toward the respective CT (two-way ANOVA; Tukey HSD; $p < 0.05$).

Days	Treatments	Number of species (S)	Pielou's index (J')	Shannon-wiener (H')
14	CT	140 \pm 18	0.86 \pm 0.013	4.26 \pm 0.063
	Ag ₂ S NPs	130 \pm 11	0.86 \pm 0.006	4.20 \pm 0.097
	AgNO ₃	117 \pm 8	0.86 \pm 0.012	4.08 \pm 0.064
28	CT	136 \pm 5	0.86 \pm 0.008	4.23 \pm 0.047
	Ag ₂ S NPs	121 \pm 3	0.88 \pm 0.009	4.23 \pm 0.036
	AgNO ₃	113 \pm 4*	0.87 \pm 0.007	4.11 \pm 0.047*

The dominant classes across control samples (Figure 2) were Acidobacteria (23.4% \pm 1.4), Alphaproteobacteria (17.3% \pm 1.6), and Betaproteobacteria (10.1% \pm 0.6). After day-14, the relative abundance of the dominant classes has not changed significantly in Ag₂S NPs-treated soil. However, a significant increase in the relative abundance of Rubrobacteria (+ 9.0% \pm 1.9; $F=6.32$, $p=0.029$), Cytophagia (+ 4.1% \pm 1.4; $F=7.25$, $p=0.02$) and Actinobacteria (+ 3.6% \pm 0.1; $F=7.25$, $p=0.02$) was observed in soil spiked with AgNO₃. Additionally, differences in relative abundance at class level were detected considering the silver form (nanoparticle *vs.* ionic), namely for Alphaproteobacteria [$F=8.08$, $p=0.02$, (+ 4.6% \pm 0.6 in AgNO₃-treated soil)] and Cytophagia [$F=15.07$, $p=0.007$, (+ 4.3% \pm 1.5 in AgNO₃-treated soil)].

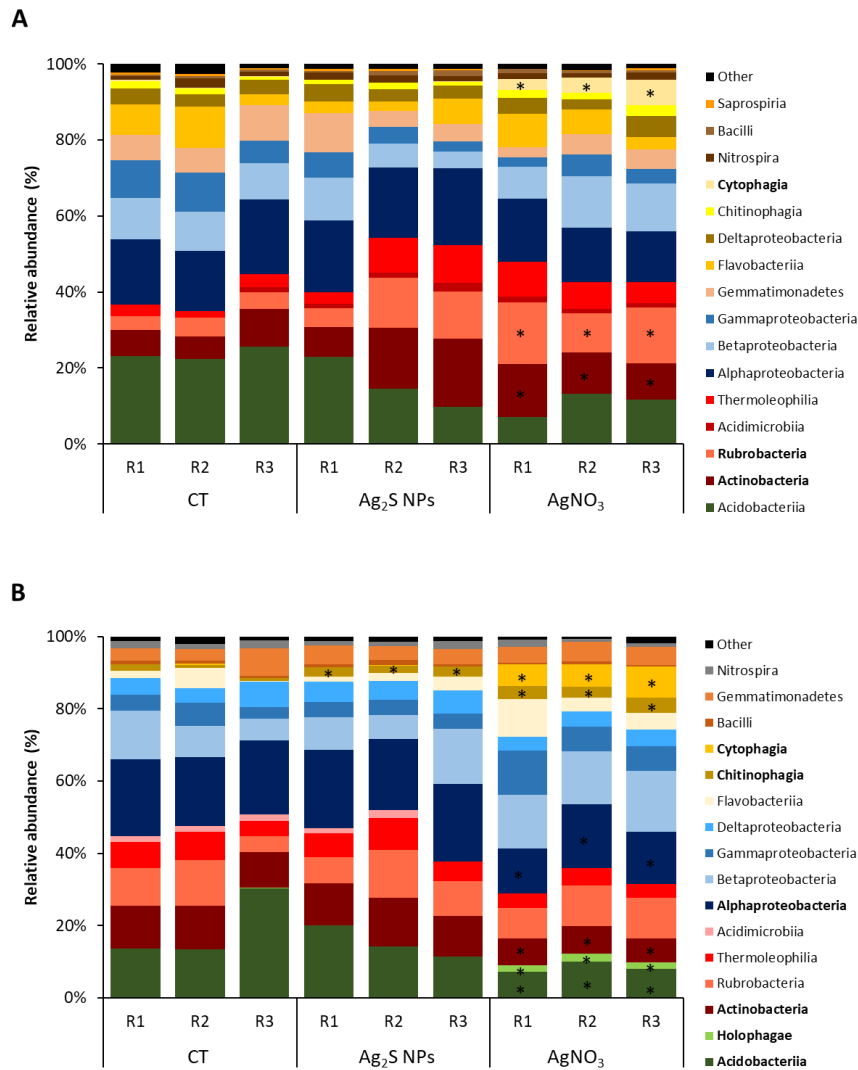


Figure 2. Relative abundance of 15 most abundant classes of soil microbiome, after day 14 (A) and 28 (B). Results of three replicates (R1, R2 and R3) are presented for non-exposed soil (CT) and for each silver treatment [$10 \text{ mg (Ag) kg}^{-1}$ soil of AgNO₃ and Ag₂S NPs]. Asterisks (*) and bold names (classes) indicate significant differences towards the respective CT, for each sampling time (one-way ANOVA, $p < 0.05$; Tukey HSD).

At the genus level, a total of 30 genera were significantly impacted in AgNO₃-treated soil (Figure 3 A) towards the respective CT. Specifically, a significant increase in the relative abundance of 14 genera was detected in AgNO₃-treated soil, 6 of which were exclusively detected in this treatment (Figure 3 and Table S3). On the other hand, 16 genera presented a significant decrease, from which eight were not detected in AgNO₃-treated soil (Table S3).

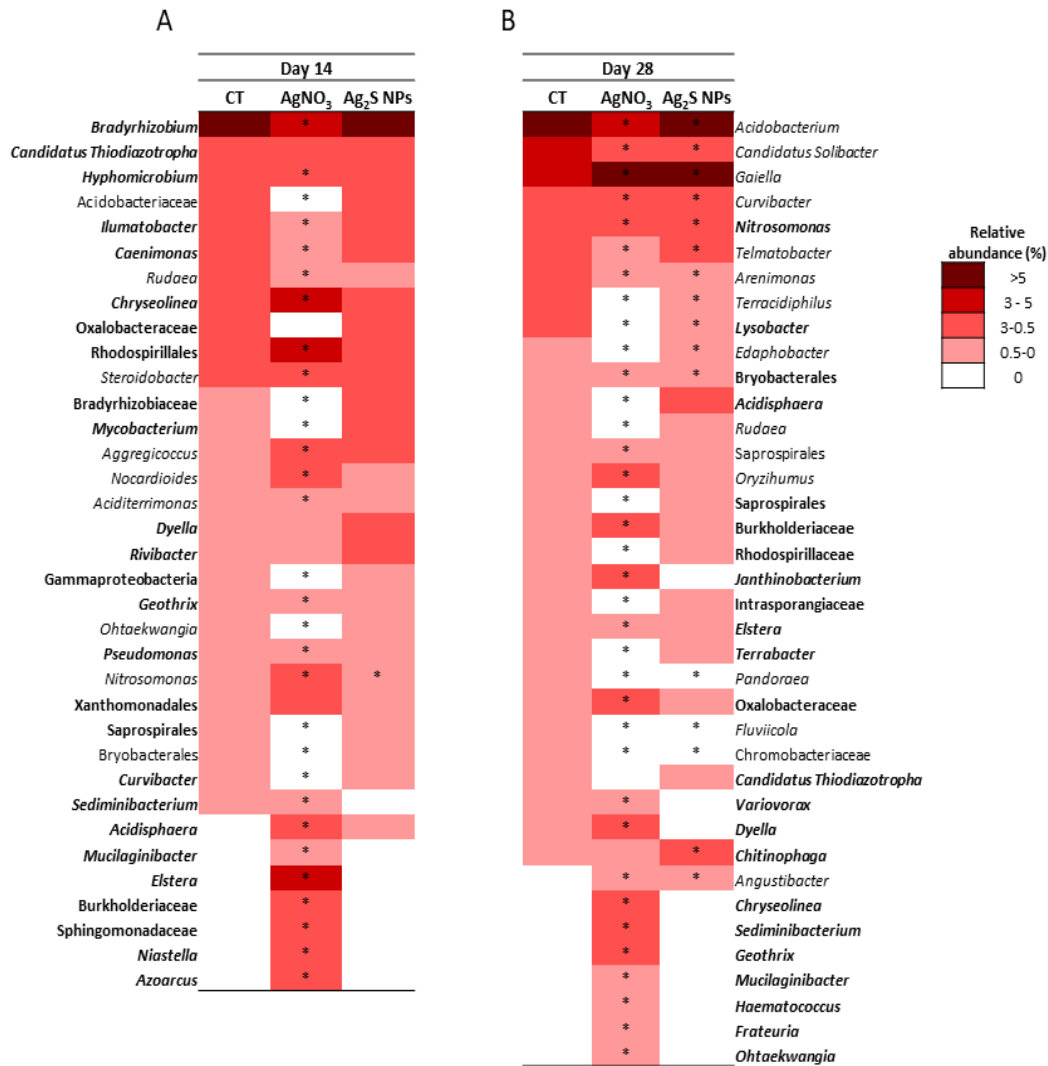


Figure 3. Relative abundance of the genera and unidentified genera affiliated with family or class significantly ($p < 0.05$) affected by Ag₂S NPs or AgNO₃ treatments, after 14 (A) or 28 (B) days of exposure. Average of three replicates ($n=3$) is presented for control (CT) and for each silver treatment [10 mg (Ag) kg⁻¹ soil of AgNO₃ and Ag₂S NPs]. Asterisk (*) indicates a significant difference between soil treatments and control samples, for each sampling time. Bold affiliation (genera or unidentified genera affiliated with family or class) name indicates a significant difference among silver forms (AgNO₃ vs. Ag₂S NPs), for each sampling time (one-way ANOVA, $p < 0.05$; Tukey HSD).

Considering the 30 most abundant OTUs for each soil treatment (Figure 4), the relative abundance of 13 OTUs significantly changed after AgNO₃ exposure, while none was significantly affected by Ag₂S NPs (Table S3). AgNO₃-treated soil presented a significant decrease in OTUs affiliated with *Bradyrhizobium* (OTU 31), *Candidatus Solibacter* (OTU 254), *Nitrosomonas* (OTU 482), *Mycobacterium* (OTU 287); and a significant increase in OTUs affiliated with *Curvibacter* (OTU 58), *Pseudomonas* (OTU

184), *Massilia* (OTU 76), *Sediminibacterium* (OTU 218), *Chryseolinea* (OTU 221), *Ohtaekwangia* (OTU 282), *Sphingomonas* (OTU 301), *Sphingomonadaceae* (OTU 599) and *Geothrix* (OTU 669) (Table S4).

In terms of the predicted microbial functional profile (Table 2), significant changes were mainly detected in AgNO₃-treated soil. For instance, in genes related to the denitrification process (*norB* gene: -6.3 %), *Quorum Sensing* (+2.0% of *solR*), transporters (-7.1% in ABC-2 type transport system ATP-binding protein, and +24.3% in phosphonate transport system substrate-binding protein), and transferases (-25.2% in serine/threonine-protein kinase). Regarding flagellar assembly, exposure to both silver forms led to a decrease of 79.3% (AgNO₃) and 26.7% (Ag₂S NPs) of the relative abundance of sequences encoding the outer membrane protein FlgP.

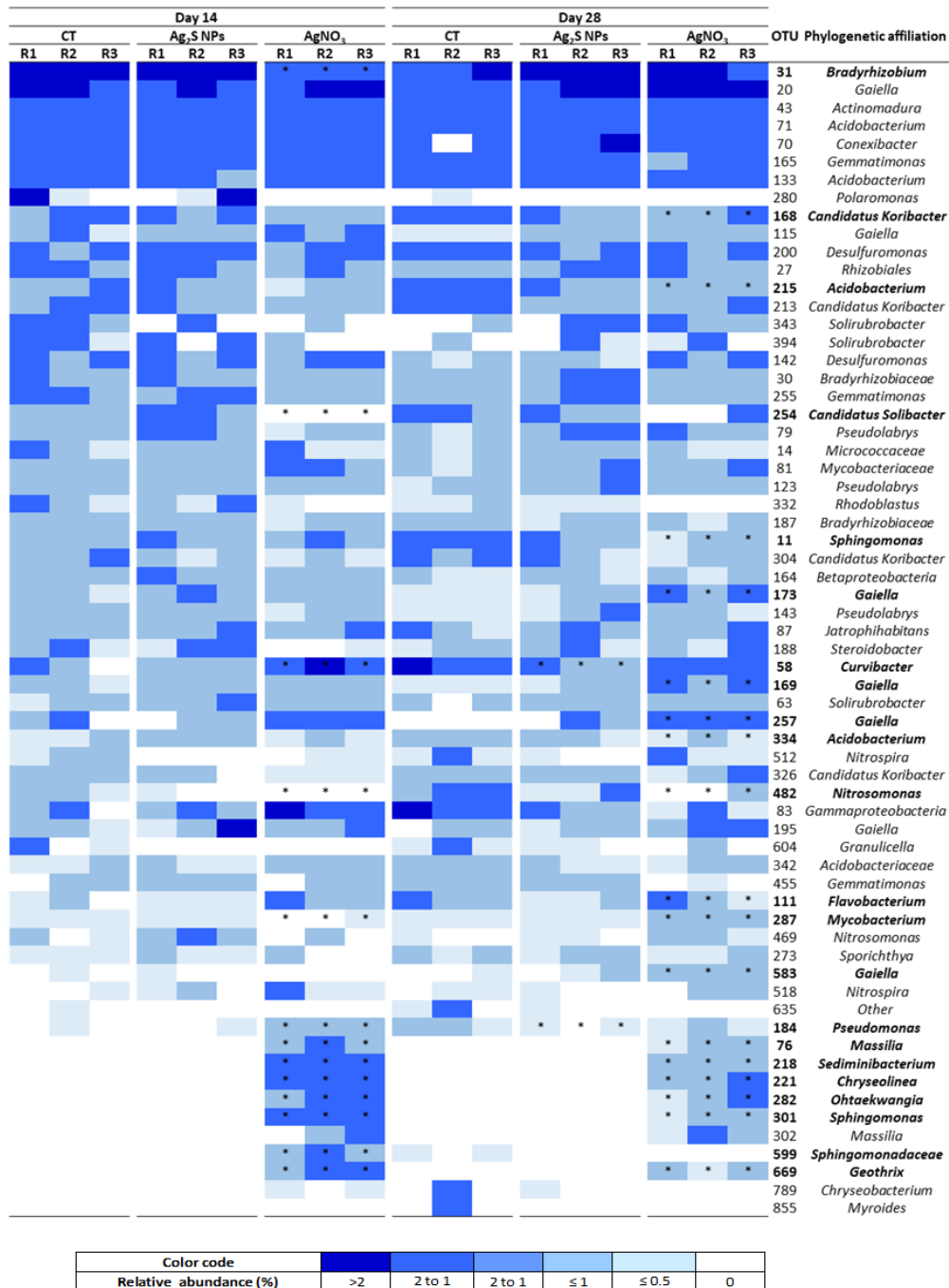


Figure 4. Relative abundance of the most represented OTUs (30 most abundant per treatment) in exposed soil at both 14 and 28 days of exposure. The color code represents the relative OTU abundance (%) in each sample. Asterisks (*) indicate significant differences towards the respective control (CT), for each sampling time (two-way ANOVA, $p < 0.05$; Tukey HSD). Bold genera names indicate significant differences between silver treatments (AgNO₃ vs. Ag₂S NPs), for each sampling time (two-way ANOVA, $p < 0.05$; Tukey HSD).

Table 2. Functional inference for the soil microbiome exposed to 10 mg (Ag) kg⁻¹ soil for AgNO₃ and Ag₂S NPs, at day 14 and 28. The average values (n=3) for each silver treatment and control (CT) were computed using the Piphillin software. The arrows indicate a decrease (↓) and increase (↑) in relative abundance of genes encoding the listed functions/products toward the respective CT. Statistical differences across the treatments were highlighted in dark-blue (■ significantly decrease) and light-blue (■ significantly increase) using two-way ANOVA (Tukey HSD, p<0.05).

KEGG Orthology	KEGG ID	Day-14				Day-28								
		AgNO ₃ vs. CT		Ag ₂ S NPs vs. CT		Ag ₂ S NPs vs. AgNO ₃		AgNO ₃ vs. CT		Ag ₂ S NPs vs. AgNO ₃				
		Tendency	P-value	Tendency	P-value	Tendency	P-value	Tendency	P-value	Tendency	P-value			
Carbohydrate metabolism	Pyruvate ferredoxin oxidoreductase delta subunit	K00171	↑		↑		↑		↓	0.001	↑	0.009	↑	<0.001
	Pyruvate ferredoxin oxidoreductase gamma subunit	K00172	↑		↑		↑		↓		↑	0.03	↑	0.011
	<i>norB</i> : Nitric oxide reductase subunit B	K04561	↓	<0.001	↓		↑	<0.001	↓		↓		↑	
	<i>nasB</i> : Assimilatory nitrate reductase electron transfer subunit	K00360	↑		↑		↑		↓	0.003	↑		↑	
	<i>nasA</i> : Assimilatory nitrate reductase catalytic subunit	K00372	↓		↓		↑		↓	0.03	↑		↑	
	<i>nirK</i> : Nitrite reductase (NO-forming)	K00368	↓		↑		↑		↑	<0.001	↑		↑	0.015
Nitrogen metabolism	<i>nifH</i> : nitrogenase iron protein NifH	K02588	↑		↑		↑		↑	0.004	↑		↑	0.038
	<i>nifK</i> : nitrogenase molybdenum-iron protein beta chain	K02591	↑		↑		↑		↑	0.004	↑		↑	0.037
	<i>nirA</i> : Ferredoxin-nitrite reductase	K00366	↓		↑		↑		↑	0.032	↑		↑	0.016
	<i>narH, narY, nxrB</i> : nitrate reductase / nitrite oxidoreductase, beta subunit	K00371	↑		↓		↓		↑	<0.001	↓	0.008	↓	<0.001
	<i>pmoA-amoA</i> : methane/ammonia monooxygenase subunit A	K10944	↑		↓		↓		↑	<0.001	↓	0.010	↓	<0.001
	<i>nrfA</i> : Nitrite reductase (cytochrome c-552)	K03385	↑		↑		↓		↓	0.040	↑		↓	0.003
	<i>nrfH</i> : Cytochrome c nitrite reductase small subunit	K15876	↓		↑		↑		↓		↑		↑	0.008
	Adenylylsulfate kinase	K00860	↓		↓		↓		↑		↓	0.049	↓	
Transferases	Sulfur carrier protein ThiS adenylyltransferase	K03148	↓		↓		↓		↓	0.004	↑	0.008	↑	
	beta-lysine N6-acetyltransferase	K21935	↑		↑		↑		↓	0.012	↑	0.011	↑	
	serine/threonine-protein kinase	K12132	↓	0.019	↓		↑		↓	0.047	↓		↑	
Oxidoreductases	ADP-reducing hydrogenase subunit HndA	K18330	↑		↑		↑		↓	0.012	↑	0.011	↑	
	NADP-reducing hydrogenase subunit HndC	K18331	↑		↑		↑		↓	0.012	↑	0.011	↑	
Transporters	<i>cusA, silA</i> : copper/silver efflux system protein	K07787	↑		↑		↑		↓	0.008	↓		↑	0.019

	<i>mdtB</i> ; multidrug efflux pump	K07788	↓	↓	↑	↓	0.003	↓	↑	0.019
	<i>mdtC</i> ; multidrug efflux pump	K07789	↓	↓	↑	↓	0.005	↓	↑	0.043
	ABC-2 type transport system ATP-binding protein	K01990	↓	↑	↑	↓	0.033	↓	↑	
	Phosphonate transport system substrate-binding protein	K02044	↑	↑	↓	↓		↑	↑	
	rhIR, phzR; LuxR family transcriptional regulator, quorum-sensing system regulator RhIR	K18099	↓	↓	↑	↑	0.023	↓	↑	0.017
<i>Quorum sensing</i>	lasR; LuxR family transcriptional regulator, quorum-sensing system regulator LasR	K18304	↓	↓	↑	↑	<0.001	↑	↓	0.001
	solR, cepR, tofR; LuxR family transcriptional regulator, quorum-sensing system regulator SolR	K19666	↑	↔	↓	↔	<0.001	↔	↔	
Flagellar assembly	outer membrane protein FlgP	K09860	↓	↓	↔	↔	0.013	↔	↔	0.024
	flagellar biosynthesis protein FlgN	K02399	↑	↓	↑	↑	0.026	↓	↑	0.002

3.1.2. Effect on soil microbiome after 28 days of exposure

At day 28, clustering and PCoA analysis showed a clear impact of both AgNO₃ and Ag₂S NPs in the soil microbiome structure (Figure 1). Control samples were arranged in a distinct branch from the exposed soils, sharing 55% of similarity (Figure 1 B). The PCoA showed a similar spatial separation, in which 74.8% of the variance was explained by two axes (PCO1=16.4% and PCO2=58.4%) (Figure 1 D). Silver exposed samples were separate from the CT along the first axis (PCO1). The Permanova analysis confirmed a significant impact of both silver forms toward CT in the bacterial community structure [PERMANOVA (Ag₂S NPs vs. CT): $t=2.71$; $P=0.001$; (AgNO₃ vs. CT) $t=1.59$; $P=0.001$]. However, differences between silver forms were not observed (PERMANOVA: $t=1.44$, $P=0.102$).

Regarding the diversity analysis (Table 1), a significant decrease in the number of OTUs observed (S : $F=4.16$, $p=0.042$) and in the Shannon-Wiener index (H' : $F=6.12$, $p=0.048$) was observed for the AgNO₃-treated soils but not for the Ag₂S NPs-treated soils.

At class level (Figure 3 B), a significant increase ($+1.4\% \pm 0.1$) in the relative abundance of Chitinophagia ($F=19.99$; $p=0.028$) was detected for Ag₂S NPs-treated soil, in comparison to CT. In AgNO₃-treated soil it was observed a significant increase in the relative abundance of Cytophagia ($6.7\% \pm 1.1$; $F=61.39$, $p<0.001$), Chitinophagia ($2.5\% \pm 0.1$; $F=61.39$, $p<0.001$), and Holophagia ($1.9\% \pm 0.1$; $F=217.58$, $p<0.001$); and a significant decrease in the relative abundance of Alphaproteobacteria ($5.4\% \pm 1.3$; $F=9.59$, $p=0.027$), Actinobacteria ($4.0\% \pm 0.5$; $F=18.89$, $p=0.07$), Acidimicrobiia ($1.7\% \pm 0.1$; $F=6.02$; $p=0.033$). Comparing silver forms, differences in relative abundance of Alphaproteobacteria ($F=9.59$, $p=0.017$, $-5.8\% \pm 1.4$, in AgNO₃-treated soils), Actinobacteria ($F=18.89$, $p=0.03$, $-4.8\% \pm 0.5$ in AgNO₃-treated soils), and Cytophagia ($F=61.40$, $p<0.001$, $+6.7\% \pm 1.4$ in AgNO₃-treated soils) were detected.

At genus level, the Ag₂S NPs significantly affected low-abundance genera (relative abundance $<2\%$). For instance, it was noted a decrease in the relative abundance of *Edaphobacter* (Acidobacteria class; -0.4%) and *Curvibacter* (Betaproteobacteria; -1.6%) and an increase of *Acidisphaera* and *Elstera* (Alphaproteobacteria; $+0.2\%$ and $+0.1\%$, respectively), an unidentified genus affiliated with Intrasporangiaceae family (Actinobacteria, $+0.3\%$); and *Chitinophaga* (Chitinophagia, $+0.3\%$) towards the control. Besides, three genera were not detected in Ag₂S NPs-treated soil while being present in control soil: *Fluviicola*, *Pandoraea* and a genus affiliated with Chromobacteriaceae. A

stronger impact at genus level was observed in AgNO₃-treated soil, where a total of 32 genera were significantly impacted (Figure 3, Table S5). In comparison to the CT, 12 genera were not detected in AgNO₃-treated soil, and seven genera were exclusively detected in soils exposed to AgNO₃, namely *Chryseolinea*, *Ohtaekwangia*, *Sediminibacterium*, *Frateuria*, *Geothrix*, *Mucilaginibacter*, and *Haematococcus*. Comparing silver forms, the abundance of 19 genera was distinctly affected (Table S5), in which 13 genera increased in abundance and six genera decreased in AgNO₃-treated soil in comparison to Ag₂S NPs soil (Table S5). Additionally, *Angustibacter* was exclusively detected in spiked soils, irrespective of the contaminant, presenting a relative abundance of 0.14% and 0.21% in Ag₂S NPs-treated and AgNO₃-treated soils (Table S5), respectively.

From the 30 most abundant OTUs for each condition (Figure 4; Table S4), the relative abundance of two OTUs [OTU 58 (*Curvibacter*) and OTU 184 (*Pseudomonas*)] significantly decreased in Ag₂S NPs-treated soil. In AgNO₃-treated soil a significant change in the relative abundance of 17 OTUs towards CT was observed. These affiliated with *Massilia* (OTU 76), *Nitrosomonas* (OTU 482), Sphingomonadales (OTU 11), *Sphingomonas* (OTU 301), *Candidatus Koribacter* (OTU 168), *Acidobacterium* (OTU 215), *Acidobacterium* (OTU 334), *Gaiella* (OTUs 173, 169, 257, and 583), *Mycobacterium* (OTU 287), *Chryseolinea* (OTU 221), *Ohtaekwangia* (OTU 282), *Sediminibacterium* (OTU 218), *Flavobacterium* (OTU 111), and *Geothrix* (OTU 669). Considering the differences among silver forms, significant differences were registered for all the OTUs mentioned above (Table S4).

At day-28, the predicted functional profile of soil Lufa 2.2 microbiome differed in soils spiked with Ag₂S NPs or AgNO₃ towards the respective CT (Table 2). In soil exposed to Ag₂S NPs, a significant decrease was observed in the average relative abundance of genes involved in the nitrification process [-16.1% of *amoA* gene (ammonia to hydroxylamine) and -11.2% of *nxB* gene (nitrite to nitrate)] and in sulfur reduction [-17.2% of *cysC* gene (sulfate to sulfide)] (Figure S2); while a significant increase was noted in genes involved in carbon fixation [encoding pyruvate ferredoxin oxidoreductase delta (+22.0%) and gamma (+65.0%) subunits]. On the other hand, in AgNO₃-treated soils, it was predicted a reduction in genetic determinants associated with assimilatory nitrate reduction (-8.0% of *nasA*, -54.2% of *nasB*, and -27.3% of *nirA*), dissimilatory nitrate reduction (-100% of *nrfA*), denitrification (-17.4% of *nirK*), nitrogen fixation (-36.3% of *nifK* and -36.3% of *nifH*); and a significant increase in

genes related to the nitrification process (+10.1% of *amoA* and +23.4% of *nxB*) (Figure S2). Besides, the relative abundance of *nrfH* gene, involved in the dissimilatory nitrate reduction, decreased in AgNO₃-treated soil (-90.4%) towards the Ag₂S NPs-treated soil (Figure S2). Regarding sulfur cycle, the relative abundance of genes related to assimilatory sulfur reduction (sulfate to sulfide) increased in soil spiked with AgNO₃ (*cysJ* gene: +24.1% toward the control and +21.0% toward the Ag₂S NPs-treated soil). Additionally, a significant decrease of genes associated to resistance mechanisms was predicted in AgNO₃-treated soil in comparison to the CT, including efflux pumps (-28.1% of *mdtB* and *mdtC*, and -23.9% of *cusA* and *silA*). Also, the relative abundance of *Quorum Sensing* transcriptional regulators [*i.e.*, *rhlR* (+48.0%) and *lasR* (+59.2%)] were predicted to increase in AgNO₃-treated soil. Finally, AgNO₃ exposure increased the relative abundance of sequences encoding the flagellar biosynthesis protein FlgN.

3.2. Abundance and diversity of ammonia-oxidizing bacteria (AOB) and nitrite-oxidizing bacteria (NOB)

The bacterial abundance was inferred from the abundance of the 16S rRNA gene, and the relative abundance of AOB and NOB was inferred from the abundance of marker genes (*amoA*, *nxB*, respectively) divided by the abundance of the 16S rRNA gene (Figure 5).

The abundance of 16S rRNA gene varied between 10⁸ to 10⁹ copies per gram of soil for each treatment (CT, Ag₂S NPs or AgNO₃), regardless of the exposure time. Significant changes were only detected for AgNO₃-treated soil, which presented 62.4% ± 1.5 and 67.4% ± 5.8 reduction of 16S rRNA gene copy numbers towards the CT and Ag₂S NPs-treated soils, respectively, after day-28 (AgNO₃ vs. CT: F=13.36, p=0.018; AgNO₃ vs. Ag₂S NPs: F=13.36, p=0.014).

A significant increase on the relative abundance of AOB-specific genes and NOB-specific genes (per 16S rRNA gene copy) was observed during the exposure period (day 14<28: p=0.008 and p=0.002, respectively), regardless of soil treatments. Comparing treatments, a higher (101.8% ± 32.7; p=0.027) relative abundance of NOB (AgNO₃ vs. CT: p=0.007) was observed at day-28 in AgNO₃-exposed soil.

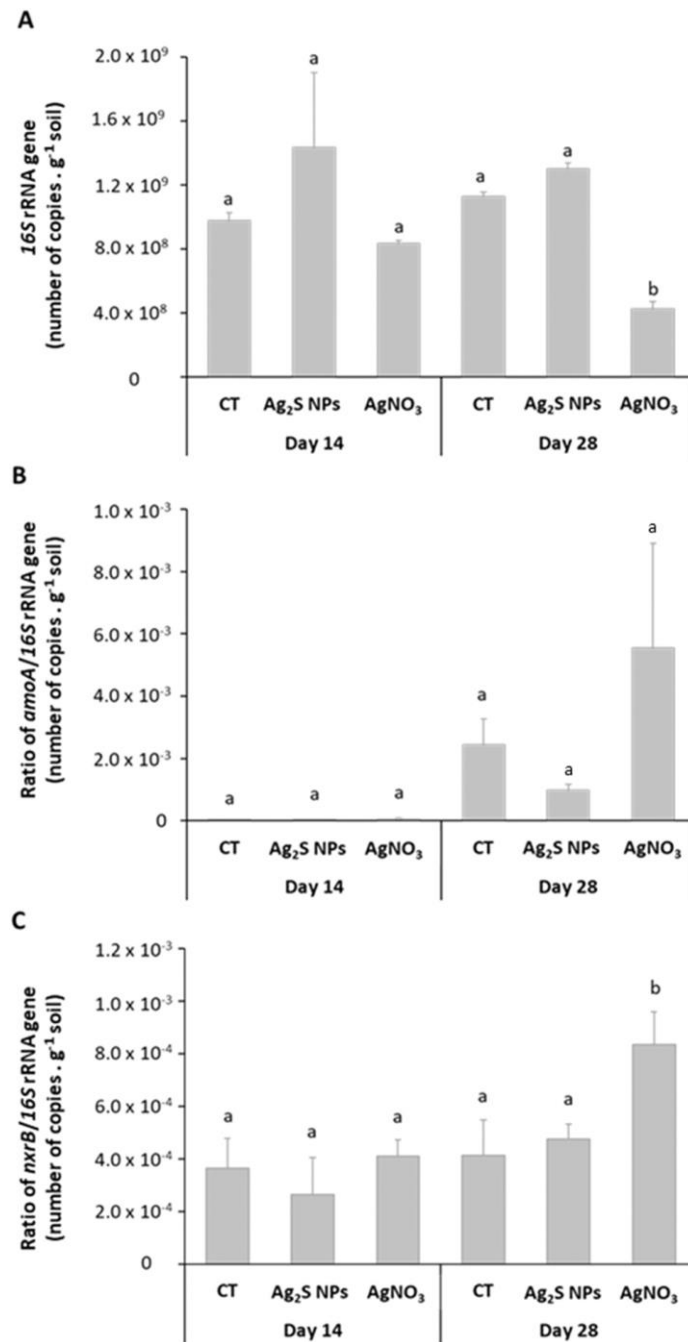


Figure 5. Copy numbers per gram of soil of 16S rRNA gene (A), and the ratio of *amoA*/16S rRNA gene (B), and *nxB*/16S rRNA gene (C) as determined by qPCR. Values represent a mean ± standard deviation of three replicates. Results are presented for non-treated soil (CT) and for soil treated with 10 mg (Ag) kg⁻¹ soil of AgNO₃ or Ag₂S NPs. The soil sampling was done at days 14 and 28. Different letters (a, b) indicate a significant difference among soil treatments for each sampling time (two-way ANOVA, $p < 0.05$; Tukey HSD).

In terms of gene diversity, from the analysis of the *amoA* and *nxB* qPCR melting curves, a distinct and time and/or treatment-dependent profile, comprising several distinct peaks, was observed suggesting the presence of different gene variants (Figure

S3 and S4). In fact, analysis of clone libraries confirmed a distinct *nxB* variant in AgNO₃-treated soil at 14 days, with 34 different nucleotides and 23 amino acid substitutions when compared to the one in control and Ag₂S NPs-treated soil at 28 days (Figure S5). Regarding the *amoA* gene, the same variant was present in all soils after 14 days (Figure S6). However, after 28 days of exposure, distinct variants of this gene were detected across the treatments. For instance, the variant detected in Ag₂S NPs-treated soil differed in one nucleotide and was predicted to encode similar a protein (did not change the number of amino acid) from the one detected in control soil (Figure S6). In AgNO₃-treated soil 2 *amoA* variants were detected, which were absent from the other soils, and differed in 9 nucleotides (2 amino acids) and 13 nucleotides (2 amino acids) from the variant detected in control soil.

Further analysis of *amoA* and *nxB* diversity was accomplished through DGGE (Figure 6 A and B). Cluster analysis of *nxB* DGGE profiles suggested a distinct nitrite-oxidizing bacterial community in AgNO₃-treated soil and CT, although still sharing similarities of 81.1% (day 14) and 79.0% (day 28). On the other hand, community exposed to Ag₂S NPs grouped closer with CT, sharing 84.3% (day 14) and 86.0% of similarity (day 28). Also, the clustering analysis revealed that the silver treatments and the time of exposure had a clear impact on the diversity of ammonia oxidizers (inferred from *amoA* gene variants). At longer exposure periods, the similarity of AOB communities exposed to Ag₂S NPs decreased towards the respective control soil (day 14=80.0% of similarity and day 28=54.0% similarity). The communities exposed to AgNO₃-treated soil showed a clear separation with control group, sharing at least 71.0%, over-time (days 14 and 28).

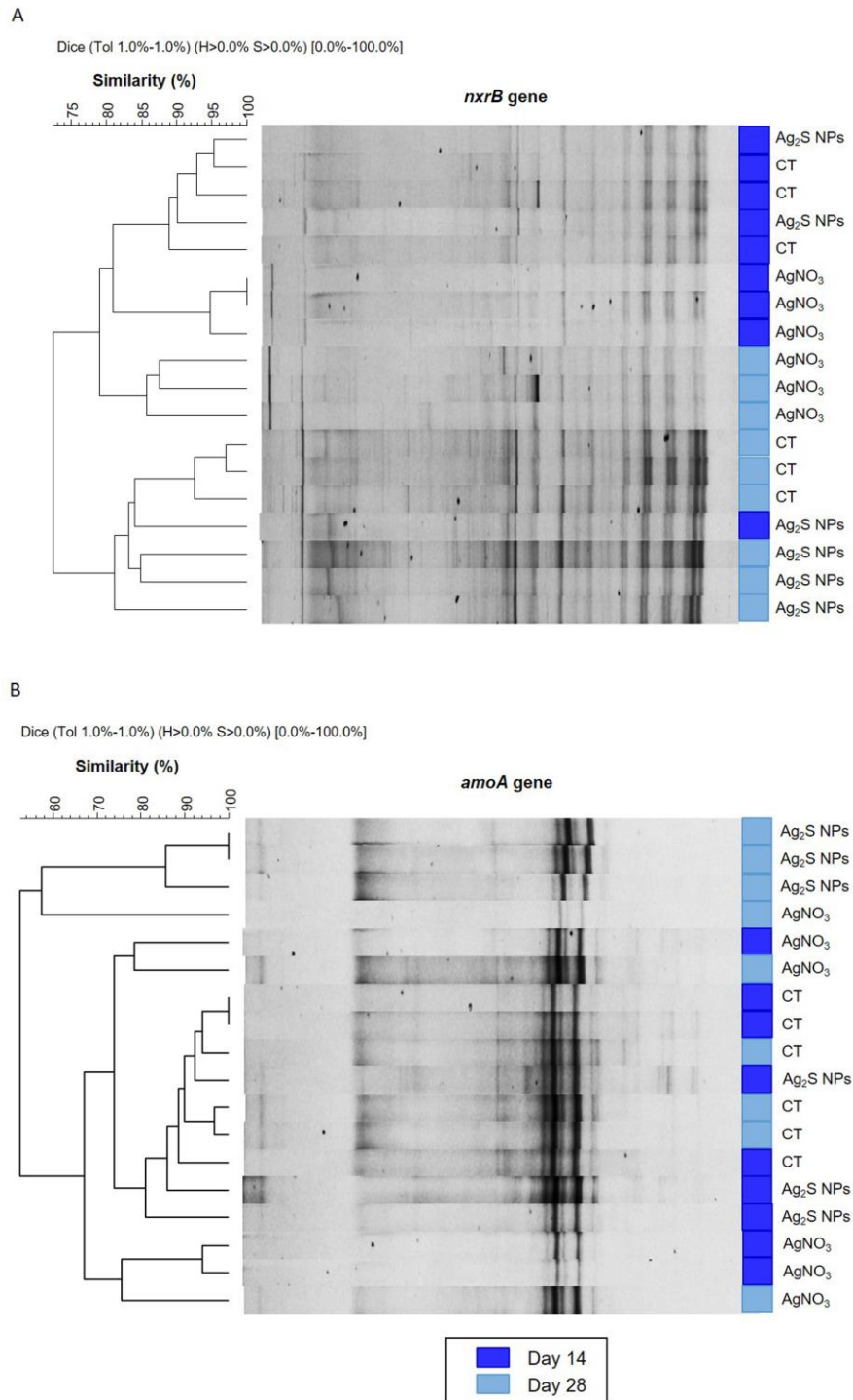


Figure 6. Clustering analysis of DGGE profiles of the *nxB* (A) and *amoA* (B) genes amplified from Lufa 2.2 soil (CT) and soil exposed to 10 mg (Ag) kg⁻¹ soil of Ag₂S NPs or AgNO₃. Soil sampling was done at days 14 and 28. The cluster was constructed based on Dice similarity.

4. Discussion

In the present study, we applied high throughput sequencing to evaluate the effect of Ag₂S NPs and AgNO₃ on soil microbiome, after 14 and 28 days of exposure, using an

indoor mesocosm experiment. In our previous work, we reported effects of Ag₂S NPs and AgNO₃ on soil microbiome structure through DGGE analysis (Peixoto *et al.*, 2020). Based on that, the current work intended to further explore the changes observed, identifying the affected bacterial phylogenetic groups and possible effects in the microbiome function, particularly in the nitrogen cycle.

In overall, our study demonstrated a soil microbiome structure (core microbiome) consistent with previous reports in natural soils (Doolette *et al.*, 2016; McGee *et al.*, 2017), including the Lufa soil (Fajardo *et al.*, 2019), where Proteobacteria, Acidobacteria, and Actinobacteria are the dominant phyla.

4.1. Silver exposure affects the soil microbiome structure and composition

The Ag₂S NPs induced a shift in the soil microbiome structure, at class and genera and OTU level, but mostly at latter exposure period (day-28). AgNO₃ exerted a stronger impact than Ag₂S NPs over-time, either at day 14 and 28. In accordance with our results, the study of Doolette and their co-authors (2016) revealed that the relative abundance of soil OTUs was significantly less sensitive to Ag₂S NPs (152 nm, PVP coated) in comparison to the silver in nano-form (AgNPs - 44 nm) and in ionic-form (AgNO₃). In literature, these distinct silver effects have been related with the different Ag⁺ dissolution/concentration rates in porewater/soils, in which a faster Ag⁺ dissolution from AgNO₃ was well documented (Schultz *et al.*, 2018; Wang *et al.*, 2017; Schlich *et al.*, 2018). Also, our previous study (Peixoto *et al.*, 2020) suggested that the Ag⁺ concentration in porewater may explain the stronger impact exerted by AgNO₃. On the other hand, the observed effect of Ag₂S NPs (day 28) may be explained by the specific-particle effect, since the dissolved/dissociated Ag⁺ concentration in porewater was similar between control and Ag₂S NPs-exposed soil (full analysis was described in Peixoto *et al.*, 2020).

Typically, healthy soils are associated with a high diversity of bacteria, reflecting greater metabolic capacity and plasticity. In our work, only for AgNO₃-treated soils was observed a significant reduction in richness and diversity, at both sampling times, probably due the higher Ag⁺ concentration in porewater (as described in our previous work, Peixoto *et al.*, 2020). A similar impact in these indexes was already reported in forest soil (Shah *et al.*, 2014) and activated sludge (Yang *et al.*, 2014; Forstner *et al.*, 2020), after exposure to AgNPs and AgNO₃. On the other hand, using environmentally

relevant concentrations (0.015, 0.15, and 1.5 $\mu\text{g kg}^{-1}$), the study by Montes de Oca-Vásquez (*et al.*, 2020) demonstrated that AgNPs did not change the diversity and composition (at phyla and genera levels) of the agricultural soil bacterial community. Although Ag₂S NPs did not affect the overall diversity of soil microbiome, some bacterial groups were significantly affected at class and genera level. For instance, Chitinophagia (Bacteroidetes phylum), known for their lignocellulose-degrading capability (Kishi *et al.*, 2017), showed to be enriched in Ag₂S NPs-treated soils, an outcome that resulted mainly from a significant increase in the relative abundance of the genus *Chitinophaga* in comparison to the CT. Similarly, this class significantly increased in AgNO₃-treated soils, but in this case due to an increase of *Sediminibacterium* (day 14 and 28) and *Niastella* (day 14). Chitinophagia class comprises endospore-forming microorganisms capable of degrading plant-derived carbohydrates in terrestrial ecosystem (Kishi *et al.*, 2017). This ability to form spores can enable these microorganisms to survive in metal-contaminated soils (Frenk *et al.*, 2013). In agreement with our results, Doolette *et al.*, (2016) also observed a significant increase of this class in both silver-treated soils (Ag₂S NPs and AgNO₃). In opposite to our results, Zhang *et al.* (2020) reported a significant decrease in the relative abundance of Chitinophagales and Chitinophagaceae in agricultural soil (pH \approx 5) exposed to 100 mg kg⁻¹ of AgNPs (20 nm), in the presence/absence of cucumber plants. This contradictory result can be explained by the distinct AgNPs type (non-sulfidized), the higher concentration tested, the absence of soil invertebrates, and the distinct plant species used, compared to our study. As for AgNO₃-treated soil, an increase in the relative abundance of Rubrobacteria (day-14), Cytophagia (days 14 and 28), Holophagia (day-28), and a decrease of Actinobacteria (days 14 and 28) Alphaproteobacteria (day-28) and Acidimicrobiia (day-28) were observed in our study. Most of these classes are commonly detected in metal-contaminated soils, mainly due to the expression of resistance mechanisms (like sporulation, efflux pumps and *Quorum Sensing*, among others) (Ward *et al.*, 2009; Chater *et al.*, 2010; Kou *et al.*, 2018). Regarding the most sensitive classes to AgNO₃, the decrease of nitrogen-fixing *Bradyrhizobium* seems to contribute to the decline of Alphaproteobacteria abundance under AgNO₃ exposure. This genus is involved in different biochemical functions in soils, including photosynthesis, induction of root nodules, symbiotic nitrogen fixation and denitrification (Jones *et al.*, 2016), suggesting that AgNO₃ negatively impact these functions. These multiple roles in nitrogen cycle and plant growth-promotion make the

ecology of *Bradyrhizobium* particularly important for agroecosystem (Jones *et al.*, 2016). Additionally, several less abundant genera (<2% in relative abundance) in the Lufa 2.2 community were affected by the silver exposure, regardless of form. For instance, the genus *Angustibacter* was exclusively detected in both silver-treated soils, suggesting its tolerance to silver. In agreement, a study from Kou and collaborators (2018) showed the same genus emerged in soils contaminated with lead, zinc and copper, at different exposure scenarios (*e.g.*, mixture or single contaminants). On the other hand, in our study, *Fluviicola* (Flavobacteriia), *Pandoraea* and an unidentified genus affiliated with Chromobacteriaceae (Betaproteobacteria) were not detected in Ag₂S NPs- and AgNO₃-treated soils in comparison to the CT. These genera might play a crucial role in nitrogen cycle, in which *Fluviicola* is involved in nitrification process (Guan *et al.*, 2020); *Pandoraea* is part of the rhizosphere, promoting plant growth and participating in the biodegradation of complex organic substances (Kumar *et al.*, 2018); and some species of the Chromobacteriaceae family are potentially involved in denitrifying processes, since they possess plastocyanin/azurin genes (Santos *et al.*, 2018). The presence of wheat in our experiment may explain these observed changes in the abundance of N-related genera. In fact, the uptake, accumulation and phytotoxicity of Ag₂S NPs (at 10 mg kg⁻¹ soil) in wheat were already reported (Wang *et al.*, 2017; Wang *et al.*, 2015), which may influence the abundance of these genera in contaminated soils.

4.2. Silver exposure affects the soil microbiome function

Observed changes in soil microbiome structure and relative abundance of different taxa, probably result in significant alterations in terms of microbiome functions. In the current study, the abundance of different genes and/or proteins related with the carbon, nitrogen and sulfur metabolisms was projected to be influenced by silver exposure. Accordingly, the negative impact of AgNPs and graphene oxides nanoparticles in the carbohydrate and amino acid metabolisms was previously described in the study from Li and their collaborators in (2019). In our study it was predicted a decrease in genes *cusA* and *silA* in AgNO₃-treated soils (day-28), involved in metal efflux. It is well reported that metallic nanoparticles (*e.g.*, AgNPs and ZnO nanoparticles) can block the activity of efflux pumps, reducing the efficiency of this resistance mechanism (Banoee *et al.* 2010). On the other hand, in our study, the AgNO₃ seems to promote the cell communication mechanisms, namely *Quorum Sensing* (QS). This increase might lead to

higher community resistance to contaminants and may also promote bacterial virulence (Ali *et al.*, 2017; Zakaria and Dhar, 2020). In addition, at longer exposure periods, in AgNO₃-treated soil a higher abundance of the flagellar biosynthesis protein FlgN was predicted, which may result in the increase of the filament polymerization in bacteria (Cairns *et al.*, 2014). In accordance, the intensification on cell motility in the presence of AgNPs was previously reported (Li *et al.*, 2019; Yan *et al.*, 2020). On the other hand, both silver forms (Ag₂S NPs and AgNO₃) negatively impacted the abundance of flagellar outer membrane lipoprotein (FlgP), after 14 days of exposure, required in motility functions as a colonization factor (Martinez *et al.*, 2009).

4.2.1. Silver exposure affects the nitrification process

Over-time, in each soil, our study revealed a significant increase in the abundance of total bacteria, AOB and NOB. This observation might result from the presence of plants and invertebrates, since it is well known that the invertebrates potentially increase the ammonia in soils, possibly favouring bacteria involved in the nitrogen cycle (Thakur and Geisen, 2019; Bouchon *et al.*, 2016). The AOB and NOB are involved in the two key steps of the nitrification process. The first step of nitrification plays a major role in sustaining the global nitrogen cycle and is accomplished primarily by the participation of AOB (Prosser *et al.*, 2011). In our experiment, the *amoA*/16S rRNA gene ratio was similar across soil treatments. In contrast, a study by Doolette and co-workers (2016) showed a decreased in abundance of this gene in AgNO₃-treated soil (pH=5.1) towards the Ag₂S NPs-treated soil, at 10 mg (Ag) kg⁻¹ soil and after 28 days of exposure. On the other hand, the study of Yan (*et al.*, 2020) demonstrated a decline of AOB and ammonia-oxidizing archaea (AOA) abundance in AgNPs-treated soil (yellow-brown loam soil; pH=7.13), at 100 mg (Ag) kg⁻¹ soil. The study of Wang *et al.* (2020) showed also a significant reduction on AOB abundance (number of *amoA* gene copies per gram of dry sediments) in AgNPs-treated sediments [10 mg (Ag) L⁻¹] towards non-exposed sediments (pH=7.15). These contradictory results may be due to differences in experimental design (*e.g.*, the presence of different plant and animal species in our study), and distinct soil properties (*e.g.*, lower pH in our study), which might influence the soil microbiome composition and structure and consequently its function. In fact, in our study, the total bacteria abundance (inferred from the 16S rRNA gene abundance) in silver-treated soils was higher than observed in the study by Doolette *et al.*, (2016). In comparison to control, the relative abundance of AOB (*e.g.*, OTU 469 affiliated with

Nitrosomonas) was significantly higher in AgNO₃-treated soils at day-28 and an increase in *amoA* sequences was predicted by functional profile inference. The second step of the nitrification process is carried out by NOB, where nitrite is oxidized to nitrate (Prosser *et al.*, 2011). Our results suggested that only AgNO₃ promote the activity/abundance of NOB in soils, in which, a significant increase in *nxB*/16S rRNA genes ratio was observed in this soil. Also, this result was corroborated by *in silico* analysis. A wide range of phyla were identified as players in this step, namely Chloroflexi, Nitrospirae, Nitrospinae and Proteobacteria (Pinto *et al.*, 2016). Accordingly, in our study, the increased abundance of *Nitrospira* (*e.g.*, OTU 518) possible contributed to the increase of *nxB* abundance in communities exposed to AgNO₃. Although Piphillin analysis predicted a decrease of *nxB* and *amoA* abundance in Ag₂S NPs-treated soils, the qPCR analysis did not detect significant alterations in these genes' abundance. This contradictory result may be due limitations of the applied methodologies. In fact, the metagenome inference (using Piphillin) is a valuable approach previously validated in several studies (Fajardo *et al.*, 2019; Yan *et al.*, 2020) but results accuracy depends on the availability of annotated reference genomes, which may lack in genome databases. Thus, in our study, the qPCR technique was used to confirm some of the identified effects, due to its high specificity and sensitivity (Kim *et al.*, 2013). Due to limitations, primer-template mismatches and the presence of PCR inhibitors (*e.g.*, metals, humic, flavic and phenolic acids) may also affect the accuracy of qPCR results (Sidstedt *et al.*, 2015; Wilson, 1997). Hence, further investigations should explore the effects on microbiome function, using other approaches such as whole-metagenome sequencing.

Interestingly, we observed distinct *amoA* or *nxB* variants in soils exposed to different treatments (especially the one exposed to AgNO₃) and over time. This result suggests a potential succession of AOB and NOB, probably with different degree of silver-tolerance. In accordance, the study by Das *et al.*, (2012) confirmed the appearance and stimulation of distinct AOB phylotypes after AgNPs and AgNO₃ exposure in natural freshwater, at 0.01 to 1 mg (Ag) L⁻¹. These authors suggested that the selection of these phylotypes may result from the presence of silver or metal-resistance genes or from their ability to survive the metal exposure by entering an inactive (*e.g.*, endospores) state (Das *et al.*, 2012). Other reports already suggested that the nitrogen content, soil pH and temperature, potentially promote the emergence of *amoA* gene variants in *Nitrosomonas* (Aigle *et al.*, 2019; Ramanathan, 2017). Also, the emergence of *nxB*

variants in *Nitrospira* can be promoted by different concentrations of nitrite, dissolved oxygen, and temperature (Maixner *et al.*, 2006; Park and Noguera, 2008; Siripong and Rittmann, 2007).

5. Conclusions

The current study demonstrates that Ag₂S NPs and AgNO₃, at 10 mg kg⁻¹ soil alter the soil microbiome structure, under a complex scenario of exposure (multi-species mesocosm). These effects were mainly detected at longer time of exposure (day-28) highlighting the importance to study these nanoparticles at long-term exposure scenarios. In Ag₂S NPs-treated soil was observed a significant increase in the abundance of Chitinophagia, suggesting a silver-tolerance effect. Also, functional analysis revealed a significative alteration in the abundance of genes involved in different metabolisms, contributing to the imbalance of crucial soil functions related with S, N and C cycles. On the other hand, AgNO₃ exerted a stronger impact on soil microbiome, *e.g.*, being observed a negative impact on richness and diversity indexes, on OTU relative abundance, on predicted functions, and on the abundance of total bacteria, when compared to soil exposed to CT and Ag₂S NPs. Distinct effects were detected concerning the silver form, suggesting a distinct mode of action. Accordingly, for soils exposed to AgNO₃, general mechanisms of defence as the QS were predicted to increase in this soil, while specific mechanisms of silver resistance (*e.g.*, genes encoding for efflux pumps) were decreased. In complex exposure scenario (indoor mesocosms including invertebrates and plants), nitrification seems to be favoured in AgNO₃-treated soil. Additionally, both silver-treated soils presented different *amoA* and *nrrB* variants, suggesting a possible emergence of bacteria phylotypes with different degrees of tolerance to silver. Further studies aiming at exploring the long-term effect of silver sulfide form, using a complex scenario of exposure and metagenomic analysis, would be helpful for developing strategies for the inclusion of this compounds in the risk assessment regulations.

6. Acknowledgements

All the authors were funded by the EU H2020 project Nano-FASE (Nanomaterial Fate and Speciation in the Environment; grant no. 646002). Thanks are due to FCT/MCTES

for the financial support to CESAM (UIDP/50017/2020+UIDB/50017/2020), through national funds, and for the PhD grant of S. Peixoto (SFRH/BD/117738/2016).

7. References

- Aigle, A., Prosser, J. I., Gubry-Rangin, C. (2019). The application of high-throughput sequencing technology to analysis of *amoA* phylogeny and environmental niche specialisation of terrestrial bacterial ammonia-oxidisers. *Environmental Microbiome*, 14(1), 3.
- Ali, S. G., Ansari, M. A., Jamal, Q. M. S., Khan, H. M., Jalal, M., Ahmad, H., Mahdi, A. A. (2017). Antiquorum sensing activity of silver nanoparticles in *P. aeruginosa*: an *in silico* study. *In Silico Pharmacology*, 5(1), 12.
- Almeida, A. R., Domingues, I., Henriques, I. (2021). Zebrafish and water microbiome recovery after oxytetracycline exposure. *Environmental Pollution*, 272, 116371.
- Amorim, C. L., Alves, M., Castro, P. M., Henriques, I. (2018). Bacterial community dynamics within an aerobic granular sludge reactor treating wastewater loaded with pharmaceuticals. *Ecotoxicology and Environmental Safety*, 147, 905-912.
- Angly, F. E., Dennis, P. G., Skarszewski, A., Vanwonderghem, I., Hugenholtz, P., Tyson, G. W. (2014). CopyRighter: a rapid tool for improving the accuracy of microbial community profiles through lineage-specific gene copy number correction. *Microbiome*, 2(1), 1-13.
- Banooee, M., Seif, S., Nazari, Z. E., Jafari-Fesharaki, P., Shahverdi, H. R., Moballegh, A., Shahverdi, A. R. (2010). ZnO nanoparticles enhanced antibacterial activity of ciprofloxacin against *Staphylococcus aureus* and *Escherichia coli*. *Journal of Biomedical Materials Research Part B: Applied Biomaterials*, 93(2), 557-561.
- Bouchon, D., Zimmer, M., Dittmer, J. (2016). The terrestrial isopod microbiome: an all-in-one toolbox for animal-microbe interactions of ecological relevance. *Frontiers in Microbiology*, 7, 1472.
- Bour, A., Mouchet, F., Silvestre, J., Gauthier, L., Pinelli, E. (2015). Environmentally relevant approaches to assess nanoparticles ecotoxicity: a review. *Journal of Hazardous Materials*, 283, 764-777.
- Cairns, L. S., Marlow, V. L., Kiley, T. B., Birchall, C., Ostrowski, A., Aldridge, P. D., Stanley-Wall, N. R. (2014). FlgN is required for flagellum-based motility by *Bacillus subtilis*. *Journal of Bacteriology*, 196(12), 2216-2226.

- Chater, K. F., Biro, S., Lee, K. J., Palmer, T., Schrempf, H. (2010). The complex extracellular biology of *Streptomyces*. *FEMS Microbiology Reviews*, 34(2), 171-198.
- Das, P., Williams, C. J., Fulthorpe, R. R., Hoque, M. E., Metcalfe, C. D., Xenopoulos, M. A. (2012). Changes in bacterial community structure after exposure to silver nanoparticles in natural waters. *Environmental Science & Technology*, 46(16), 9120-9128.
- Doolette, C. L., Gupta, V. V., Lu, Y., Payne, J. L., Batstone, D. J., Kirby, J. K., McLaughlin, M. J. (2016). Quantifying the sensitivity of soil microbial communities to silver sulfide nanoparticles using metagenome sequencing. *PloS one*, 11(8), e0161979.
- Eren, A. M., Morrison, H. G., Lescault, P. J., Reveillaud, J., Vineis, J. H., Sogin, M. L. (2015). Minimum entropy decomposition: unsupervised oligotyping for sensitive partitioning of high-throughput marker gene sequences. *The ISME Journal*, 9(4), 968-979.
- Fajardo, C., Costa, G., Nande, M., Botías, P., García-Cantalejo, J., Martín, M. (2019). Pb, Cd, and Zn soil contamination: Monitoring functional and structural impacts on the microbiome. *Applied Soil Ecology*, 135, 56-64.
- Frenk, S., Ben-Moshe, T., Dror, I., Berkowitz, B., Minz, D. (2013). Effect of metal oxide nanoparticles on microbial community structure and function in two different soil types. *PloS one*, 8(12), e84441.
- Forstner, C., Orton, T. G., Wang, P., Kopittke, P. M., Dennis, P. G. (2020). Wastewater Treatment Processing of Silver Nanoparticles Strongly Influences Their Effects on Soil Microbial Diversity. *Environmental Science & Technology*, 54(21), 13538-13547.
- Geitner, N.; Hendren, C.; Cornelis, G.; Kaegi, R.; Lead, J.; Lowry, G.; Lynch, I.; Nowack, B.; Petersen, E.; Bernhardt, E.; Brown, S.; Chen, W.; de Garidel-Thoron, C.; Hanson, J.; Harper, S.; Jones, K.; von der Kammer, F.; Kennedy, A.; Kidd, J.; Matson, C.; Metcalfe, C.; Pedersen, J.; Peijnenburg, W.; Quik, J.; Rodrigues, S. M.; Rose, J.; Sayre, P.; Simonin, M.; Svendsen, C.; Tanguay, R.; Tufenkji, N.; van Teunenbroek, T.; Thies, G.; Tian, Y.; Rice, J.; Turner, A.; Liu, J.; Unrine, J.; Vance, M.; White, J.; Wiesner, M. (2020). Harmonizing across environmental nanomaterial testing media for increased comparability of nanomaterial datasets. *Environmental Science: Nano*, 7(1), 13-36.

- Giese, B., Klaessig, F., Park, B., Kaegi, R., Steinfeldt, M., Wigger, H., Gottschalk, F. (2018). Risks, release and concentrations of engineered nanomaterial in the environment. *Scientific Reports*, 8(1), 1-18.
- Guan, X., Gao, X., Avellan, A., Spielman-Sun, E., Xu, J., Laughton, S. N., Zhang, R. (2020). CuO nanoparticles alter the rhizospheric bacterial community and local nitrogen cycling for wheat grown in a calcareous soil. *Environmental Science & Technology*, 54(14), 8699-8709.
- Iwai, S., Weinmaier, T., Schmidt, B. L., Albertson, D. G., Poloso, N. J., Dabbagh, K., DeSantis, T. Z. (2016). Piphillin: improved prediction of metagenomic content by direct inference from human microbiomes. *PloS one*, 11(11), e0166104.
- Jansson, J. K., Hofmockel, K. S. (2018). The soil microbiome—from metagenomics to metaphenomics. *Current opinion in Microbiology*, 43, 162-168.
- Jones, F. P., Clark, I. M., King, R., Shaw, L. J., Woodward, M. J., Hirsch, P. R. (2016). Novel European free-living, non-diazotrophic *Bradyrhizobium* isolates from contrasting soils that lack nodulation and nitrogen fixation genes—a genome comparison. *Scientific Reports*, 6, 25858.
- Kaegi, R., Voegelin, A., Sinnet, B., Zuleeg, S., Hagendorfer, H., Burkhardt, M., Siegrist, H. (2011). Behavior of metallic silver nanoparticles in a pilot wastewater treatment plant. *Environmental Science & Technology*, 45(9), 3902-3908.
- Kim, J., Lim, J., Lee, C. (2013). Quantitative real-time PCR approaches for microbial community studies in wastewater treatment systems: applications and considerations. *Biotechnology Advances*, 31(8), 1358-1373.
- Kisand, V., Cuadros, R., Wikner, J. (2002). Phylogeny of culturable estuarine bacteria catabolizing riverine organic matter in the northern Baltic Sea. *Applied and Environmental Microbiology*, 68(1), 379-388.
- Kishi, L. T., Lopes, E. M., Fernandes, C. C., Fernandes, G. C., Sacco, L. P., Alves, L. M. C., Lemos, E. G. (2017). Draft genome sequence of a *Chitinophaga* strain isolated from a lignocellulose biomass-degrading consortium. *Genome Announcements*, 5(3), e01056-16.
- Kou, S., Vincent, G., Gonzalez, E., Pitre, F. E., Labrecque, M., Brereton, N. J. (2018). The response of a 16S ribosomal RNA gene fragment amplified community to lead, zinc, and copper pollution in a Shanghai field trial. *Frontiers in microbiology*, 9, 366.

- Kumar, M., Verma, S., Gazara, R. K., Kumar, M., Pandey, A., Verma, P. K., Thakur, I. S. (2018). Genomic and proteomic analysis of lignin degrading and polyhydroxyalkanoate accumulating β -proteobacterium *Pandoraea* sp. ISTKB. *Biotechnology for Biofuels*, 11(1), 154.
- Li, G. F., Huang, B. C., Zhang, Z. Z., Cheng, Y. F., Fan, N. S., Jin, R. C. (2019). Recent advances regarding the impacts of engineered nanomaterials on the anaerobic ammonium oxidation process: performances and mechanisms. *Environmental Science: Nano*, 6(12), 3501-3512.
- Liu, S., Wang, C., Hou, J., Wang, P., Miao, L., Fan, X., Xu, Y. (2018). Effects of Ag and Ag₂S nanoparticles on denitrification in sediments. *Water Research*, 137, 28-36.
- Maixner, F., Noguera, D. R., Anneser, B., Stoecker, K., Wegl, G., Wagner, M., Daims, H. (2006). Nitrite concentration influences the population structure of *Nitrospira*-like bacteria. *Environmental Microbiology*, 8(8), 1487-1495.
- Martinez, R. M., Dharmasena, M. N., Kirn, T. J., Taylor, R. K. (2009). Characterization of two outer membrane proteins, FlgO and FlgP, that influence *Vibrio cholerae* motility. *Journal of Bacteriology*, 191(18), 5669-5679.
- Martín-Pozo, L., de Alarcón-Gómez, B., Rodríguez-Gómez, R., García-Córcoles, M. T., Çipa, M., Zafra-Gómez, A. (2019). Analytical methods for the determination of emerging contaminants in sewage sludge samples. A review. *Talanta*, 192, 508-533.
- Martens, A., (2005). Denitrification, *In* Encyclopedia of soils in the environment, Elsevier, 378-382, ISBN 9780123485304.
- McGee, C. F., Storey, S., Clipson, N., Doyle, E. (2018). Concentration-dependent responses of soil bacterial, fungal and nitrifying communities to silver nano and micron particles. *Environmental Science and Pollution Research*, 25(19), 18693-18704.
- McGillicuddy, E., Murray, I., Kavanagh, S., Morrison, L., Fogarty, A., Cormican, M., Morris, D. (2017). Silver nanoparticles in the environment: Sources, detection and ecotoxicology. *Science of the Total Environment*, 575, 231-246.
- Montes de Oca-Vásquez, G. M., Solano-Campos, F., Vega-Baudrit, J. R., López-Mondéjar, R., Odriozola, I., Vera, A., Bastida, F. (2020). Environmentally relevant concentrations of silver nanoparticles diminish soil microbial biomass

- but do not alter enzyme activities or microbial diversity. *Journal of Hazardous Materials*, 391, 122224.
- Nelson, M. B., Martiny, A. C., Martiny, J. B. (2016). Global biogeography of microbial nitrogen-cycling traits in soil. *Proceedings of the National Academy of Sciences*, 113(29), 8033-8040.
- Nkongolo, K. K., Narendrula-Kotha, R. (2020). Advances in monitoring soil microbial community dynamic and function. *Journal of Applied Genetics*, 1-15.
- Peixoto, S., Khodaparast, Z., Cornelis, G., Lahive, E., Etxabe, A. G., Baccaro, M., Papadiamantis, A.G., Gonçalves, S.F., Lynch, I., Busquets-Fite, M., Puentes, V., Loureiro, S., Henriques, I. (2020). Impact of Ag₂S NPs on soil bacterial community—A terrestrial mesocosm approach. *Ecotoxicology and Environmental Safety*, 206, 111405.
- Pester, M., Maixner, F., Berry, D., Rattei, T., Koch, H., Lückner, S., Loy, A. (2014). *NxrB* encoding the beta subunit of nitrite oxidoreductase as functional and phylogenetic marker for nitrite-oxidizing Nitrospira. *Environmental Microbiology*, 16(10), 3055-3071.
- Pinto, A. J., Marcus, D. N., Ijaz, U. Z., Bautista-de Lose Santos, Q. M., Dick, G. J., Raskin, L. (2016). Metagenomic evidence for the presence of comammox Nitrospira-like bacteria in a drinking water system. *Mosphere*, 1(1).
- Prosser, J. I. (2011) Soil nitrifiers and nitrification. Nitrification, eds Ward BB, Arp DJ, Ramanathan, B., Boddicker, A. M., Roane, T. M., Mosier, A. C. (2017). Nitrifier gene abundance and diversity in sediments impacted by acid mine drainage. *Frontiers in Microbiology*, 8, 2136.
- Reinsch, B. C., Levard, C., Li, Z., Ma, R., Wise, A., Gregory, K. B., Lowry, G. V. (2012). Sulfidation of silver nanoparticles decreases *Escherichia coli* growth inhibition. *Environmental Science & Technology*, 46(13), 6992-7000.
- Rotthauwe, J. H., Witzel, K. P., Liesack, W. (1997). The ammonia monooxygenase structural gene *amoA* as a functional marker: molecular fine-scale analysis of natural ammonia-oxidizing populations. *Applied and Environmental Microbiology*, 63(12), 4704-4712.
- Santos, A. B., Costa, P. S., do Carmo, A. O., da Rocha Fernandes, G., Scholte, L. L. S., Ruiz, J., Nascimento, A. M. A. (2018). Insights into the genome sequence of *Chromobacterium amazonense* isolated from a tropical freshwater lake. *International Journal of Genomics*, 2018, 1-10.

- Schlich, K., Hoppe, M., Kraas, M., Schubert, J., Chanana, M., Hund-Rinke, K. (2018). Long-term effects of three different silver sulfide nanomaterials, silver nitrate and bulk silver sulfide on soil microorganisms and plants. *Environmental Pollution*, 242, 1850–1859.
- Schultz, C. L., Gray, J., Verweij, R. A., Busquets-Fité, M., Puentes, V., Svendsen, C., Matzke, M. (2018). Aging reduces the toxicity of pristine but not sulphidised silver nanoparticles to soil bacteria. *Environmental Science: Nano*, 5(11), 2618–2630.
- Shah, V. Jones, J., Dickman, J., Greenman, S. (2014). Response of soil bacterial community to metal nanoparticles in biosolids. *Journal of Hazardous Materials*, 274, 399–403.
- Sidstedt, M., Jansson, L., Nilsson, E., Noppa, L., Forsman, M., Rådström, P., Hedman, J. (2015). Humic substances cause fluorescence inhibition in real-time polymerase chain reaction. *Analytical Biochemistry*, 487, 30-37.
- Siripong, S., Rittmann, B. E. (2007). Diversity study of nitrifying bacteria in full-scale municipal wastewater treatment plants. *Water research*, 41(5), 1110-1120.
- Starnes, D. L., Unrine, J. M., Starnes, C. P., Collin, B. E., Oostveen, E. K., Ma, R., Tsyusko, O. V. (2015). Impact of sulfidation on the bioavailability and toxicity of silver nanoparticles to *Caenorhabditis elegans*. *Environmental Pollution*, 196, 239-246.
- Tavares, R. D., Tacão, M., Figueiredo, A. S., Duarte, A. S., Esposito, F., Lincopan, N., Henriques, I. (2020). Genotypic and phenotypic traits of blaCTX-M-carrying *Escherichia coli* strains from an UV-C-treated wastewater effluent. *Water Research*, 184, 116079.
- Thakur, M. P., Geisen, S. (2019). Trophic regulations of the soil microbiome. *Trends in Microbiology*, 27(9), 771-780.
- Turner S., Pryer KM., Miao VP., Palmer JD. 1999. Investigating deep phylogenetic relationships among cyanobacteria and plastids by small subunit rRNA sequence analysis. *The Journal of Eukaryotic Microbiology* 46:327–338.
- Wang, C., Liu, S., Hou, J., Wang, P., Miao, L., Li, T. (2020). Effects of silver nanoparticles on coupled nitrification–denitrification in suspended sediments. *Journal of Hazardous Materials*, 389, 122130.
- Wang, P., Lombi, E., Sun, S., Scheckel, K. G., Malysheva, A., McKenna, B. A., Kopittke, P. M. (2017). Characterizing the uptake, accumulation and toxicity of

- silver sulfide nanoparticles in plants. *Environmental Science: Nano*, 4(2), 448-460.
- Wang, P., Menzies, N. W., Lombi, E., Sekine, R., Blamey, F. P. C., Hernandez-Soriano, M. C., Kopittke, P. M. (2015). Silver sulfide nanoparticles (Ag₂S-NPs) are taken up by plants and are phytotoxic. *Nanotoxicology*, 9(8), 1041-1049.
- Ward, N. L., Challacombe, J. F., Janssen, P. H., Henrissat, B., Coutinho, P. M., Wu, M., Barabote, R. D. (2009). Three genomes from the phylum Acidobacteria provide insight into the lifestyles of these microorganisms in soils. *Applied and Environmental Microbiology*, 75(7), 2046-2056.
- Wilson, I. G. (1997). Inhibition and facilitation of nucleic acid amplification. *Applied and Environmental Microbiology*, 63(10), 3741.
- Wu, J., Bai, Y., Lu, B., Li, C., Menzies, N. W., Bertsch, P. M., Kopittke, P. M. (2020). Application of sewage sludge containing environmentally-relevant silver sulfide nanoparticles increases emissions of nitrous oxide in saline soils. *Environmental Pollution*, 265, 114807.
- Yan, C., Huang, J., Cao, C., Li, R., Ma, Y., Wang, Y. (2020). Effects of PVP-coated silver nanoparticles on enzyme activity, bacterial and archaeal community structure and function in a yellow-brown loam soil. *Environmental Science and Pollution Research*, 27(8), 8058-8070.
- Yang, Y., Quensen, J., Mathieu, J., Wang, Q., Wang, J., Li, M., Alvarez, P. J. (2014). Pyrosequencing reveals higher impact of silver nanoparticles than Ag⁺ on the microbial community structure of activated sludge. *Water Research*, 48, 317-325.
- Zakaria, B. S., Dhar, B. R. (2020). Changes in syntrophic microbial communities, EPS matrix, and gene-expression patterns in biofilm anode in response to silver nanoparticles exposure. *Science of The Total Environment*, 139395.
- Zhang, H., Huang, M., Zhang, W., Gardea-Torresdey, J. L., White, J. C., Ji, R., Zhao, L. (2020). Silver nanoparticles alter soil microbial community compositions and metabolite profiles in unplanted and cucumber-planted soils. *Environmental Science & Technology*, 54(6), 3334-3342.

8. Supplementary material

8.1. List of Figures

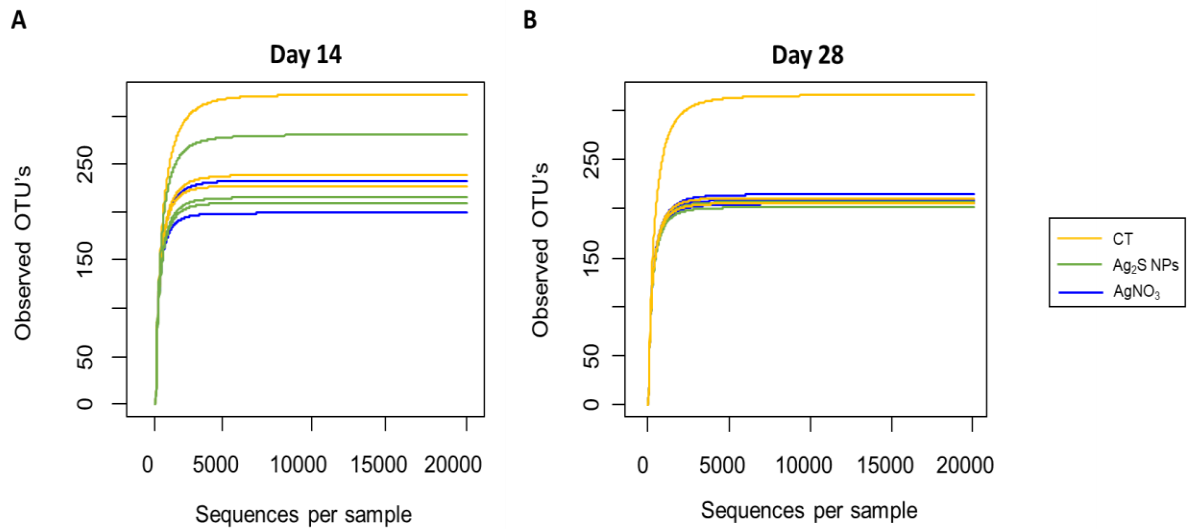


Figure S1. Rarefaction curves of OTUs as function of the number of reads. Results of three replicates are presented for control (CT) and for each treatment [10 mg (Ag) kg⁻¹ soil of AgNO₃ and Ag₂S NPs]. The soil sampling was done at day 14 (A) and day 28 (B). The sequencing effort reaches an average of 53117.

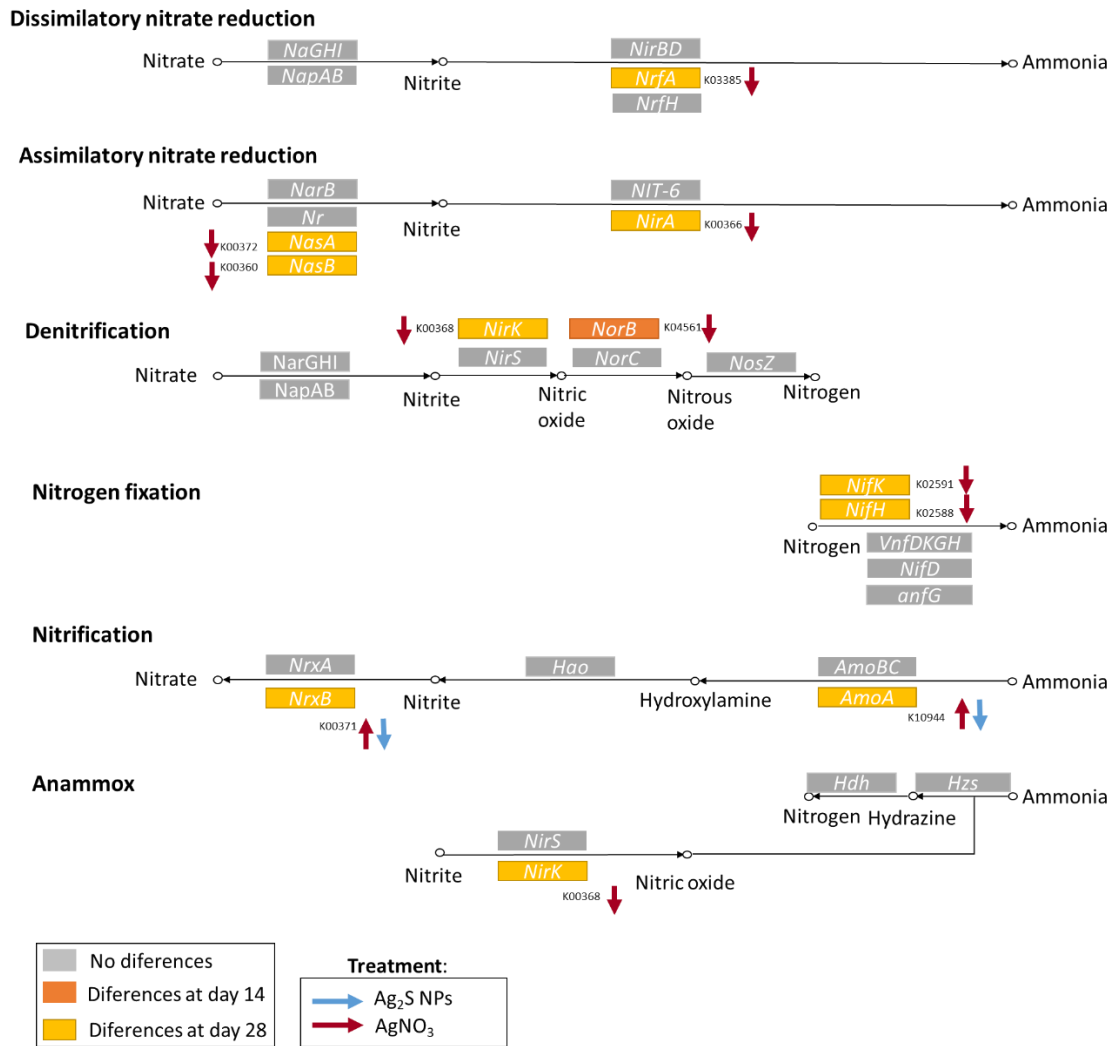


Figure S2. Nitrogen metabolism of soil microbiome exposed to 10 mg (Ag) kg⁻¹ of Ag₂S NPs or AgNO₃. The data was based on predicted relative abundance of nitrogen-related genes. Different colors (■ no differences; ■ differences at day 14; and ■ differences at day 28) represent significant differences in the silver forms towards the respective control (two-way ANOVA; Tukey HSD; p<0.05). The arrows indicate the significant increased (↑) or decreased (↓) in the relative abundance of genes between silver treatments (blue: Ag₂S NPs; red: AgNO₃) toward the respective control (two-way ANOVA; Tukey HSD; p<0.05).

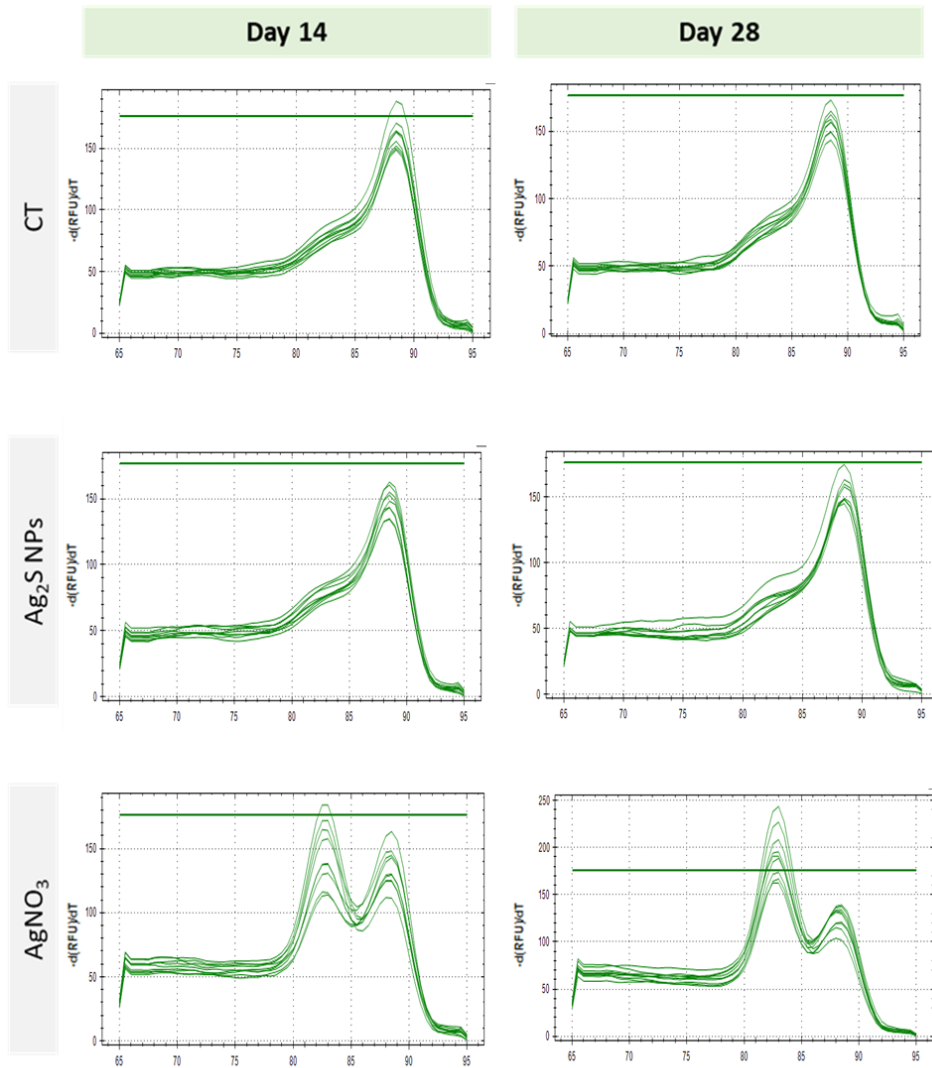


Figure S3. Melting curves for *nxB* gene amplified from Lufa 2.2 soil (CT), and soils exposed to 10 mg kg⁻¹ of Ag₂S NPs or AgNO₃, after 14 and 28 days of exposure.

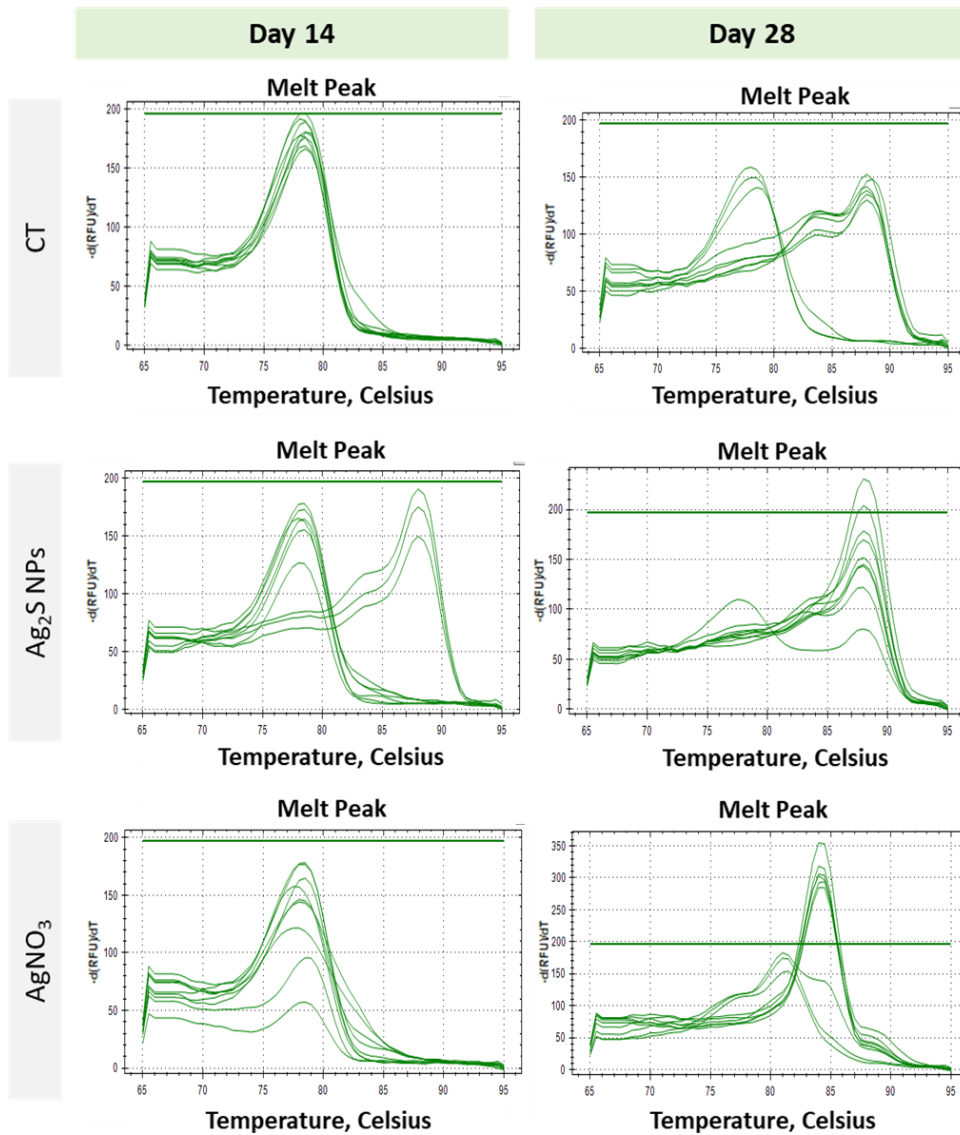


Figure S4. Melting curves for *amoA* gene amplified from Lufa 2.2 soil (CT), soils exposed to 10 mg kg^{-1} of Ag_2S NPs or AgNO_3 , after 14 and 28 days of exposure.

```

CT - day 28:      GGTGGGCCAGGCGGCGATCGGATACATTCGGACGGACCAAGAGTGGCGGTTTCGTGAACATCTATGAAGA
Ag2S NPs - day 28: GGTGGGCCAGGCGGCGATCGGATACATTCGGACGGACCAAGAGTGGCGGTTTCGTGAACATCTATGAAGA
AgNO3 - day 14:  GGTGGGCCAGGCGGCGATCGGCTACATCCGGACGGACCAAGAGTGGCGATTTCGTCAATATCTATGAGGA

CT - day 28:      TACGGCGACCTCGATGCGGTCGTTGGTCTGAAGGAATCGACAGATCAGGATTTTCGAGAGATGAGCCCTGG
Ag2S NPs - day 28: TACGGCGACCTCGATGCGGTCGTTGGTCTGAAGGAATCGACAGATCAGGATTTTCGAGAGATGAGCCCTGG
AgNO3 - day 14:  TACGGCGACCTCGATGCGGGCCCTCGTGAAGGCATCGACAAGACCGGATTCTCAGGGACGAACCGTGG

CT - day 28:      CGTTTGACGGGCAGCAGTCTGCCGGAGCATGAAACATTCTTTTCTATCTCCAGCGGATTTGCAACCAC
Ag2S NPs - day 28: CGTTTGACGGGCAGCAGTCTGCCGGAGCATGAAACATTCTTTTCTATCTCCAGCGGATTTGCAACCAC
AgNO3 - day 14:  AAGATGACGGGCAGCAGTCTGCCGGAGCATGAGACCTTCTTTCTATCTCCAGCGGATCTGCAACCAC

CT - day 28:      TGCACGTATCCAGGCTGCCTG
Ag2S NPs - day 28: TGCACGTATCCAGGCTGCCTG
AgNO3 - day 14:  TGCACGTATCCCGGCTGCTTG

```

Figure S5. Multiple Sequence Alignments of *nxB* sequences, using Clustal Omega software. Treatments represented the soil microbiome exposed to 10 mg (Ag) kg⁻¹ soil of Ag₂S NPs or AgNO₃ or non-exposed (CT), at 14 and 28 days of exposure. Grey color indicates differences in nucleotides compared between treatments.

1-AgNO ₃ - day 28:	ATGATACCGGGAGCGCTGGTCATGGACACCGTCCTGCTGCTGACCCGCAACTGGATGGTC
2-AgNO ₃ - day 28:	ATGATACCGGGAGCGCTGGTCATGGACACCGTCCTGCTGCTCACCGCAACTGTTTGGTC
3-AgNO ₃ - day 14:	ATGATCCAGGCGCTTGATGATGGATACGATTCCTGCTGTTGACGGGTAACCTGGCTGATT
4-Ag ₂ S NPs - day 28:	ATGATACCGGGAGCGCTGGTCATGGACACCGTCCTGCTGCTGACCCGCAACTGGATGGTC
5-CT - day 28:	ATGATACCGGGAGCGCTGGTCATGGACACCGTCCTGCTGCTGACCCGCAACTGGATGGTC
1-AgNO ₃ - day 28:	ACAGCCCTGATTGGCGGGCGCGCTTTGGTCTTTTGGTCTACCCGGGCAACTGGCCGATA
2-AgNO ₃ - day 28:	ACAGCCCTGATTGGCGGGCGCGCTTTGGTCTTTTGGTCTACCCGGGCAACTGGCCGATA
3-AgNO ₃ - day 14:	ACAGCTCTGTTAGGCGGTGGTTTCTTTGGACTATTCTTCTACCCAGGCAACTGGCCGATA
4-Ag ₂ S NPs - day 28:	ACAGCCCTGATTGGCGGGGCGCGCTTTGGTCTTCTGTTCTACCCGGGCAACTGGCCATT
5-CT - day 28:	ACAGCCCTGATTGGCGGGGCGCGCTTTGGTCTTCTGTTCTACCCGGGCAACTGGCCATT
1-AgNO ₃ - day 28:	TTTGGCCCCACCCACTGCCGCTGGTAGCTGAAGGCGTACTGCTGTCGTTGGCCGACTAC
2-AgNO ₃ - day 28:	TTTGGCCCCACCCACTGCCGCTGGTAGCTGAAGGCGTACTGCTGTCGTTGGCCGACTAC
3-AgNO ₃ - day 14:	TCTGGTCCAACCCACTTACCATTGGTAGTAGAAGGCGTACTGCTGTCAGTAGCTGACTAC
4-Ag ₂ S NPs - day 28:	TTTGGCCGACCCACTGCCGCTGGTAGCTGAAGGCGTACTGCTGTCGTTGGCCGACTAC
5-CT - day 28:	TTTGGCCGACCCACTGCCGCTGGTAGCTGAAGGCGTACTGCTGTCGTTGGCCGACTAC
1-AgNO ₃ - day 28:	ACCGGCTTTCTGTATGTACGCACCGGCACGCCTGAGTACGTGCGCCTGATCGAACAAAGGC
2-AgNO ₃ - day 28:	ACCGGCTTTCTGTATGTACGCACCGGCACGCCTGAGTACGTGCGCCTGATCGAACAAAGGC
3-AgNO ₃ - day 14:	ACCGGCTTCTGTATGTACGTACCGGTACACCGGAATACGTACGCCTGATTGAACAAAGGC
4-Ag ₂ S NPs - day 28:	ACCGGCTTCTGTATGTACGCACCGGCACGCCGAGTACGTGCGCCTGATCGAACAAAGGC
5-CT - day 28:	ACCGGCTTCTGTATGTACGCACCGGCACGCCGAGTACGTGCGCCTGATCGAACAAAGGC
1-AgNO ₃ - day 28:	TCGCTGCGAACCTTTGGCGGGCACACTACGGTCATTGCGGCATTCTTCTCCGCGTTTGTGTC
2-AgNO ₃ - day 28:	TCGCTGCGAACCTTTGGCGGGCACACTACGGTCATTGCGGCATTCTTCTCCGCGTTTGTGTC
3-AgNO ₃ - day 14:	TCAGTGCCTACCTTTGGTGGTCACACCACAGTGATTGCGAGCTTCTTCTCAGCCTTCGTA
4-Ag ₂ S NPs - day 28:	TCGCTGCGAACCTTTGGCGGGCACACTACGGTCATTGCGGCATTCTTCTCCGCGTTTGTGTC
5-CT - day 28:	TCGCTGCGAACCTTTGGCGGGCACACTACGGTCATTGCGGCATTCTTCTCCGCGTTTGTGTC
1-AgNO ₃ - day 28:	TCCATGCTCATGTTCTGCGTGTGGTGGTACTTTGGCAAAGTCTACTGCACCGCCTTCTAC
2-AgNO ₃ - day 28:	TCCATGCTCATGTTCTGCGTGTGGTGGTACTTTGGCAAAGTCTACTGCACCGCCTTCTAC
3-AgNO ₃ - day 14:	TCCATGCTGATGTTCTGCGTATGGTGGTACTTTGGCAAAGTCTACTGCACCGCCTTCTAC
4-Ag ₂ S NPs - day 28:	TCCATGCTCATGTTCTGCGTGTGGTGGTACTTTGGCAAAGTCTACTGCACCGCCTTCTAC
5-CT - day 28:	TCCATGCTCATGTTCTGCGTGTGGTGGTACTTTGGCAAAGTCTACTGCACCGCCTTCTAC

Figure S6. Multiple sequence alignment of *amoA* variants, using Clustal Omega software. A representative of each variant per treatment was included. Treatments include soil exposed for 14 and 28 days to 10 mg (Ag) kg⁻¹ soil Ag₂S NPs or AgNO₃ or non-exposed (CT). Grey color indicates differences in nucleotides compared between treatments.

8.2. List of Tables

Table S1. Primer sequences and thermocycling conditions for ammonia-oxidizing bacteria (*amoA* gene) and nitrite-oxidizing bacteria (*nxB* gene), and total bacteria (16S rRNA gene).

Target	Molecular method	Primer's sequence (5' – 3')	Thermocycling conditions	Melting curve	Reference
Ammonia-oxidizing bacteria (α -subunit)	Denaturing gradient gel electrophoresis	<i>amoA</i> -1F GC: CCGCCGCGCGGGCGGGCGGGGCGGGGACGG GGGGGGTTTCTACTGGTGGT; <i>amoA</i> -2R: CCCCTCKGSAAAGCCTTCTTC [K = G or T, S = G or C]	98 °C for 3 min; followed by 40 cycles consisting of 98 °C for 30 s, annealing 51°C for 45 s and 60 °C for 45 s. Final extension 72°C for 30 min.	-	Gremion <i>et al.</i> , 2004
	qPCR	<i>amoA</i> -1F: GGGGTTTCTACTGGTGGT; <i>amoA</i> -2R: CCCCTCKGSAAAGCCTTCTTC [K = G or T, S = G or C]	98 °C for 3 min; followed by 40 cycles consisting of 98 °C for 30 s, and 51°C for 45 s	Temperature ramping from 60 to 95 °C.	Rotthauwe <i>et al.</i> , 1997
Nitrite-oxidizing bacteria (<i>Nitrospira</i>)	Denaturing gradient gel electrophoresis	<i>nxB</i> -169F-GC: CGCCCGCCGCGCGGGCGGGGCGGGG CACGGGGGTACAGTTGGTGAACA; <i>nxB</i> -638R: CGGTCTGGTCRATCA	98 °C for 3 min; followed by 40 cycles consisting of 98 °C for 30 s, annealing 52°C for 45 s and 60 °C for 45 s. Final extension 72°C for 30 min.	-	Pester <i>et al.</i> , 2014
	qPCR	<i>nxB</i> -169F: TACATGTGGTGAACA; <i>nxB</i> -638R: CGGTCTGGTCRATCA	98 °C for 3 min; followed by 40 cycles consisting of 98 °C for 30 s and 52°C for 45 s	Temperature ramping from 60 to 95 °C.	Pester <i>et al.</i> , 2014
Total bacteria	qPCR	338F: GACTCCTACGGGAGGCAGCAG 518R: ATTACCGGGCTGCTGG	95 °C for 3 min; followed by 40 cycles consisting of 95 °C for 30 s, and 55°C for 45 s	Temperature ramping from 60 to 95 °C.	Muyzer <i>et al.</i> , 1993

Table S2. Number of reads and OTUs per sample after each sequence data processing step.

Treatment	Sampling time (days)	Replicate	Input sequences	Sequences after preprocessing	Sequences after chimera removal	Sequences assigned to OTU	Sequences assigned to taxa	Count after lineage-specific copy-number correction	Median sequence length after pre-processing
AgNO ₃	14	R1	139340	139113	133924	55137	55137	28392	421
		R2	136803	136611	131368	56865	56779	29305	422
		R3	190139	189867	188173	83219	83047	44789	422
	28	R1	137726	137508	134113	62035	62035	28220	422
		R2	107885	107696	103554	42988	42988	21933	422
		R3	115893	115720	113771	48128	48128	23643	422
CT	14	R1	139317	139117	133591	52136	51997	26371	422
		R2	115290	115097	110604	40632	40518	21127	422
		R3	119892	119728	117859	54565	54305	30854	407
	28	R1	142478	142250	138935	54802	54802	30180	419
		R2	125249	125065	121533	46681	46681	24876	421
		R3	127281	127077	124752	58162	57941	35066	407
Ag ₂ S NPs	14	R1	117900	117682	115004	47569	47308	26633	416
		R2	113522	113344	110152	42568	42496	24007	409
		R3	128314	128137	122085	44572	44492	23646	407
	28	R1	164679	164449	160655	57248	57119	32032	419
		R2	165700	165455	162546	61834	61727	34048	416
		R3	134794	134568	130431	48698	48607	25845	422

Table S3. Statistical analysis of the relative abundance of soil genera, at day 14, using the one-way ANOVA. Treatments represented the soil microbiome non-exposed (CT), and soils exposed to Ag₂S NPs or AgNO₃. In table, multi-comparisons, using the Tukey HSD test, were done considering differences between sampling treatment. The confidence value $p < 0.05$.

Day 14			
Genus	Treatment	F	p
<i>Bradyrhizobium</i>	CT x Ag ₂ S NPs	70.64	0.981
	CT x AgNO ₃		0.038
	Ag ₂ S NPs x AgNO ₃		0.031
<i>Chryseolinea</i>	CT x Ag ₂ S NPs	150.39	0.994
	CT x AgNO ₃		0.007
	Ag ₂ S NPs x AgNO ₃		0.008
<i>Steroidobacter</i>	CT x Ag ₂ S NPs	60.18	0.815
	CT x AgNO ₃		0.037
	Ag ₂ S NPs x AgNO ₃		0.081
Rhodospirillales	CT x Ag ₂ S NPs	80.17	1.000
	CT x AgNO ₃		0.029
	Ag ₂ S NPs x AgNO ₃		0.030
<i>Hyphomicrobium</i>	CT x Ag ₂ S NPs	100.70	0.390
	CT x AgNO ₃		0.048
	Ag ₂ S NPs x AgNO ₃		0.010
<i>Nocardioides</i>	CT x Ag ₂ S NPs	60.38	0.996
	CT x AgNO ₃		0.046
	Ag ₂ S NPs x AgNO ₃		0.051
<i>Ilumatobacter</i>	CT x Ag ₂ S NPs	140.43	0.965
	CT x AgNO ₃		0.010
	Ag ₂ S NPs x AgNO ₃		0.007
<i>Nitrosomonas</i>	CT x Ag ₂ S NPs	50.97	0.867
	CT x AgNO ₃		0.042
	Ag ₂ S NPs x AgNO ₃		0.079
<i>Caenimonas</i>	CT x Ag ₂ S NPs	110.17	0.963
	CT x AgNO ₃		0.018
	Ag ₂ S NPs x AgNO ₃		0.013
Aciditerrimonas	CT x Ag ₂ S NPs	130.82	0.957
	CT x AgNO ₃		0.011
	Ag ₂ S NPs x AgNO ₃		0.008
Bradyrhizobiaceae	CT x Ag ₂ S NPs	120.62	0.950
	CT x AgNO ₃		0.014
	Ag ₂ S NPs x AgNO ₃		0.010
Gammaproteobacteria	CT x Ag ₂ S NPs	530.21	0.859
	CT x AgNO ₃		<0.001
	Ag ₂ S NPs x AgNO ₃		<0.001
Acidobacteriaceae	CT x Ag ₂ S NPs	100.76	0.121
	CT x AgNO ₃		0.008
	Ag ₂ S NPs x AgNO ₃		0.136
<i>Aggregicoccus</i>	CT x Ag ₂ S NPs	90.96	0.330
	CT x AgNO ₃		0.011
	Ag ₂ S NPs x AgNO ₃		0.067
<i>Mycobacterium</i>	CT x Ag ₂ S NPs	130.07	0.803
	CT x AgNO ₃		0.015
	Ag ₂ S NPs x AgNO ₃		0.008
<i>Pseudomonas</i>	CT x Ag ₂ S NPs	110.19	0.868
	CT x AgNO ₃		0.012
	Ag ₂ S NPs x AgNO ₃		0.021
<i>Geothrix</i>	CT x Ag ₂ S NPs	90.86	0.904
	CT x AgNO ₃		0.016
	Ag ₂ S NPs x AgNO ₃		0.026
<i>Sediminibacterium</i>	CT x Ag ₂ S NPs	120.16	0.856
	CT x AgNO ₃		0.010
	Ag ₂ S NPs x AgNO ₃		0.017
Acidisphaera	CT x Ag ₂ S NPs	150.54	1.000
	CT x AgNO ₃		0.007
	Ag ₂ S NPs x AgNO ₃		0.007
Saprospirales	CT x Ag ₂ S NPs	320.82	0.093
	CT x AgNO ₃		0.004
	Ag ₂ S NPs x AgNO ₃		<0.001
Rudaea	CT x Ag ₂ S NPs	80.43	0.254
	CT x AgNO ₃		0.015
	Ag ₂ S NPs x AgNO ₃		0.130

<i>Ohtaekwangia</i>	CT x Ag ₂ S NPs	50.13	0.706
	CT x AgNO ₃		0.049
	Ag ₂ S NPs x AgNO ₃		0.136
Bryobacterales	CT x Ag ₂ S NPs	50.40	0.160
	CT x AgNO ₃		0.041
	Ag ₂ S NPs x AgNO ₃		0.559
<i>Curvibacter</i>	CT x Ag ₂ S NPs	500.40	0.915
	CT x AgNO ₃		<0.001
	Ag ₂ S NPs x AgNO ₃		<0.001
<i>Mucilagimibacter</i>	CT x Ag ₂ S NPs	350.73	1.000
	CT x AgNO ₃		<0.001
	Ag ₂ S NPs x AgNO ₃		<0.001
<i>Elstera</i>	CT x Ag ₂ S NPs	1070.28	1.000
	CT x AgNO ₃		<0.001
	Ag ₂ S NPs x AgNO ₃		<0.001
Burkholderiaceae	CT x Ag ₂ S NPs	600.39	1.000
	CT x AgNO ₃		<0.001
	Ag ₂ S NPs x AgNO ₃		<0.001
Sphingomonadaceae	CT x Ag ₂ S NPs	15320.24	1.000
	CT x AgNO ₃		<0.001
	Ag ₂ S NPs x AgNO ₃		<0.001
<i>Niastella</i>	CT x Ag ₂ S NPs	340.40	1.000
	CT x AgNO ₃		<0.001
	Ag ₂ S NPs x AgNO ₃		<0.001
<i>Azoarcus</i>	CT x Ag ₂ S NPs	490.52	1.000
	CT x AgNO ₃		<0.001
	Ag ₂ S NPs x AgNO ₃		<0.001
<i>Candidatus Thiodiazotropha</i>	CT x Ag ₂ S NPs	80.39	0.683
	CT x AgNO ₃		0.052
	Ag ₂ S NPs x AgNO ₃		0.019
<i>Rivibacter</i>	CT x Ag ₂ S NPs	140.46	0.080
	CT x AgNO ₃		0.080
	Ag ₂ S NPs x AgNO ₃		0.004
<i>Rhodopila</i>	CT x Ag ₂ S NPs	10.18	0.758
	CT x AgNO ₃		0.340
	Ag ₂ S NPs x AgNO ₃		0.711
<i>Dyella</i>	CT x Ag ₂ S NPs	50.65	0.259
	CT x AgNO ₃		0.317
	Ag ₂ S NPs x AgNO ₃		0.035
Oxalobacteraceae	CT x Ag ₂ S NPs	70.71	0.297
	CT x AgNO ₃		0.139
	Ag ₂ S NPs x AgNO ₃		0.019
Xanthomonadaceae	CT x Ag ₂ S NPs	70.92	0.349
	CT x AgNO ₃		0.112
	Ag ₂ S NPs x AgNO ₃		0.018

Table S4. Statistical analysis of the abundance of the most represented OTUs (30 most abundant per treatment) in exposed soil at days 14 and 28. Two-way ANOVA was applied considering a $p < 0.05$ (Tukey HSD method).

Sampling time (day)	OTU ID	Treatments	F	p
14	31	CT x Ag ₂ S NPs	13.800	0.805
		CT x AgNO ₃		0.013
		AgNO ₃ x Ag ₂ S NPs		0.007
	58	CT x Ag ₂ S NPs	0.250	0.994
		CT x AgNO ₃		0.007
		AgNO ₃ x Ag ₂ S NPs		0.008
	143	CT x Ag ₂ S NPs	4.953	0.307
		CT x Ag		0.346
		AgNO ₃ x Ag ₂ S NPs		0.045
	187	CT x Ag ₂ S NPs	21.110	0.144
		CT x AgNO ₃		0.014
		AgNO ₃ x NP		0.002
	254	CT x Ag ₂ S NPs	33.997	0.716
		CT x AgNO ₃		0.001
		AgNO ₃ x Ag ₂ S NPs		0.001
	301	CT x Ag ₂ S NPs	52.922	1.000
		CT x AgNO ₃		<0.001
		AgNO ₃ x Ag ₂ S NPs		1.000
	218	CT x Ag ₂ S NPs	334.749	<0.001
		CT x AgNO ₃		<0.001
		AgNO ₃ x Ag ₂ S NPs		<0.001
	221	CT x Ag ₂ S NPs	144.463	1.000
		CT x AgNO ₃		<0.001
		AgNO ₃ x Ag ₂ S NPs		<0.001
	282	CT x Ag ₂ S NPs	75.582	1.000
		CT x AgNO ₃		<0.001
		AgNO ₃ x Ag ₂ S NPs		<0.001
	669	CT x Ag ₂ S NPs	171.947	1.000
		CT x AgNO ₃		<0.001
		AgNO ₃ x Ag ₂ S NPs		<0.001
184	CT x Ag ₂ S NPs	48.856	.815	
	CT x AgNO ₃		<0.001	
	AgNO ₃ x Ag ₂ S NPs		<0.001	
599	CT x Ag ₂ S NPs	101.315	1.000	
	CT x AgNO ₃		<0.001	
	AgNO ₃ x Ag ₂ S NPs		<0.001	
76	CT x Ag ₂ S NPs	36.878	1.000	
	CT x AgNO ₃		0.001	
	AgNO ₃ x Ag ₂ S NPs		0.001	
58	CT x Ag ₂ S NPs	5.767	0.045	
	CT x AgNO ₃		0.081	
	AgNO ₃ x Ag ₂ S NPs		0.890	
215	CT x Ag ₂ S NPs	5.644	0.170	
	CT x AgNO ₃		0.037	
	AgNO ₃ x Ag ₂ S NPs		0.484	
11	CT x Ag ₂ S NPs	7.053	0.179	
	CT x AgNO ₃		0.022	
	AgNO ₃ x Ag ₂ S NPs		0.284	
115	CT x Ag ₂ S NPs	17.602	0.004	
	CT x AgNO ₃		0.007	
	AgNO ₃ x Ag ₂ S NPs		0.889	
173	CT x Ag ₂ S NPs	9.272	0.448	
	CT x AgNO ₃		0.013	
	Ag x Ag ₂ S NPs		0.061	
169	CT x Ag ₂ S NPs	10.395	0.184	
	CT x AgNO ₃		0.009	
	AgNO ₃ x Ag ₂ S NPs		0.101	
257	CT x Ag ₂ S NPs	8.680	0.176	
	CT x AgNO ₃		0.014	
	AgNO ₃ x Ag ₂ S NPs		0.171	
334	CT x Ag ₂ S NPs	5.529	0.107	
	CT x AgNO ₃		0.044	
	AgNO ₃ x Ag ₂ S NPs		0.770	
482	CT x Ag ₂ S NPs	5.046	0.430	
	CT x AgNO ₃		0.044	
	AgNO ₃ x Ag ₂ S NPs		0.238	

455	CT x Ag ₂ S NPs	33.849	0.777
	CT x AgNO ₃		0.001
	AgNO ₃ x Ag ₂ S NPs		0.001
287	CT x Ag ₂ S NPs	26.396	0.497
	CT x AgNO ₃		0.001
	AgNO ₃ x Ag ₂ S NPs		0.003
221	CT x Ag ₂ S NPs	35.552	0.001
	CT x AgNO ₃		1.000
	Ag x Ag ₂ S NPs		0.001
218	CT x Ag ₂ S NPs	261.290	1.000
	CT x AgNO ₃		<0.001
	AgNO ₃ x Ag ₂ S NPs		<0.001

Table S5. Statistical analysis of the relative abundance of soil genera, at day 28, using the one-way ANOVA. Treatments represented the soil microbiome non-exposed (CT), and soils exposed to Ag₂S NPs or AgNO₃. In table, multi-comparisons, using the Tukey HSD test, were done considering differences between sampling treatment. The confidence value $p < 0.05$.

Genus	Day 28	
	Treatment	P
<i>Acidobacterium</i>	CT x Ag ₂ S NPs	0.154
	CT x AgNO ₃	5.15
	Ag ₂ S NPs x AgNO ₃	0.046
<i>Candidatus Solibacter</i>	CT x Ag ₂ S NPs	14.72
	CT x AgNO ₃	0.101
	Ag ₂ S NPs x AgNO ₃	0.004
<i>Gaiella</i>	CT x Ag ₂ S NPs	6.32
	CT x AgNO ₃	0.145
	Ag ₂ S NPs x AgNO ₃	0.029
<i>Curvibacter</i>	CT x Ag ₂ S NPs	5.80
	CT x AgNO ₃	0.045
	Ag ₂ S NPs x AgNO ₃	0.080
<i>Nitrosomonas</i>	CT x Ag ₂ S NPs	10.09
	CT x AgNO ₃	0.998
	Ag ₂ S NPs x AgNO ₃	0.018
<i>Telmatobacter</i>	CT x Ag ₂ S NPs	9.50
	CT x AgNO ₃	0.105
	Ag ₂ S NPs x AgNO ₃	0.011
<i>Arenimonas</i>	CT x Ag ₂ S NPs	11.66
	CT x AgNO ₃	0.070
	Ag ₂ S NPs x AgNO ₃	0.007
<i>Terracidiphilus</i>	CT x Ag ₂ S NPs	10.32
	CT x AgNO ₃	0.121
	Ag ₂ S NPs x AgNO ₃	0.009
<i>Lysobacter</i>	CT x Ag ₂ S NPs	8.94
	CT x AgNO ₃	0.895
	Ag ₂ S NPs x AgNO ₃	0.019
<i>Edaphobacter</i>	CT x Ag ₂ S NPs	11.47
	CT x AgNO ₃	0.031
	Ag ₂ S NPs x AgNO ₃	0.009
Bryobacterales	CT x Ag ₂ S NPs	7.96
	CT x AgNO ₃	0.960
	Ag ₂ S NPs x AgNO ₃	0.037
Acidisphaera	CT x Ag ₂ S NPs	99.79
	CT x AgNO ₃	0.029
	Ag ₂ S NPs x AgNO ₃	0.000
<i>Rudaea</i>	CT x Ag ₂ S NPs	11.81
	CT x AgNO ₃	0.062
	Ag ₂ S NPs x AgNO ₃	0.007
Saprospirales	CT x Ag ₂ S NPs	6.53
	CT x AgNO ₃	0.913
	Ag ₂ S NPs x AgNO ₃	0.037
<i>Oryzihumus</i>	CT x Ag ₂ S NPs	6.86
	CT x AgNO ₃	0.213
	Ag ₂ S NPs x AgNO ₃	0.023
Saprospirales	CT x Ag ₂ S NPs	7.63
	CT x AgNO ₃	0.075
	Ag ₂ S NPs x AgNO ₃	0.021
Burkholderiaceae	CT x Ag ₂ S NPs	14.03
	CT x AgNO ₃	0.814
	Ag ₂ S NPs x AgNO ₃	0.013
Rhodospirillaceae	CT x Ag ₂ S NPs	4.80
	CT x AgNO ₃	0.278
	Ag ₂ S NPs x AgNO ₃	0.049
<i>Janthinobacterium</i>	CT x Ag ₂ S NPs	11.21
	CT x AgNO ₃	0.568
	Ag ₂ S NPs x AgNO ₃	0.031
Intrasporangiaceae	CT x Ag ₂ S NPs	15.61
	CT x AgNO ₃	0.033
	Ag ₂ S NPs x AgNO ₃	0.162
<i>Elstera</i>	CT x Ag ₂ S NPs	53.67
	CT x AgNO ₃	0.004
	Ag ₂ S NPs x AgNO ₃	0.005
<i>Terrabacter</i>	CT x Ag ₂ S NPs	5.68
	CT x AgNO ₃	0.361
		0.225

	Ag ₂ S NPs x AgNO ₃		0.035
<i>Pandoraea</i>	CT x Ag ₂ S NPs	8.86	0.025
	CT x AgNO ₃		0.025
	Ag ₂ S NPs x AgNO ₃		1.000
Oxalobacteraceae	CT x Ag ₂ S NPs	37.82	0.994
	CT x AgNO ₃		0.001
	Ag ₂ S NPs x AgNO ₃		0.001
<i>Fluviicola</i>	CT x Ag ₂ S NPs	25.99	0.002
	CT x AgNO ₃		0.002
	Ag ₂ S NPs x AgNO ₃		1.000
Chromobacteriaceae	CT x Ag ₂ S NPs	10.58	0.017
	CT x AgNO ₃		0.017
	Ag ₂ S NPs x AgNO ₃		1.000
<i>Candidatus Thiodiazotropha</i>	CT x Ag ₂ S NPs	9.17	0.051
	CT x AgNO ₃		0.512
	Ag ₂ S NPs x AgNO ₃		0.014
<i>Variovorax</i>	CT x Ag ₂ S NPs	11.79	0.551
	CT x AgNO ₃		0.028
	Ag ₂ S NPs x AgNO ₃		0.008
<i>Dyella</i>	CT x Ag ₂ S NPs	16.44	0.987
	CT x AgNO ₃		0.007
	Ag ₂ S NPs x AgNO ₃		0.006
<i>Angustibacter</i>	CT x Ag ₂ S NPs	12.80	0.036
	CT x AgNO ₃		0.006
	Ag ₂ S NPs x AgNO ₃		0.303
<i>Chryseolinea</i>	CT x Ag ₂ S NPs	16.34	1.000
	CT x AgNO ₃		0.006
	Ag ₂ S NPs x AgNO ₃		0.006
<i>Sediminibacterium</i>	CT x Ag ₂ S NPs	256.62	1.000
	CT x AgNO ₃		<0.001
	Ag ₂ S NPs x AgNO ₃		<0.001
<i>Geothrix</i>	CT x Ag ₂ S NPs	14.47	1.000
	CT x AgNO ₃		0.008
	Ag ₂ S NPs x AgNO ₃		0.008
<i>Mucilaginibacter</i>	CT x Ag ₂ S NPs	33.21	1.000
	CT x AgNO ₃		0.001
	Ag ₂ S NPs x AgNO ₃		0.001
<i>Haematococcus</i>	CT x Ag ₂ S NPs	46.76	1.000
	CT x AgNO ₃		<0.001
	Ag ₂ S NPs x AgNO ₃		<0.001
<i>Chitinophafa</i>	CT x Ag ₂ S NPs	10.62	0.013
	CT x AgNO ₃		0.887
	Ag ₂ S NPs x AgNO ₃		0.023
<i>Frateuria</i>	CT x Ag ₂ S NPs	440.96	1.000
	CT x AgNO ₃		<0.001
	Ag ₂ S NPs x AgNO ₃		<0.001

Chapter 8

General discussion and concluding remarks

1. General discussion

This thesis contributes to increase knowledge on the response of soil microbiome to metal-based NMs, including different formulations of copper and an aged form of silver, and to determine if these responses change in the presence of crucial edaphic components in the terrestrial ecosystem. These responses were also assessed under distinct experimental designs. One of the main outcomes of this thesis is the fact that it adds valuable data for future risk assessment studies regarding the ecotoxicological effects of metal-based NMs in terrestrial compartments. To achieve our main goals, several hypotheses (H_I to H_V) were tested, and main results are discussed in the present section.

H_I: Metal-based ENMs induce changes in soil microbiome

To test this hypothesis, it was of great relevance to assess the responses of the soil microbiome to metal-based NMs at various levels of community organization, *i.e.*, targeting the functional, structural and compositional levels. In fact, an effort to assess the effects of these NMs using different microbiological levels has been noted in the literature, as we previously described in Chapter 1 (Table 1). However, an integrative approach using these methodologies is rarely used. At the functional level, soil microbiome was analysed targeting the soil enzymatic activities, the physiological profiling, the abundance of specific bacterial groups [*e.g.*, culturable P-SB, HB or nitrification bacterial community (using the qPCR)], and/or predicted functional analysis (*e.g.*, relative abundance of functional genes related to the nitrogen cycle).

Concerning the functional level, our work showed that metal-based NMs potential reduce the β -glucosidase (copper and silver -based NMs; Chapter 3 and 6), dehydrogenase (copper-based NMs; Chapter 4), acid phosphatase (copper- and silver-based NMs; Chapter 5 and 6), arylsulfatase (copper-based NMs; Chapter 4) and urease (copper-based NMs; Chapter 4) activities, which may disrupt some functions in soil related to the carbon, phosphorous, sulfur and nitrogen cycles, essentials to maintain the soil fertility and plant growth. The analysis of enzymatic activities provides an important information about the ability of soil microorganisms to regulate the biogeochemical processes in soil (Nannipieri *et al.*, 2018), which allow us to infer on the impact of these NMs on soil functionality. Additionally, this is a simple, rapid, inexpensive method and recently regulated by ISO 20130:2018 (ISO, 2018), which

provides a great advantage in its use in ecotoxicological studies. Since the nutrient cycles are not influenced by only one enzyme (Nannipieri *et al.*, 2018), caution in data analysis is still needed. Additionally, to assess the metabolic activity, the carbon utilization pattern was established via the Biolog[®]Ecoplate method. This method is time-effective and allowed to obtain broad data (*e.g.*, including 31 substrates), and the carbon substrate indexes (*e.g.*, AWCD, SAWCD or AUC) allowed us to infer the physiological state of the microbial communities after exposure to the contaminants. For instance, a significant increase in the carbon utilization was detected in soils exposed to Kocide[®]3000 (Chapter 3) and to nCuO (Chapter 4). As indicated in these Chapters, the observed impact may be due to the activation of copper-tolerance mechanisms, like efflux pumps, which required a higher energy demand (Xing *et al.*, 2020). Although, this method only represents the culturable fraction of microbial community and only targets the fast-growing organisms (Karimi and Fard, 2017) it showed to be adequate for assessing the impact of different NMs in the soil (Samarajeewa *et al.*, 2017; Samarajeewa *et al.*, 2020). Based on bacteria cultivation, an inhibitory effect on abundance of P-SB was observed for the AgNO₃-exposed soils (Chapter 6), suggesting the impair of phosphorous solubilization, which may negatively impact the crop growth and soil fertility (Nautiyal, 1999). On the other hand, nCu(OH)₂ led to a significant increase in these bacteria counts, which suggests the activation of resistance mechanisms in this community (Berg *et al.*, 2012). Although the culture-dependent methods are known to assess less than 1% of total bacteria in soil, this microbial parameter showed to be sensitive to metal-based NMs contamination (Vasileiadis *et al.*, 2015).

On the other hand, molecular methodologies, combining the PCR-DGGE and massive parallel sequencing (NGS), were used to conduct a comprehensive analysis of NMs role in the soil microbiome structure, composition and function. Regarding the PCR-DGGE analysis, it was used in our study as a global overview of the soil microbiome structure and diversity. This technique is commonly used due to its low cost and time-effectiveness (Nannipieri *et al.*, 2019). In this thesis, different communities were targeted, such as bacterial [*e.g.*, total bacteria (16S rRNA gene), ammonia-oxidizing bacteria (*amoA* gene) and nitrite-oxidizing bacteria (*nrxB* gene)] and fungal (ITS region) communities. In general, this work showed that the bacterial community structure greatly responded to the contaminant's exposure, being detected significant changes in the diversity indexes in soil exposed to Ag- and Cu-based NMs (Chapter 3,

5, and 6). Additionally, the responses of fungal communities were analysed in Chapter 3, due to the fungicide properties of Kocide[®]3000. As a result, the highest concentration tested of this nanopesticide decreased the diversity and richness of the fungal community (in the absence of invertebrates). Thus, our work highlights the importance to assess the structure of this microbial community to evaluate the impact of the NMs in soil. Albeit the effects of NMs were mainly assessed on bacterial communities, more studies are required to assess the impact of this NMs in fungal and other communities (*e.g.*, archaea). In fact, the negative impact of Cu-based nanopesticides was already reported on soil fungal and other eukaryote communities' structure and composition (Zhang *et al.*, 2020; Carley *et al.*, 2020). Additionally, the PCR-DGGE technique was also performed in our work to select samples to be used for a deeper analysis using NGS (Chapter 4 and 6). In fact, only 1 to 2% of the microbial population, representing dominant species present in an environmental sample, was cover in the PCR-DGGE analysis (Karimi and Fard, 2017). On the other hand, the decreased cost of NGS analysis observed over the years (Nannipieri *et al.*, 2019), and its high sensitivity, contributed to its increasingly frequent use in ecotoxicology studies. In fact, this methodology allowed us to identify changes in specific bacterial groups (even at low percentage of abundance), and associated them to different soil functions (*e.g.*, classes and genera associated to the nitrogen cycle). For instance, in Chapter 7, the increase of the relative abundance of Chitinophagia linked to lignocellulose-degrading activity, was observed in Ag₂S NPs and AgNO₃ -treated soils, when compared to the control. On the other hand, in copper-treated soils a decrease of the relative abundance of bacteria involved in decomposition of organic matter [Acidobacteria in Kocide[®]3000, nCuO, and Cu(OH)₂-i treated soil] and regulation of nitrogen cycle [Flavobacteriia in nCu(OH)₂ treated soil] was detected towards the control. Also, the increased abundance of copper-tolerant bacteria, such as Clostridia (Kocide[®]3000) and Gemmatimonadetes [nCu(OH)₂], was detected in copper-treated soils towards the control.

The use of the transversal microbiome analysis was a key point in our work for a robust analysis and comprehensive evaluation of Ag- and Cu- based NMs effects. Due to deeper outcome regarding bacterial community structure, composition, and functionally inference, our work widely recommends the use of NGS analysis as a microbial endpoint for the environmental risk assessment of these contaminants. Yet, the NGS analysis should also be complemented with culture-dependent (*e.g.*, carbon utilization

pattern, enzymatic activities and bacterial counts) and/or with other culture-independent (*e.g.*, qPCR) methodologies; to obtain the global picture of soil microbiome.

As discussed above, our results confirm that metal-based NMs alter the soil microbiome, at the functional, structural and compositional levels. Nevertheless, these effects were dependent on the metal-type NMs, NMs formulation, concentrations tested and exposure period. Additionally, the detection of the impact of these contaminants in soil microbiome was dependent on the complexity of the experimental assays and on the applied microbial endpoints. Concerning the Cu-based NMs, the impact of commercial Cu(OH)₂-nanopesticide (Kocide[®]3000) (Chapter 3, 4 and 5), nCuO and lab-synthesized nCu(OH)₂ (Chapter 4 and 5) was assessed in this work, under relevant environmental concentrations [recommended concentration applied of Kocide[®]3000 in soil: 0.45 (single), 19.86 (season) and/or 50 mg (Cu) kg⁻¹ soil (maximum applied for several crops)]. Although all tested concentrations suggested an impact on soil microbial communities' structure and function, the highest copper concentration showed a stronger impact regarding Kocide[®]3000-treated soil (50 mg kg⁻¹ soil > 19.86 mg kg⁻¹ soil > 0.45 mg kg⁻¹ soil; Chapter 3 and 5). One of the changes recorded was the inhibition of different soil enzymatic activities. In accordance, a concentration-dependent effect of Cu-based NMs in soil microbiome was also reported (Simonin *et al.*, 2018 a, b; Zhang *et al.*, 2019; Zhang *et al.*, 2020). However, a contradictory effect can be found in literature when is applied the lowest recommended concentrations (*e.g.*, one application per event for Kocide[®]3000 - 6.68 mg/L), in which some studies showed a detrimental effect on bacterial communities using a sequential application of Kocide[®]3000 (a total of three events per year) (Carley *et al.*, 2020, Simonin *et al.*, 2018 b). Additionally, these contradictory results may also be explained by the distinct procedure used to apply copper to soil. Depending on the application method, only 10-75% of ingredient active in pesticides can reach the soil compartment (Kah *et al.*, 2018). For instance, in these studies (Carley *et al.*, 2020, Simonin *et al.*, 2018b), the nanopesticide was sprayed on crops, which may lead to loss of this product in air and/or plant tissues. In our studies, the contamination procedure was through the addition of copper directly in the soil, thus assuming a copper accumulation scenario in soil.

Additionally, our work (Chapter 3 and 4) showed also a distinct impact on soil microbiome concerning the copper formulation (fully discussed below - H_{III}). On the other hand, the Ag₂S NPs were used in our study as a model of sulfidation of silver NPs in WWTP (sulfidation degree = 100%), in Chapter 6 and 7. Since the lower degree of

sulfidation is typically associated with increased toxicity of silver to the soil microbiome (Reinsch *et al.*, 2012), and generally to biota, the evaluation of the effects of these NPs allowed us to infer the potential risk of aged AgNPs resulting from WWTP sulfidation processes, to the soil microbiome. Regarding the Ag-based NMs, we used a concentration 1000 or 25 times higher than the predicted environmental concentrations for 2050 [10 mg (Ag) kg⁻¹ soil] for agricultural or sludge-treated soils, respectively (Giese *et al.*, 2018) (Chapter 6 and 7). Although this concentration is not relevant from an ecological point of view, we consider that the analysis of its impact will contribute to understand the Ag₂S NPs effects in a not-too-distant future, since the predicted concentration of AgNPs is still increasing overtime (Giese *et al.*, 2018). Also, previous studies demonstrated that, at this concentration, Ag₂S NPs exerted toxic effects to soil organisms, *e.g.*, in nematodes (Starnes *et al.*, 2015), plants (Wang *et al.*, 2017) and microorganisms (Doolette *et al.*, 2016), adding more information to the already existing, which increases the relevance of this study.

An increased concentration of metal-based NMs in soil is predicted overtime, not only due to the frequent use of nano-products but also due to their persistence in the terrestrial compartment (McKee and Filser, 2016; Giese *et al.*, 2018; Ballabio *et al.*, 2018). Recently, the effects of silver and copper-based nanopesticides on soil microbiome have been studied at both short- and -longer exposure periods (Simonin *et al.*, 2018 a, b; Carley *et al.*, 2020; Zhang *et al.*, 2020). However, contradictory effects were reported, probably due to the distinct NMs concentrations and experimental designs used. In addition, time is a crucial parameter which influences NMs behaviour and therefore toxicity. In the current thesis, the copper- (Chapter 4) and silver- (Chapter 6 and 7) based NMs mainly affect the soil functioning at longer exposure periods (day 28), highlighting the relevance of studying these NMs at long-term exposures. Therefore, in Chapter 3, the impact of Kocide[®]3000 was investigated after 90 days of exposure, showing a significant effect on soil microbiome at the structure (bacterial and fungal communities) and function (carbon cycle) level. In accordance, at this exposure period, few studies showed a significant influence of copper-based NMs on soil enzymatic activity (Simonin *et al.*, 2018 a, b). On the other hand, exposure during one year showed a detrimental effect of NMs on soil bacterial community structure/composition and/or function (Carley *et al.*, 2020; Simonin *et al.*, 2018b). In fact, the potential functional redundancy of these bacterial communities' over-time was

reported in NMs-treated soils (Zhai *et al.*, 2019), suggesting a recovery of affected functions by the activity of other microorganisms (Allison and Martiny, 2008).

Distinct experimental designs have been performed to understand the impact of NMs in both terrestrial and aquatic compartments, being the microcosm and mesocosm experiments the most used approaches (Bidwell, 2020). According to Bidwell (2020), the main difference between these approaches is based on the size of the system, in which microcosms are smaller. The main advantage of using the small lab scale setup is its cost-effectiveness, and the fact that it allows to evaluate the effects of many contaminants with simplified procedures, and the avoidance of confusing variables (Huckabee, 1985). In this point of view, a microcosm-based approach was performed in Chapter 3 to understand the impact of Kocide®3000 on soil microbiome structure and function during 90 days of exposure and the presence/absence of the *P. pruinosus*. This approach was valuable, in our study, not only to infer the impact of the nanopesticide in soil microbiome structure, diversity and function but also to infer the potential attenuation of these effects when soil invertebrates were present. Accordingly, several studies also using this simple approach demonstrated the effect of silver or copper-based NMs on the soil microbiome (Zhang *et al.*, 2020; Simonin *et al.*, 2018 a, b; Peyrot *et al.*, 2014). On the other hand, using this simple design is difficult to evaluate the impact of contaminants from an agroecosystem's perspective (Bour *et al.*, 2015). Thus, currently, several studies recommend the use of mesocosms-based experiments to study the effects of NMs in soil, which facilitate the extrapolation of the impact of these contaminants at the ecosystem level (Bour *et al.*, 2015; Carley *et al.*, 2020; Forstner *et al.*, 2019). Having this in view, indoor mesocosms experiments were performed to investigate the impact of Cu-based NMs (Chapter 4) or Ag₂S NPs (Chapter 6 and 7) in the soil microbiome. Additionally, the inclusion of different species of organisms in this works revealed to be a relevant approach. In fact, the accumulation/uptake of NMs in agroecosystems (*e.g.*, in soil, invertebrates and/or plants) may result in negative consequences to human health (*e.g.*, via food chain) and to soil fertility (*e.g.*, soil microbiome) (Dang *et al.*, 2019; Dai *et al.*, 2020). This approach was relevant in our study not only to understand the impact of these NMs on soil microbiome (*i.e.*, from bulk and/or rhizosphere - Chapter 5) but also on parameters related to the animals and plants (*e.g.*, biomass, metal uptake and accumulation; not included in this thesis).

Contradictory results regarding the impact of these NMs on soil microbiome were also reported for agricultural soil, which may be due to distinct soil properties (Simonin *et*

et al., 2018 a). In fact, different soil pH, organic matter and water content, might influence not only the NMs bioavailability in soils but also the soil microbiome abundance, structure and composition (Simonin *et al.*, 2018 a; Shahsavari *et al.*, 2017). As a consequence, the NMs toxicity can be altered (Simonin *et al.*, 2018 a, Zhang *et al.*, 2020). For these reasons, the Lufa 2.2 soil was selected to test our hypothesis, since this is a natural and standard soil commonly used in ecotoxicology studies, and harbours a well-studied microbiome (Fajardo *et al.*, 2019; Bastos *et al.*, 2014).

III: Distinct formulations of ENMs distinctly affect the soil microbiome function, structure and composition

Distinct effects on soil microbiome composition and predicted functions were observed in soils spiked with Cu-based NMs (Chapter 4). Although the same concentration of copper was tested, the distinct formulations may justify these distinct observed effects in soil microbiome (Chapter 4 and 5). Although the impact of Kocide[®]3000 is primarily attributed to the presence of the active ingredient (Zhang *et al.*, 2020), the effect of excipients cannot be excluded. In fact, 73.5% of excipients are present in the commercial formulation of Kocide[®]3000, and distinct toxic effects of the Cu(OH)₂ in the commercial formulation and the ionic form were observed in Chapter 3 and 4. Additionally, the highest aggregation state of nCu(OH)₂ in solution (in deionised water after 4 h) compared with the commercial formulation Kocide[®]3000 (Li *et al.*, 2019), suggested a lower toxicity of nCu(OH)₂ at longer time of exposure. On the other hand, the prolonged dissolution of nCuO in soil suggests a later toxic effect on soil microbiome (Spielman-Sun *et al.*, 2018), which is in accordance with our results (Chapter 4 and 5). Additionally, the ionic dissolved fraction (Cu²⁺ or Ag⁺) is generally indicated as the primary factor of the antimicrobial action of metal-based NPs (Reinsch *et al.*, 2012; McNeilly *et al.*, 2021). For this reason, in each experiment performed in our work was included an ionic control [Cu(OH)₂-i and AgNO₃]. Concerning the Cu exposure, the ionic fraction dissolved was according to the following pattern, after days 14 and 28: Cu(OH)₂-i > Kocide[®]3000 ~ nCuO > nCu(OH)₂. In opposite, in Chapter 3, Kocide[®]3000 showed the highest dissolved fraction in comparison to the Cu(OH)₂-i, probably due to the use of different copper extraction methods. In fact, the DTPA (Chapter 4) method has been suggested as more effective to extract copper in soil than the porewater extraction method (Rodrigues *et al.*, 2021). For instance, this method

targets not only the total “labile” metal in soil (*i.e.*, free ions in soil porewater) but also the metallic ions associated with soil organic matter (like, the organic-bound fractions in soil) (Gao *et al.*, 2017). Notwithstanding, the complexity of the experimental design, exposure time, presence of biota may also contribute to these distinct observations. Additionally, regarding the silver-based NMs, a higher impact of AgNO₃ in soil microbiome structure and functions was observed in comparison to the effect exerted by Ag₂S NPs (Chapter 6 and 7), probably due to the higher Ag⁺ concentration in porewater measured in soil exposed to AgNO₃. These results agree with literature as we described in Table 1 - Chapter 1, in which the toxicity increased following the pattern: Ag₂S NPs < AgNPs < AgNO₃.

On the other hand, the particle-specific effect and oxidative stress are also considered decisive in toxicity of the NMs to microorganisms (McNeilly *et al.*, 2021; Lakshmeesha *et al.*, 2020), which can also explain the observed distinct impacts between formulations.

H_{III}: The presence of invertebrates influences the effects of metal-based ENMs on soil microbiome

To test this hypothesis, experiments were conducted using microcosms (Chapter 3) and indoor-mesocosms to study the impact of Cu-based NMs (Chapter 4 and 5) or Ag₂S NPs (Chapter 6). In Chapter 3, long-term impact of Cu-based nanopesticide in soil microbiome was evaluated in the presence/absence of the soil dwelling detritivore *Porcellionides pruinosus* (Crustacea, Isopoda), as a member of the terrestrial compartment. The obtained results suggested that the invertebrate may attenuate the effects of this nanopesticide on soil microbiome. For instance, the fungal community diversity and the carbon-utilization pattern were only affected by the contaminant when this organism was absent. Nevertheless, the path of this attenuation effect is still unclear. We hypothesized that effects are due to the microbial growth stimulus resulting from the presence of these organisms in soil. In fact, the presence of this invertebrate might increase the oxygen level and nutrients in soil by the deposition of nitrogen-enriched faeces, influencing the pH levels in soil; which may influence the soil microbiome abundance (Abd El-Wakeil, 2015). In addition, the abundance and composition of the soil microbiome can also be directly influenced by the presence of this organism in soil, through the introduction of microbiota from their body (gut system) and/or as a part of product excretion (*e.g.*, faecal particles) (Zimmer & Topp,

2002; Bouchon *et al.*, 2016; Bray *et al.*, 2019). For example, the study of Bouchon *et al.* (2016) reported that the bacterial community associated to the faeces of *A. vulgare* is composed of Alphaproteobacteria, Gammaproteobacteria and Mollicutes. Thus, due to the introduction of this community in soils, the dynamic of soil microbiome might be changed. In addition, the food preference of this terrestrial isopod for fungal communities has been reported (Zimmer & Topp, 2002), which might also influence both fungal and bacterial community abundance and/or composition in the terrestrial compartment (Hibbing *et al.*, 2010). On the other hand, isopods activity in soil probably changes the soil properties (such as pH and organic matter), which may promote the aggregation of NMs in soils (Lead *et al.*, 2018). As a consequence, this promoted aggregation may diminish the toxic effect of these contaminants in soil (Zhang *et al.*, 2019).

In addition, different species of soil invertebrates (*e.g.*, isopods, earthworms and mealworms), commonly used in ecotoxicology assays (Bour *et al.*, 2015), were included in the indoor mesocosm experiments (Chapters 4, 5, 6, and 7). Since the responses of soil microbiome changed in the presence of the invertebrates (as confirmed in Chapter 3), the inclusion of different species of invertebrates in these experiments might also increase the relevance of our study.

Some variability among soil samples was observed in our work (Chapter 4 and 5), which may be derived from the potential mobilization of the NMs in soil by the organisms' activity (*e.g.*, bioturbation) or organism's mortality. Accordingly, the use of more than three replicates per treatment is recommended, although difficult in higher tier, complex testing systems. In overall, these results highlight the importance to include not only *P. pruinosus* (Chapter 3), but also other invertebrate species to assess the impact of the copper- and silver- based NMs in the terrestrial ecosystem (Chapter 4, 5, 6, and 7).

H_{IV}: Metal-based ENMs affect the soil rhizosphere bacterial community

Although previous studies showed that Cu-based NMs exerts a toxic effect on the plants' growth and bulk soil microbiome structure (Zhang *et al.*, 2018, Zhai *et al.*, 2019), not much is known about the influence of these NMs on the soil microbiome associated with the root system when different invertebrate's species are included in the same experiment. In fact, the responses of rhizosphere to the contaminants are usually tested as a simple experimental design with/without plant, such as the rhizobox design

(Wei *et al.*, 2018). The study of the rhizosphere microbiome in contaminated soils is also relevant in an agronomic perspective because soil microbiome can stimulate the plant defence to phytopathogens and regulate soil fertility (Philippot *et al.*, 2013; Yuan *et al.*, 2018). Thus, in Chapter 5, the exposure to Cu NMs led to a reduced soil enzymatic activity (*i.e.*, acid phosphatase, arylsulfatase and urease) in the rhizosphere soil, which may be a result of the presence of root exudates. This impact was distinct from that observed in the bulk soil, concerning the type of enzyme tested and exposure time. For instance, the application of copper NMs, under complex exposure scenario, may impair the regulation of the P cycle (*e.g.*, by the reduced AP activity), after 14 days but only in rhizosphere soil. This negative impact may disrupt the soil fertility and reduce the growth/quality of plants (Wei *et al.*, 2019). In fact, negative impacts of copper-based NPs on wheat growth and root elongation were previously detected (Dimkpa *et al.*, 2012; Zhang *et al.*, 2018).

Although the influence of root exudates was not directly evaluated in this study, their presence might stimulate the dissolution of copper formulations in soil (Spielman-Sun *et al.*, 2018), which agrees with the earlier effects observed in our study (*i.e.*, enzymatic activity at day 14). Additionally, the root exudates can also stimulate the abundance of beneficial soil microbiome, which can support some functions affected and attenuate the impact of NMs on soils over-time (Zhai *et al.*, 2019). Due to the distinct impact observed between the rhizosphere and bulk soil microbiome, we recommend to analyse both soils microbiome (1) in the experiments with and without plants to avoid some confusing variables (like, soil invertebrates), and (2) using the NGS method to understand the role of root exudates in the soil microbiome composition.

H_V: The metal-based ENMs change the nitrogen cycle

Some changes in the bacterial phylotypes and predicted gene abundance involved in the nitrogen cycle were detected in soils exposed to NMs (Chapter 4 and 7). Concerning the predicted functional analysis, a decreased abundance of genes linked to the nitrification (Chapter 7) and denitrification (Chapter 4) were projected in Ag- and Cu- NMs treated soils, respectively. These results confirm our hypothesis (H_V), suggesting that metal NMs-exposure negatively impact the nitrogen transformation (*i.e.*, decreasing the *amoA* and *nxrB* genes) and increase the loss of nitrogen in agroecosystems (*i.e.*, decreasing the *nirS* and *nosZ* genes). As a consequence, a nitrogen-use efficiency for plant growth and

soil fertility can be compromised (McGee *et al.*, 2020). These observed changes may result from the reduced abundance of specific bacterial groups detected in contaminated soil, *e.g.*, *Bacillus* (Chapter 4), *Nitrosomonas* (AOB) and *Nitrospira* (NOB) (Chapter 6) genera. These genera were already suggested as mediating these specific processes in the soil (Nelson *et al.*, 2016), and were also reported to be significantly affected by the NMs exposure in previous studies (Guan *et al.*, 2020; Zhang *et al.*, 2020).

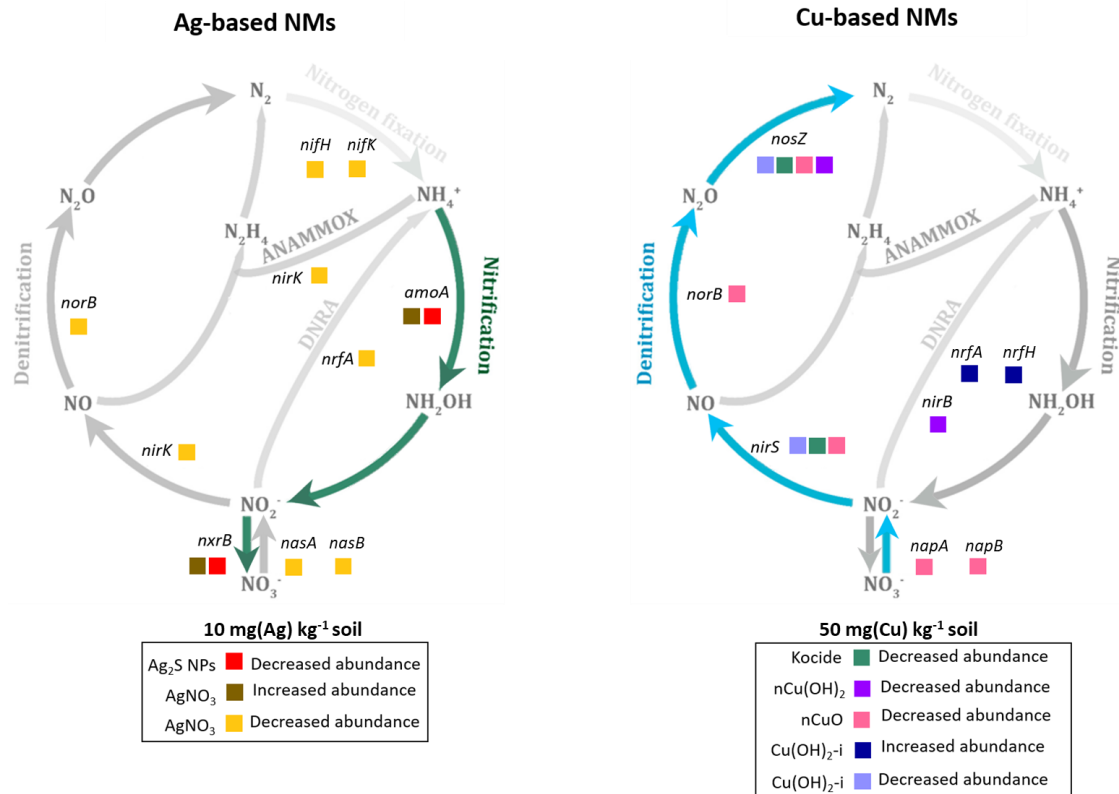


Figure 1. Nitrogen metabolism of soil microbiome exposed to silver- [Ag₂S NPs or AgNO₃ at 10 mg (Ag) kg⁻¹] or copper- based NMs [Kocide[®]3000, nCu(OH)₂, nCuO, or Cu(OH)₂-i at 50 mg (Cu) kg⁻¹]. The data was only based on predicted relative abundance of nitrogen-related genes, previously described in Chapter 4 and Chapter 7, using the Piphillin software. Green and blue arrows indicate the steps in the nitrogen cycle significantly affected by silver- or copper- based NMs exposure, respectively. Gray arrows indicate the steps in the nitrogen cycle not affected by NMs exposure.

Despite the valuable outcome of the predicted functional analysis, the dependency of data deposition in databases used by the Piphillin software can be the main problem of this analysis (Iwai *et al.*, 2016). For this reason, the qPCR was performed in Chapter 7 to confirm the predicted impact of silver (Ag₂S NPs and AgNO₃) in the abundance of both *amoA* and *nrxB* genes, involved in nitrification. Although the increased abundance of both genes in AgNO₃-treated soil was confirmed by qPCR analysis, the

negative impact of Ag₂S NPs was not detected. This molecular method has been used in microbial ecology studies, due to their sensitivity and reproductivity (Kim *et al.*, 2013). In fact, considering our results, this technique was a valuable complement in the predicted functional analysis. Due to some advantages of qPCR analysis (described in Chapter 7), other methodologies can also be used to confirm these results, such as DGGE, NGS and microarrays (*i.e.*, GeoChip as fully described in He *et al.*, 2007). Additionally, distinct variants of *amoA* and *nxrB* genes seem to emerge in Ag-treated soils, suggesting that silver tolerant ammonia-oxidizing (AOB) and nitrite-oxidizing (NOB) bacteria were selected in this treated soil. In fact, the activation of resistance mechanisms (like, cell communication mechanisms - *Quorum Sensing*, and flagellar biosynthesis protein) was predicted in our study, which may support this tolerance effect. In accordance, the study of Das *et al.*, 2012 also reported that variants in AgNO₃ and AgNPs -treated soils may result from the resistance mechanisms. In agreement, different studies already reported a tolerant effect of Ag-based NMs in bacterial community related to the nitrogen cycle (Zhang *et al.*, 2020; Guan *et al.*, 2020). From a methodological perspective, the DGGE and clone libraries used in our study showed to be a fast and cost-effective approach to confirm the diversity of AOB and NOB communities. However, the identification of the AOB and NOB phylotypes affected by the silver exposure should be further explored (*e.g.*, using the NGS analysis).

2. Final remarks and future directions

In this thesis distinct experimental designs and microbial methodologies were used to assess the impact of metal-based NMs on the structure, composition and functions of the soil microbiome. It emphasised the relevance of including microbiome analysis in ecotoxicological research as well as in risk assessment regulation. Although our results highly indicate the NGS as the better method to estimate the impact of these NMs, complementary methodologies targeting the functional level should also be considered (*e.g.*, soil enzymatic activities).

In overall, our results suggested that the metal-based NMs negatively affected the soil microbiome, which is essential for several agroecosystems services. For instance, the intentional application of copper-based NMs in agriculture might affect the functionality of the terrestrial ecosystem (Chapter 3, 4 and 5), through the observed reduction of

microbial processes associated with carbon (*e.g.*, DHA and β -glucosidase activities, and CLPP), nitrogen (*e.g.*, UA activity and, denitrification), and sulfur (*e.g.*, arylsulfatase activity) cycles. On the other hand, the exposure to Ag₂S NPs (unintentional source of NMs in the soil) showed a slight impact on the soil microbiome structure, composition and function, with changes in the phosphorous and carbon cycles. Thus, at a microbiome perspective, the presence of these metal-based NMs has a potential environmental risk to the soil ecosystem, highlighting the importance to regulate the use of these compounds in agriculture. Nevertheless, more studies are needed to confirm this potential negative impact targeting several conventional ecotoxicological endpoints (like plant growth, fruit/vegetable nutritional value, invertebrates' mortality and reproduction, among others). Additionally, this thesis provides relevant information on ecotoxicological experimental designs to assess the impact of metal-based NMs in soil, highlighting the relevance of using a more realistic framework (*e.g.*, indoor-mesocosms), which also should include the soil biota as an essential element of the ecosystem. The later impact of Ag- and Cu- based NMs revealed the relevance to study these NMs at long-term exposure.

Finally, to conclude, this thesis highlights the relevance of using a multidisciplinary and integrative approach (microbial ecotoxicology) to understand the risk of using these NMs on the agroecosystems. Further studies also should use the microbial endpoints to complement the conventional ecotoxicology studies and should be included in the risk assessment of the NMs.

Based on our results, new questions and hypotheses were raised concerning the:

I. Metal-based NMs formulation:

- Due to the distinct impact of commercial nanopesticide and nCu(OH)₂ on soil microbiome, as suggested in Chapters 3, 4, and 5, the excipients in the nanopesticide and the dispersive agent in nCu(OH)₂ may influence the toxic effect on soil microbiome and or Cu²⁺ dissolution rates. So, these agents should be investigated in future studies.
- The root exudates may promote the Cu²⁺ dissolution, which can be dependent on the copper formulation (Chapter 5). Thus, studies including the presence and absence of plants should be further considered, addressing distinct copper extraction methods, such as porewater, DTPA, and CaCl₂ methods (as used by Gao *et al.*, 2017; Rodrigues *et al.*, 2021).

II. Experimental design:

- Due to the frequent application of these NMs in the terrestrial compartment (*e.g.*, Kocide[®]3000 can be applied two or three times depended on the severity of crop diseases), a re-exposure scenario with several concentrations, sampling times, and presence/absence of soil target and non-target organisms, should be addressed in future studies. For this, the use of a Pollution-Induced Community Tolerance framework (Blanck *et al.*, 2002) with NGS method is suggested, to understand if the metal tolerance effect is altered (induced, reduced or not change) in a re-exposure scenario.
- Due to the potential later impact of metal-based NMs observed in both Chapters 4 and 6, long-term exposure effects to these NMs should be further explored.
- Due to the potential decreased loss of N, as suggested in Chapter 4 (by the predicted reduction of relative abundance of *nirS* and *nosZ* genes), we hypothesized that the leaching of nitrate from agricultural soils to aquatic ecosystems may occur. Thus, the quantification of N (total, NO₃⁻ and NO₂⁻) in leaching, collected from terrestrial mesocosms, should be performed to confirm this potential environmental problem.
- The potential impact of soil invertebrates and plants on the soil properties (such as oxygen level, nutrient content and soil pH) should be deeper explored to understand their influence on soil microbiome composition and function.
- Soil might be a reservoir for different types of NMs, not exclusively for the metallic ones. Additionally, the application of fertilizers, with natural or industrial origin, can stimulate the soil microbiome activity, which might change the soil microorganism's responses to NMs' exposure. Thus, further studies should focus on the combined effects of metal-NMs and fertilizers on the soil microbiome, using different endpoints like soil enzymatic activities, carbon utilization patterns and microbiome composition.

III. Microbial related endpoint:

- Since copper present a fungicide property, the structure and composition of fungal communities (in both bulk and rhizosphere soil) should also be further explored in the Cu-treated soil (Chapter 4 and 5).
- The predicted functional analysis suggests a potential impact of Cu- and Ag- based NMs in the relative abundance of genes associated to different nutrient cycles (*e.g.*, C, N and S) and bacterial resistance mechanisms (*e.g.*, efflux pumps and quorum-sensing) (Chapter 4 and 7). The effects on these processes should be confirmed by independent (*e.g.*, qPCR, NGS analysis) and/or dependent culture methods (*e.g.*, characterization of soil bacterial/fungal isolates by susceptibility assays, biofilm formation assays, among others).
- Due to the potential negative impact of metal-based NMs in the nitrification and denitrification processes, the quantification of total nitrification using conventional ecotoxicology methods (*i.e.*, substrate-induced nitrification - OECD Method No. 216) should be considered in future studies. Additionally, the Archaea and Comammox communities are also suggested as mediators in ammonia oxidation, so future studies should assess the impact of Ag-based NMs in these communities.

3. References

- Abd El-Wakeil, K. F. (2015). Effects of terrestrial isopods (Crustacea: Oniscidea) on leaf litter decomposition processes. *The Journal of Basic & Applied Zoology*, 69, 10-16.
- Allison, S. D., Martiny, J. B. (2008). Resistance, resilience, and redundancy in microbial communities. *Proceedings of the National Academy of Sciences*, 105, 11512-11519.
- Ballabio, C., Panagos, P., Lugato, E., Huang, J. H., Orgiazzi, A., Jones, A., Montanarella, L. (2018). Copper distribution in European top soils: An assessment based on LUCAS soil survey. *Science of The Total Environment*, 636, 282-298.

- Bastos, A. C., Prodana, M., Oliveira, J. M. M., Calh a, C. F., Santos, M. J. G., Soares, A. M. V. M., Loureiro, S. (2014). Water-extractable priority contaminants in LUFA 2.2 soil: back to basics, contextualisation and implications for use as natural standard soil. *Ecotoxicology*, 23(9), 1814-1822.
- Berg, J., Brandt, K. K., Al-Soud, W. A., Holm, P. E., Hansen, L. H., S rensen, S. J., Nybroe, O. (2012). Selection for Cu-tolerant bacterial communities with altered composition, but unaltered richness, via long-term Cu exposure. *Applied and Environmental Microbiology*, 78(20), 7438-7446.
- Bidwell, J. R. (2020). In vivo ecotoxicology models. In An introduction to interdisciplinary toxicology (pp. 507-523). Academic Press.
- Blanck, H. (2002). A critical review of procedures and approaches used for assessing pollution-induced community tolerance (PICT) in biotic communities. *Human and Ecological Risk Assessment*, 8(5), 1003-1034.
- Bouchon, D., Zimmer, M., Dittmer, J. (2016). The terrestrial isopod microbiome: An all-in-one toolbox for animal-microbe interactions of ecological relevance. *Frontiers in Microbiology*, 7, 1–19.
- Bour, A., Mouchet, F., Silvestre, J., Gauthier, L., Pinelli, E. (2015). Environmentally relevant approaches to assess nanoparticles ecotoxicity: a review. *Journal of Hazardous Materials*, 283, 764-777.
- Bray, N., Wickings, K. (2019). The roles of invertebrates in the urban soil microbiome. *Frontiers in Ecology and Evolution*, 7, 359.
- Carley, L. N., Panchagavi, R., Song, X., Davenport, S., Bergemann, C. M., McCumber, A. W., Simonin, M. (2020). Long-term effects of copper nanopesticides on soil and sediment community diversity in two outdoor mesocosm experiments. *Environmental Science & Technology*, 54(14), 8878-8889.
- Dai, Y., Wang, Z., Zhang, L., Jiang, Z., Pu, S., Fan, Q., Xing, B. (2020). Transfer and transformation of CeO₂ NPs along a terrestrial trophic food chain. *Environmental Science: Nano*, 7(2), 588-598.
- Dang, F., Chen, Y. Z., Huang, Y. N., Hintelmann, H., Si, Y. B., Zhou, D. M. (2019). Discerning the sources of silver nanoparticle in a terrestrial food chain by stable isotope tracer technique. *Environmental Science & Technology*, 53(7), 3802-3810.
- Das, P., Williams, C. J., Fulthorpe, R. R., Hoque, M. E., Metcalfe, C. D., Xenopoulos, M. A. (2012). Changes in bacterial community structure after exposure to silver

- nanoparticles in natural waters. *Environmental Science & Technology*, 46(16), 9120-9128.
- Dimkpa, C. O., McLean, J. E., Latta, D. E., Manangón, E., Britt, D. W., Johnson, W. P., Anderson, A. J. (2012). CuO and ZnO nanoparticles: phytotoxicity, metal speciation, and induction of oxidative stress in sand-grown wheat. *Journal of Nanoparticle Research*, 14(9), 1-15.
- Doolette, C. L., Gupta, V. V., Lu, Y., Payne, J. L., Batstone, D. J., Kirby, J. K., McLaughlin, M. J. (2016). Quantifying the sensitivity of soil microbial communities to silver sulfide nanoparticles using metagenome sequencing. *PLoS one*, 11(8), e0161979.
- Fajardo, C., Costa, G., Nande, M., Botías, P., García-Cantalejo, J., Martín, M. (2019). Pb, Cd, and Zn soil contamination: Monitoring functional and structural impacts on the microbiome. *Applied Soil Ecology*, 135, 56-64.
- Forstner, C., Orton, T. G., Wang, P., Kopittke, P. M., Dennis, P. G. (2019). Soil chloride content influences the response of bacterial but not fungal diversity to silver nanoparticles entering soil via wastewater treatment processing. *Environmental Pollution*, 255, 113274.
- Gao, X., Spielman-Sun, E., Rodrigues, S. M., Casman, E. A., Lowry, G. V. (2017). Time and nanoparticle concentration affect the extractability of Cu from CuO NP-amended soil. *Environmental Science & Technology*, 51(4), 2226-2234.
- Giese, B., Klaessig, F., Park, B., Kaegi, R., Steinfeldt, M., Wigger, H., Gottschalk, F. (2018). Risks, release and concentrations of engineered nanomaterial in the environment. *Scientific Reports*, 8(1), 1-18.
- Guan, X., Gao, X., Avellan, A., Spielman-Sun, E., Xu, J., Laughton, S. N., Zhang, R. (2020). CuO nanoparticles alter the rhizospheric bacterial community and local nitrogen cycling for wheat grown in a calcareous soil. *Environmental Science & Technology*, 54(14), 8699-8709.
- He, Z., Gentry, T. J., Schadt, C. W., Wu, L., Liebich, J., Chong, S. C., Zhou, J. (2007). GeoChip: a comprehensive microarray for investigating biogeochemical, ecological and environmental processes. *The ISME journal*, 1(1), 67-77.
- Hibbing, M. E., Fuqua, C., Parsek, M. R., Peterson, S. B. (2010). Bacterial competition: surviving and thriving in the microbial jungle. *Nature Reviews Microbiology*, 8(1), 15-25.

- Huckabee, J. W., (1985). Evaluation of tests to predict chemical injury to ecosystems: Microcosms. *In* Methods for estimating risk of chemical injury: Human and non-human biota and ecosystems. J. Wiley & Sons, N.Y. pp. 637–674.
- ISO, 2018. ISO 20130:2018: Soil quality — Measurement of enzyme activity patterns in soil samples using colorimetric substrates in micro-well plates. Accessed 25 May 2021. <https://www.iso.org/standard/67074.html>
- Iwai, S., Weinmaier, T., Schmidt, B. L., Albertson, D. G., Poloso, N. J., Dabbagh, K., DeSantis, T. Z. (2016). Piphillin: improved prediction of metagenomic content by direct inference from human microbiomes. *PloS one*, 11(11), e0166104.
- Kah, M., Kookana, R. S., Gogos, A., Bucheli, T. D. (2018). A critical evaluation of nanopesticides and nanofertilizers against their conventional analogues. *Nature Nanotechnology*, 13(8), 677-684.
- Karimi, E., Mohseni Fard, E. (2017). Nanomaterial effects on soil microorganisms. *Soil Biology*, 137–200.
- Kim, J., Lim, J., Lee, C. (2013). Quantitative real-time PCR approaches for microbial community studies in wastewater treatment systems: applications and considerations. *Biotechnology Advances*, 31(8), 1358-1373.
- Lakshmeesha, T. R., Murali, M., Ansari, M. A., Udayashankar, A. C., Alzohairy, M. A., Almatroudi, A., Niranjana, S. R. (2020). Biofabrication of zinc oxide nanoparticles from *Melia azedarach* and its potential in controlling soybean seed-borne phytopathogenic fungi. *Saudi Journal of Biological Sciences*, 27(8), 1923-1930.
- Lead, J. R., Batley, G. E., Alvarez, P. J., Croteau, M. N., Handy, R. D., McLaughlin, M. J., Schirmer, K. (2018). Nanomaterials in the environment: behavior, fate, bioavailability, and effects - an updated review. *Environmental Toxicology and Chemistry*, 37(8), 2029-2063.
- Li, J., Rodrigues, S., Tsyusko, O. V., Unrine, J. M. (2019a). Comparing plant–insect trophic transfer of Cu from lab-synthesised nano-Cu(OH)₂ with a commercial nano-Cu(OH)₂ fungicide formulation. *Environmental Chemistry*, 16(6), 411-418.
- McGee, C. F., Storey, S., Clipson, N., Doyle, E. (2018). Concentration-dependent responses of soil bacterial, fungal and nitrifying communities to silver nano and micron particles. *Environmental Science and Pollution Research*, 25(19), 18693-18704.

- McKee, M. S., Filser, J. (2016). Impacts of metal-based engineered nanomaterials on soil communities. *Environmental Science: Nano*, 3(3), 506-533.
- McNeilly, O., Mann, R., Hamidian, M., Gunawan, C. (2021). Emerging Concern for Silver Nanoparticle Resistance in *Acinetobacter baumannii* and Other Bacteria. *Frontiers in Microbiology* 12, 894-914.
- Nannipieri, P., Penton, C. R., Purahong, W., Schloter, M., Van Elsas, J. D. (2019). Recommendations for soil microbiome analyses. *Biology and Fertility of Soils*. 55:765–766.
- Nannipieri, P., Trasar-Cepeda, C., Dick, R. P. (2018). Soil enzyme activity: a brief history and biochemistry as a basis for appropriate interpretations and meta-analysis. *Biology and Fertility of Soils*, 54(1), 11-19.
- Nautiyal, S. C. (1999). An efficient microbiological growth medium for screening phosphate solubilizing microorganisms. *FEMS Microbiology Letters*, 170(436), 265–270.
- Nelson, M. B., Martiny, A. C., Martiny, J. B. (2016). Global biogeography of microbial nitrogen-cycling traits in soil. *Proceedings of the National Academy of Sciences*, 113(29), 8033-8040.
- Park, H. D., Noguera, D. R. (2008). Nitrospira community composition in nitrifying reactors operated with two different dissolved oxygen levels. *Journal Microbiology Biotechnology*, 18(8), 1470-1474.
- Peyrot, C., Wilkinson, K. J., Desrosiers, M., Sauvé, S. (2014). Effects of silver nanoparticles on soil enzyme activities with and without added organic matter. *Environmental Toxicology and Chemistry*, 33(1), 115-125.
- Philippot, L., Raaijmakers, J. M., Lemanceau, P., Van Der Putten, W. H. (2013). Going back to the roots: the microbial ecology of the rhizosphere. *Nature Reviews Microbiology*, 11(11), 789-799.
- Reinsch, B., Levard, C., Li, Z., Ma, R., Wise, A., Gregory, K. B., Lowry, G. V. (2012). Sulfidation of silver nanoparticles decreases *Escherichia coli* growth inhibition. *Environmental Science and Technology*, 46(13), 6992–7000.
- Rodrigues, S., Bland, G. D., Gao, X., Rodrigues, S. M., Lowry, G. V. (2021). Investigation of pore water and soil extraction tests for characterizing the fate of poorly soluble metal-oxide nanoparticles. *Chemosphere*, 267, 128885.
- Samarajeewa, A. D., Velicogna, J. R., Princz, J. I., Subasinghe, R. M., Scroggins, R. P., Beaudette, L. A. (2017). Effect of silver nano-particles on soil microbial growth,

- activity and community diversity in a sandy loam soil. *Environmental Pollution*, 220, 504-513.
- Samarajeewa, A. D., Velicogna, J. R., Schwertfeger, D. M., Princz, J. I., Subasinghe, R. M., Scroggins, R. P., Beaudette, L. A. (2021). Ecotoxicological effects of copper oxide nanoparticles (nCuO) on the soil microbial community in a biosolids-amended soil. *Science of The Total Environment*, 763, 143037.
- Shahsavari, E., Aburto-Medina, A., Khudur, L. S., Taha, M., Ball, A. S. (2017). From microbial ecology to microbial ecotoxicology. *In Microbial Ecotoxicology* (pp. 17-38). Springer, Cham.
- Simonin, M., Cantarel, A. A., Crouzet, A., Gervais, J., Martins, J. M., Richaume, A. (2018a). Negative effects of copper oxide nanoparticles on carbon and nitrogen cycle microbial activities in contrasting agricultural soils and in presence of plants. *Frontiers in Microbiology*, 9, 3102.
- Simonin, M., Colman, B. P., Tang, W., Judy, J. D., Anderson, S. M., Bergemann, C. M., Bernhardt, E. S. (2018b). Plant and microbial responses to repeated Cu(OH)₂ nanopesticide exposures under different fertilization levels in an agroecosystem. *Frontiers in Microbiology*, 9, 1769.
- Spielman-Sun, E., Lombi, E., Donner, E., Avellan, A., Etschmann, B., Howard, D., Lowry, G. V. (2018). Temporal evolution of copper distribution and speciation in roots of *Triticum aestivum* exposed to CuO, Cu(OH)₂, and CuS nanoparticles. *Environmental Science & Technology*, 52(17), 9777-9784.
- Starnes, D. L., Unrine, J. M., Starnes, C. P., Collin, B. E., Oostveen, E. K., Ma, R., Tsyusko, O. V. (2015). Impact of sulfidation on the bioavailability and toxicity of silver nanoparticles to *Caenorhabditis elegans*. *Environmental Pollution*, 196, 239-246.
- Vasileiadis, S., Puglisi, E., Trevisan, M., Scheckel, K. G., Langdon, K. A., McLaughlin, M. J., Donner, E. (2015). Changes in soil bacterial communities and diversity in response to long-term silver exposure. *FEMS Microbiology Ecology*, 91(10), 1–11.
- Wang, P., Lombi, E., Sun, S., Scheckel, K. G., Malysheva, A., McKenna, B. A., Kopittke, P. M. (2017). Characterizing the uptake, accumulation and toxicity of silver sulfide nanoparticles in plants. *Environmental Science: Nano*, 4(2), 448–460.

- Wei, Z., Gu, Y., Friman, V. P., Kowalchuk, G. A., Xu, Y., Shen, Q., Jousset, A. (2019). Initial soil microbiome composition and functioning predetermine future plant health. *Science Advances*, 5(9), eaaw0759.
- Xing, C., Chen, J., Zheng, X., Chen, L., Chen, M., Wang, L., Li, X. (2020). Functional metagenomic exploration identifies novel prokaryotic copper resistance genes from the soil microbiome. *Metallomics*, 12 (3), 387-395.
- Yuan, J., Zhao, J., Wen, T., Zhao, M., Li, R., Goossens, P., Shen, Q. (2018). Root exudates drive the soil-borne legacy of aboveground pathogen infection. *Microbiome*, 6(1), 1-12.
- Zhai, Y., Hunting, E. R., Liu, G., Baas, E., Peijnenburg, W. J., Vijver, M. G. (2019). Compositional alterations in soil bacterial communities exposed to TiO₂ nanoparticles are not reflected in functional impacts. *Environmental research*, 178, 108713.
- Zhang, X., Xu, Z., Qian, X., Lin, D., Zeng, T., Filser, J., Kah, M. (2020). Assessing the impacts of Cu(OH)₂ nanopesticide and ionic copper on the soil enzyme activity and bacterial community. *Journal of Agricultural and Food Chemistry*, 68(11), 3372-3381.
- Zhang, Z., Ke, M., Qu, Q., Peijnenburg, W. J. G. M., Lu, T., Zhang, Q., Qian, H. (2018). Impact of copper nanoparticles and ionic copper exposure on wheat (*Triticum aestivum* L.) root morphology and antioxidant response. *Environmental Pollution*, 239, 689-697.
- Zimmer, M., Topp, W. (2002). The role of coprophagy in nutrient release from feces of phytophagous insects. *Soil Biology and Biochemistry*, 34(8), 1093-1099.

Annexes

1. Annex 1

A1. Copyright Licence Terms and Conditions for Figures in Chapter 1.

A1.1. Figure 2 (page 6): Scheme of ENMs sources and released in the terrestrial environment.

ELSEVIER LICENSE
TERMS AND CONDITIONS

Apr 05, 2021

This Agreement between University of Aveiro -- Sara Peixoto ("You") and Elsevier ("Elsevier") consists of your license details and the terms and conditions provided by Elsevier and Copyright Clearance Center.

0504/2021

RightLink Private License

License Number	5042601085496	Format	both print and electronic
License date	Apr 05, 2021	Are you the author of this Elsevier chapter?	No
Licensed Content Publisher	Elsevier	Will you be translating?	No
Licensed Content Publication	Elsevier Books	Title	Effects of nanomaterials on the soil microbiome: nano-agrochemicals and biosolids' applications
Licensed Content Title	Soil Pollution	Institution name	University of Aveiro
Licensed Content Author	Susana Loureiro, Paula S. Tourinho, Geert Cornelis, Nico W. Van Den Brink, Maria Diez-Ortiz, Socorro Vázquez-Campos, Vicenç Fornas-Portillo, Claus Svendsen, Cornelis A.M. Van Gestel	Expected presentation date	Sep 2021
Licensed Content Date	Jan 1, 2018	Portions	Figure 7.1, image on page 162
Licensed Content Pages	30	Requestor Location	University of Aveiro Campus Santiago Aveiro, 3810 • 193 Portugal Attn: University of Aveiro
Start Page	161	Publisher Tax ID	GB 494 6272 12
End Page	190	Total	0.00 EUR
Type of Use	reuse in a thesis/dissertation		
Portion	figures/tables/illustrations		
Number of figures/tables/illustrations	1		

<https://s101.copyright.com/AppDispatchServlet>

A1.2. Figure 3 (page 11): Predicted environmental concentrations in Europe regarding the presence of AgNPs (tonnes Ag per km²) (Kuenen *et al.*, 2020) or Copper (mg Cu kg⁻¹ vineyards soil) (Ballabio *et al.*, 2018). Permission request: May 2021.

(Ballabio *et al.*, 2018)



RightsLink[®]

? Help ✉ Email Support

Publisher: Elsevier

Copyright © 1969, Elsevier

Creative Commons

This is an open access article distributed under the terms of the [Creative Commons CC-BY](#) license, which permits unrestricted use, distribution, and reproduction in any medium, provided the original work is properly cited.

You are not required to obtain permission to reuse this article.

To request permission for a type of use not listed, please contact [Elsevier Global Rights Department](#).

Are you the [author](#) of this Elsevier journal article?

(Kuenen *et al.*, 2020)

1. Environmental Science : Nano 

0,00 EUR

Article: Inventory of country-specific emissions of engineered nanomaterials throughout the life cycle

ISSN	2051-8153	Publisher	Royal Society of Chemistry
Type of Use	Republish in a thesis/dissertation	Portion	Image/photo/illustration

[Hide Details](#)

LICENSED CONTENT


Publication Title	Environmental Science : Nano	Rightsholder	Royal Society of Chemistry
Article Title	Inventory of country-specific emissions of engineered nanomaterials throughout the life cycle	Publication Type	Journal
Author/Editor	Royal Society of Chemistry (Great Britain),	Start Page	3824
Date	01/01/2014	End Page	3839
Language	English	Issue	12
Country	United Kingdom of Great Britain and Northern Ireland	Volume	7

REQUEST DETAILS

Portion Type	Image/photo/illustration	Distribution	Worldwide
Number of images / photos / illustrations	1	Translation	Original language of publication
Format (select all that apply)	Electronic	Copies for the disabled?	No
Who will republish the content?	Academic institution	Minor editing privileges?	No
Duration of Use	Life of current edition	Incidental promotional use?	No
Lifetime Unit Quantity	Up to 499	Currency	EUR
Rights Requested	Main product		

A1.3. Figure 4 (page 13): Conceptual diagram of the major transformations that engineered nanomaterials (ENMs) might undergo in the environment.

Permission request: May 2021.

 **Transformations of Nanomaterials in the Environment**
Author: Gregory V. Lowry, Kelvin B. Gregory, Simon C. Apte, et al
Publication: Environmental Science & Technology
Publisher: American Chemical Society
Date: Jul 1, 2012
Copyright © 2012, American Chemical Society

PERMISSION/LICENSE IS GRANTED FOR YOUR ORDER AT NO CHARGE


This type of permission/license, instead of the standard Terms & Conditions, is sent to you because no fee is being charged for your order. Please note the following:

- Permission is granted for your request in both print and electronic formats, and translations.
- If figures and/or tables were requested, they may be adapted or used in part.
- Please print this page for your records and send a copy of it to your publisher/graduate school.
- Appropriate credit for the requested material should be given as follows: "Reprinted (adapted) with permission from (COMPLETE REFERENCE CITATION), Copyright (YEAR) American Chemical Society." Insert appropriate information in place of the capitalized words.
- One-time permission is granted only for the use specified in your request. No additional uses are granted (such as derivative works or other editions). For any other uses, please submit a new request.

If credit is given to another source for the material you requested, permission must be obtained from that source.

[BACK](#) [CLOSE WINDOW](#)

A1.4. Figure 5 (page 14): Schematic overview of the main fate-determining parameters of ENMs in soil-water systems. Permission request: May 2021.



Fate and Bioavailability of Engineered Nanoparticles in Soils: A Review
Author: Geert Cornelis, , Kerstin Hund-Rinke, et al
Publication: Critical Reviews in Environmental Science & Technology
Publisher: Taylor & Francis
Date: Dec 17, 2014
Rights managed by Taylor & Francis

Thesis/Dissertation Reuse Request

Taylor & Francis is pleased to offer reuses of its content for a thesis or dissertation free of charge contingent on resubmission of permission request if work is published.

[BACK](#) [CLOSE](#)

A1.5. Figure 6 (page 16): Nanoparticles and ions mode of action in (A) bacteria and (B) fungi cells. Permission request: May 2021.

(McNeilly *et al.*, 2021)



[Front Microbiol.](#) 2021; 12: 652863.

PMCID: PMC8085274

Published online 2021 Apr 16. doi: [10.3389/fmicb.2021.652863](https://doi.org/10.3389/fmicb.2021.652863)

PMID: [33936010](https://pubmed.ncbi.nlm.nih.gov/33936010/)

Emerging Concern for Silver Nanoparticle Resistance in *Acinetobacter baumannii* and Other Bacteria

[Oliver McNeilly](#)¹, [Riti Mann](#)¹, [Mohammad Hamidian](#)^{1,*} and [Cindy Gunawan](#)^{1,2,*}

► [Author information](#) ► [Article notes](#) ► [Copyright and License information](#) ► [Disclaimer](#)

[Copyright](#) © 2021 McNeilly, Mann, Hamidian and Gunawan.

This is an open-access article distributed under the terms of the Creative Commons Attribution License (CC BY). The use, distribution or reproduction in other forums is permitted, provided the original author(s) and the copyright owner(s) are credited and that the original publication in this journal is cited, in accordance with accepted academic practice. No use, distribution or reproduction is permitted which does not comply with these terms.

(Lakshmeesha *et al.*, 2020)



Biofabrication of zinc oxide nanoparticles from *Melia azedarach* and its potential in controlling soybean seed-borne phytopathogenic fungi

Author:

T.R. Lakshmeesha, M. Murali, Mohammad Azam Ansari, Arakere C. Udayashankar, Mohammad A. Alzohairy, Ahmad Almatroudi, Mohammad N. Alomary, Sarah Mousa Maadi Asiri, B.S. Ashwini, Naveen Kumar Kalagatur, Chandra S. Nayak, S.R. Niranjana

Publication: Saudi Journal of Biological Sciences

Publisher: Elsevier

Date: August 2020

© 2020 The Author(s). Published by Elsevier B.V. on behalf of King Saud University.

Creative Commons Attribution-NonCommercial-No Derivatives License (CC BY NC ND)

This article is published under the terms of the Creative Commons Attribution-NonCommercial-No Derivatives License (CC BY NC ND). For non-commercial purposes you may copy and distribute the article, use portions or extracts from the article in other works, and text or data mine the article, provided you do not alter or modify the article without permission from Elsevier. You may also create adaptations of the article for your own personal use only, but not distribute these to others. You must give appropriate credit to the original work, together with a link to the formal publication through the relevant DOI, and a link to the Creative Commons user license above. If changes are permitted, you must indicate if any changes are made but not in any way that suggests the licensor endorses you or your use of the work.

Permission is not required for this non-commercial use. For commercial use please continue to request permission via Rightslink.

[BACK](#)

[CLOSE WINDOW](#)

A1.6. Figure 7 (page 19): Schematic of three biogeochemical cycles of carbon, nitrogen and phosphorous in terrestrial ecosystems. Permission request: May 2021.



**AMERICAN
SOCIETY FOR
MICROBIOLOGY**

Forest Soil Bacteria: Diversity, Involvement in Ecosystem Processes, and Response to Global Change

Author: Salvador Lladó, Rubén López-Mondéjar, Petr Baldrian
Publication: Microbiology and Molecular Biology Reviews
Publisher: American Society for Microbiology
Date: Apr 12, 2017

Copyright © 2017, American Society for Microbiology

Permissions Request

ASM authorizes an advanced degree candidate to republish the requested material in his/her doctoral thesis or dissertation. If your thesis, or dissertation, is to be published commercially, then you must reapply for permission.

[BACK](#) [CLOSE WINDOW](#)